Loughborough University

This item is held in Loughborough University's Institutional Repository (https://dspace.lboro.ac.uk/) and was harvested from the British Library's EThOS service (http://www.ethos.bl.uk/). It is made available under the following Creative Commons Licence conditions.

creative commons

COMMONS DEED

Attribution-NonCommercial-NoDerivs 2.5

You are free:

- to copy, distribute, display, and perform the work

Under the following conditions:

Attribution. You must attribute the work in the manner specified by the author or licensor.

Noncommercial. You may not use this work for commercial purposes.

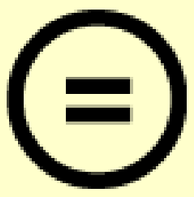

No Derivative Works. You may not alter, transform, or build upon this work.

- For any reuse or distribution, you must make clear to others the license terms of this work.
- Any of these conditions can be waived if you get permission from the copyright holder.

Your fair use and other rights are in no way affected by the above.

This is a human-readable summary of the Legal Code (the full license).

Disclaimer

For the full text of this licence, please go to:
http://creativecommons.org/licenses/by-nc-nd/2.5/

INVESTIGATION OF PARAMETERS AFFECTING THE IGNITION OF ARC DISCHARGES AND THE DEVELOPMENT OF A HIGH FREQUENCY IGNITION SUPPLY

by

Mansour Saiepour B.Sc., M.Sc., PGCE, AMIEE

A DOCTORAL THESIS

Submitted in partial fulfilment of the requirements for the award of PhD of the Loughborough University of Technology, 1991.

Supervisor: Dr J E Harry

Department of Electronic and Electrical Engineering

© by M Saiepour 1991

ABSTRACT

Non-contact ignition of TIG welding arcs has been studied. The variation of dc voltage with dc current of combined ac-dc discharges indicated that an ac-dominated discharge, a dc-dominated discharge and a transition region exist during the initial current rise after breakdown from cold. These measurements enabled the conditions for reliable ignition of dc arcs using a continuous sinusoidal hf source to be predicted.

The minimum current to sustain a cold arc and the time taken to reach the steady-state were investigated using a novel capacitor discharge supply. The results showed that to initiate a 3 mm TIG welding arc from cold supplied by a power supply with an open circuit voltage of 80 V, a minimum current of about 0.9 A may be required and the time taken for the arc to reach the steady-state may take several hundred milliseconds.

The results of investigations on combined ac-dc discharges, minimum current to sustain a cold arc and the time taken to reach the steady-state indicated that for safe, interference-free and reliable non-contact arc ignition, a continuous sinusoidal hf supply was the best method. A high voltage (about 3 kV) and high current (about 1 A) were required simultaneously to initiate a 3 mm TIG arc from cold. A single continuous sinusoidal hf supply required an ignition power of the order of 1.35 kW which was not feasible.

An arc ignition method using two continuous sinusoidal hf supplies has been devised which provides safe, interference-free and reliable arc ignition, and which requires less than 75% of the output power of a single continuous sinusoidal hf system. A solid-state hf ignition system based on the new method was designed and constructed.

ACKNOWLEDGEMENTS

I am grateful to my supervisor Dr. J.E. Harry for initiating this work and for his encouragement and guidance which have been invaluable.

I wish to thank SERC and NEI Weldcontrol for the financial support of the CASE award for this work.

I am grateful to my present employers British Steel Technical, Swinden Laboratories for allowing me some time for visits to Loughborough University in order to complete the thesis.

Finally, I would like to thank my family for their understanding and support over the years.

To my God, who made this possible

CONTENTS

LIST OF FIGURES

CHAPTER 5

APPENDIX 5

LIST OF TABLES

List of Symbols and Definitions of Terms

symbol		unit
d	electrode separation	mm
e	charge on an electron (1.6×10^{-19})	C
f	frequency	Hz
i_d	instantaneous discharge current	A
k	Boltzmann's constant (1.38×10^{-23})	JK^{-1}
p	gas pressure	b
r_d	instantaneous discharge resistance	Ω
$r_{d(av.)}$	average combined discharge resistance	Ω
t	time	s
t_{min}	time taken for a cold arc to be self-sustained	s
Δt_0	period of current zero	s
v_c	instantaneous capacitor voltage	V
v_d	instantaneous discharge voltage	V
C_p	specific heat capacity at constant pressure	$Jkg^{-1}K^{-1}$
D	arc column diameter	mm
E	electric field	Vm^{-1}
E_0	peak value of ac electric field	Vm^{-1}
I_d	dc discharge current	A
$I_{d(dc)}$	dc current in a combined ac-dc discharge	A
I_i	initial discharge current	A
I_m	peak current of an ac discharge	A
I_{min}	minimum current required to sustain a clod arc	A

I_{sc}	short circuit current	A
I_t	dc current in a combined ac-dc discharge at the transition region	A
J	current density	Am^{-2}
K	thermal conductivity	$Wm^{-1}K^{-1}$
$R_{d(hf+dc)}$	resistance of a combined ac-dc discharge	Ω
T	temperature	K
V_b	breakdown voltage	kV
V_c	initial capacitor voltage	V
V_d	dc discharge voltage	V
$V_{d(dc)}$	dc voltage in a combined ac-dc discharge	V
V_i	reignition voltage	V
V_m	peak voltage of an ac discharge	V
V_{oc}	open circuit voltage	V
V_t	dc voltage of a combined ac-dc discharge at the transition region	V
α	Townsend's first ionisation coefficient	-
γ	Townsend's second ionisation coefficient	-
μ_+	mobility of positive ions	$m^2V^{-1}s^{-1}$
ρ	gas density	kgm^{-3}
$\rho_{av.}$	average gas density during the development of the arc column	kgm^{-3}
ρ_0	gas density at °C	kgm^{-3}
Ø	thermionic work function	eV

Definition of Some of the Terms Used

Words that could cause some ambiguity have been defined to assist in the clarification of the text.

Ignition, initiation, starting, establishment - the stage at which an arc becomes self-sustaining.

Cold arc - the arc just after breakdown from cold in which the thermal processes at the cathode and the column are insignificant.

Cold column - an arc column in which field ionisation is dominant and thermal ionisation is insignificant.

Hot column - an arc column in which thermal ionisation is dominant and field ionisation is insignificant.

Thermally developed column - an arc column which has acquired a higher temperature (after breakdown from cold) due to the increase in thermal ionisation and has reached a stable temperature.

Combined discharge - a discharge which is supplied with current from two or more power sources.

Temporary arc - a short duration arc resulting from glow to arc transitions.

CHAPTER 1

INTRODUCTION

1.0 INTRODUCTION

Safe initiation of welding arcs has always presented difficulties. Non-contact arc initiation techniques use high frequency (hf), high voltage pulse trains which have a high harmonic content, are not always effective and may cause considerable damage to semiconductors. The high frequency output necessary for operator safety results in the connections to the electrodes and the electrodes themselves having a major effect on the ignition circuit. The supply circuit behaves like a transmission line with the values of resistance, capacitance and inductance being both frequency and geometry dependent. This leads to unreliable and unpredictable arc initiation under apparently similar conditions.

The problem of damage to semiconductors has been made greater by the use of microprocessors and computers to control arc welding processes. The high frequency ignition source acts as a spark transmitter resulting in both transmission along conductors and airborne transmission. This results in unpredictable damage to semiconductor components in power supplies and associated computer controlled equipment used in automated welding supplies.

Any attachments to the welding terminals such as leads, torches and worktables are capable of acting as antennae and transmit radio frequency radiation which may be radiated to computers unconnected to the welding equipment such as microprocessor controlled servo-hydraulic systems. Attempts to minimise radiated interference have been made by keeping the welding cables as short, straight, close together, and as close to the ground or floor as possible.

Power lines are capable of directly conducting high frequency energy which may cause interference directly

or by radiation from these power lines to computers which are used as for example data retrieval and analysis systems.

Radiation from the welding circuit can be picked up by underground metal objects or unshielded wiring in the immediate vicinity, conducted some distance, and re-radiated. This can also be a troublesome source of interference.

The techniques that are used for the ignition of welding arcs, have been developed empirically. The literature is confined largely to industrial practice and very little information is available on the minimum requirements for satisfactory arc ignition.

The purpose of this work is to
i) study the minimum requirements for a dc arc to initiate, using either dc or ac ignition sources and
ii) develop a reliable, safe and (radio frequency interference) RFI-free ignition system which may be suitable for use with microprocessor controlled welding equipment.

1.1 Structure of the Thesis

The overall structure of the thesis is shown in Fig. 1.1. Electrical breakdown and discharge processes relevant to arc initiation (Chap. 2), and methods used for ignition together with their associated problems (Chap. 3), have been reviewed.

Chap. 4 describes the preliminary investigations into high-voltage breakdown using dc and ac up to 800 kHz. Static dc discharges were used to determine the conditions under which a dc discharge will initiate a dc arc. The time required for the starting discharge to allow the main supply to provide sufficient current for the arc to sustain itself was investigated.

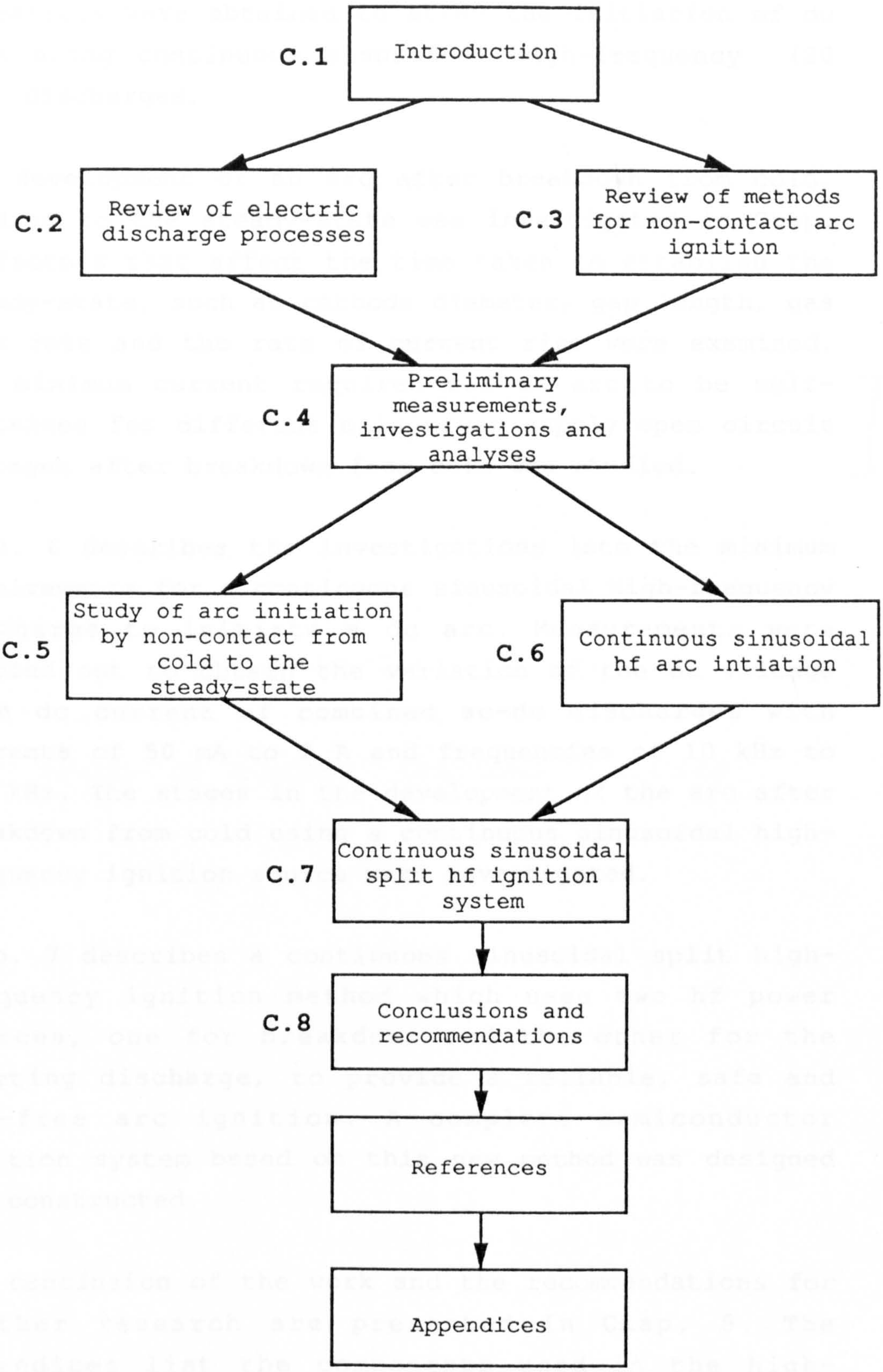

Fig.1.1 Structure of the Thesis

Voltage-current characteristics for combined ac-dc discharges were obtained to study the initiation of dc arcs using continuous sinusoidal high-frequency (20 kHz) discharges.

The development of an arc after breakdown from cold, leading to the steady-state was investigated in Chap. 5. Factors that affect the time taken to establish the steady-state, such as cathode diameter, gap length, gas flow rate and the rate of current rise were examined. The minimum current required for an arc to be self-sustained for different main power supply open circuit voltages after breakdown from cold was studied.

Chap. 6 describes the investigations into the minimum requirements for a continuous sinusoidal high-frequency discharge to initiate a dc arc. Measurements were carried out to obtain the variation of the dc voltage with dc current of combined ac-dc discharges with currents of 50 mA to 2 A and frequencies of 10 kHz to 800 kHz. The stages in the development of the arc after breakdown from cold using a continuous sinusoidal high-frequency ignition source were investigated.

Chap. 7 describes a continuous sinusoidal split high-frequency ignition method which uses two hf power sources, one for breakdown and the other for the starting discharge, to provide a reliable, safe and RFI-free arc ignition. A complete semiconductor ignition system based on this new method was designed and constructed.

The conclusion of the work and the recommendations for further research are presented in Chap. 8. The appendices list the components used in the high-frequency high-voltage generator and each hf module of the split hf system, the static V-I chracteristics for arcs, the time taken for an arc column to thermally develop and a description of the rotating load line model.

CHAPTER 2

REVIEW OF ELECTRIC DISCHARGE PROCESSES

2.1 ELECTRIC BREAKDOWN OF GASES

The gas in an arc gap needs to be initially broken down by the application of a high voltage across the gap. This section deals with phenomena that are likely to be encountered in non-contact initiation of arc discharges. High-voltage breakdown using dc and ac have been considered.

2.1.1 DC Breakdown

The electrical conductivity of a gas depends on the degree to which it is ionised. Under normal conditions, any gas contains an amount of electrons and positive ions which are produced by for example photo-ionisation or cosmic radiation. When these charged particles are made to accelerate and gain energy by the application of a large enough electric field of the order of 3 $kVmm^{-1}$ in air, they ionise other gas atoms in their path by collision and further electrons and positive ions are produced. This process can develop into a chain reaction resulting in an electron avalanche which leads to a complete breakdown of the gas.

The initiation of a gas discharge requires two conditions to be satisfied:
i) an electron moving through the gas should produce an electron avalanche by collision processes,
ii) as a result of the avalanche further electrons should be generated in the gas or at the cathode so that a continuous supply of charge may continue.

Electrons are removed to the anode and positive ions to the cathode by the action of the electric field. The conditions in such an avalanche are expressed in terms of the distance x of the electron from its starting point and Townsend's first ionisation coefficient α, which is the number of ion-pairs created by one electron per unit length of its path in the direction of the electric field. For one electron starting, n

electrons appear at a distance x nearer to the anode where $n=e^{\alpha x}$ (Howatson 1976). The number of positive ions per avalanche is $e^{\alpha x}-1$. These ions bombard the cathode and generate new (secondary) electrons which lead to new avalanches. A total of $\gamma(e^{\alpha x}-1)$ secondary electrons are produced where γ is Townsend's second ionisation coefficient and is the number of electrons emitted from the cathode per ion. Breakdown can occur only when

$$\gamma(e^{\alpha x}-1) \geq 1$$

disregarding the value 1 with respect to $e^{\alpha x}$,

$$\gamma e^{\alpha x} \geq 1$$

which is known as the Townsend breakdown criterion and indicates that the rate of generation of electrons is balanced by their rate of loss to the electrodes.

The quantities α and γ are both functions of E/p where E is the electric field and p the gas pressure. They also depend on the type of gas and γ is also dependent on the cathode material. The breakdown voltage V_b is therefore a function of the product of the gas pressure p and electrode separation d. The relation between V_b and pd is given by the Paschen curve indicated in Fig. 2.1 which shows the variation of V_b with pd in different gases, and shows that there is a minimum value for V_b. At high values of pd, α becomes relatively small due to the small amount of energy that the electrons pick up from the electric field per free path and therefore V_b becomes relatively large. At low values of pd, V_b also increases due to the small number of possible collisions. Between those extreme values of pd there is a value corresponding to the minimum value of V_b. The minimum breakdown voltages and the corresponding pd values using iron electrodes in different gases are shown in Table 2.1.

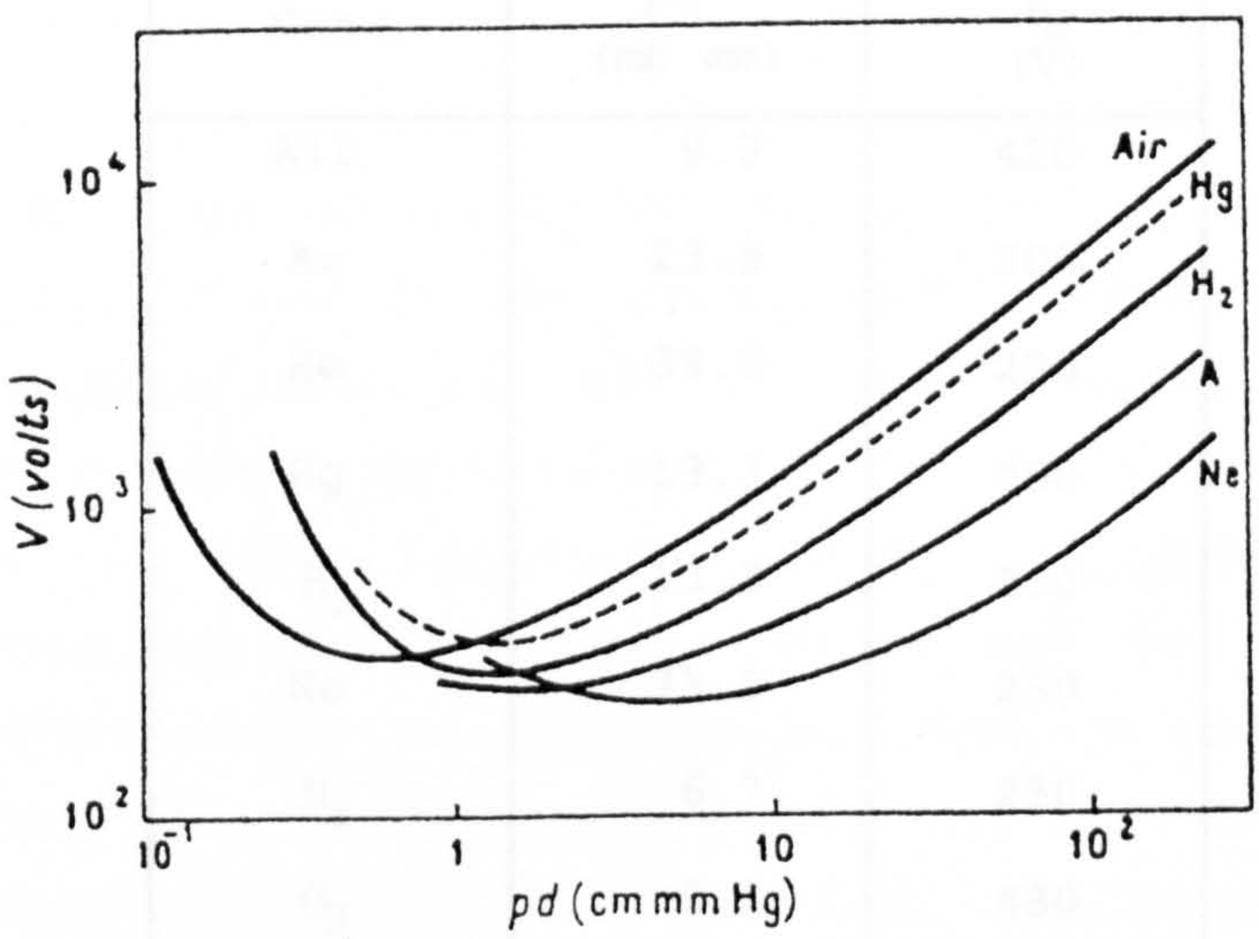

Fig.2.1 Paschen curves for different gases (Papoular 1965).

Gas	pd (mb mm)	V_b (V)
Air	9.3	420
Ar	23.9	300
He	39.9	220
Hg	13.3	450
H_2	13.3	250
Ne	73.2	230
N_2	6.7	230
O_2	5.3	480

Table 2.1 Measured values for the minimum breakdown voltage and corresponding values for pd using iron electrodes (von Engel 1983).

Gas	pd (mb mm)	V_b (V)
Air	9.3	420
Ar	23.9	300
He	39.9	220
Hg	13.3	450
H_2	13.3	250
Ne	73.2	230
N_2	6.7	230
O_2	5.3	480

Table 2.1 Measured values for the minimum breakdown voltage and corresponding values for pd using iron electrodes (von Engel 1983).

Townsend breakdown depends on secondary electron emission from the cathode and is therefore affected by the transit time of positive ions. The time required for this type of breakdown is of the order of 10^{-4} s which is greater than the positive ion transit time of about 6.5×10^{-6} s for a 3 mm gap in air at atmospheric pressure.

The Townsend theory may not apply at atmospheric pressure which is of interest to studies on the ignition of welding arcs. This was found to be due to the observed time lag of the order of 10^{-7} s which was less than the positive ion transit time (Kuffel et al 1984). A fundamentally different type of breakdown takes place when an electron avalanche grows to 10^8 - 10^9 electrons. This is the case for air when pd $\geq$ 10-20 b mm. This breakdown process is called Kanal, streamer or space charge breakdown and is based on the deformation of the electric field by the presence of a space charge between the electrodes and may also rely on photo-ionisation in the gas but not on positive ion bombardment of the cathode. This space charge which plays a part only when the electron avalanche exceeds the critical limit of 10^8 - 10^9 electrons, leads to the formation of an ionised channel between the electrodes in a very short time of the order of 10^{-7} s.

Electrode gaps in argon have lower breakdown voltages than in air because argon is a monatomic gas and needs less energy for ionisation than a polyatomic gas which is dissociated before ionisation can take place, despite the higher ionisation potential of argon (15.8 eV) compared with nitrogen (14.5 eV) or oxygen (13.6 eV). Oxygen is also an electro-negative gas which causes an increased loss of electrons by attachment resulting in an increased breakdown voltage.

A point-plane gap has a lower breakdown voltage than a gap between two uniform spheres. This is due to the

field concentration and the formation of a positive ion space charge above the point electrode. The electrons have higher velocities near the pointed electrode due to the higher voltage gradient at the point than in a uniform field and leave more positive ions behind resulting in a positive ion space charge. Conditions at the cathode surface such as temperature, affect the secondary electron emission process which is required for the discharge to be self-sustaining; for example a cathode with a higher temperature than a colder one would enhance electron emission and lower the breakdown voltage. Non-contact ignition of arcs between cold electrodes will therefore require higher breakdown voltages than in gaps in which an arc previously existed. The breakdown voltages of electrode gaps measured by different investigators using different shapes of electrodes in air and argon at atmospheric pressure are shown in Fig. 2.2.

2.1.2 AC Breakdown

The breakdown voltage of a gap for an alternating voltage at 50 Hz is similar to that for dc conditions. If the frequency is increased to a value at which positive ions have insufficient time to cross the gap in half a cycle, a positive space charge is gradually built up in the gap leading to field distortion and a lowering of the breakdown voltage below the dc value. At much higher frequencies, the breakdown mechanism is further complicated because of the amplitude of oscillations of electrons in the gap becoming comparable with the gap length so that cumulative ionisation may be produced in the gap by an electron travelling many times the gap length in the direction of the alternating field.

The breakdown voltages for frequencies up to 20 kHz for gaps up to 25 mm between spheres of 62.5 mm diameter in air at atmospheric pressure have been found to be

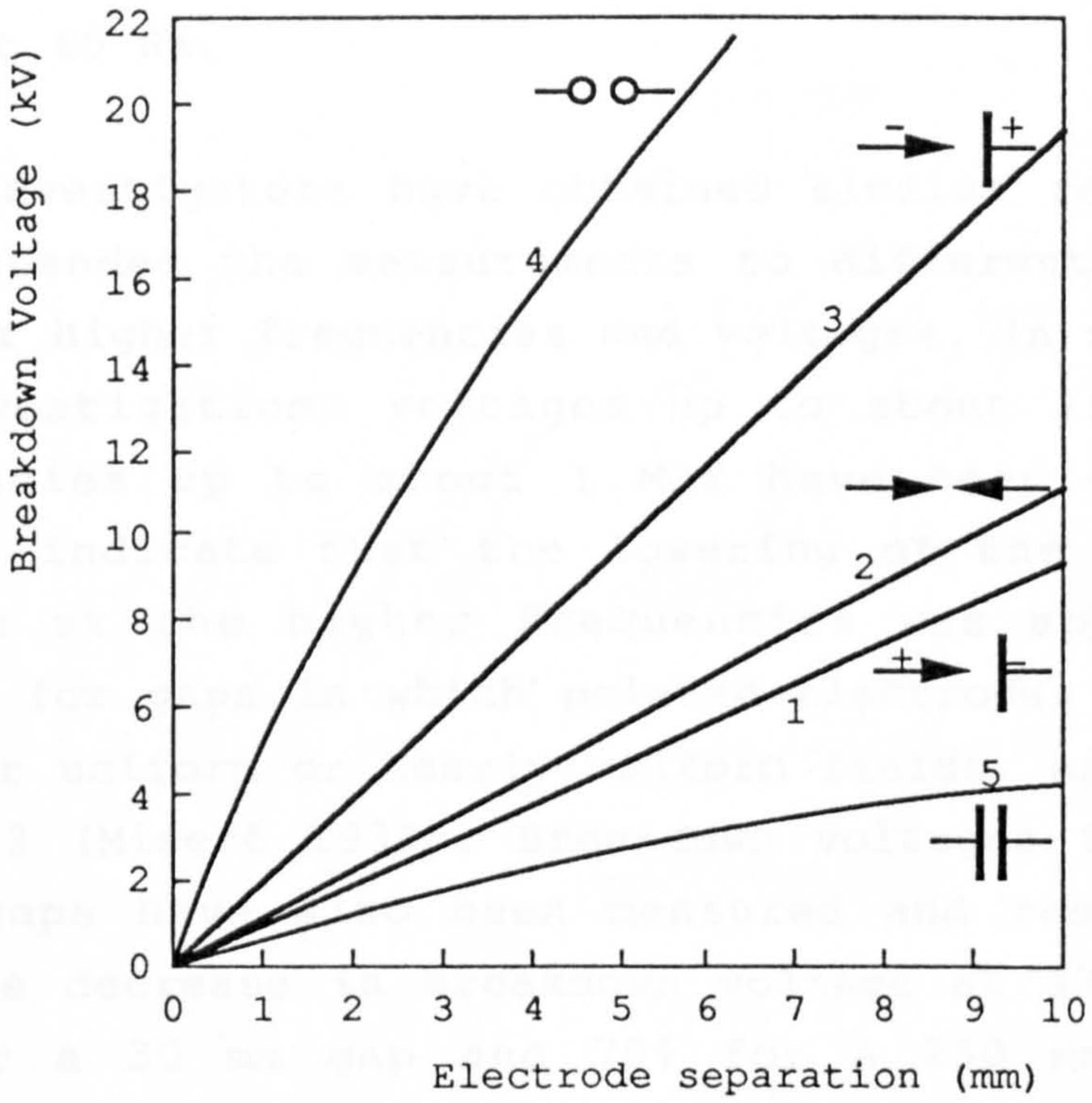

Fig.2.2 Variation of breakdown voltage with electrode separation for different electrode geometries in air (curves 1, 2, 3 and 4) and in argon (curve 5) (Romalo 1969).

similar to dc breakdown voltages (Reukema 1928). A progressive lowering of the breakdown voltage of a given gap occurred as the frequency was raised from 20 kHz to 60 kHz but for higher frequencies, up to the maximum of 425 kHz used by Reukema, the breakdown voltage of a gap was constant at about 15% below the value at 60 Hz.

Other investigators have obtained similar results and have extended the measurements to different types of gaps for higher frequencies and voltages. In several of the investigations voltages up to about 150 kV and frequencies up to about 1 MHz have been used. The results indicate that the lowering of the breakdown voltage at the higher frequencies was appreciably greater for gaps in which pointed electrodes were used than for uniform or nearly uniform fields, as shown in Fig. 2.3 (Miseré 1932). Breakdown voltages for point-plane gaps have also been measured and results show that the decrease in breakdown voltage at 370 kHz was 46% for a 30 mm gap and 70% for a 250 mm gap, as compared with the 50 Hz values (Luft 1937).

The results of investigations on the breakdown of gaps between spheres or plates indicate a critical gap length below which the breakdown voltage is independent of the frequency; the critical gap length decreasing with increasing frequency (Lassen 1931, Miseré 1932, Müller 1934). This critical gap length has been measured to be 4.5 mm at 110 kHz and 0.9 mm at 995 kHz (Müller 1934). Consideration of positive ion mobilities shows that these critical gaps correspond approximately to those for which accumulation of positive ions may occur in the gap with a consequent space-charge distortion of the electric field and a lowering of the breakdown voltage. The critical frequency at which this critical gap length is just possible is given by:

$$f = \frac{\mu_+ E_0}{2 \pi d}$$

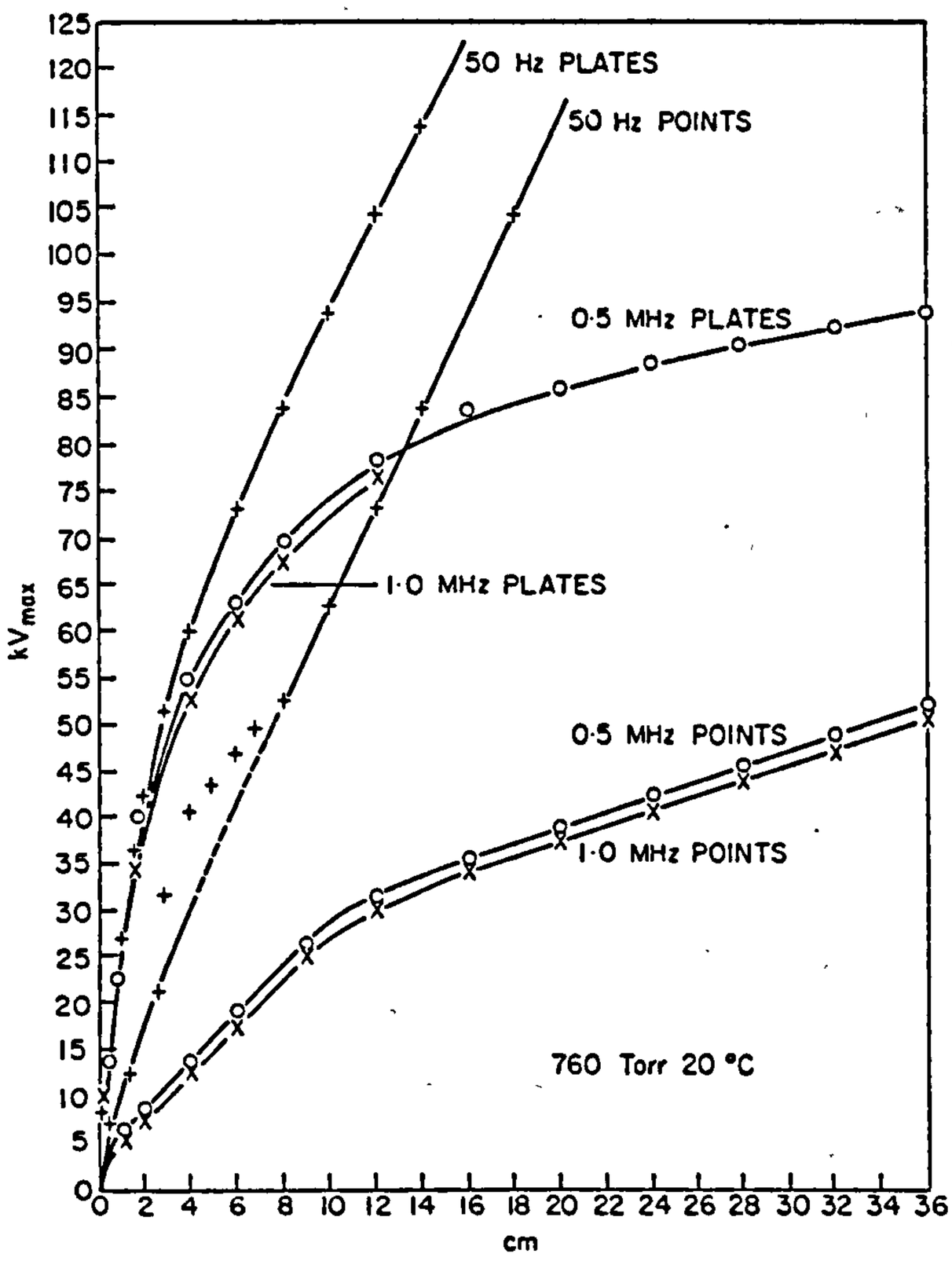

Fig.2.3 Peak breakdown voltage in air at atmospheric pressure as a function of gap length between plates and between points for frequencies of 50 Hz, 0.5 MHz and 1 MHz (Meek and Craggs 1978).

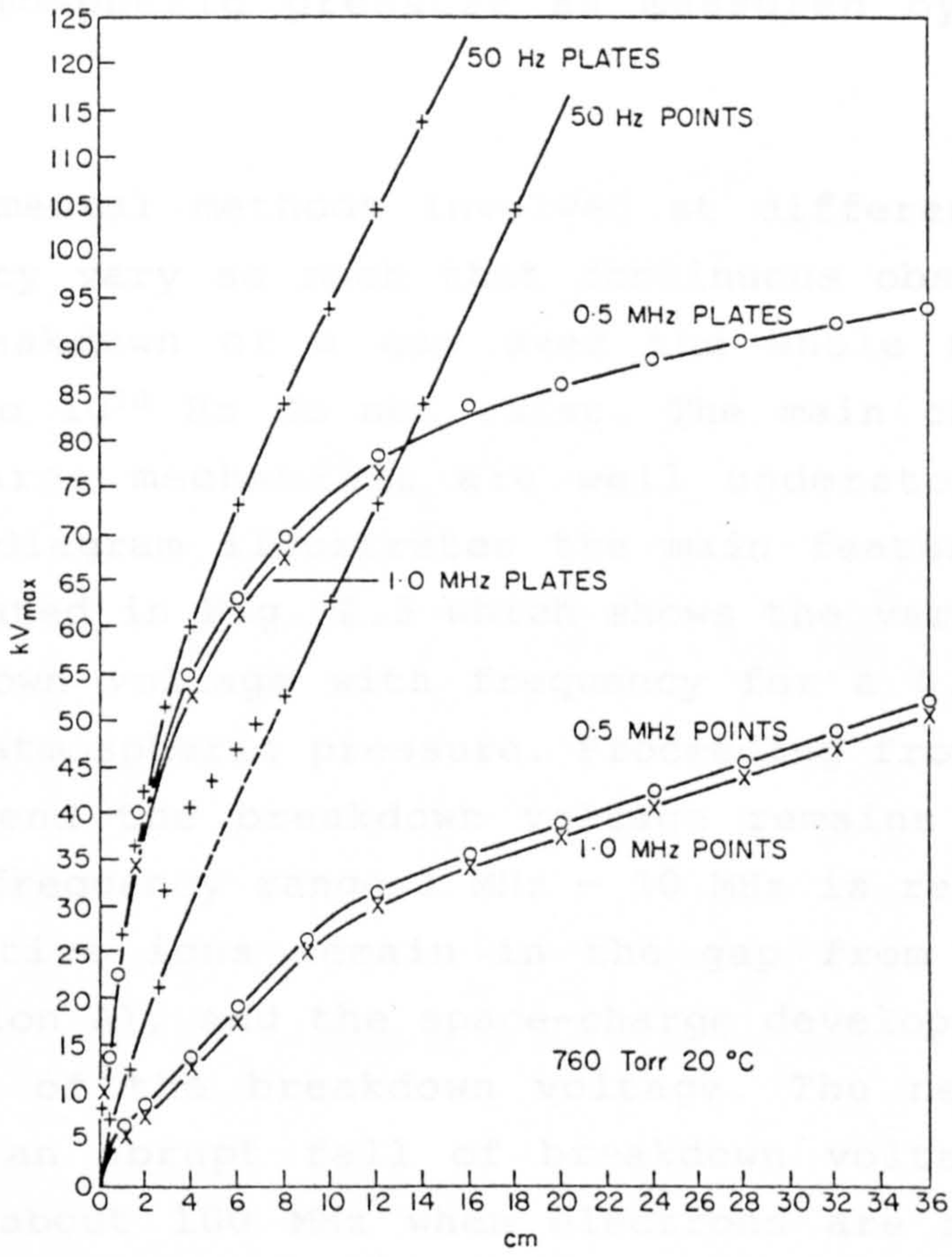

Fig.2.3 Peak breakdown voltage in air at atmospheric pressure as a function of gap length between plates and between points for frequencies of 50 Hz, 0.5 MHz and 1 MHz (Meek and Craggs 1978).

where μ_+ is the mobility of positive ions, E_0 is the peak value of the alternating field, and d is the electrode separation. This is illustrated in Fig. 2.4 which shows the variation of the breakdown voltage with the electrode separation at different frequencies in air at atmospheric pressure as measured by Lassen (1931).

The experimental methods involved at different ranges of frequency vary so much that continuous observations on the breakdown of a gap over the whole frequency range up to 10^{10} Hz do not exist. The main changes in the discharge mechanisms are well understood and a composite diagram illustrates the main features. This is illustrated in Fig. 2.5 which shows the variation of the breakdown voltage with frequency for a 0.4 mm gap in air at atmospheric pressure. Proceeding from the low frequency end the breakdown voltage remains constant until the frequency range 1 MHz - 10 MHz is reached, at which positive ions remain in the gap from cycle to cycle (region A), and the space-charge developed causes a lowering of the breakdown voltage. The next major change is an abrupt fall of breakdown voltage which occurs at about 100 MHz when electrons are no longer removed from the gap in each cycle (region B).

AC breakdown has been reviewed by Nasser (1971), and Meek and Craggs (1978), and a comprehensive collection of references is given by Muehe (1965). A summary of experimental work carried out on the breakdown of gaps with spherical electrodes using sinusoidal hf high voltages is given in Table 2.2.

2.2 ELECTRIC DISCHARGES

The characteristics of a discharge that results after breakdown of a gap between two electrodes depends on the type of gas, the gas pressure, the electrode separation, material and geometry, and the parameters

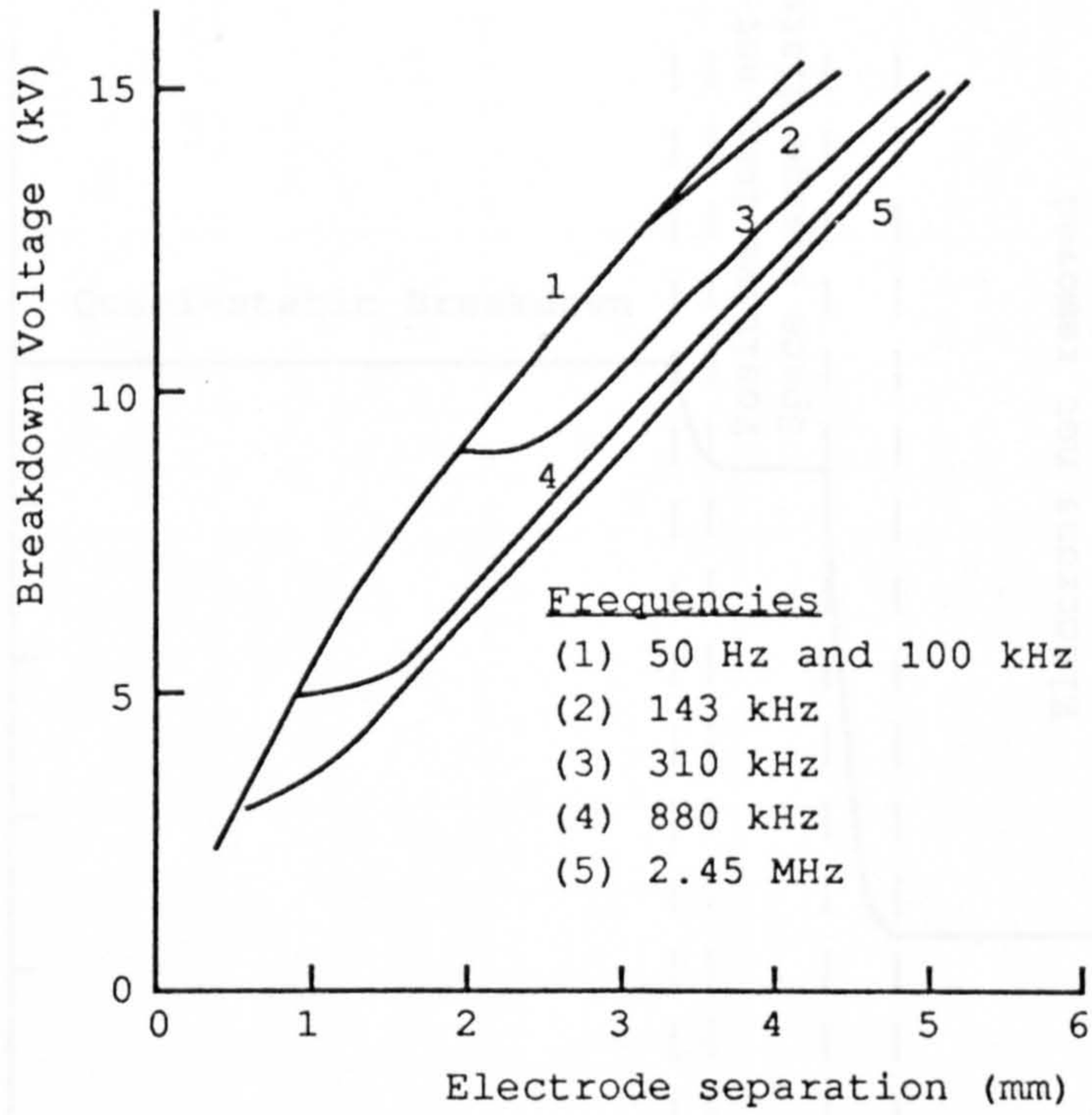

Fig.2.4 Variation of breakdown voltage with gap length at different frequencies in air at atmospheric pressure (Lassen 1931).

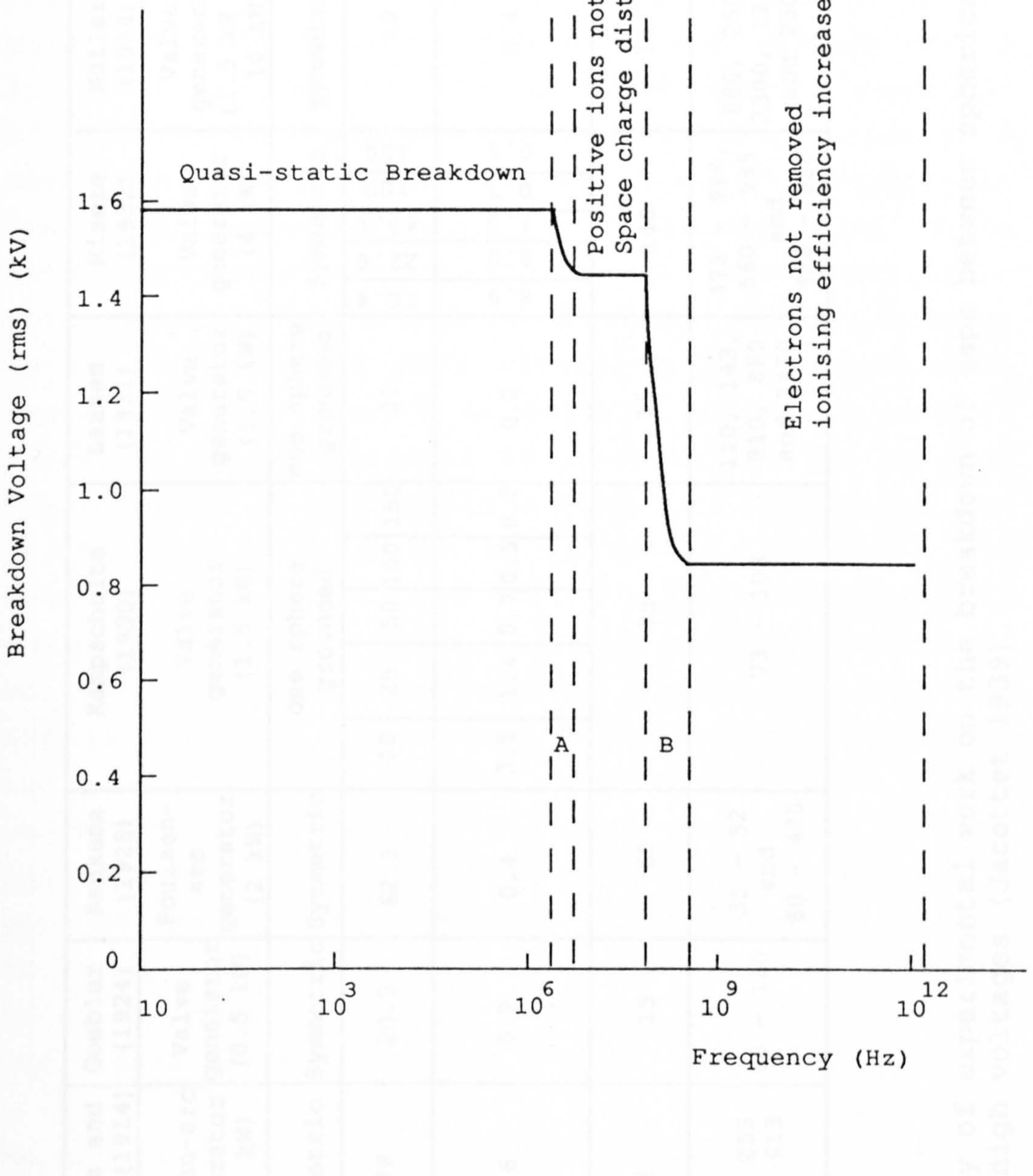

Fig.2.5 Variation of breakdown voltage with frequency for a 0.4 mm gap in air at atmospheric pressure (Prowse 1950).

Reference	Clarke and Ryan (1914)	Goebler (1924)	Reukema (1928)	Kampschulte (1930)					Lassen (1931)	Misere (1932)					Müller (1934)	Luft (1937)
HF generator	Poulsen-arc generator (15 kW)	Valve generator (0.5 kW)	Poulsen-arc generator (2 kW)	Valve generator (1.5 kW)					Valve generator (1.5 kW)	Valve generator (4 kW)					Valve generator (1.5 kW and 10 kW)	Valve generator (4 kW)
Arrangement of spheres	Symmetric	Symmetric	Symmetric	one sphere grounded					one sphere grounded	Symmetric					Symmetric	Symm. and one grounded
Sphere diameter (mm)	178	20.5	62.5	10	25	50	100	150	25	16.4	22.6	49.1	100	150	10	50 and 100
Ratio of gap separation to sphere diameter	0.16	0.2	0.4	3.5	1.4	0.7	0.3	0.2	0.2	8.5	8.0	1.5	0.7	0.5	0.4	1.2, 0.65 and 0.4
Highest voltage used (kV)	74	15	65	75					15	140					14	130
Frequency (kHz)	123, 255 and 613	85 - 120	35 - 52 and 60 - 425	73 - 108					110, 143, 310, 880 and 2450	473 - 995, 560 - 995 and 428 - 850					880, 2500, 3300, 12000 and 25000	360, 370, 460 and 470

Table 2.2 A survey of experimental work on the breakdown of gaps between spherical electrodes using undamped hf high voltages (Jacottet 1939).

of the external circuit such as the applied voltage and series resistance.

The voltage-current characteristics of a discharge may be determined using a circuit such as that shown in Fig. 2.6. If the current is slowly increased by reducing the series resistance, the appearance of the discharge, the current density and the voltage across it will vary. Fig. 2.7 indicates the order of magnitude of steady-state voltages and currents which occur in a discharge at a pressure of about 1 mb. A discharge is generally classified into three groups according to the discharge current. The first part of the characteristic which occurs at a current of less than 10^{-5} A, is known as the Townsend or dark discharge. It is not self-sustaining and requires an external source to produce electrons either directly by ionising the gas or from the cathode. If the supply voltage is increased or the stabilising resistance is reduced to increase the current to about 10^{-4} A, a glow discharge is established which normally has almost a constant voltage with changes in current. Only the steady-state arc is normally of interest under welding operations but glow discharges are also reviewed because i) a glow phase may also occur in an ignition process ii) the ignition methods investigated in the present work use a glow as the starting discharge. Increasing the current to about 1 A, causes the discharge to suddenly change to an arc which has a more intense light, lower voltage and higher temperature than a glow.

An arc is divided into three main regions; the cathode fall, the anode fall and the positive column. Fig. 2.8 shows the voltage distribution along a dc arc. An arc discharge has a high current density of several hundred Amm^{-2} on the electrodes and up to 1 Amm^{-2} in the column, a low cathode fall voltage of about 10 V which is much smaller than in a glow discharge (≈300 V) and large temperature and voltage gradients especially near the

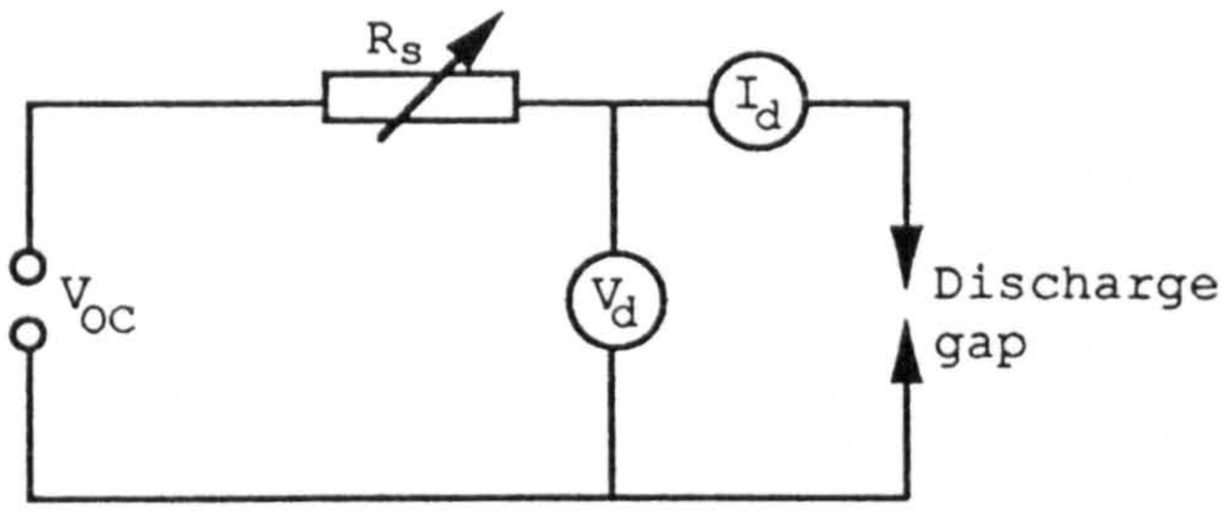

Fig.2.6 Circuit used to determine the V-I characteristics of an electric discharge.

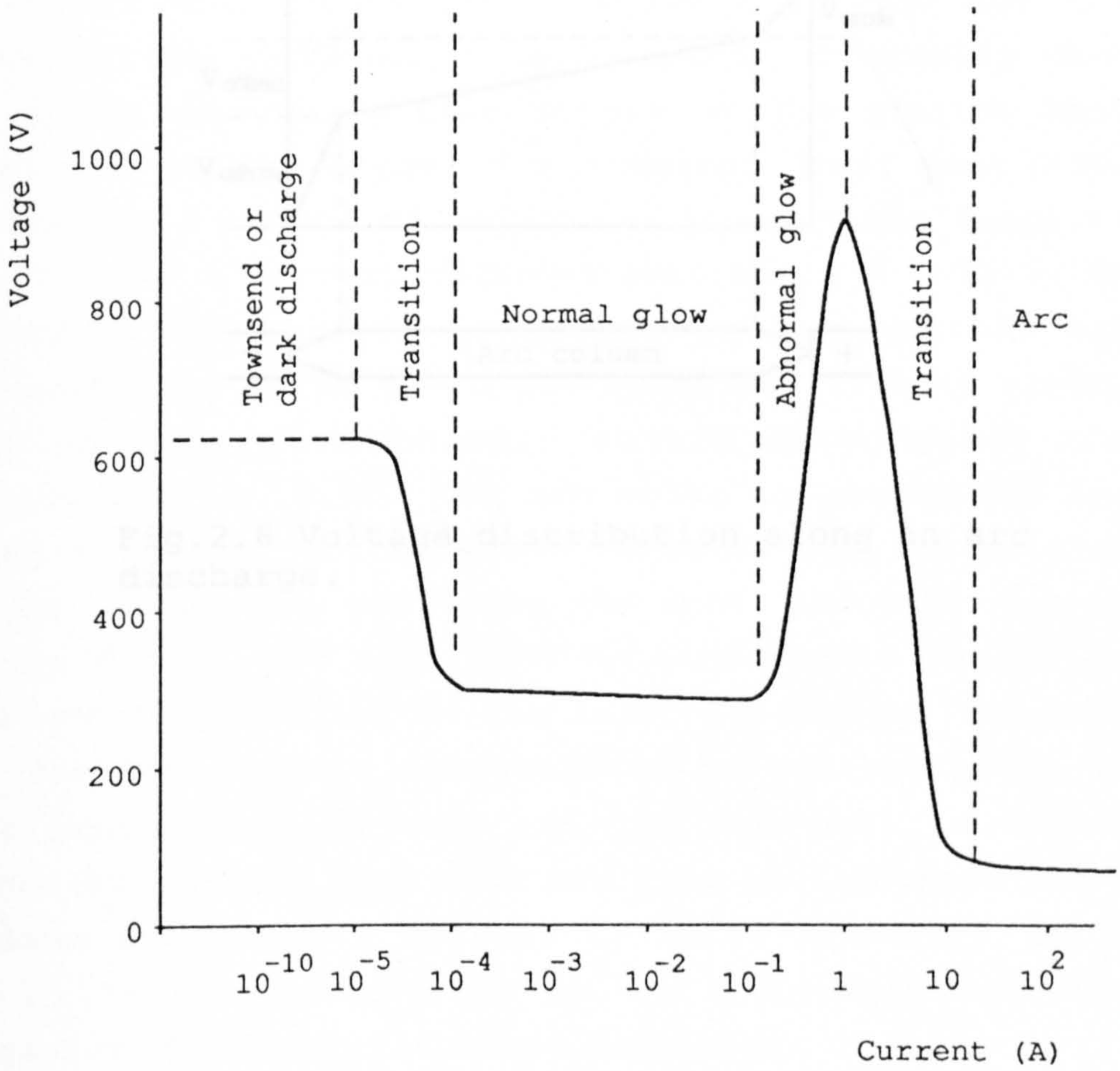

Fig.2.7 steady-state V-I characteristic of a discharge at a pressure of about 1 mb (Somerville 1959).

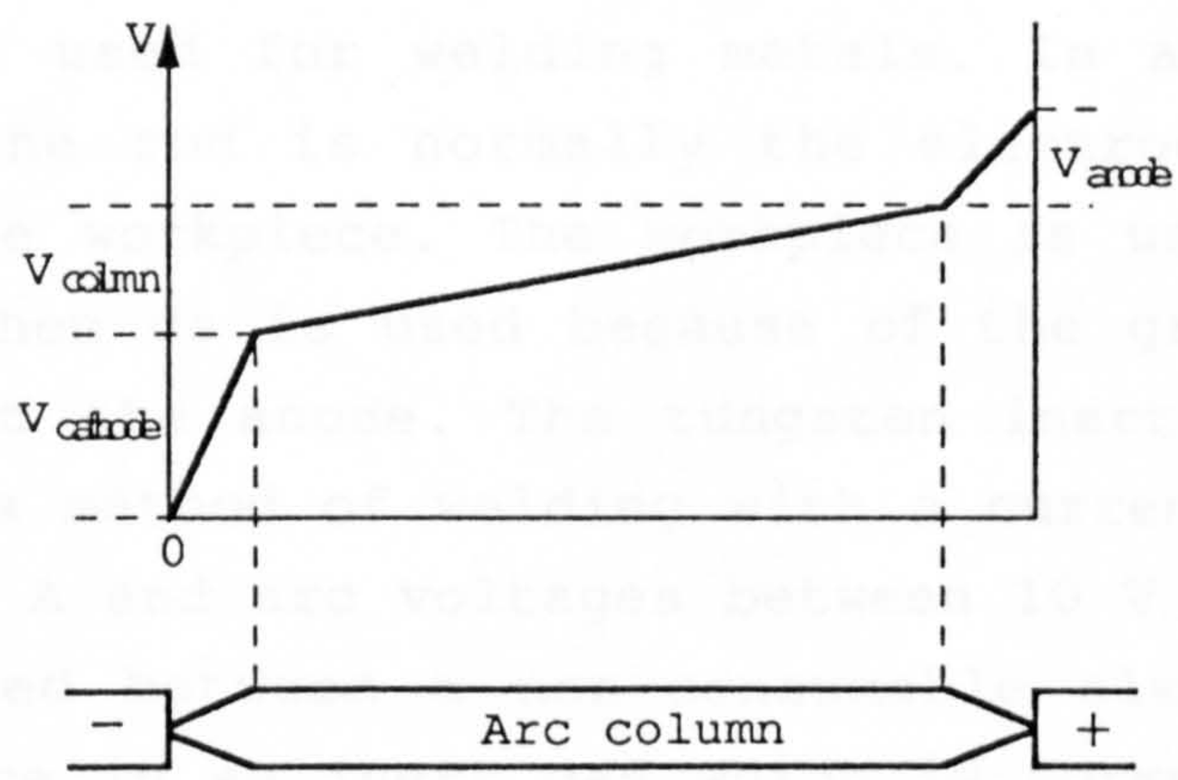

Fig.2.8 Voltage distribution along an arc discharge.

electrode regions. Arcs and glow discharges are not completely separable and it is possible that a discharge may operate with arc roots but retain its high voltage glow column or it may have an arc column with glow roots (Harry and Evans 1988, Guile 1971). Electric arcs and glows have been extensively discussed in several publications such as Edels 1961, Papoular 1965, Nasser 1971, Cobine 1958, Somerville 1959, von Engel 1965, Hoyaux 1968, Howatson 1976 and Hirsh et al 1978.

The high temperature (≈6000 K) of an arc at atmospheric pressure is used for welding metals. In arc welding processes the rod is normally the electrode and the plate is the workpiece. The workpiece is usually made the anode when dc is used because of the greater heat developed at the anode. The tungsten inert gas (TIG) process is a method of welding with a current range of 10 A to 500 A and arc voltages between 10 V - 15 V. It is maintained between a non-consumable electrode and the workpiece in an inert gas which is normally argon, flowing through a ceramic nozzle surrounding the electrode (Fig. 2.9). The arc melts the workpiece and forms a pool of molten metal to which the filler wire may be added, thus providing the weld. Contamination of the weld-pool and electrode by atmospheric oxygen or nitrogen is prevented by the inert gas shroud. The zone of greatest heat is concentrated in the workpiece so that penetration is deep and the weld-pool is narrow (Lancaster 1986). Each size and type of electrode has a maximum and minimum current carrying capacity. Table 2.3 gives a general guide to the approximate current range for different electrode diameters.

2.2.1 The Cathode

The mechanisms of electron emission from the cathode of a glow discharge are by secondary emission through ion bombardment and by photoelectric emission through radiation from the discharge plasma.

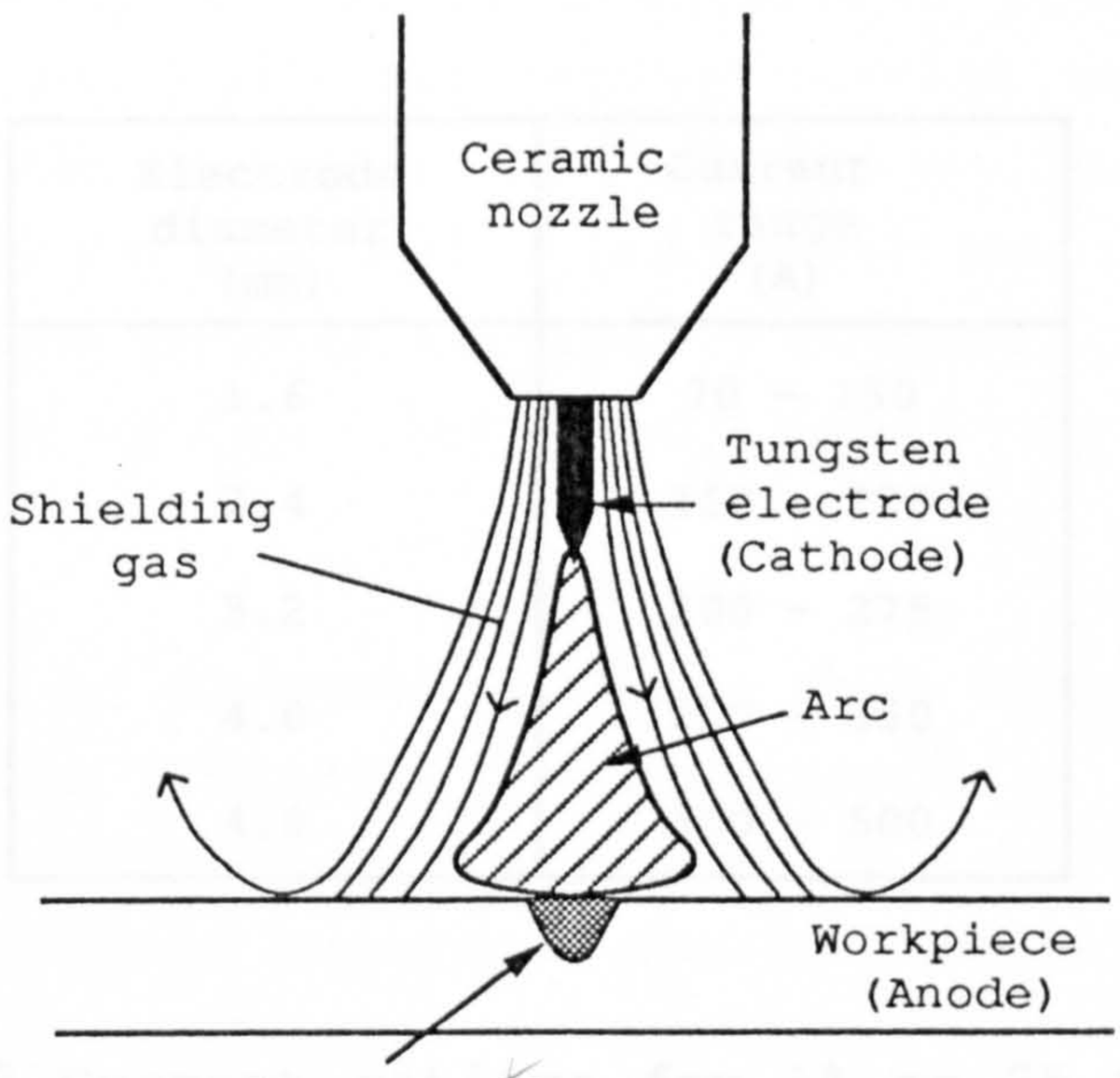

Fig.2.9 Tungsten inert gas welding arc with a dc electrode negative connection.

Electrode diameter (mm)	Current range (A)
1.6	70 - 150
2.4	150 - 225
3.2	200 - 275
4.0	250 - 350
4.8	300 - 500

Table 2.3 Current ratings for 1% or 2% thoriated tungsten electrodes using argon shielding gas and dc electrode negative (Cary 1979).

These necessitate the high cathode fall voltage of a glow discharge of about 300 V which depends mainly on a combination of the gas type and cathode material, varying little with the pressure, the electrode separation and the discharge current. Table 2.4 summarises the approximate values of the normal cathode fall voltage for different combinations of electrode and gas. The current density at the cathode of a glow discharge is proportional to the gas pressure and is 1 Amm^{-2} - 10 Amm^{-2} in air at atmospheric pressure and remains constant with increasing current at a given pressure if the cathode surface is not completely covered by the cathode spot. Increasing the current so that the cathode becomes completely covered, causes the current density to increase until an arc is established.

The mechanisms of electron emission from the cathode of an arc are more efficient than those for a glow. The electrons are normally emitted by a combination of thermionic and field emission. The cathode fall voltage is therefore low typically of the order of 10 V (Table 2.5). The cathode materials used for electric arcs can be described as either thermionic such as tungsten and carbon or cold-cathode materials such as copper and iron. Some measured values of fall voltages are shown in Table 2.5. The cathode fall voltage of arcs has been shown to increase at low currents of the order of 3 A or less which causes an increase in the arc voltage (Bauer and Schulz 1954, Busz-Peuckert and Finkelnburg 1956, Goldman 1966); this may be of significance to the initial stages of arc initiation when the current is still low and a higher arc voltage will be more difficult to sustain.

The mechanisms of electron emission from the two types of cathode are different. When cathodes are of refractory materials such as tungsten with boiling points of 4000 K or higher, thermionic emission is

Cathode material	Cathode fall voltage (V)						
	Air	Ar	H_2	N_2	O_2	He	CO_2
Al	229	100	170	180	311	140	-
Ag	280	130	216	150	-	162	-
Cu	375	130	214	208	-	177	460
Fe	269	165	250	215	290	150	-
Pt	277	131	276	216	364	165	475
Zn	277	119	184	216	354	143	410
K	180	-	-	170	-	59	460
Ni	226	-	-	200	-	160	-

Table 2.4 Glow discharge cathode fall voltages (Thomson et al 1933 and von Engel et al 1934).

Electrode material	Current (A)	Cathode fall (V)	Anode fall (V)	Reference
C	up to 20	9 - 11	11 - 12	von Engel et al (1934)
C	-	10	20	Mason (1937)
C	-	10	-	Finkelnburg (1948)
Cu	up to 20	8 - 9	2 - 6	von Engel et al (1934)
Cu	up to 6	16	-	Kesaev (1965)
Fe	up to 300	5 - 12	2 - 10	von Engel et al (1934)
Fe	up to 6	15.1	-	Kesaev (1965)
W	up to 6	16.1	-	Kesaev (1965)

Table 2.5 Measured arc cathode and anode fall voltages in air at atmospheric pressure (Knight 1984).

responsible for producing sufficient electrons to supply the arc current. The current density of 10^6 Am^{-2} - 10^8 Am^{-2} of the electrons emitted from the cathode is given by the Richardson-Dushman equation (Richardson 1921, Dushman 1923):

$$J = A\ T^2\ e^{-\left(\frac{e\ \varnothing}{k\ T}\right)}$$

the constant A has a value of about 6×10^5 $Am^{-2}K^{-2}$ for most metals, $\varnothing$ is the thermionic work function of the cathode surface, e is the charge on an electron and k is Boltzmann's constant. T is the surface temperature in Kelvin. If cathode materials with low boiling points (cold-cathode) such as copper (≈2600 K) are used the cathode current densities are normally higher than 10^{10} Am^{-2} and the cathode spot moves over the cathode surface (Guile 1971). The movement of the cathode spot is of significance to arc ignition from cold when the cathode has not yet reached a thermionic emission temperature, and will be discussed in section 2.2.5. The main mechanism of electron emission for non-thermionic cathodes may be field emission. The characteristics of the two types of electron emission have been extensively reviewed by Guile (1971) and are summarised in Table 2.6.

2.2.2 The Anode

The anode has a fall voltage across a very thin region (≈10^{-5} m) near its surface due to a negative space-charge owing to the high concentration of electrons (Cobine 1958, Somerville 1959). The anode fall voltage in an arc is relatively small, generally in the range of 1 V - 10 V for metallic anodes and 10 V - 20 V for carbon anodes and it depends on the energy required for electrons to ionise the anode vapour atoms (Lancaster 1986). The arc anode generally attains higher temperatures than the cathode (Table 2.7) and this is used advantageously in welding. It is heated by

Thermionic cathodes	Non-thermionic cathodes
Operate at high temperatures in excess of 3.5×10^3 K	Operate at a wide range of temperatures, less than 3×10^3 K
Low current density ($10-100$ Amm^{-2})	High current density (10^4-10^5 Amm^{-2} or higher)
Slow moving or fixed cathode spot	Rapidly moving cathode spot

Table 2.6 Characteristics of emission processes at an arc cathode (Guile 1971).

Electrode material	Gas	Current (A)	Cathode temperature ($\times 10^3$ K)	Anode temperature ($\times 10^3$ K)
Al	Air	9	3.4	3.4
C	Air	2 - 12	3.5	4.2
C	N_2	4 - 10	3.5	4.0
Cu	Air, N_2	10 - 20	2.2	2.4
Fe	Air, N_2	4 - 17	2.4	2.6
Mg	Air	< 10	3.0	3.0
Ni	Air, N_2	4 - 20	2.37	2.45
W	Air	2 - 4	3.0	4.25
Zn	Air	2	2.35	2.35

Table 2.7 Arc cathode and anode temperatures at atmospheric pressure (von Engel et al 1934).

bombardment of its surface by electrons which are accelerated in the electric field of the anode fall region and heat transfer by thermal conduction from the arc. The high temperature of the anode may not be essential for the operation of the arc, and investigations have shown that the arc may be operated with a water cooled anode in which case no anode material was found in the arc (Cobine 1958); this may also imply that arc initiation may not be affected by the anode temperature unlike the cathode which should reach a high enough temperature to establish a thermally stable cathode spot.

2.2.3 The Positive Column

The discharge column has a lower voltage gradient and current density than the cathode and anode fall regions. The type of gas used affects the characteristics of the column.

The positive column of a glow discharge is dominated by field ionisation rather than thermal ionisation. The voltage gradient along the positive column of a glow discharge in air at atmospheric pressure decreases from 145 Vmm^{-1} at 0.01 A to 9 Vmm^{-1} at 0.5 A and the current density increases from 0.3 Amm^{-2} at 0.02 A to 0.55 Amm^{-2} at 0.1 A (Gambling and Edels 1954). It is possible to maintain a stable glow discharge at pressures up to several atmospheres, but there is a tendency for a glow to change into an arc for pressures above about 14 mb (Howatson 1976).

A free-burning arc column at atmospheric pressure is in thermal equilibrium; its electrical conductivity is maintained by thermal ionisation and it has a constant electric field of the order of 1 Vmm^{-1} for long arcs in the range 50 mm - 100 mm with currents of 10^2 A - 10^4 A (King 1961, Lancaster 1986). The thermal ionisation within the arc column is caused by the high gas

temperature, which in turn is established and maintained by the energy given up by the ions and electrons in collision with the gas particles. The energy of the ions and electrons is obtained directly from the electric field. The maintenance of the arc column is by thermal ionisation, but this is only an intermediate process by which electrical energy is converted into heat (Cobine 1958). The thermal characteristics of the arc column are governed by the transport properties such as thermal conductivity of the gas used.

Monatomic gases like argon and helium ionise to give:

$$Ar \rightarrow Ar^{+} + e$$

but polyatomic gases such as nitrogen and oxygen undergo dissociation into atoms before ionisation:

$$N_2 \rightarrow 2N \qquad \text{at dissociation}$$

$$2N \rightarrow 2N^{+} + 2e \qquad \text{at ionisation}$$

which increases the energy required for ionisation. An arc can normally be initiated more easily in a monatomic gas due to the lower total ionisation energy required. An arc operating in a diatomic gas has a higher voltage than an arc of equal length in a monatomic gas due to the higher column voltage gradient (Fig. 2.10). Discharges in electro-negative gases such as oxygen require an even higher energy for ionisation due to the loss of electrons from the column by attachment to neutral atoms or molecules to form negative ions, resulting in a higher column voltage gradient. Some monatomic gases such as helium with an ionisation potential of 24.58 eV require a higher energy for ionisation than some diatomic gases such as nitrogen and oxygen resulting in a higher column voltage gradient (Fig. 2.10) and consequently a higher

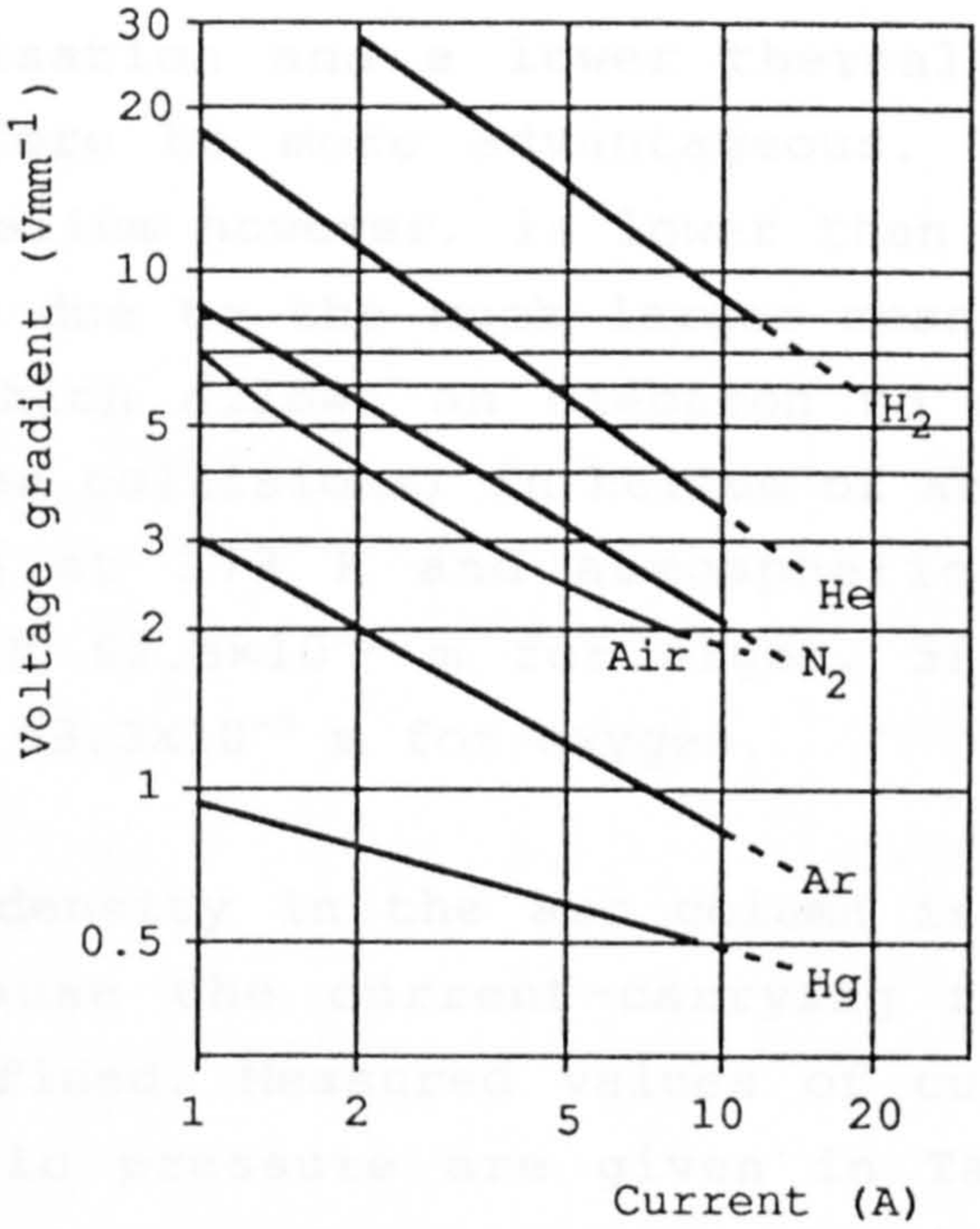

Fig.2.10 Arc column voltage gradient as function of current (Suits 1939).

arc voltage. The thermal conductivity (which affects the heat transfer from the column to its boundaries) of helium of about 0.42 $Wm^{-1}K^{-1}$ at 1273 K and atmospheric pressure is much higher than that for argon 0.05 $Wm^{-1}K^{-1}$, nitrogen 0.07 $Wm^{-1}K^{-1}$ and oxygen 0.09 $Wm^{-1}K^{-1}$ hence a helium discharge loses heat more quickly and the column voltage gradient is further increased. For the rapid establishment of a steady-state, heat losses from the column should be minimised to increase the thermal ionisation and a lower thermal conductivity would therefore be more advantageous. The breakdown voltage of helium however, is lower than that of argon which may be due to the much larger mean free path of electrons (which allows an electron to gain a higher energy between collisions) in helium of about 173.6×10^{-9} m at 273 K and atmospheric pressure as compared with 62.6×10^{-9} m for argon, 58.8×10^{-9} m for nitrogen and 63.3×10^{-9} m for oxygen.

The current density in the arc column is difficult to measure because the current-carrying region is not precisely defined. Measured values of current density at atmospheric pressure are given in Table 2.8. The diameter of low current arcs up to 10 A in nitrogen has been found to be directly proportional to the square root of the arc current. The radius of the arc column has been measured to be constant between 20A and 200A (King 1954).

2.2.4 The Glow to Arc Transition

The following observations are normally made when there is a transition from a glow discharge to an arc discharge.

a) The cathode glow which is characterised by a large diameter on the surface of the cathode, changes to a number of intensely bright arc spots of high current density (Guile 1971).

Current density (Amm^{-2})	Gas	Reference
0.06	Nitrogen	Suits (1939)
0.32	Argon	Suits (1939)
1.0	Air	Pfender (1978)
2.0	Air	King (1954)

Table 2.8 Measured values of current density in the arc column at atmospheric pressure (Knight 1984).

b) The diameter of the positive column of the glow discharge which is normally larger than the column of the arc discharge at a constant power input decreases, resulting in an increase in the intensity of the light emitted from the column and also the average gas temperature.

c) A change from the high voltage, low current condition of the glow discharge to the lower voltage, higher current condition of the arc discharge occurs. Rapid fluctuations between these two states occur until either the external circuit or the discharge conditions allow one state to become stable.

The cause of the transitions can be divided into two categories; electrode dominated processes and column dominated processes as discussed below.

2.2.4.1 Electrode dominated processes

The factors affecting the glow to arc transition when using thermionic cathodes are mainly those affecting the heat transfer at the cathode surface such as gas, gas pressure, gas flow rate and cathode size, shape and material. The transition may take place continuously or discontinuously and the abnormal glow phase may or may not be present.

The glow to arc transition for non-thermionic cathodes does not depend on raising the cathode temperature to emit more electrons. The transition is almost always discontinuous and the abnormal glow phase is not present. The main mechanism for the glow to arc transition occurring with non-thermionic cathodes appears to depend on the presence of insulating particles on the cathode surface (Hancox 1960, Maskrey and Dugdale 1962, Holliday and Isaacs 1966). The insulating particles become charged by positive ion bombardment to a high potential which causes breakdown

of the insulating particles and a burst of vapour above the cathode surface is produced. The increased electrical conductivity due to the vapour causes a local increase in current density which increases the amount of vapour produced and the high current density arc cathode spot is established. Polishing the metal surface and heat treatment to remove the surface contaminants may prevent arcing (Maskrey and Dugdale 1962), and the impurity content of the cathode was found to affect the arcing rate (Fan 1939, Holliday and Isaacs 1966). A review of the non-thermionic glow to arc transition is given by Lutz (1974).

2.2.4.2 Column dominated processes

Glow to arc transitions can occur even when the electrodes are carefully polished and heat treated to remove the contaminants. The glow to arc transition may be caused by an increase in gas pressure or discharge current and can be attributed to heating of the discharge column. Thermal ionisation is dominant in an arc column whereas in a glow column, field ionisation is dominant (section 2.2.3).

Investigations on steady-state discharges in hydrogen using a 3 mm gap at atmospheric pressure, have shown that increasing the current up to 1 A causes the column diameter to increase. At about 1 A increase in current caused the column diameter to gradually decrease and produce an increased luminosity at the centre. At about 1.5 A a critical current was reached when a sudden contraction occurred, resulting in the formation of a bright red concentrated column with a diameter of the order of 0.3 mm, which was shown to occur simultaneously with a sudden discontinuity in the column voltage gradient and current density. Further increase in current above 1.5 A resulted in an increase in both luminosity and diameter of this concentrated column (Gambling and Edels 1956).

The column constriction coincided with a minimum in the measured excitation temperatures of about 3000 K and 4000 K. These temperatures are close to the temperature (≈3500 K) at which the thermal conductivity of hydrogen reaches its peak and then begins to decrease (Edels 1961). The decrease in thermal conductivity may have caused the increase in temperature resulting in an increase in thermal ionisation leading to a constriction into an arc column. The sudden transition from the glow column to an arc column therefore may have been due to a critical gas temperature (≈3500 K). Similar work carried out by Price et al (1955) showed that despite the formation of the constricted column, the cathode still possessed the normal negative glow and cathode dark space characteristic of a glow discharge, showing that the column constriction is not due to any transitions at the cathode and is dependent only on the thermal conditions in the column.

For large electrode separations (>50 mm) in which the positive column is not influenced by electrode effects, the voltage gradient of a free-burning discharge column in air or nitrogen at atmospheric pressure has been measured over a current range of 10^{-4} A - 10^{4} A and the results showed that no sudden transitions in the voltage gradient occurred; the glow column gradually changed to an arc column as the current was increased (King 1961).

2.2.5 Arc Stability

Two factors control the stability of an arc discharge; external stability where the interaction of the arc with its supply circuit is important and the internal stability where the conditions within the discharge such as decay and reformation of cathode spots and the positive column have an effect. Instabilities caused by these should be eliminated to achieve reliable arc ignition.

The external stability of an electric arc requires the sum of the gradients of the arc characteristic and the gradient of the load line to be positive (Kaufmann 1900),

i.e. $dv/di + R > 0$

where dv/di = dynamic resistance of the arc

R = stabilising resistance.

The power supply load line and arc characteristic are illustrated in Fig. 2.11. The power supply load line intersects the discharge characteristic at points A and B such that at the steady-state

$$V_d = V_{OC} - IR$$

Referring to Fig. 2.11 point A is stable because an increase in the dc current by for example some transient condition, decreases the voltage across the discharge. This increases the difference between the dc applied voltage and the discharge voltage (because of inductance in the circuit) and therefore the current decreases; as a result point A is restored. When the dc current decreases the voltage across the discharge becomes larger. This decreases the difference between the dc applied voltage and the discharge voltage, and therefore the current will increase and point A is again restored. Point B is unstable because an increase in current will make the discharge operate at point A and a decrease in current will extinguish the discharge. In power supplies used for welding it is normal practice to improve ignition and increase the stability of the arc by using a value of series impedance greater than that required by the Kaufmann criterion. DC welding arcs are normally operated with a ratio of open circuit voltage to arc voltage of up to 4:1.

Fig.2.11 Interaction of the characteristics of the arc and the power source for arc stability.

The Kaufmann criterion may be satisfied but the lifetime of arcs may be finite depending on the maintenance of the cathode spot and the column. The stability of short arcs (≈5 mm) has been shown to be related to the phenomena associated with the extinction and reformation of the cathode spot on cold cathodes and the arc life was found to vary with the electrode material and to increase with the arc current (Cobine and Farrall 1960, Kesaev 1963 I and II).

A thermionic cathode in the initial stages of arc ignition from cold may have a temperature which is too low for thermionic emission to take place and may be non-thermionic (Table 2.6). The cathode spot on a non-thermionic cathode after initiation from cold has been shown to move from one position to another in about 10^{-7} s (Froome 1947). The cathode spot on a cold TIG arc cathode moves around rapidly similar to that on a non-thermionic cathode and this may cause unreliable arc initiation.

The arc may be extinguished in very short times (about 10^{-9} s) due to the disruption of the cathode fall region which is not in thermal equilibrium (Cassie 1958). It may take 10^{-5} s - 5×10^{-5} s to establish the cathode fall region (Betz and Karrer 1937, Froome 1948).

Investigations on the re-ignition of arcs show the significance of the cathode temperature on arc ignition from cold. A clear distinction in the re-ignition mechanisms exist for thermionic cathodes and cold-cathodes. When a cold-cathode arc is interrupted the positive ion space-charge can disappear in less than 10^{-6} s and be replaced by a low conductivity neutral cathode region but the recovery process in the column occurs more slowly resulting in spark re-ignition owing to the spark breakdown of the neutral cathode region. When arcs with thermionic cathodes are interrupted a neutral cathode region is not produced

because the high temperature of the cathode results in an electron cloud around the cathode surface and the total conductivity remains finite which causes thermal re-ignition because breakdown of a neutral region is not required (Crawford and Edels 1960, Edels and Whittaker 1962).

Methods of improving the stability of high current electric arcs include the introduction of compounds of low ionisation potential into the arc stream with cored, coated or impregnated electrodes.

The addition of either thoria (thorium oxide) or zirconia (zirconium oxide) to pure tungsten increases the electron emission thus giving better arc initiation and improved arc stability particularly at low currents. The addition of lanthanum oxide or yttrium oxide to the tungsten cathode produces even better arc ignition and stability (Persits et al 1979, Ushio and Matsuda 1986). Alloyed electrodes give a longer life than plain tungsten electrodes, carry higher currents and are less likely to give tungsten inclusions in the weld. The end of the electrode is normally tapered to a sharp point to concentrate the cathode spot on the end of the electrode and thus provide a more stable arc (Fig. 2.9). The angle of the taper influences certain characteristics of a TIG arc such as the V-I characteristic, distribution of thermal flux and pressure on the anode spot resulting in a variation in weld width and depth of penetration (Kohei 1968, Savage 1965, Chihoski 1970, Erokhin 1971). The angle also has an influence on the arc temperature, the electrical conductivity, its transverse dimensions and consequently the weld width and depth of penetration (Mechev et al 1976).

A further source of instability is due to variations occurring in the arc column caused by for example gas flow. This causes the arc to take up a continually

changing shape and as a result the arc voltage varies with the length of the column causing fluctuations in the current which may cause extinction. After extinction the column may remain highly ionised and conducting for several hundred microseconds. The re-ignition voltage depends on the time it is applied after arc interruption. The variation of the re-ignition voltage with time for a 20 A arc in different gases using tungsten electrodes for a gap length of 2 mm at a pressure of 0.14 b has been measured (Kelham 1954). The gases recovered their electric strength in the order oxygen, nitrogen, air and argon with re-ignition voltages of 6.5 kV, 5.2 kV, 5.0 kV and 2.8 kV respectively at 8 ms after interruption. The rate of deionisation of the column depended on factors such as recombination and diffusion coefficients and thermal properties. The mean recovery rates decreased as the arc length increased which was attributed to the reduced effect of the electrode surfaces in cooling and deionising the column. The processes at the column of a short arc (5 mm or less) are influenced by the electrodes but where long arcs are considered the deionisation phenomena at the column are dominant (Slepian 1928 and 1930). The effect of instability in the column on arc extinction has more effect when the column is still cold and field ionisation is dominant such as in the initial stages of arc ignition from cold when there is little thermal ionisation. This is because in a cold (field dominated) arc column, delays due to thermal inertia are insignificant.

2.2.6 AC Discharges

The characteristic of an ac discharge at frequencies of lower than about 100 Hz, is similar to the dc discharge having the same current, except that breakdown must take place at the beginning of each half-cycle of current. The discharge in a resistive circuit in which

current and voltage are in phase, deionises after a current zero before the voltage has time to build up in the reverse direction and the discharge extinguishes at each current zero. The breakdown voltage after each current zero has a transient component (re-ignition voltage) due to the discontinuity in current owing to the extinction. The reignition voltage depends on the rate at which the gas deionises and the size and material of the electrodes because of their effect on cooling the discharge and the secondary ionisation coefficient (section 2.2.5).

The relation between current and voltage in each half-cycle following breakdown at low frequencies, is similar to that of the static characteristic because the discharge reaches equilibrium in times much less than one half-period. The discharge will not have time to reach equilibrium during each half-cycle as the frequency increases, so that for increasing current the degree of ionisation and hence the discharge impedance will be appropriate to a smaller current than actually flows. This results in a higher voltage than for a dc discharge with the same current, and for a decreasing current the voltage will be lower than for a dc discharge of equal current, and therefore a hysteresis results (Fig. 2.12).

The frequency at which the degree of ionisation in the discharge remains almost constant depends on the current and the gap length. If the frequency is such that the degree of ionisation and hence the conductivity remain constant, the discharge will behave as a fixed resistance and its characteristic loses its negative slope and becomes almost linear (Fig. 2.12).

The re-ignition voltage of ac discharges in gaps of 0.025 mm - 0.625 mm at atmospheric pressure has been measured in the frequency range 0.15 MHz - 1 MHz and current range of 0.3 A - 0.8 A (Schwab and Hotz 1970).

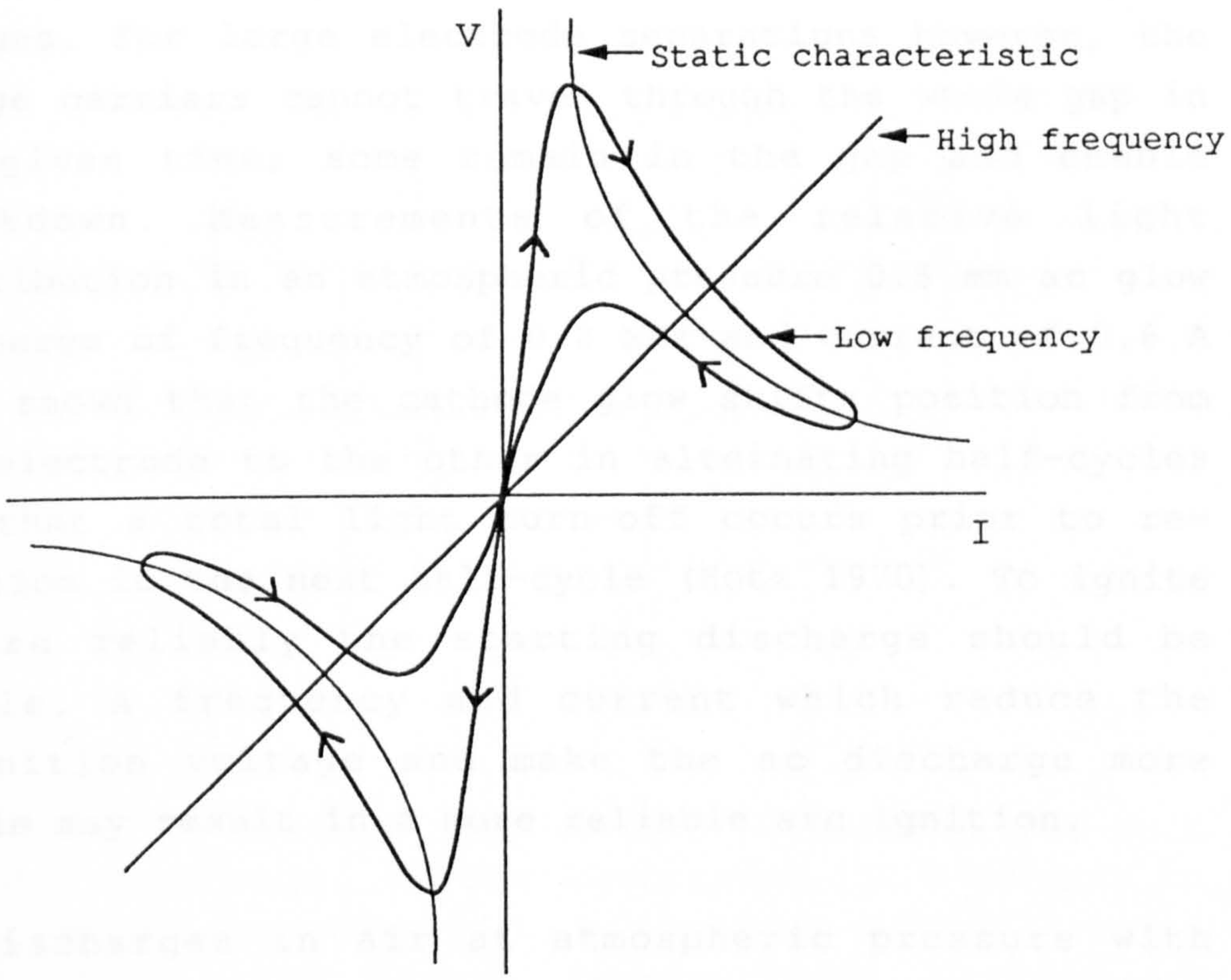

Fig.2.12 Static and dynamic discharge characteristics.

The re-ignition voltage at constant frequency increased with electrode separation up to a maximum value after which it suddenly decreased and stayed low for a further increase in the gap length. It was shown that for each frequency there was a critical gap length at which reignition was not required. The explanation given for this effect was that at relatively small electrode separations all charge carriers could be removed from the discharge gap before re-ignition and breakdown take place without support from space charges. For large electrode separations however, the charge carriers cannot travel through the whole gap in the given time; some remain in the gap and enable breakdown. Measurements of the relative light distribution in an atmospheric pressure 0.5 mm ac glow discharge of frequency of 0.2 MHz and current of 0.6 A have shown that the cathode glow shifts position from one electrode to the other in alternating half-cycles and that a total light turn-off occurs prior to re-ignition in the next half-cycle (Hotz 1970). To ignite an arc reliably the starting discharge should be stable. A frequency and current which reduce the reignition voltage and make the ac discharge more stable may result in a more reliable arc ignition.

AC discharges in air at atmospheric pressure with electrode separations up to 2.5 mm and a frequency of 1 MHz - 30 MHz with currents of 0.05 A - 0.8 A operated as ac glow and with currents of 0.8 A - 2 A operated as ac arc discharges. The discharge voltage was high (≥275 V) for glows and low (≥30 V) for arcs (Schwab 1967, 1971). Fig. 2.13 shows typical waveforms of voltage and current for a 1 MHz arc discharge. Little work has been carried out on ignition of arcs using ac discharges. It is not known whether a minimum discharge current, voltage or power are needed, and whether the ac starting discharge should be a glow or an arc.

The re-ignition voltage at constant frequency increased with electrode separation up to a maximum value after which it suddenly decreased and stayed low for a further increase in the gap length. It was shown that for each frequency there was a critical gap length at which reignition was not required. The explanation given for this effect was that at relatively small electrode separations all charge carriers could be removed from the discharge gap before re-ignition and breakdown take place without support from space charges. For large electrode separations however, the charge carriers cannot travel through the whole gap in the given time; some remain in the gap and enable breakdown. Measurements of the relative light distribution in an atmospheric pressure 0.5 mm ac glow discharge of frequency of 0.2 MHz and current of 0.6 A have shown that the cathode glow shifts position from one electrode to the other in alternating half-cycles and that a total light turn-off occurs prior to re-ignition in the next half-cycle (Hotz 1970). To ignite an arc reliably the starting discharge should be stable. A frequency and current which reduce the reignition voltage and make the ac discharge more stable may result in a more reliable arc ignition.

AC discharges in air at atmospheric pressure with electrode separations up to 2.5 mm and a frequency of 1 MHz - 30 MHz with currents of 0.05 A - 0.8 A operated as ac glow and with currents of 0.8 A - 2 A operated as ac arc discharges. The discharge voltage was high (≥275 V) for glows and low (≥30 V) for arcs (Schwab 1967, 1971). Fig. 2.13 shows typical waveforms of voltage and current for a 1 MHz arc discharge. Little work has been carried out on ignition of arcs using ac discharges. It is not known whether a minimum discharge current, voltage or power are needed, and whether the ac starting discharge should be a glow or an arc.

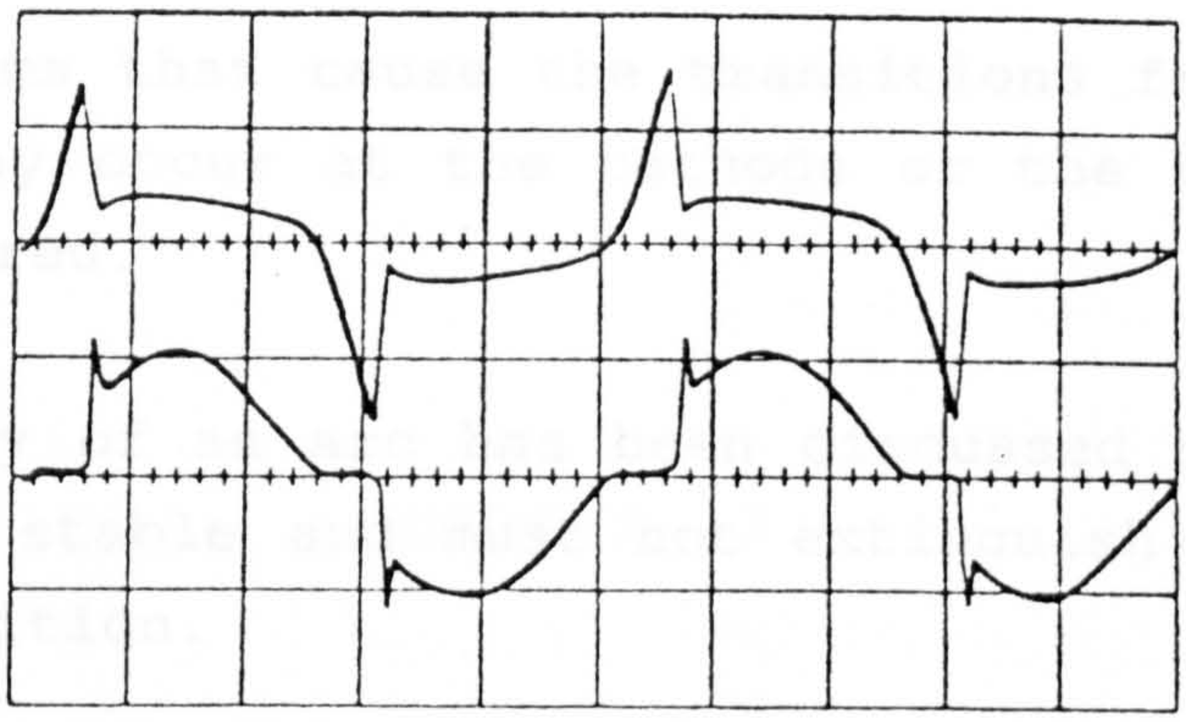

Fig.2.13 Voltage and current waveforms for a 1 MHz discharge. Carbon electrodes, 0.7 mm gap in air at atmospheric pressure. Upper trace: Voltage, 200 V/div. Lower trace: Current, 1 A/div. (Schwab 1971).

2.2.7 Summary

Breakdown of arc gaps using dc and ac voltages has been reviewed; reliable breakdown is initially needed for non-contact arc ignition to be achieved.

The different regions and mechanisms of arc and glow discharges using dc or ac supplies have been discussed. These are relevant to non-contact arc initiation for both the starting discharge and the main arc.

The mechanisms that cause the transitions from glow to arc which may occur at the cathode or the column have been considered.

The stability of an arc has been discussed because the arc must be stable and must not extinguish to achieve reliable ignition.

CHAPTER 3

A REVIEW OF METHODS FOR NON-CONTACT ARC IGNITION

3.0 A REVIEW OF METHODS FOR NON-CONTACT ARC IGNITION

Touch starting is not desirable for tungsten inert gas (TIG) welding arcs. It is not suitable for mechanised equipment, the electrodes may stick and become difficult to separate, the tungsten cathode can become contaminated and increased electrode erosion may occur. Non-contact arc ignition in which an external high-voltage power source is used to break down and ionise the arc gap and allow the main arc to establish is necessary. A further advantage is that the arc length may be set in advance which is useful for automatic welding equipment.

Arc welding power sources normally have an output voltage of less than 100 V to conform to safety regulations such as the British Standards (B.S. 638). This voltage is too low to break down the arc gap. A voltage of higher than about 3 kV is required to break down a 3 mm TIG arc gap. A separate high-voltage source is therefore coupled to the output of the main power supply to break down the gap and provide a conducting path for the main current.

3.1 PHYSICAL PRINCIPLES OF ARC INITIATION

Arc initiation is a complex phenomenon involving the gas, electrodes (such as electrode shape, material and surface layers) and the electrical circuit. An arc becomes self-sustained when

i) the gas between the electrodes becomes ionised and

ii) the cathode emits sufficient electrons either thermionically as for example for a tungsten cathode which should reach a temperature of higher than about 3500 K, or by field emission for which the voltage gradient at the cathode should exceed 10^9 Vm^{-1} or a combination of both.

The voltage across the gap collapses suddenly from a

value close to the breakdown voltage in a time of the order of 10^{-8} s, after which a pronounced step may be in evidence and by about 10^{-6} s the voltage is only some tens of volts (Somerville 1959). After a time of the order of 10 μs the current density in the spark channels at atmospheric pressure has usually fallen from its initial value of about 10^9 Am^{-2} to about 3×10^7 Am^{-2}, and slowly decreasing with time to the value characteristic of the stable arc which may be as low as 10^5 Am^{-2}. Cavenor and Meyer (1969) have identified a number of phases in the development of the spark channel. A glow structure is first formed, a diffuse glow develops and a filamentary glow is then established, after which a transition to an arc phase takes place, all of which occur in less than 1 μs.

Arcs occurring in times shorter than 10^{-4} s are transient reactions and cannot involve thermal ionisation, because the durations are not long enough for thermal equilibrium to be established among electrons, positive ions and gas particles which takes a time of the order of 1 ms (Suits 1936). Short duration arcs have a much higher column voltage gradient than steady-state arcs because most of the ionisation in the column is by electron collisions or field ionisation (Cobine 1958).

An arc-like cathode fall is established in 1 μs, the rapidly changing transient phase of the cathode processes is very short, and there appears to be a quasi-stable state set up at the cathode similar to that in the channel (Somerville 1959). The initial rapid movement of the cathode spot in the first 1 μs from breakdown and rate of growth of current exclude the possibility of thermionic electron emission from the cathode, while the high current densities of greater than 10^{10} Am^{-2} observed, favour field emission (Froome 1948).

There appears to have been very little investigation of the initiation of welding arcs. It is not known whether the arc requires a sufficient voltage, current or power to be reliably established following spark breakdown. Romalo (1969) has considered the arc column theory to find the minimum required current (I_{min}) for an arc to become self-sustained. He assumed that the arc column was in thermal equilibrium and that it was a uniform resistive conductor between the cathode and anode. He then used the power supply load line and the static arc characteristic to derive an equation for I_{min}:

$$I_{min} > \frac{\pi K_{T_i}^2 \, l_0}{\eta \, u_0 \left(\frac{dK}{dT}\right)_T}$$

where K_{Ti} is the thermal conductivity of the gas at a temperature T_i, at which the thermal conductivity becomes significant (assumed to be about 6000 K), l_0 is the gap length, η is a coefficient accounting for thermal losses of the arc towards the electrodes and u_0 is the power supply open circuit voltage. A value of I_{min} of about 2.5 A for a 3 mm gap in nitrogen was calculated assuming an open circuit voltage of 80 V. This equation gives a value for I_{min} in argon of about 0.59 A.

The relation developed by Romalo may be inaccurate because:

i) the column is not yet thermally developed and therefore the column theory under thermal equilibrium may not be applicable.

ii) the electrode fall voltages may need to be taken into account because in short arcs of the order of 5 mm or less, they constitute a large proportion of the total arc voltage.

Pykal (1975) has used short duration (15 μs) ignition pulses to investigate the initiation of TIG welding

arcs. The measured value of I_{min} was 3 or 4 times greater than that found by Romalo. High speed Schlieren photographs of the arc at the initial stages of its formation indicated that it is necessary for an arc cathode fall region to establish before an arc can initiate and that the arc column and anode region are not as important.

The external ignition source in non-contact arc initiation from cold, causes spark breakdown and establishes the initial transitions; further transitions to the arc phase are sustained by the main power supply over much longer periods. The time to reach the steady-state may take minutes, during which slow processes such as convection and thermal conduction in the gas and in the electrodes take place (Somerville 1959). The effects of the energy exchange between the electrodes and gas upon the electrical conductivity indicates that cooling of the gas increases as the electrode separation is reduced and produces a relatively more rapid decay of free charge and electrical conductivity (Crawford and Edels 1960). Studies on the reignition of spark channels in short (1 mm - 5 mm) gaps in air at atmospheric pressure for tungsten and copper, have shown that the cooling effect was increased with larger electrodes (Churchill et al. 1961). Somerville (1959) assuming a semi-infinite metal with a plane surface which receives heat energy from a cathode spot over that surface at a rate of Q, shows that to reach a surface temperature T, the time (t) is given by: $t = \pi KS\rho T^2/4Q^2$, where K, S and ρ are the thermal conductivity, specific heat and density of the cathode respectively. It can be seen that t varies with the square of T and inversely with the square of Q. Therefore the cathode material which has specific values for K, S, ρ and T, and the rate of gain in thermal energy by the cathode determine the time taken to reach the steady-state.

3.2 EFFECT OF THE MAIN POWER SUPPLY ON ARC INITIATION

It is known that an arc is not always established despite spark breakdown of the arc gap. If a visible discharge is obtained in the gap, then breakdown has been achieved and failure to start the arc must be associated with the main power source which has not succeeded in maintaining conduction after the spark has collapsed. Therefore, for the arc to be established, the main power supply should have a rate of rise of current high enough to reach a minimum value of current (I_{min}) in the time that the ignition pulse exists.

Melton (1981) has investigated the increase in the main arc current by applying a short circuit load to a welding power supply. This was to provide consistent results and avoid the variations inevitable in striking an arc such as effects of electrode surface and shielding gas. The measurements gave the highest rate of current rise since the effect of the arc resistance was eliminated. A silicon-controlled rectifier switch was used to close the output of the welding power supply and the rise in current was measured using a low-inductance shunt and an oscilloscope with a bandwidth of 50 MHz. The results showed that for single-phase and three-phase supplies the average current increase over the first 3 ms was about 10^4 As^{-1} and was similar when using a transductor (magnetic) or thyristor converter for current control. Melton has also shown that the final current setting of the welding supply affected the rate of current rise. For a single-phase transductor-controlled welding supply, doubling the output current from 50 A to 100 A resulted in a corresponding increase in the rate of rise of current from 0.5×10^4 As^{-1} to 10^4 As^{-1}. This was found by Brown (1976) to affect arc ignition reliability where a minimum current setting of 100 A was required with a transductor-controlled welding supply to ensure arc

initiation from a dc spark. The ripple in the output voltage of the main power supply affected the rate of current rise since the higher output voltage caused a higher rate of rise of current. Ignition may therefore be more reliable if an attempt to ignite the arc is made when the output voltage is at its peak.

Needham (1969) has suggested the use of a non-inductive auxiliary power source connected in parallel with the main power supply to provide a high rate of rise of current of the order of 10^6 As^{-1}. The auxiliary power source which has a higher voltage and lower current can be designed to give about 10 A within 10 μs and lasting for 1 ms, to assist in igniting the arc and in maintaining conduction until the welding supply can take over. In the initial 10 μs or so the current from the auxiliary power source raises the temperature of the tungsten tip more rapidly and it prevents the tendency to erratic movement which occurs at low current if the cathode is not thermally established.

A further difficulty in arc initiation caused by the main power supply is that even if di/dt is high enough, arc extinction may occur. This is due to the underdamped oscillations in current superimposed on the main current, owing to the discharge of any effective capacitance in parallel with the main supply through the output leads during the initial current rise. This difficulty may be overcome by using an LCR network connected in parallel with the main supply to provide overdamping of the transients. Melton (1981) has shown that the supplementary current from an LCR network having a capacitance of 20 μF, a resistance of 12 Ω and an inductance of 500 μH exhibited a broad peak of current waveform at 4 A over 50 μs - 100 μs which covered the time at which the current from the welding supply passed through its minimum level. When this network was used the combined current no longer fell below 5 A. This combination enabled an arc to be

intiated under conditions which previously was impossible with the welding supply alone. Fig. 3.1 shows the main current waveforms before and after superimposing the current from the LCR network.

3.3 ARC INITIATION USING HIGH-FREQUENCY HIGH-VOLTAGE SPARKS

The most common method for non-contact initiation of TIG welding arcs is the use of high-frequency high-voltage generators to obtain hf sparks with a peak voltage of about 4 kV and frequency of about 2.5 MHz to break down and ionise the gap. Fig. 3.2 shows a basic circuit in which a high-voltage transformer charges the capacitor every half cycle up to the breakdown voltage of the spark-gap. When the spark-gap breaks down, the tuned circuit consisting of C_1 and the primary of the air core transformer (T_2), resonates and the transfer of electrical energy between the electric field of C_1 and the magnetic field of the primary creates a high-frequency oscillatory current in the circuit which is coupled into the welding line and superimposed on the welding current through the secondary of T_2. The instantaneous peak power of the spark-gap oscillator is several killowatts but the mean rating is only about 20 W.

Spark-gap oscillators are relatively safe because hf current does not penetrate the human body but tracks across the skin. Each hf spark has a duration of 5 μs - 10 μs and more than a thousand sparks may occur each second and several seconds may elapse before the arc strikes. There may be a train of 10-20 sparks for each half cycle of the 50 Hz supply with an average interval of 0.5 ms between consecutive sparks (Fig. 3.3). A duration of 10 ms of each spark will allow the main current from a typical welding supply with a rate of rise of current of 10^4 As^{-1}, to reach only 0.1 A, which may not be sufficient for the arc to maintain itself.

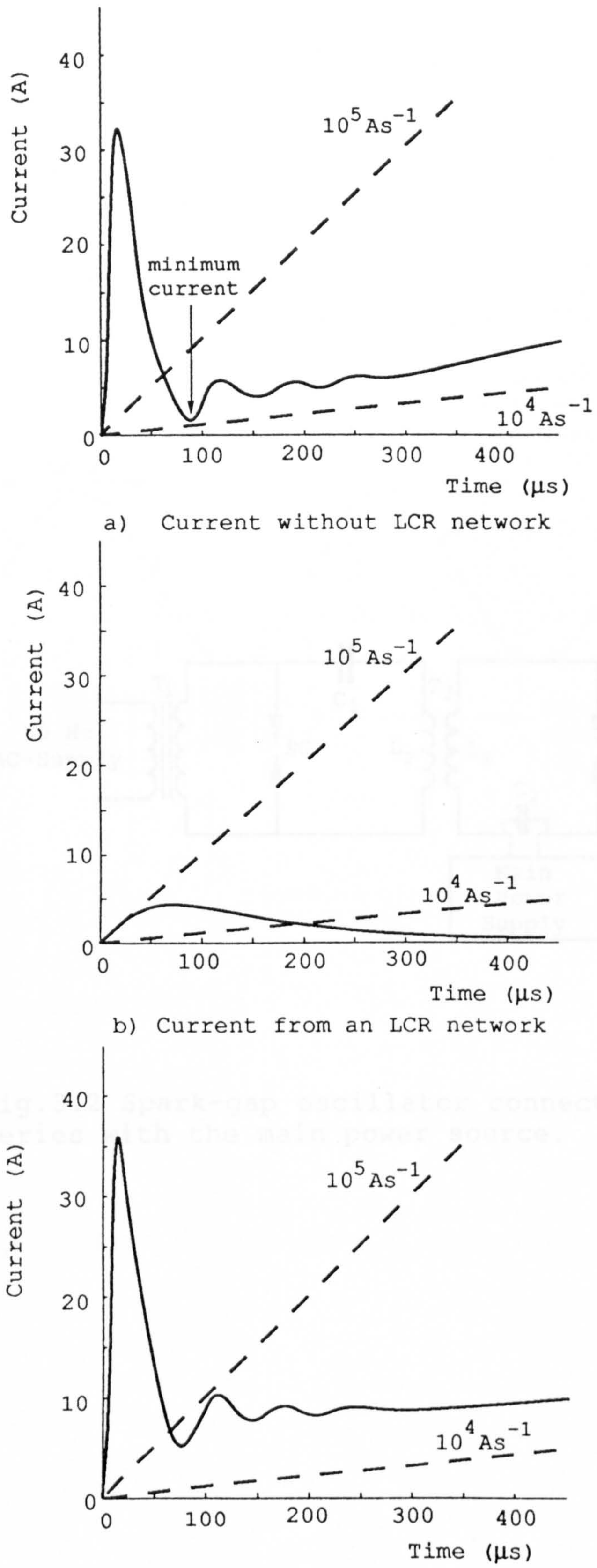

Fig.3.1 Main current waveforms before and after superimposing the current from an LCR network (Melton 1981).

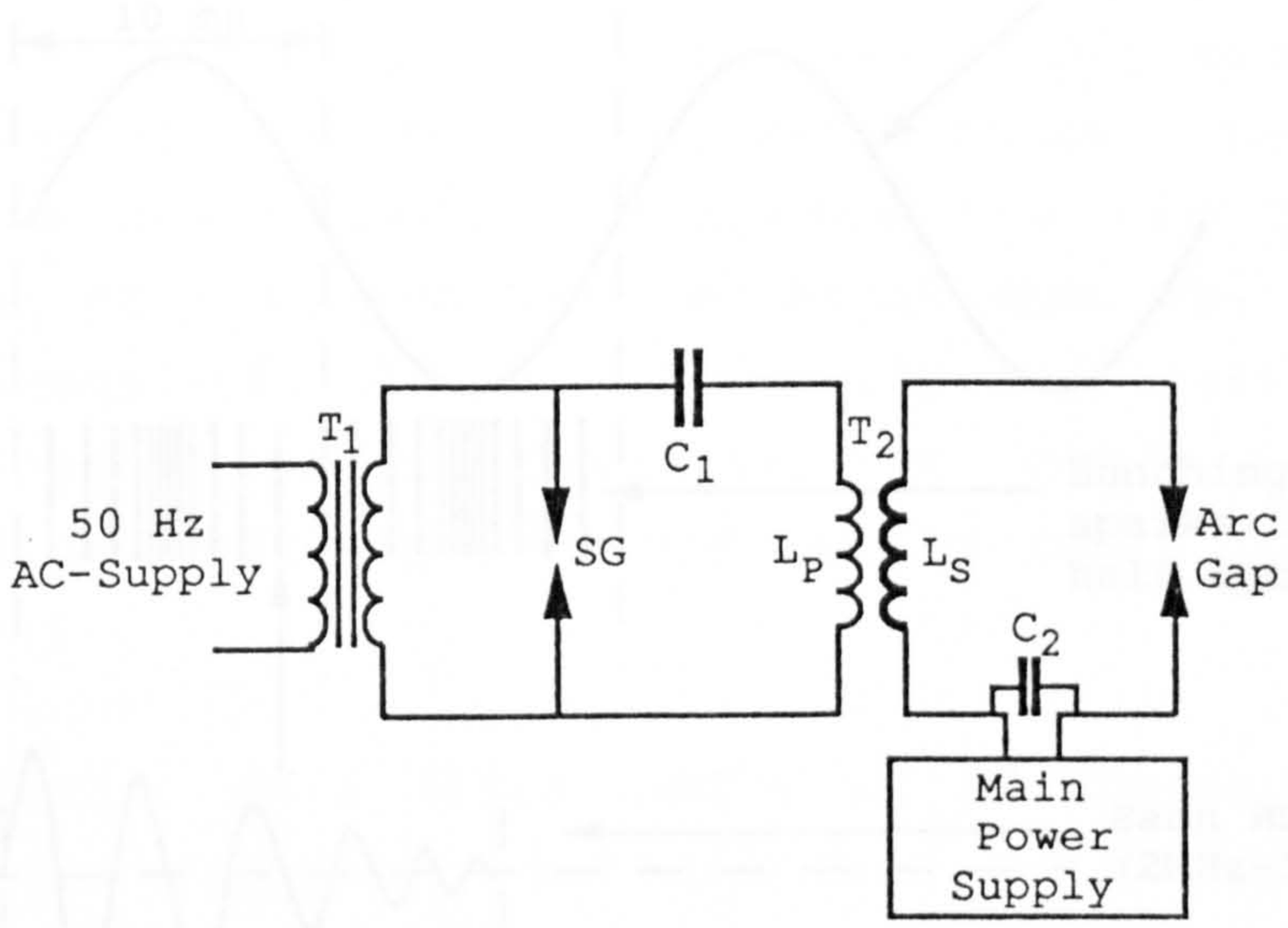

Fig.3.2 Spark-gap oscillator connected in series with the main power source.

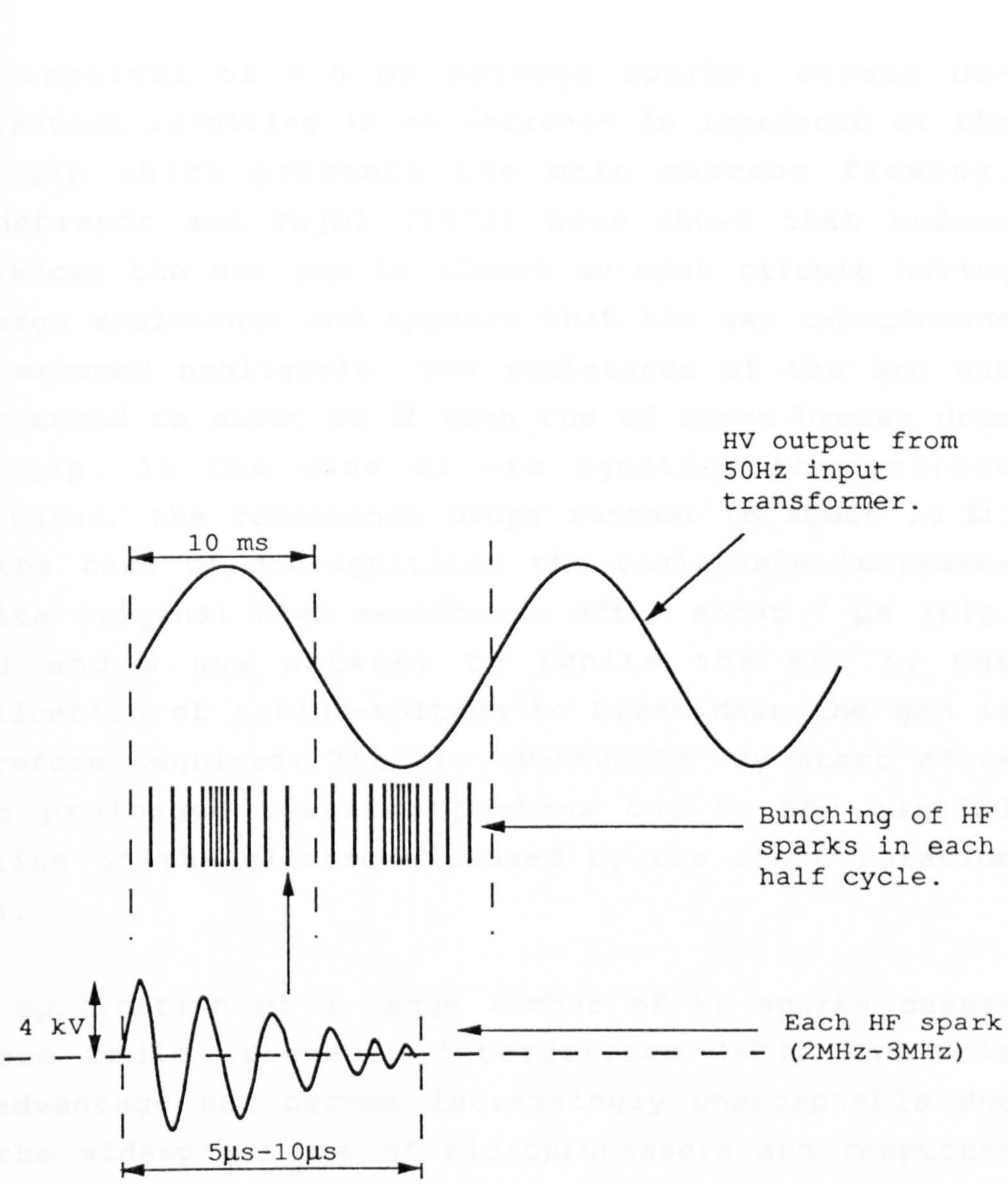

Fig.3.3 Typical output from a spark-gap oscillator.

The interval of 0.5 ms between sparks, causes de-ionisation resulting in an increase in impedance of the arc gap which prevents the main current flowing. Hildebrandt and Tajbl (1973) have shown that before breakdown the arc gap is almost an open circuit having a large resistance and appears that the gap capacitance was assumed negligible. The resistance of the arc gap is reduced to about 50 Ω when the hf spark breaks down the gap. In the case of arc ignition the current increases, the resistance drops further to about 10 Ω. In the case of non-ignititon the resistance increases to its original high resistance after about 7 μs (Fig. 3.4) and a new attempt to ignite the arc by the application of a high-voltage to break down the gap is therefore required. The arc eventually may start after such prolonged sparking perhaps due to the partial heating of the electrode caused by the short duration arcs.

The application of a large number of hf sparks causes severe radio frequency interference (RFI) and this disadvantage has become increasingly unacceptable due to the widespread use of microprocessors and computers in welding. This interference affects computers connected by transducers to the plates to be welded, which are used for data retrieval and analysis and microprocessors and computers un-connected to the welding equipment such as microprocessor controlled servo-hydraulic systems. Makhlin et al (1979) have measured the voltage level of the interference caused by spark-gap oscillators. The conducted interference measured at the mains supply to the spark-gap oscillators was in the voltage range of 100 - 130 dB relative to 1 μV and the frequency range was 0.15 MHz - 30 MHz. He also showed that even if mains interference suppression filters were used a considerable amount of RFI still existed. Correy et al (1986) have investigated the possibility of eliminating radiated RFI by using metallic shielding structures. It was

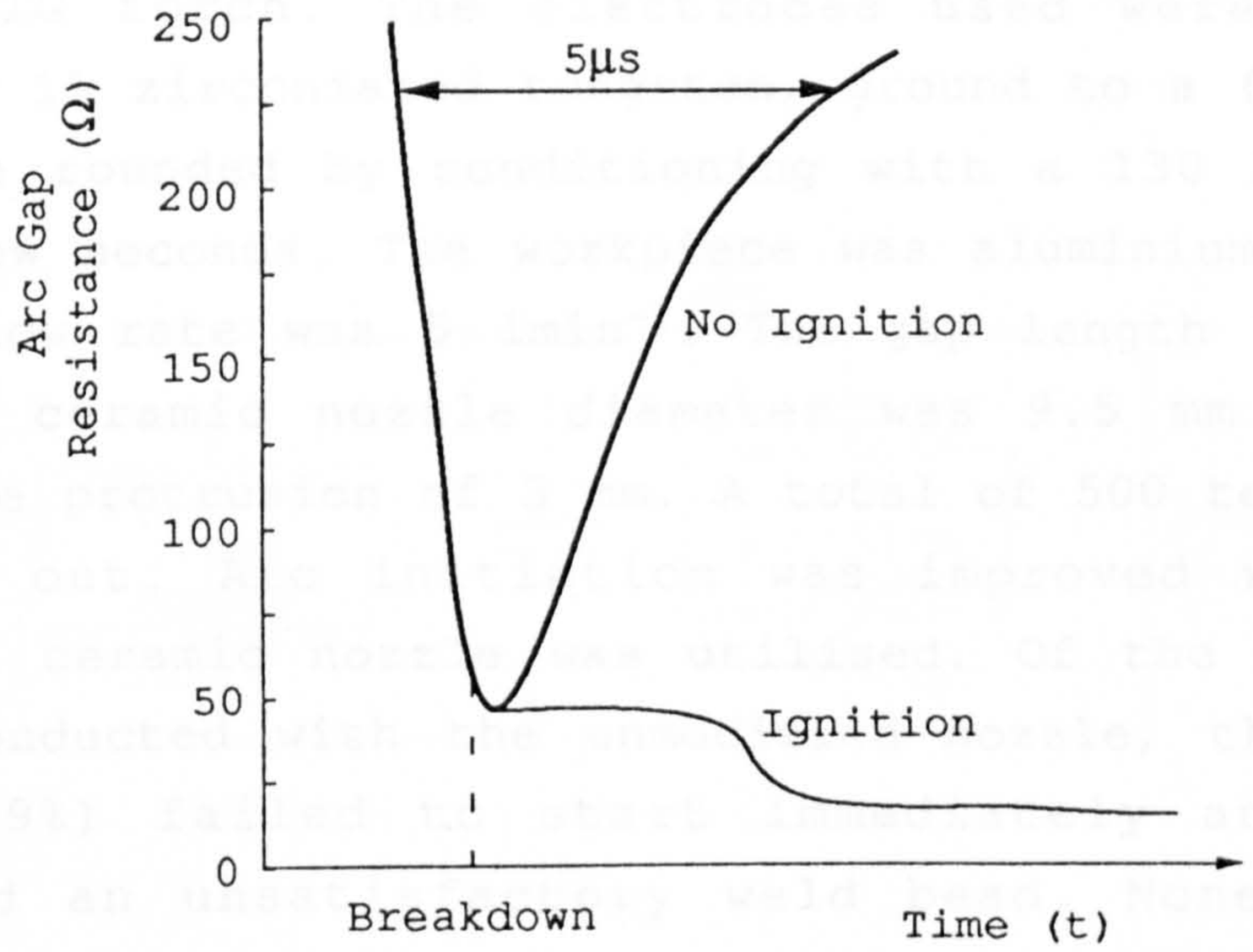

Fig.3.4 Variation of the arc gap resistance with time after spark breakdown from cold (Hildebrandt and Tajbl 1973).

concluded that this method of reducing RFI was very costly and that shielding structure design is a trial and error process that might never attain the required shielding level.

Brown (1976) showed that breakdown and arc initiation may be improved by touching the side or earthing the ceramic nozzle of the TIG torch. An ac power supply with an open circuit voltage of 100 V and an hf ignition source was connected to an air-cooled type TW150 TIG torch. The electrodes used were 2.4 mm diameter 1% zirconiated tungsten, ground to a 60° point and then rounded by conditioning with a 130 A ac arc for a few seconds. The workpiece was aluminium and the argon flow rate was 5 $lmin^{-1}$. The gap length was 2 mm and the ceramic nozzle diameter was 9.5 mm with an electrode protrusion of 3 mm. A total of 500 tests were carried out. Arc initiation was improved when the modified ceramic nozzle was utilised. Of the first 54 tests conducted with the unmodified nozzle, thirty-two (i.e. 59%) failed to start immediately and hence produced an unsatisfactory weld bead. None of the following 446 tests conducted with the modified nozzle failed to initiate immediately. It was emphasised that the results do not imply that such a modification to the ceramic nozzle of all TIG torches will necessarily produce similar improvement, and that hf arc initiation is an unpredictable process.

An hf ignition source should be coupled to the main power supply in such a way that no damage occurs due to the high-voltages, RFI is minimised and power losses are reduced. There are two main methods of connecting an hf ignition source to the main power supply. The first is a parallel connection as shown in Fig. 3.5. L and C form a low pass filter to protect the main power supply and prevent loss of hf power due to diversion of the hf current through the supply. L is a ferrite core dc choke designed to saturate at a current just above

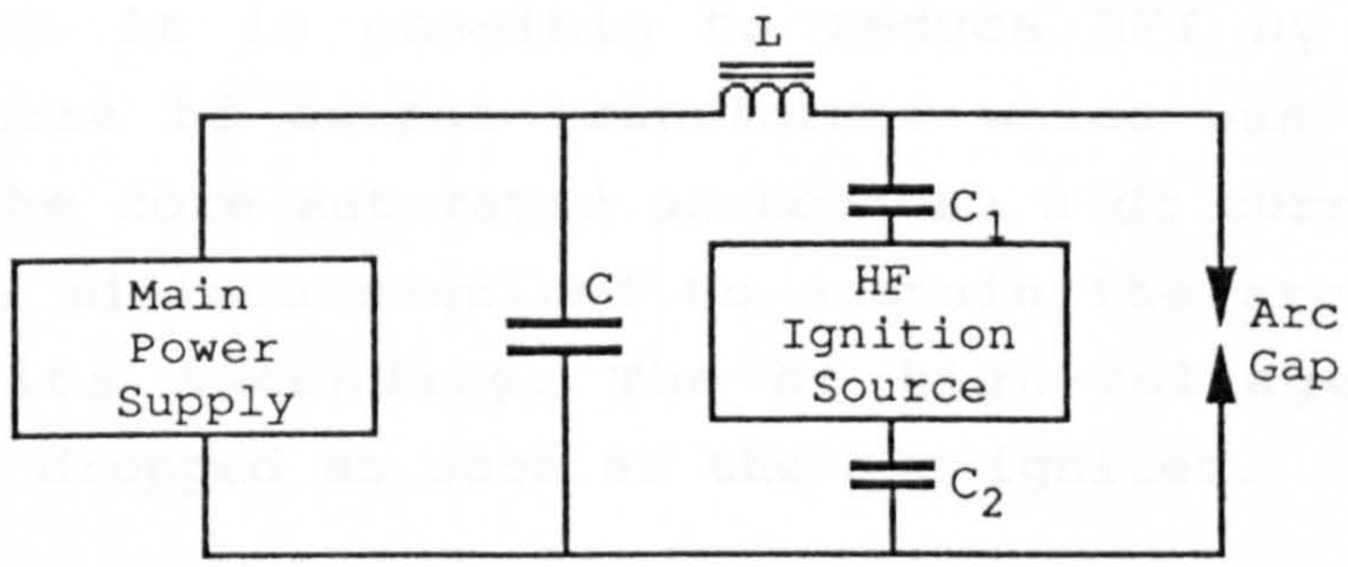

Fig.3.5 Parallel connection of an HF ignition source

the required minimum arc current (I_{min}) for the arc to be self-sustained. C_1 and C_2 are dc blocking capacitors to prevent the dc current flowing through the hf source. A careful design of the choke (L) can help minimise RFI, because as soon as the arc reaches I_{min} and becomes self-sustained, the hf current will flow through L and C and not through the welding cable. The advantage of this method of connection is that the output transformer can be compact and the ignition source can be used with any welding current. The second method is a series connection as shown in Fig. 3.2. The secondary of the hf output transformer must carry the welding current and hence it is bulky. Gufan (1965) has shown that it is possible to reduce RFI by using a ferrite core hf output transformer which was designed so that the core saturated as soon as a dc current just above the minimum required to sustain the arc, flowed through its secondary. The hf high-voltage output therefore dropped as soon as the arc ignited.

3.4 ARC INITIATION BY HIGH-VOLTAGE DC

The feasibility of using a high-voltage dc pulse for TIG arc initiation to overcome the problem of electrical interference caused by the conventional high frequency spark system, has been investigated by Brown (1976). A thyristor controlled pulse generator was used to produce pulses of about 1 ms duration. The basic arrangement of the circuit for a high-voltage dc ignition system is shown in Fig. 3.6. Isolation from the main power source was achieved with a high-voltage diode which prevents the high-voltage dc from appearing at the main power source terminals.

The required breakdown voltage was investigated using an air-cooled TIG torch with argon shielding gas of flow rate of 4.5 $lmin^{-1}$ and a stainless steel workpiece. The electrodes were 2.4 mm diameter 1% thoriated, 1% zirconiated or pure tungsten and were either rounded or

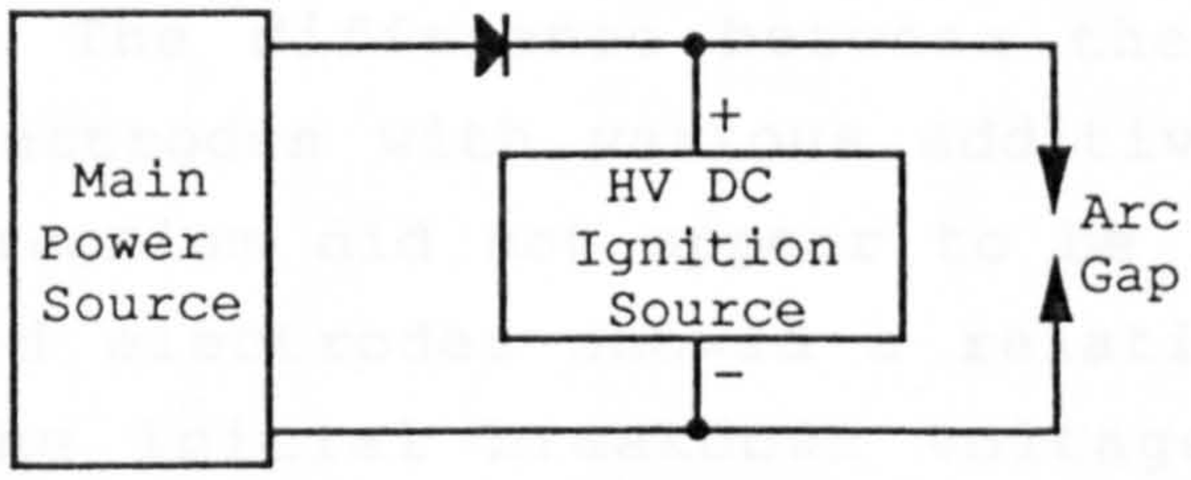

Fig.3.6 Basic circuit for arc initiation using a dc high-voltage pulse.

pointed (60°) tip. The gap length was 2 mm. Each electrode was tested after grinding and cleaning, and the first breakdown voltage recorded as the initial breakdown. A second reading taken typically 30 s after the initial breakdown was termed the subsequent breakdown. Further tests were also carried out with the tungsten tip rounded up by previously using a low current (25 A) electrode positive arc for a few seconds to melt the tungsten tip. The results of the tests are shown in Fig. 3.7, where each point indicates the mean of twelve separate tests, together with the standard deviation from the mean (thus 63% of the results lay within the extremes of the arrows). Many of the results, particularly the initial breakdowns showed a large scatter. The difference between the breakdown voltages of electrodes with various additives such as thorium and zirconium did not appear to be significant but the pointed electrodes showed a relatively small decrease in the initial breakdown voltage over the blunt electrodes. The cause of the relatively large difference between the initial and subsequent breakdown voltages may be the presence of impurities or emission sites formed during the initial breakdown causing a lower subsequent breakdown voltage.

Tests were carried out to examine the effect of temperature on arc initiation (Brown 1976). A 2.4 mm diameter 2% thoriated tungsten electrode at a gap length of 2 mm from a stainless steel workpiece was used. The argon flow rate was 4.5 $lmin^{-1}$. The initial breakdown voltage was considerably reduced as the temperature of the electrode and shielding gas was increased. It was shown that at 20 °C the initial breakdown voltage was about 4.5 kV and the subsequent breakdown voltage was about 2 kV but at 150 °C, the initial and subsequent breakdown voltages were almost equal at about 2 kV. Preheating the electrode may thus offer an improvement in starting efficiecy at lower applied voltages.

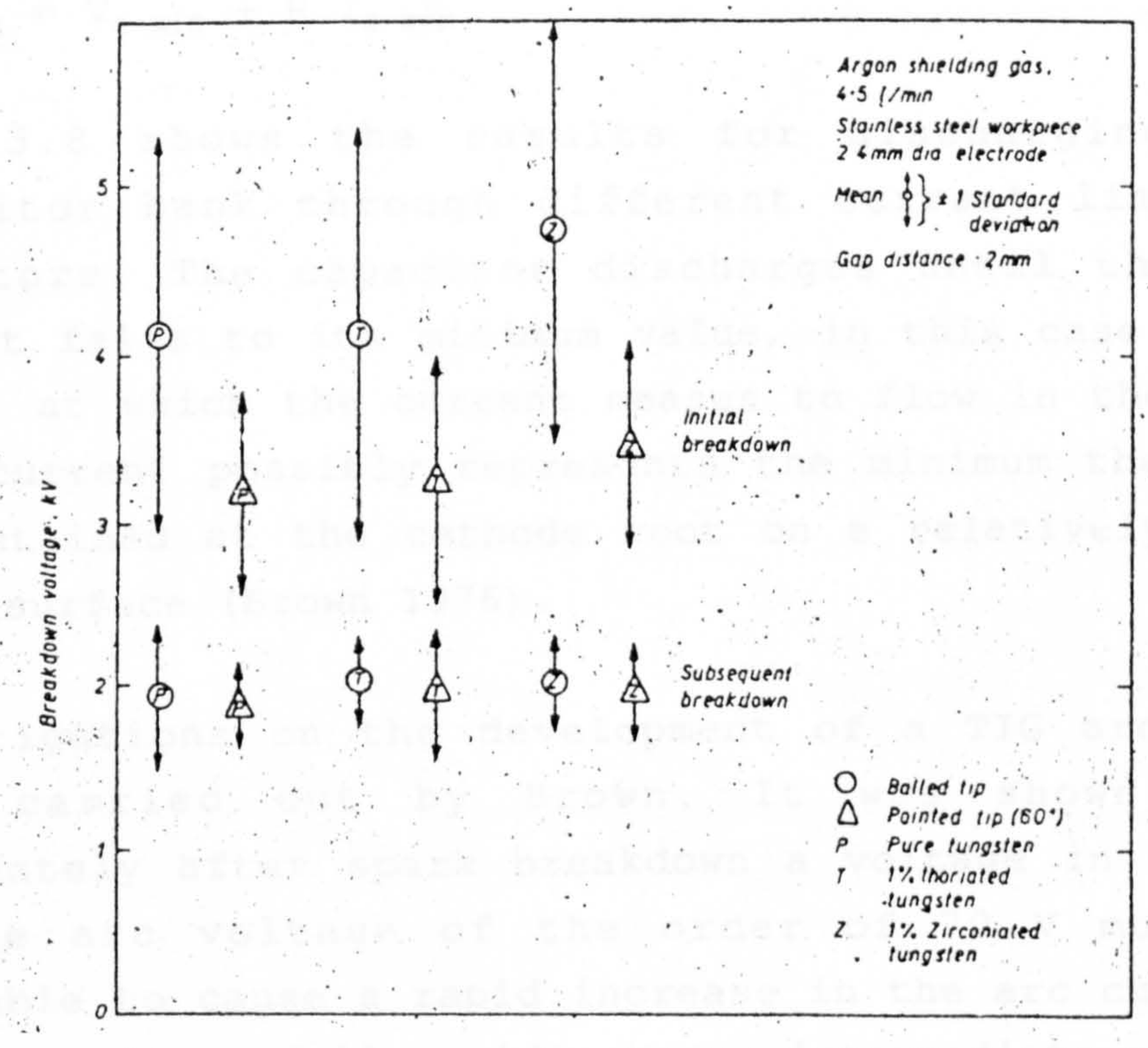

Fig.3.7 Variation of initial and subsequent breakdown voltages (Brown 1976).

Tests were also carried out using a charged capacitor bank and current limiting resistor to determine the voltage and current for reliable and rapid formation of an arc. It was found that the residual capacitor voltage V_c was related to the minimum arc voltage V_a in addition to a voltage derived from the minimum arc current I_{min} and the current limiting resistor R:

$$V_{c\,min} = V_{a\,min} + R.I_{a\,min}$$

Fig. 3.8 shows the results for discharging the capacitor bank through different current limiting resistors. The capacitor discharges until the arc current falls to its minimum value, in this case about 0.4 A, at which the current ceases to flow in the arc. This current possibly represents the minimum that can be sustained at the cathode root on a relatively cold metal surface (Brown 1976).

Investigations on the development of a TIG arc were also carried out by Brown. It was shown that immediately after spark breakdown a voltage in excess of the arc voltage of the order of 70 V must be available to cause a rapid increase in the arc current. The arc voltage fell rapidly to an intermediate voltage of around 25 V which appeared to be associated with a cold unstable arc. This value is in agreement with that stated by Pykal (1975). Once the arc was stabilised the voltage fell to around 10 V - 15 V which is characteristic of a TIG arc in thermal equilibrium.

DC arc initiation does not ensure an immediate and reliable ignition unless the voltage is very high of the order of 10 kV. The high voltage dc must be limited in magnitude and duration for safety reasons. A dc pulse from a high voltage supply will penetrate the human body and cause muscular contractions which may affect heart action (Biegelmeier and Rotter 1971). The severity of the shock will depend on the magnitude and

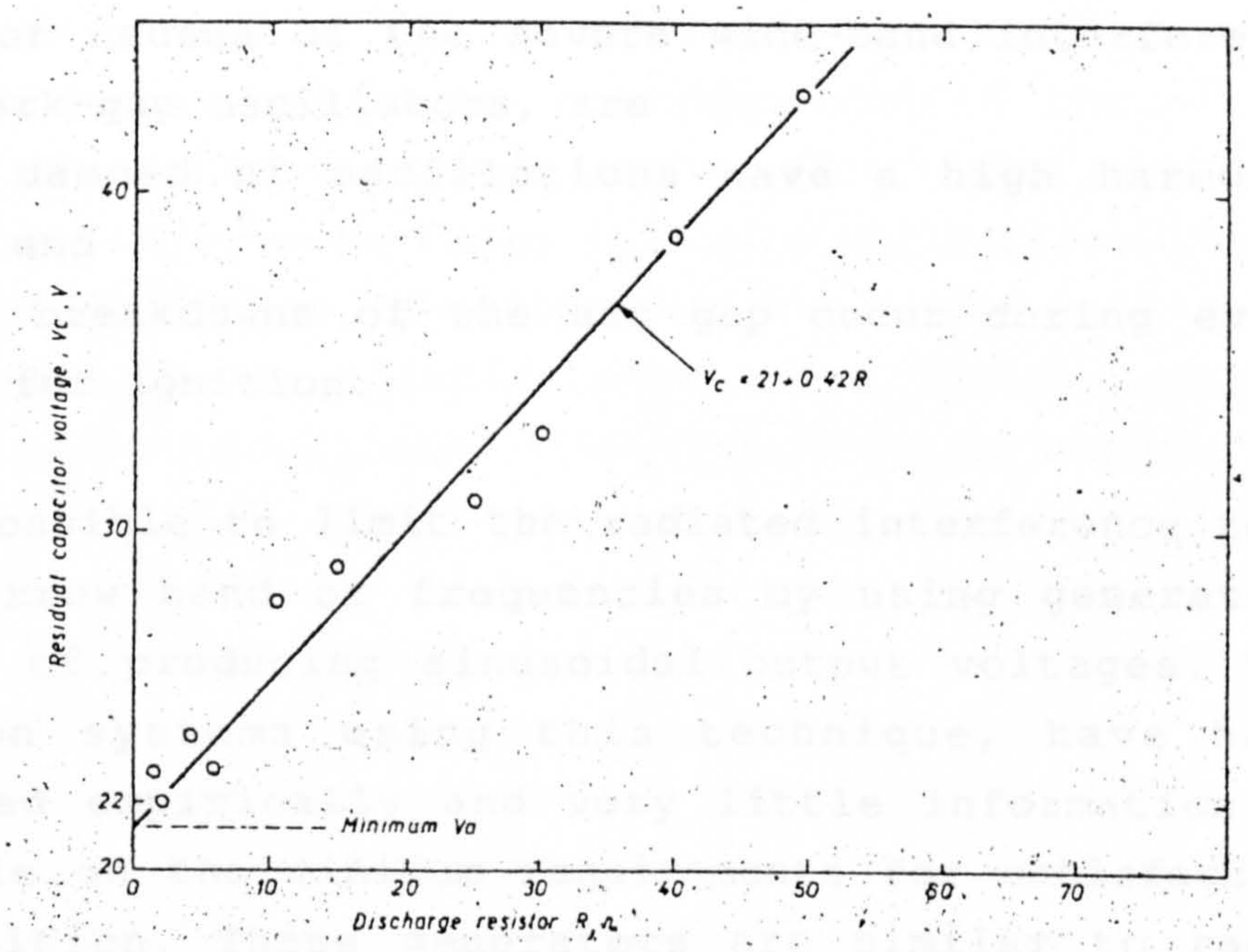

Fig.3.8 Residual capacitor voltage as function of discharge limiting resistor value (Brown 1976).

duration of the pulse. A 5 kV pulse of 500 µs duration may not cause an electric shock but can cause muscular contractions which may result in fatal accidents in hazardous environments.

3.5 CONTINUOUS SINUSOIDAL HIGH-FREQUENCY HIGH-VOLTAGE

Two major causes of the severe wide-band interference from spark-gap oscillators, are
a) the damped hf oscillations have a high harmonic content and
b) many breakdowns of the arc gap occur during every attempt for ignition.

It is possible to limit the radiated interference to a very narrow band of frequencies by using generators capable of producing sinusoidal output voltages. The ignition systems using this technique, have been developed empirically and very little information is available on the minimum requirements for satisfactory arc ignition. These generators are similar to radio transmitters and have been found to be unsatisfactory unless they are very powerful and consequently very costly.

Volff and Hammerslag (1951) developed an arc ignition system consisting of a crystal controlled valve oscillator feeding a power amplifier stage having two valves in parallel. An output frequency of about 13.56 MHz which was in a frequency band permissible to industrial apparatus was used. The generator was capable of generating an hf output power of about 100 W. The length of the welding cable was adjusted to minimise the loss of power, due to standing waves set up on the welding cable. It was therefore necessary to have a length such that a voltage maximum appeared at the welding torch. A length of about 2.77 m was used for the cable between the ignition source and the torch which was 1/8 of a wavelength. Volff and Hammerslag

showed that the generation of a continuous high-frequency for arc ignition, at a relatively low power input was difficult to achieve.

There are several disadvantages in using high frequencies of the order of few MHz for arc ignition. The length of the welding cable needs to be such that due to the standing waves a maximum voltage appears at the welding torch. During normal use the welding cable may be coiled, stretched out, supported in the air or laid on an electrically conducting floor. The resulting changes in impedances cause multiple reflections, which alter the position of voltage maximum and may cause large impedance mismatches between the ignition source and the welding circuit. The effect is to reduce the voltage available at the electrode for arc ignition. A second disadvantage of using a high-voltage source having a frequency of the order of a few MHz is radiation from the welding cable which acts as a transmitting antenna, since the length of the cable is long in comparison with a quarter-wavelength. A third disadvantage is that the capacitive reactance of the arc gap becomes important and a capacitive current will flow which increases losses.

Air Reduction Company (1955) developed an arc ignition system which was a class-C push-pull valve Hartley oscillator operating at low frequencies of the order of 50 kHz - 500 kHz. The low frequencies were used to avoid the disadvantages such as power loss and radiation caused when high frequencies of the order of a few MHz are used. This was made possible by the use of a ferrite core output transformer for the high-frequency high-voltage generator which saturated when the welding current flowed through the secondary due to arc ignition. However, no values of output power were given and may have been higher than 1 kW.

3.6 SUMMARY

The review indicates that failure to achieve reliable non-contact arc initiation may be caused by the cold arc and the main power supply during the initial current rise. The cold arc may become self-sustained when the current reaches 1 A - 2 A within about 100 μs, but it may take several milliseconds to reach a steady-state at thermal equilibrium. A cold arc in which field ionisation is dominant may extinguish more easily than an arc in which thermal ionisation is dominant because in a cold arc, delays due to thermal inertia are insignificant. A temporary decrease in current owing to an oscillatory initial current rise supplied by the main power source may therefore extinguish the arc.

Spark-gap oscillators are relatively safe, require a small average power of only about 20 W and are simple and cheap, however, they can be unreliable and cause severe electrical interference.

The high-voltage dc method of arc ignition is almost interference-free and may require small amounts of power. For reliable ignition however, the high-voltage source should operate for a long time of the order of 1 ms which may be unsafe.

The continuous sinusoidal hf method of arc ignition has the advantages from each of the other two methods such as safety, reliability and free of interference but a high power (several kW) source would be required which may be large and expensive.

This review has enabled the relative merits of the indvidual methods to be considered. A programme of work based on studying arc ignition using dc and continuous sinusoidal hf methods was therefore undergone to develop a method which overcomes these limitations.

CHAPTER 4

PRELIMINARY MEASUREMENTS, INVESTIGATIONS AND ANALYSES

4.0 PRELIMINARY MEASUREMENTS, INVESTIGATIONS AND ANALYSES

Reliable arc ignition is essential because if the arc fails to initiate, the gap must be broken down again and if this process is repeated, it may cause severe radio frequency interference.

An analysis of the requirements to ensure immediate breakdown of the arc gap, formation of a suitable starting discharge and subsequent establishment of a stable low voltage arc is needed to design an efficient arc initiation power source.

There is little published work on the characteristics of the conducting path which during the initiation process is carrying current from both the ignition source and the main power supply.

The purpose of the preliminary investigations was to obtain information on the

a) breakdown voltage.

b) discharge voltage, current and power which allow the establishment of dc arcs using either dc or sinusoidal hf ignition sources.

c) minimum requirements for an arc ignition power source by considering the combined discharge which is formed during the intermediate stage between the time of breakdown and the time of establishment of the arc.

4.1 BREAKDOWN MEASUREMENTS

Initially a non-contact arc ignition source must produce sufficient output voltage to break down the arc gap. The breakdown voltage at atmospheric pressure is affected by the gas, condition of the electrodes such as shape, temperature, and surface roughness, and the frequency of the applied voltage.

For gaps in argon, most work is carried out using dc and there is little data available on breakdown voltages of gaps in argon using high frequencies especially for short (1 mm - 5 mm) point-plane gaps similar to TIG arc welding gaps.

The purpose of the initial investigation is to
i) measure breakdown voltages which would be used in subsequent work to determine approximate values of the minimum output voltage required for an ignition source.
ii) obtain familiarity with the difficulties in producing sinusoidal high frequency high voltages to efficiently break down electrode gaps.
iii) investigate the possibility of reducing the breakdown voltage by using a sufficiently high frequency.

4.1.1 Electrode Arrangements and Power Sources

For the uniform field measurements, 10 mm diameter copper spheres in air with a maximum gap separation of 3 mm were used having a gap length to sphere diameter ratio of less than 0.4, to obtain an almost uniform electric field within the test gap. For non-uniform field measurements gap separations up to 5 mm were used employing a Weldcraft WP-26 200A air cooled TIG torch, the tungsten cathode being 2% thoriated, 2.4 mm diameter, axially ground to a 45° included angle with 5 mm protrusion from a ceramic nozzle of 8 mm internal diameter either in free air or having 99.95% purity argon flowing with a rate of 5 $lmin^{-1}$ through it, and the anode was a copper plate.

The applied voltages were dc, 50 Hz or frequencies from 10 kHz to 800 kHz to determine whether there was a variation in the breakdown voltage with frequency; the power sources had to be designed and constructed due to the high voltages.

The dc power supply (Fig. 4.1) consisted of a 3-phase high voltage transformer with two secondary windings on each limb, with a variable output voltage of over 15 kV at up to 1.4 A. The output ripple voltage was reduced by having star-delta connected secondaries to increase the ripple frequency to (12 × 50 Hz) 600 Hz and by using LC filtering.

The output over a range of 10 kHz - 50 kHz was produced using a signal generator to supply a valve audio amplifier connected to a specially designed high voltage (7 kV) ferrite core transformer (Fig. 4.2). A capacitor was used to limit the current after breakdown.

For frequencies over the range 50 kHz - 800 kHz, a high frequency high voltage generator was designed. The circuit diagram of the high-frequency high-voltage generator is shown in Fig. 4.3, the list of components is given in Appendix 1 and Fig. 4.4 shows a photograph of the interior of the generator.

The sinusoidal input voltage which was varied to obtain the required output voltage, was fed through C_1 into a cathode coupled phase splitter (V_1, V_2) which produced two amplified antiphase voltages to drive the push-pull output stage (V_3, V_4) to convert the (8 kV max.) dc power supply into an hf power at (0 - 6 kV) and (0 - 2 A).

The anodes of the beam tetrodes (V_1, V_2) were supplied by a constant voltage of +500 V from a separate dc auxiliary supply through resistors R_2 and R_6 and a common-mode ferrite core inductor (L_1, L_2) to increase the ac output from each valve as it fell with frequency. The outputs from the anodes were coupled to the control grids of V_3 and V_4 which required a maximum grid to grid peak voltage of 300 V through C_5 and C_6.

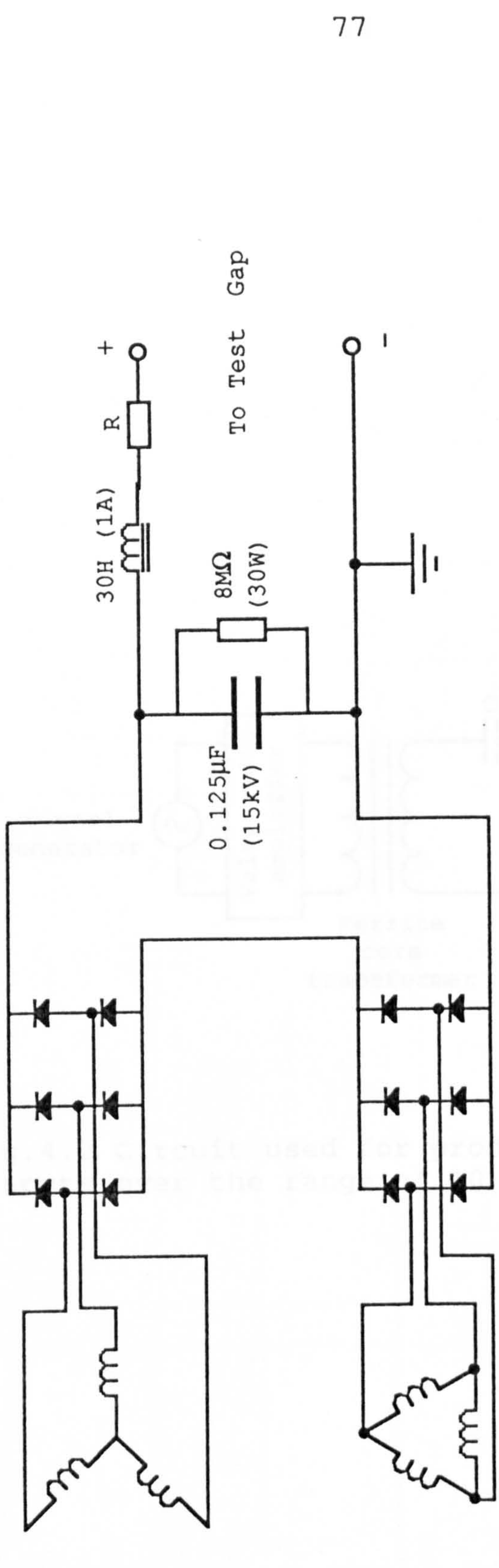

Fig.4.1 High voltage DC power supply

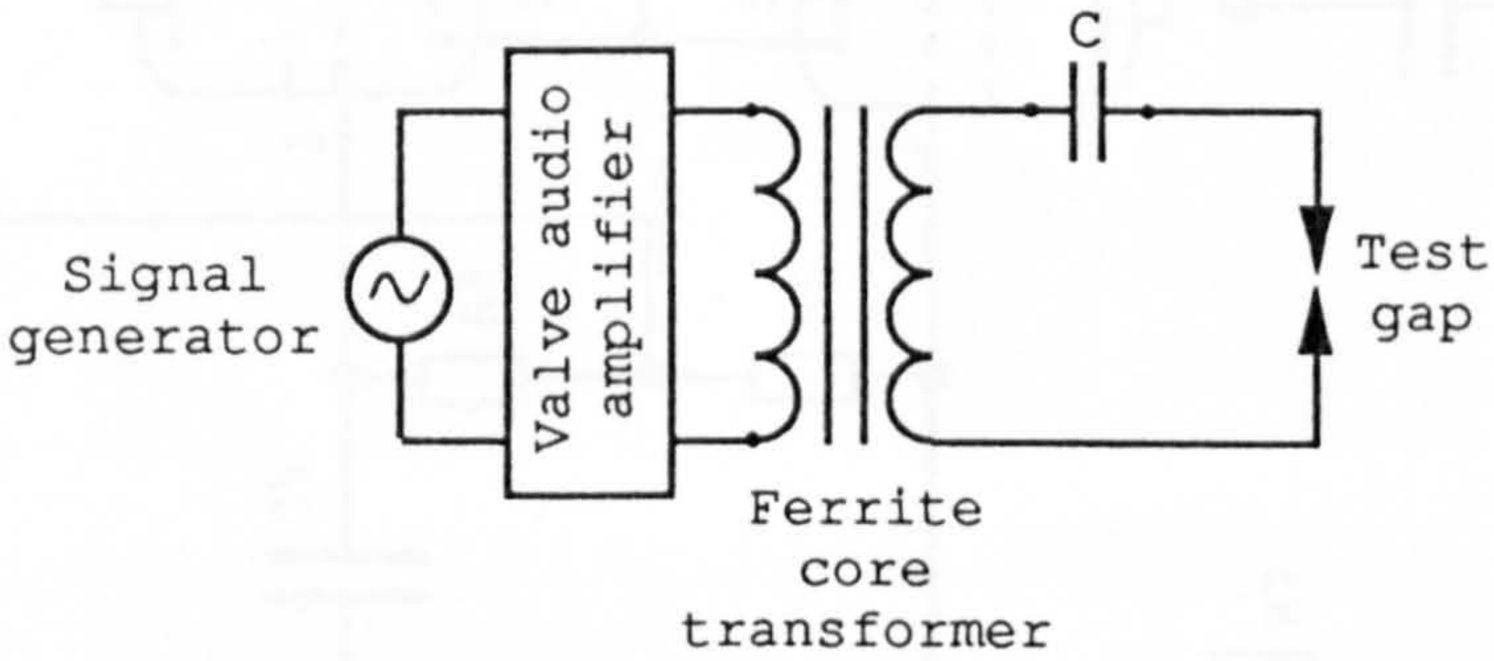

Fig.4.2 Circuit used for producing the outputs over the range of 10 kHz-50 kHz.

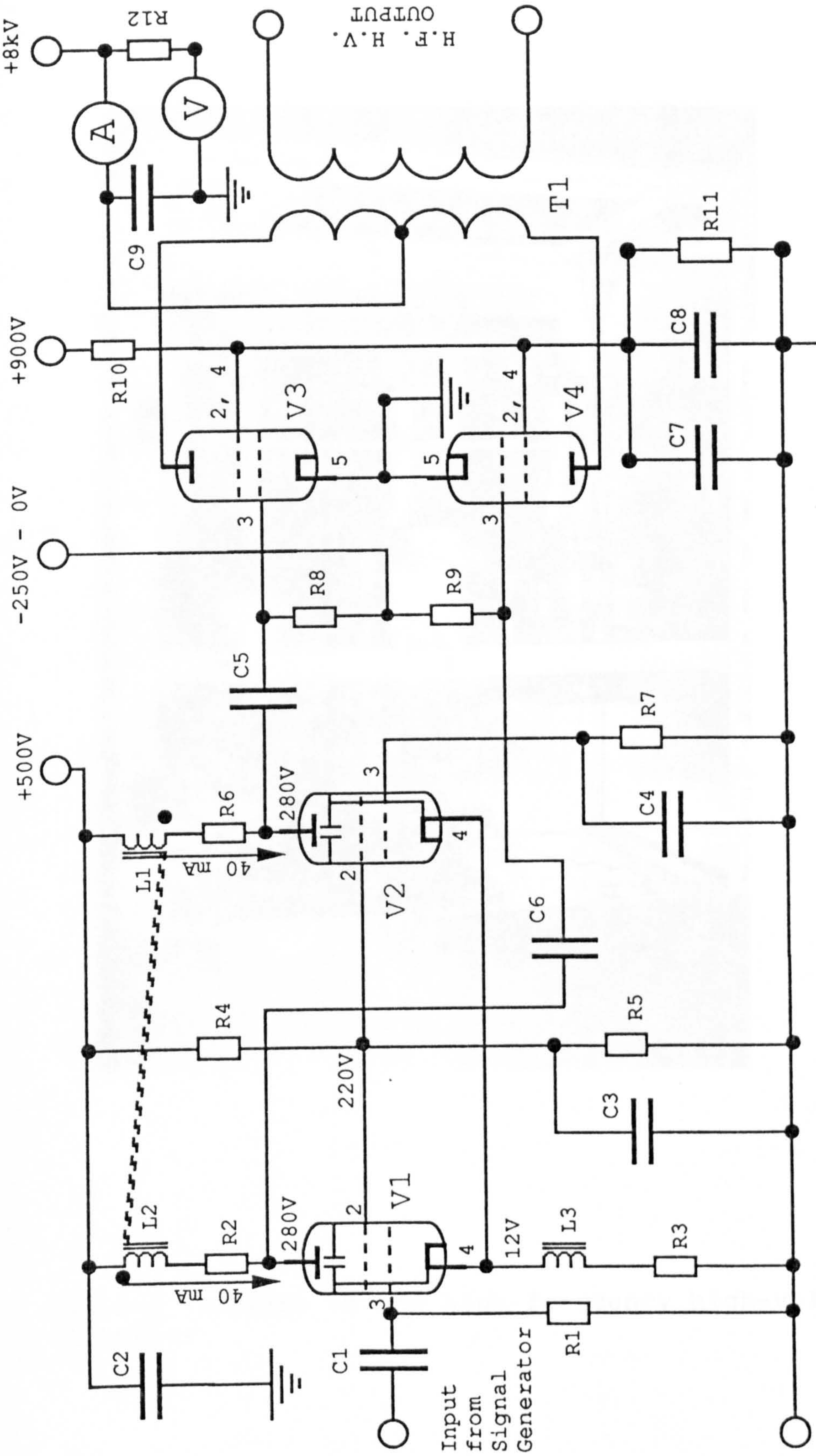

Fig.4.3 High-Frequency High-Voltage Generator

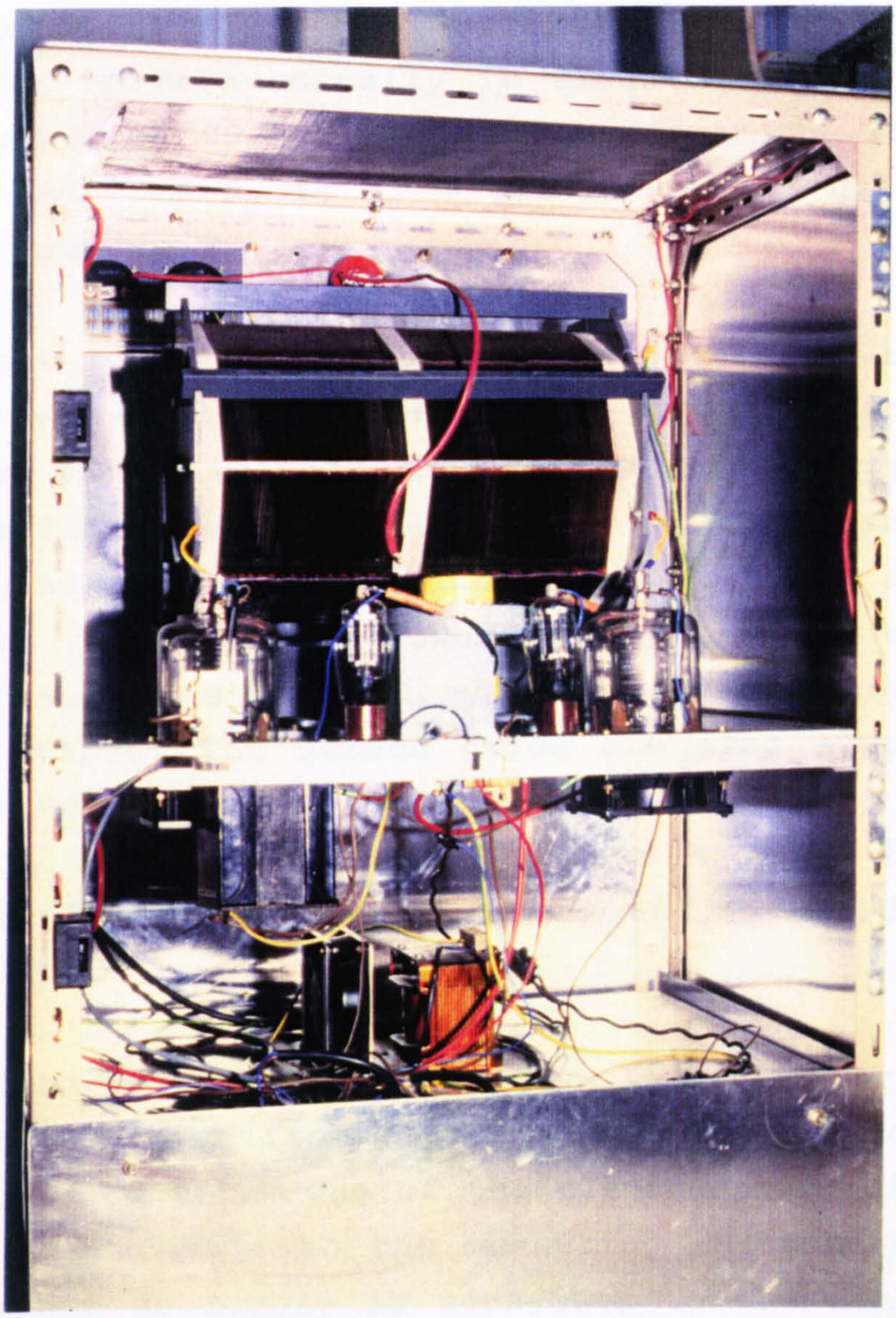

Fig.4.4 Interior of the high-frequency high-voltage generator

The screen grids are held at 220 V by the potential divider R_4 and R_5. The inductor L_3 increases the input signal to V_2 that appears at its cathode, which tends to decrease at high frquencies. The control grids are both held at about ground level using R_1 and R_7. When the valves operate normally in class-A with an anode current of about 40 mA, the voltage across the (common) cathode resistor R_3 is 12 V and hence the grid bias voltages are -12 V.

The output power tetrodes, are connected in common-cathode push-pull which enables a higher efficiency, twice the output voltage for the same input dc voltage and a better sinusoidal output due to suppression of the even harmonics. The control grid voltages are set using the dc auxiliary power supply through current limiting resistors R_8 and R_9 and can be varied to obtain maximum output. The screen grids are also supplied a constant voltage of +900 V from the auxiliary supply through a current limiting resistor R_{10}. R_{11} forms a potential divider with R_{10}, and C_7 and C_8 are by-pass capacitors.

The output push-pull air-core transformer (T_1), provides isolation from the high voltage dc and makes it possible to earth one of the electrodes of the test gap to avoid damage to the measuring instruments. The high voltage dc supply is connected to the centre-tap of T_1 and the current is fed to the anodes of V_3 and V_4 through each half of the primary. An output voltage of about 6 kV was possible at frequencies as high as 800 kHz.

A 20 kV oscilloscope probe with a bandwidth of more than 6 MHz was used to measure the breakdown voltage. The value of voltage just before breakdown of the gap at which the breakdown voltage dropped suddenly and a discharge appeared was recorded as the breakdown voltage (peak for ac). The breakdown voltages after the

first breakdown were lower, hence to obtain breakdown voltage values for cold cathodes, a duration of 30 s was allowed to elapse between measurements. Each measurement was repeated 20 times and the average of the values that varied by less than ±20% was recorded.

4.1.2 Results of Breakdown Measurements

The variation of breakdown voltage with gap separation for dc, 50 Hz and frequencies of 10 kHz - 800 kHz are shown in Fig. 4.5. The curves show the average of the readings which varied by ±20%. For a sphere gap of 3 mm separation in air, the breakdown voltage was about 12 kV corresponding to a voltage gradient of 4 $kVmm^{-1}$ (compared with 3 $kVmm^{-1}$ for gaps of longer than 10 mm in air) and for a point-plane in air it reduced by about 50% to about 6 kV corresponding to 2 $kVmm^{-1}$ and in argon it was lowered by about 75% to about 3 kV corresponding to 1 $kVmm^{-1}$.

The breakdown voltage of all the gaps under these experimental conditions, remained approximately constant with increasing frequency up to 800 kHz.

A non-contact ignition source should have an output voltage of at least equal to the breakdown voltage of the arc gap. The results of this section show the variation of the minimum required output voltage from an ignition source with electrode separation for sphere gaps in air, point to plane gaps in air and typical TIG arc gaps.

4.2 TEMPORARY ARC DISCHARGES FROM GLOW TO ARC TRANSITIONS AND THE EFFECT OF THE POWER SUPPLY

Glow to arc transitions have been observed during the investigations on arc ignition. This made it difficult to analyse the requirements of the starting discharge. Glow to arc transitions and the effect of power supply parameters were therefore investigated.

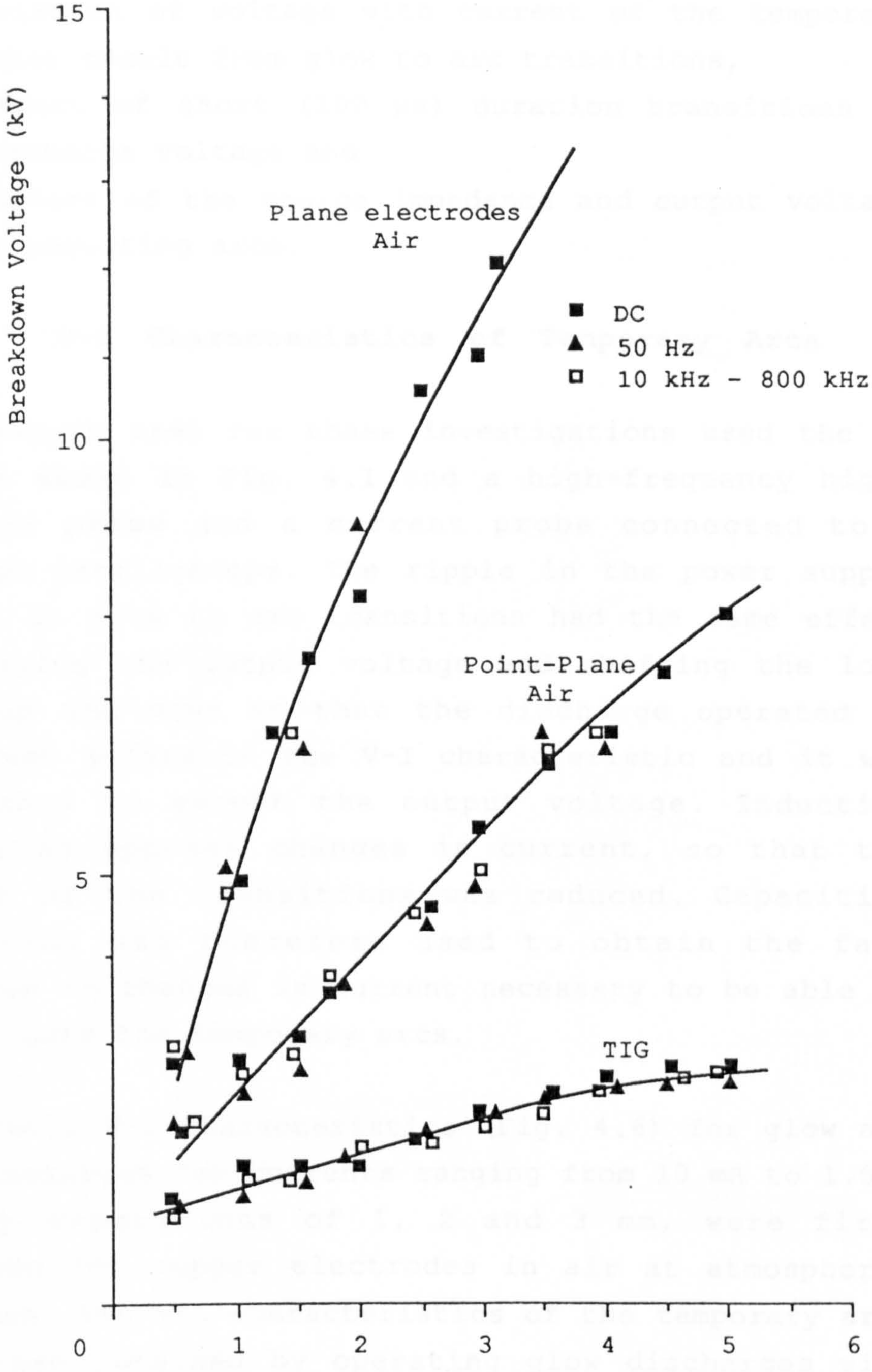

Fig.4.5 Variation of breakdown voltage with electrode separation.

The purpose of the work in this section was to investigate the

i) variation of voltage with current of the temporary arcs that result from glow to arc transitions,

ii) effect of short (100 μs) duration transitions on the discharge voltage and

iii) effect of the source impedance and output voltage on the resulting arcs.

4.2.1 V-I Characteristics of Temporary Arcs

The circuit used for these investigations used the dc source shown in Fig. 4.1 and a high-frequency high-voltage probe and a current probe connected to a storage oscilloscope. The ripple in the power supply output on glow to arc transitions had the same effect as varying the output voltage and shifting the load line up and down so that the discharge operated at different points on the V-I characteristic and it was necessary to smooth the output voltage. Inductive filtering opposes changes in current, so that the effect of the transitions was reduced. Capacitive filtering was therefore used to obtain the fast response to changes in current necessary to be able to investigate the temporary arcs.

The static V-I characteristics (Fig. 4.6) for glow and arc discharges for currents ranging from 10 mA to 1.5 A at gap separations of 1, 2 and 3 mm, were first obtained for copper electrodes in air at atmospheric pressure. The V-I characteristics of the temporary arcs were then obtained by operating glow discharges with currents of 0.1 A to 0.5 A and measuring the voltage and current at the glow to arc transition simultaneously on a storage oscilloscope. Fig. 4.7 shows a typical transition from a 0.3 A glow to a temporary arc. The measurements were repeated 20 times and the mean of the values which varied between ±10% were recorded. The V-I characteristics for the temporary arcs are shown dotted in Fig. 4.6.

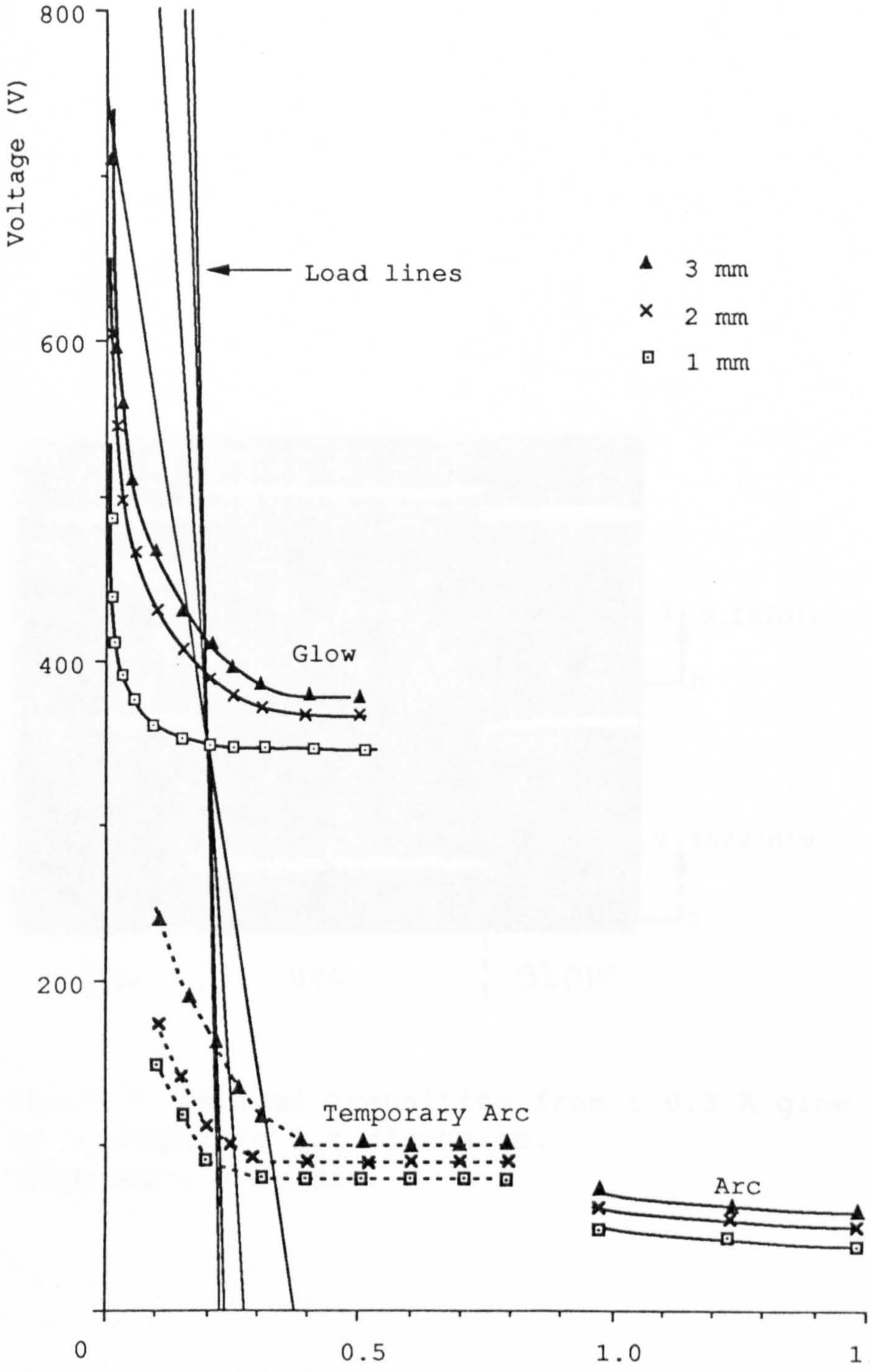

Fig.4.6 V-I characteristics of static glows and arcs and temporary arcs.

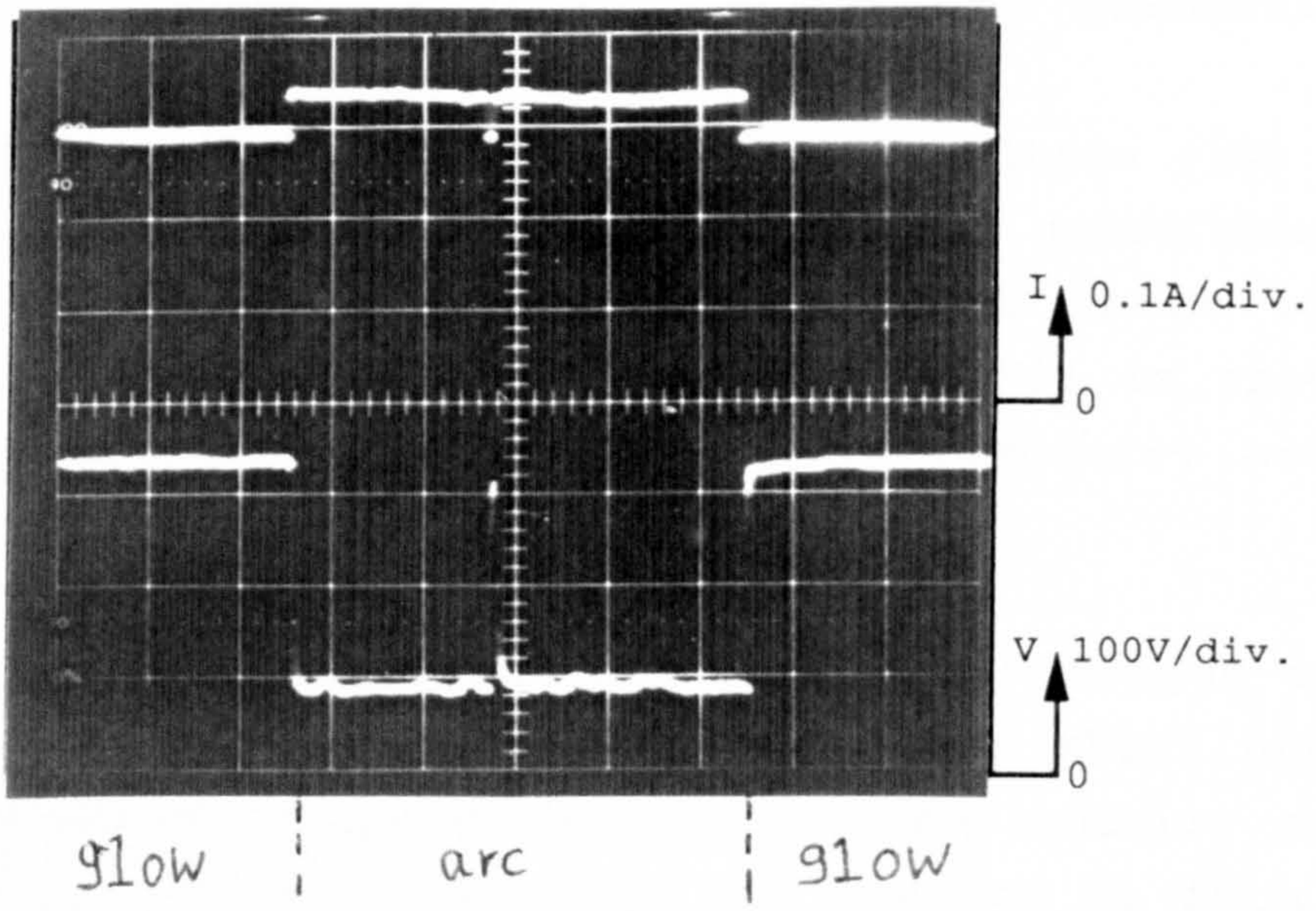

Fig.4.7 Typical transition from a 0.3 A glow to a temporary arc discharge.
Time-base: 2 ms/div.

Below about 0.1 A, more than 20 minutes elapsed before a transition took place and when it occurred, the duration was only about 100 μs (Fig. 4.8). This caused a sharp rise in voltage of the temporary arcs.

Fig. 4.6 also shows that for currents between 0.5 A and 0.8 A the discharge was not a stable arc but changed to a glow for about 100 μs at intervals of about 1 s (at a current of 0.8 A). Fig. 4.9 shows a typical short duration arc to glow transition.

4.2.1.1 Effect of duration of each transition

The resulting discharge had a higher voltage (160 V for 1 mm gap at a current of 0.1 A) when short duration glow to arc transitions of less than about 100 μs occurred than for longer durations. This is shown by the sharp rise in voltage of the temporary arc V-I curves of Fig. 4.6.

One possible explanation for the higher voltage of the short duration arcs, may be that (for short gaps of less than 5 mm length) heating the cathode causes copper oxide inclusions on the surface to form. The work function of copper oxide of 1.76 V, is relatively low compared with that of copper of about 4.38 V, and hence it can provide extra ionisation by thermal electron emission which becomes the dominant component of the cathode emission current. The duration of each transition may be governed by the amount of oxide available on the cathode which provides the extra ionisation to maintain the arc. The amount of oxide depends on the amount of heating at the cathode which increases with current. The oxide inclusion may not be large enough to provide sufficient ionisation for enough time (up to 0.5 ms or more) to allow the column to ionise sufficiently. The column will not have time to heat up and increase its current density above a critical value to constrict the column and become an

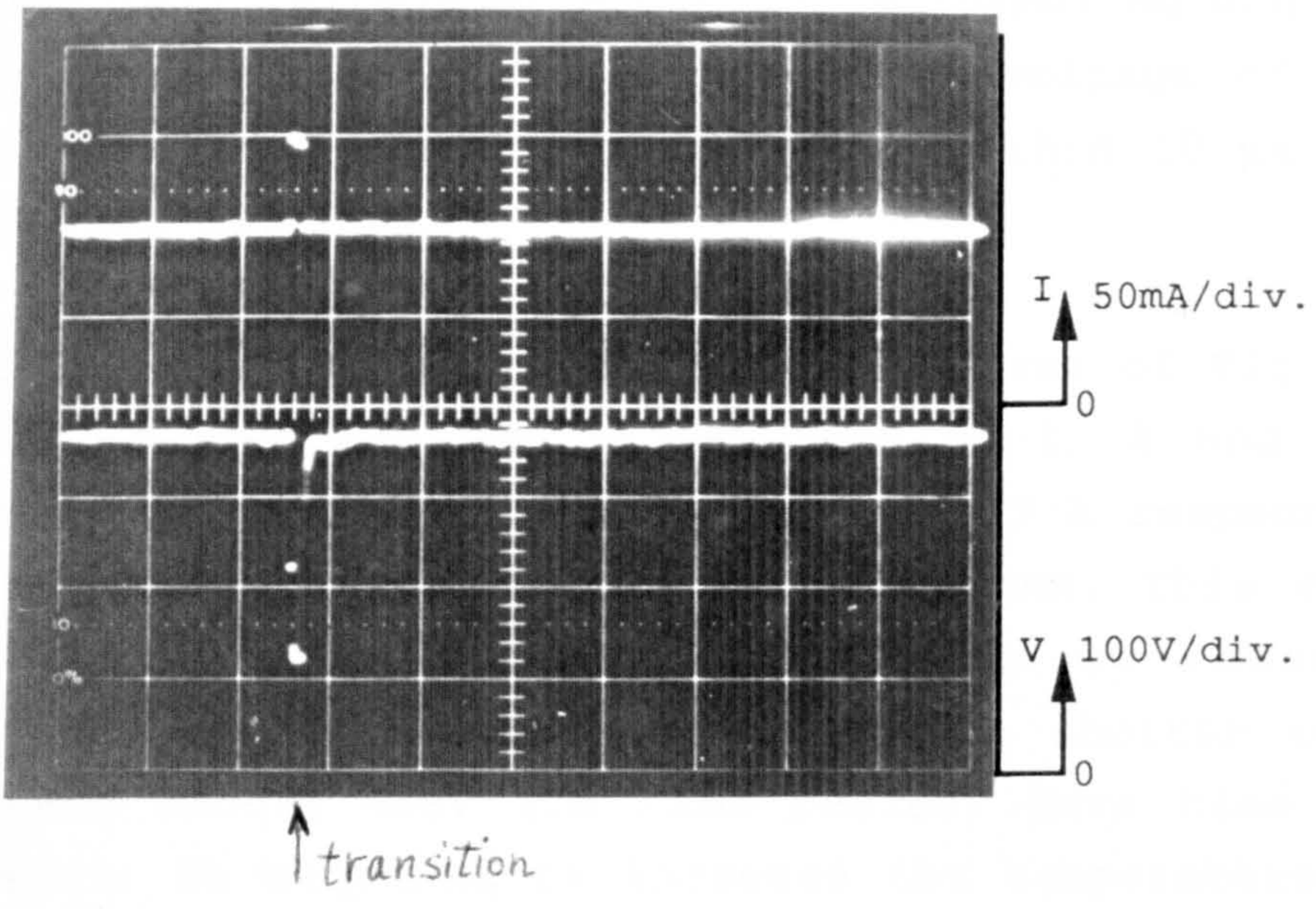

Fig.4.8 A short duration glow to arc transition. Time-base: 2 ms/div.

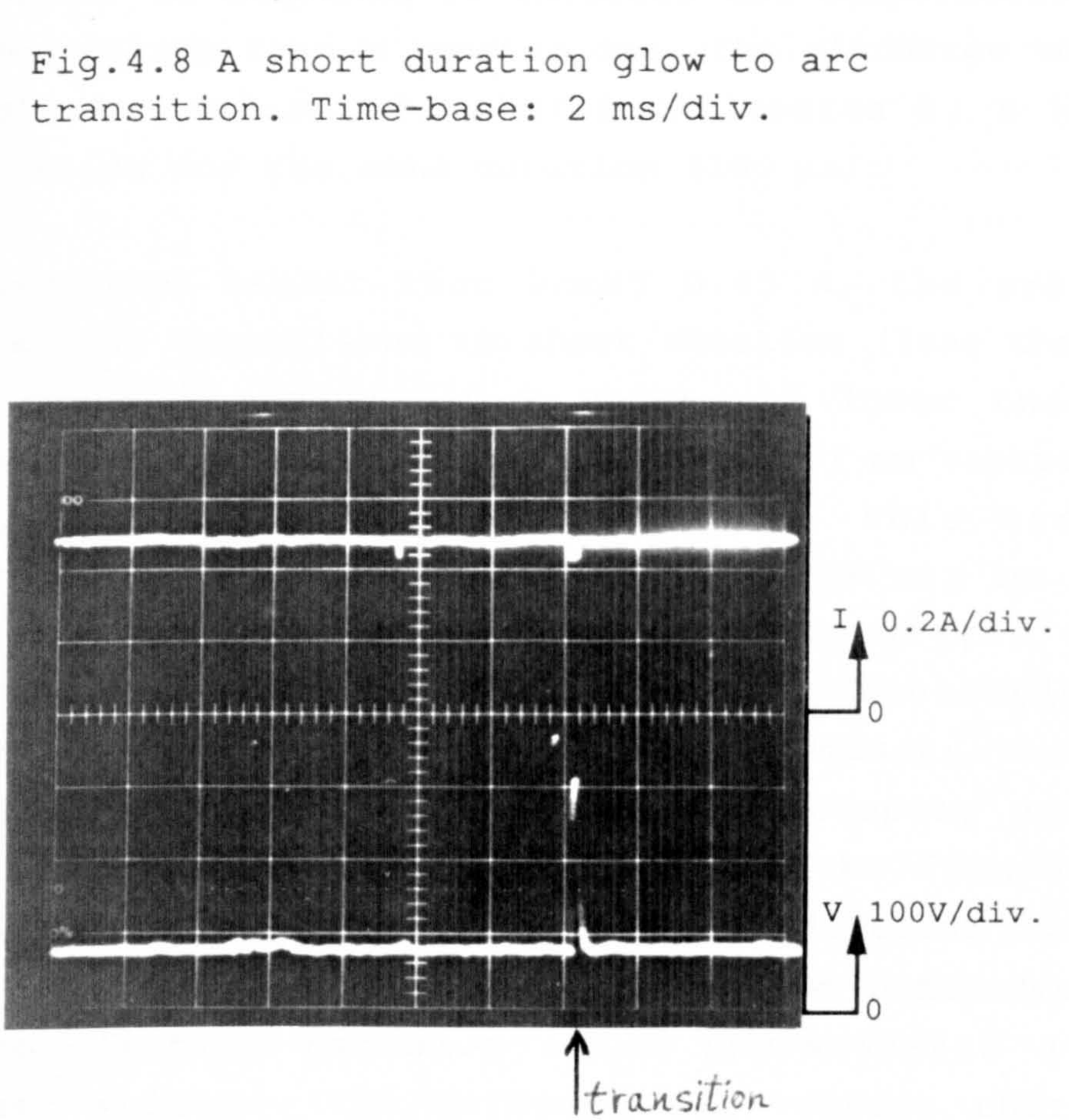

Fig.4.9 A short duration arc to glow transition. Time-base: 2 ms/div.

arc column (Gambling and Edels 1956). The voltage across the column will therefore be higher. The glow cathode fall voltage of about 285 V (Gambling and Edels 1954) changes to an arc cathode fall voltage of about 10 V (von Engel and Steenbeck 1934) within 10 μs (Betz and Karrer 1937).

The slope of the temporary arc V-I curves of Fig. 4.6, became steeper for gap separations of 1, 2 and 3 mm, starting at less than 0.2, 0.25 and 0.3 A respectively and depended on the length of the column. This may be because more heat input is required to raise the temperature of a longer column than a shorter one by the same amount over the same period. More time would therefore be required to increase the temperature of a longer column than a shorter one. The discharge voltage of shorter columns is therefore lowered by a higher proportion for the same duration (100 μs).

At currents higher than about 0.45 A, the arcs had occasional transitions to short duration (less than 100 μs) glows at about 310 V which was lower than the normal glow voltage of about 350 V for 1 mm separation. Fig. 4.9 is a typical example of this type of transition. A possible reason for this may be that, immediately after the disappearance of the oxide inclusion, production of the extra ionisation by thermal electron emission as the dominant emission mechanism from the oxide, ceases abruptly and the electron emission that follows, will be from a pure copper cathode. This would require a different dominant electron emission mechanism such as ion bombardment or photo-electric emission which necessitates a much higher voltage. The cathode fall voltage therefore increases quickly to a glow cathode fall voltage. Within the thermally ionised column, the extra ions and electrons will diminish in number due to cooling and de-ionising influences such as recombination, diffusion or discharge into the electrodes. This de-ionisation

requires a finite time to be effected and the positive column may remain highly ionised. The column will have a lower impedance and voltage if it does not have sufficient time to de-ionise and cool down to the extent required to have the lower conductivity of a normal glow column before the formation of a new oxide inclusion.

4.2.1.2 Effect of the slope of the power supply load lines

The slope of the power supply load line was decreased by decreasing the series resistance from 15 kΩ to 2 kΩ (Fig. 4.6), keeping the glow current of 0.2 A, constant. Simultaneous displays for voltage and current on a storage oscilloscope for a 0.2 A, 1 mm glow discharge, are shown in Fig. 4.10. The temporary arc current increased from 0.22 A to 0.32 A and the results showed that the output voltage of the power source and the series resistance had an effect on altering the current and voltage of the temporary arcs.

The reason for the effect of the slope of the power supply load line on the temporary arc current may be explained as follows. A temporary increased contribution of a more efficient mechanism of electron emission by thermionic emission occurs due to the existence of the oxide surface inclusions. The cathode fall voltage reduces from about 285 V to about 10 V, so that the total discharge voltage decreases. An increase in current will therefore occur to a value determined by the output voltage of the power source and the series resistance. The increase in current causes an increase in the column temperature which causes the thermal conductivity of air to suddenly decrease (King 1954). This results in a constriction of the column, increased current density and eventually a reduction in the voltage gradient across the column (Gambling and Edels 1956). A further increase in current takes place

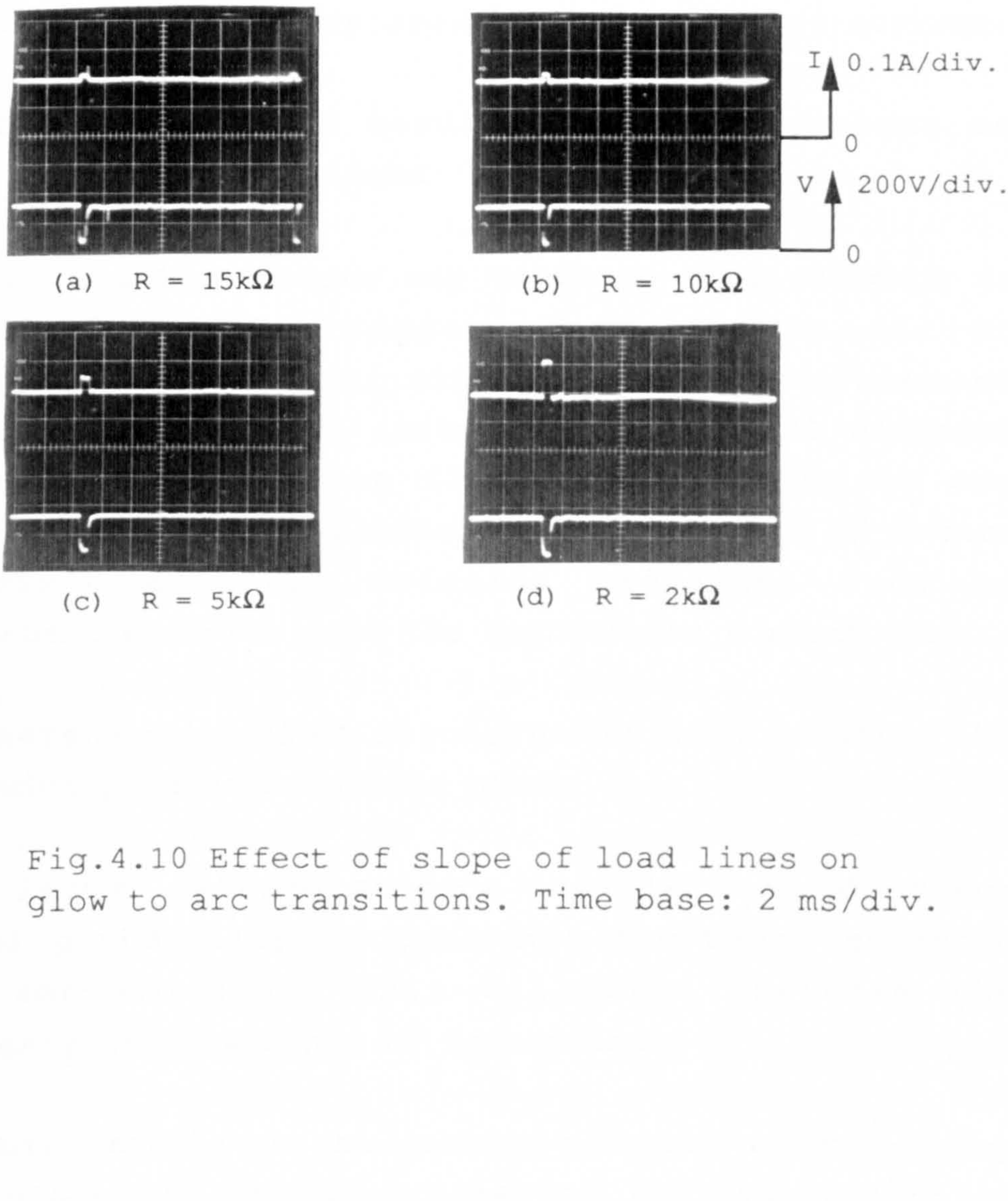

(a) R = 15kΩ (b) R = 10kΩ

(c) R = 5kΩ (d) R = 2kΩ

Fig.4.10 Effect of slope of load lines on glow to arc transitions. Time base: 2 ms/div.

which is again limited by the interaction of the discharge characteristic with the slope of the power source load line. Each transition on the oscillogram corresponded to the intersection point on the temporary arc V-I curve. The points where the load lines cross the V-I curves of the static glow and temporary arc discharges are possible operating points. The stable operating point would be at the lower voltage and higher current where the load line intersects the temporary arc V-I curve. Decreasing the slope of the load line increases the current available and therefore the resulting temporary arc will have a higher current.

4.2.2 Discussion of Results of Investigations on Glow to Arc Transitions

Glow to arc transitions may occur at glow currents as low as 0.1 A for copper electrodes in air at atmospheric pressure, although in this series of experiments they were infrequent (one in 20 minutes) and of short duration (100 μs). The glow to arc transitions can be explained by the presence of a more efficient electron emission mechanism such as thermionic emission from the cathode for a short time.

An increase in glow discharge current causes the following processes to take place:

i) A larger cathode surface area is covered, hence higher probability of including a site of enhanced electron emission. This will then increase the frequency of occurrence of transitions.

ii) More heating at the cathode and more oxidation may take place for the same area and the evaporation of these oxide layers provides metal vapour and more electrons, hence an arc is formed. The arc duration depends on the presence of this mechanism which is favourable to the existence of the arc and which may be governed by the size of each oxide inclusion.

The V-I characteristics for temporary arcs for currents between 0.1 A and 0.8 A are similar to the static arc V-I characteristics. Arcs may exist at currents as low as 0.1 A for copper electrodes in air at atmospheric pressure, although only temporarily.

Fully developed arcs occurred at currents above a threshold value varying with separation (Fig. 4.6). A longer column appeared to require a longer duration to reach the same low voltage as a shorter column. For low current (0.1 A) glows using copper cathodes, the arcs had durations too short for the column to heat up and ionise sufficiently to develop into an arc column but the cathode fall voltage increased quickly to a glow cathode fall voltage and this caused the temporary arcs to attain a higher voltage. This may be due to constriction of the column which is governed by dissociation and thermal effects such as a sudden drop in the thermal conductivity of the gas at a critical temperature (King 1954, Gambling and Edels 1956) and the finite times required for these ionising and de-ionising influences to allow the column reach the critical temperatures.

At currents of 0.5 A to 0.8 A, occasional arc to glow transitions occurred (Fig. 4.9) which had durations too short for the column to cool down and de-ionise sufficiently to have the lower conductivity of a glow column. This caused the voltage across the temporary glows to be lower than the normal glow value.

It is therefore possible by changing the output voltage and series resistance of the power supply to affect the resulting glow to arc transitions to decrease or increase the current, voltage and duration of the temporary arcs.

4.3 ARC IGNITION USING DC DISCHARGES

Little work has been carried out in analysing the requirements for non-contact ignition of dc arcs. In the work in this section the requirements of the initial conducting path (starting discharge) to allow the main arc to establish are investigated experimentally. The combined discharge which is supplied by the two power sources is also examined and an attempt has been made to find analytically the minimum requirements of a dc ignition source for the non-contact ignition of dc arcs by considering the electrical circuit.

4.3.1 Stages in the Development of an Arc and a Summary of the Investigations

Non-contact ignition uses two power sources. A high voltage source to breakdown the gap and provide sufficient ionisation to allow the flow of the main dc current, and a main arc power supply. The developments leading to the establishment of the arc may be divided into four stages as follows:

i) Breakdown of the gap by the application of a high voltage using an external dc source.

ii) Establishment of a dc starting discharge which provides a suitable conduction path for the main power source current.

iii) Beginning of the main dc current flow and formation of a combined discharge supplied by both dc power sources.

iv) Increase of the main current at a rate determined by the discharge and the main power source characteristics, to the minimum required arc current (I_{min}) to sustain the arc.

The first stage may occur by having an ignition source of output voltage at least equal to the breakdown voltage of the gap. Breakdown of the gap does not

however guarantee arc ignition and the second stage must then take place.

The suitable conduction path was examined separately by using steady-state dc glow and arc discharges as the starting discharges to allow the flow of the main dc current to initiate dc arcs (section 4.3.2). This method eliminated any difficulties or uncertainties that the breakdown stage may cause. The use of a continuous discharge eliminated the need for a high di/dt arc power source which would be necessary when a short duration starting discharge is used.

The combined discharge during the third stage, was studied using a steady-state dc discharge supplied by two power sources simultaneously (section 4.3.3). This made it possible to find the relationship between the combined discharge voltage and current, and the open circuit voltages and series resistances of the two power sources.

In the fourth and last stage just after the formation of the combined discharge, until I_{min} is reached, the main current increases at a rate governed by the output voltages and source impedances of the two power sources and the behaviour of the combined discharge.

The main arc may be self-maintained only when the main current reaches a minimum value. The starting discharge (or ignition pulse) should therefore exist for a time sufficient for it to be self-sustained.

By knowing the current and duration of the ignition pulse which should allow the main current reach I_{min}, the parameters of the ignition source were then found.

4.3.2 Requirements of the Starting Discharge

A series of investigations using copper electrodes made of 17 mm diameter rods with hemispherical ends with 3 mm separation in air at atmospheric pressure, were carried out to
i) find the limiting values of voltage, current, and power of the starting discharge to achieve ignition,
ii) determine whether the physical mechanisms of the starting discharge, for example glow or arc, affect the ignition process.

Three different dc power supplies were used to obtain a wide range of output voltages up to 2 kV and output currents up to 20 A to maintain the discharge. The circuit used for these investigations is shown in Fig. 4.11 (Saiepour and Harry 1990).

The type of starting discharge whether glow or arc did not appear to be important, as long as the condition $V_{OC2}>V_{d1}$ where V_{OC2} is the open circuit voltage of the main source and V_{d1} is the discharge voltage supplied by the starting power source alone, was satisfied. Provided the main power supply was able to maintain the main arc, there appeared to be no limiting values for the starting discharge voltage, current or power to allow the arc to develop.

A further series of investigations, using glow discharge currents of about 0.2 A and voltages of about 420 V as the starting discharge, showed that even when V_{OC2} at about 400 V, was less than V_{d1}, and the glow discharge appeared to be stable, the main arc initiated. The reason for this effect was found to be due to the temporary (100 μs - 300 μs) decreases in the starting discharge voltage to about 100 V. This was because of the occasional glow to arc transitions (section 4.2) which appeared to last long enough under these experimental conditions, for the main current to

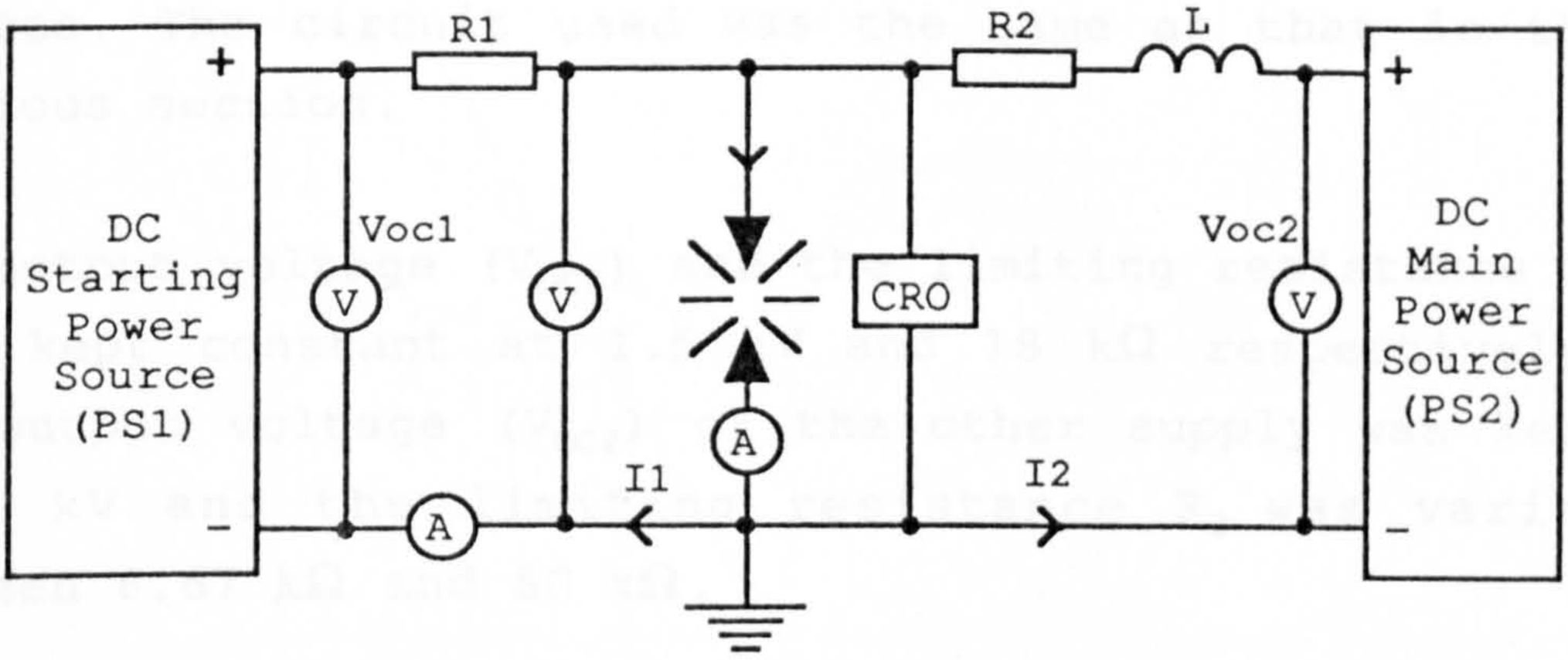

Fig.4.11 Circuit used for investigating the requirements of DC starting discharges.

reach the required I_{min} of about 0.4 A to 3 A (Chap. 3) to sustain the arc.

4.3.3 Variation of Voltage with Current of One Discharge Supplied by Two Power Sources

The ignition source causes breakdown of the gap and establishes the starting discharge and the main power supply adds its current to this. A series of investigations using static glow discharges of currents up to 140 mA was carried out to determine the variation of the combined discharge voltage with current, and series resistance and output voltage of the two power sources. The circuit used was the same as that in the previous section.

The output voltage (V_{OC1}) and the limiting resistance R_1 were kept constant at 1.5 kV and 18 kΩ respectively, the output voltage (V_{OC2}) of the other supply was kept at 1 kV and the limiting resistance R_2 was varied between 6.67 kΩ and 80 kΩ.

Fig. 4.12 shows an example of the measurements carried out for a combined discharge current of about 140 mA and voltage of about 450 V. The combined discharge current (I_d), is the sum of I_1 and I_2 and the operating point lies on the discharge V-I characteristic, but not on any of the two load lines. Therefore:

$$I_1 = \frac{V_{oc1} - V_d}{R_1} \quad , \quad I_2 = \frac{V_{oc2} - V_d}{R_2}$$

$$\text{and} \quad I_d = \frac{V_{oc1} - V_d}{R_1} + \frac{V_{oc2} - V_d}{R_2} \qquad (4.1)$$

Equation (4.1) describes the combined discharge voltage (V_d) and current related to the output voltage and resistance of the two power sources.

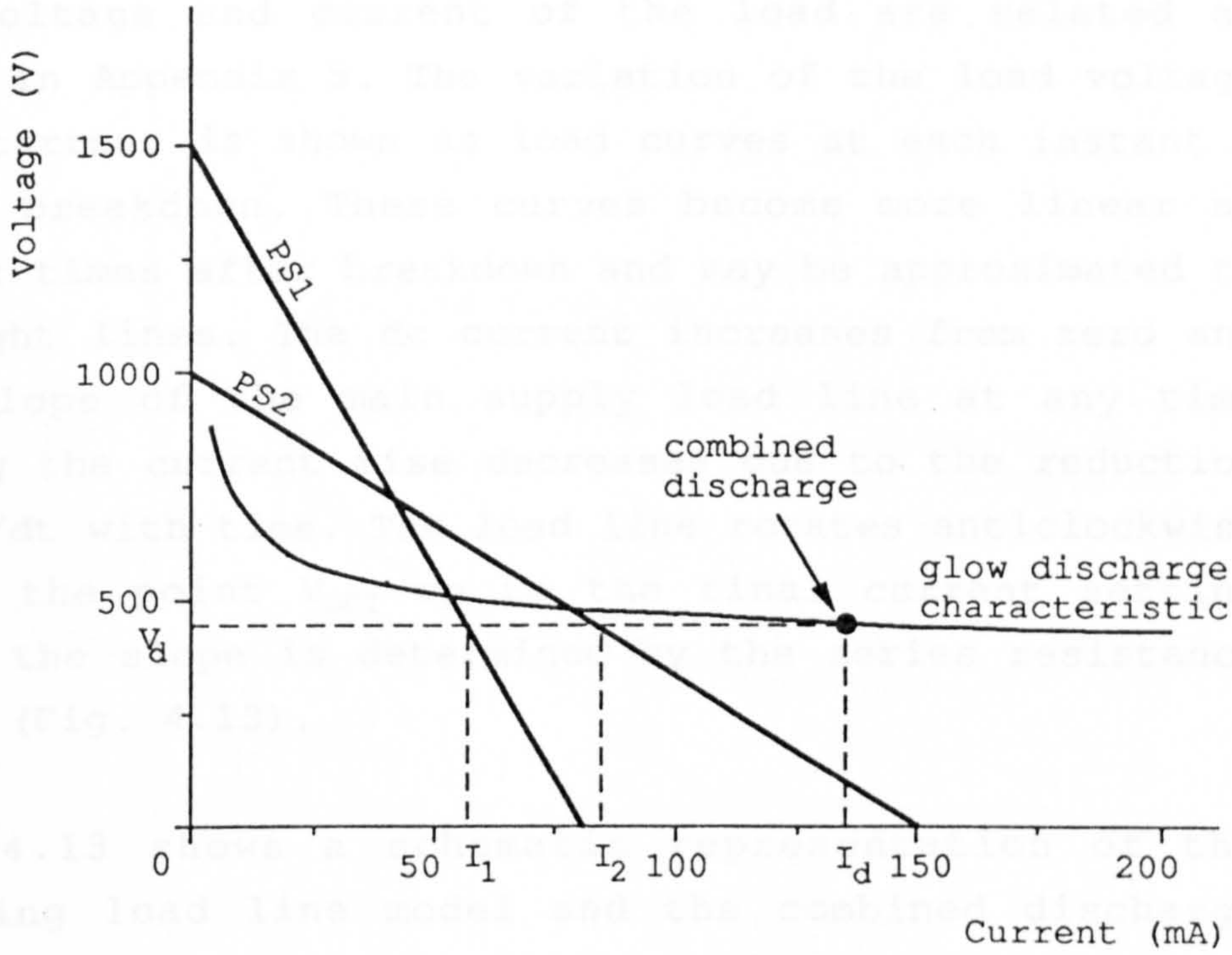

Fig.4.12 Variation of the combined discharge voltage and current with output voltage and resistance of the two power sources.

4.3.4 Variation of Current with Time During the Initial Current Rise

The ignition process may be regarded as complete when the arc current reaches a minimum value (I_{min}) to sustain the arc.

During the initial current rise in an inductive circuit the voltage and current of the load are related as shown in Appendix 5. The variation of the load voltage with current is shown as load curves at each instant t after breakdown. These curves become more linear at longer times after breakdown and may be approximated to straight lines. The dc current increases from zero and the slope of the main supply load line at any time during the current rise decreases due to the reduction in di/dt with time. The load line rotates anticlockwise about the point V_{OC2} up to the final current setting where the slope is determined by the series resistance alone (Fig. 4.13).

Fig. 4.13 shows a schematic representation of the rotating load line model and the combined discharge during the current rise. The slope of the rotating load line determines the position of the operating point (or combined discharge), and the load line intersects the V-I curve at the time when the arc becomes self-sustained. Equation (4.1) was therefore modified to give the combined discharge current (i_d) during the current rise:

$$i_d = \frac{V_{OC1} - v_d}{R_1} + i_2 \qquad (4.2)$$

where i_2 is the instantaneous discharge current supplied by the main power source. For ignition to be achieved i_2 must become higher than I_{min}.

The combined discharge resistance (r_d) in series with R_2 at any time (t) during the initial current rise may

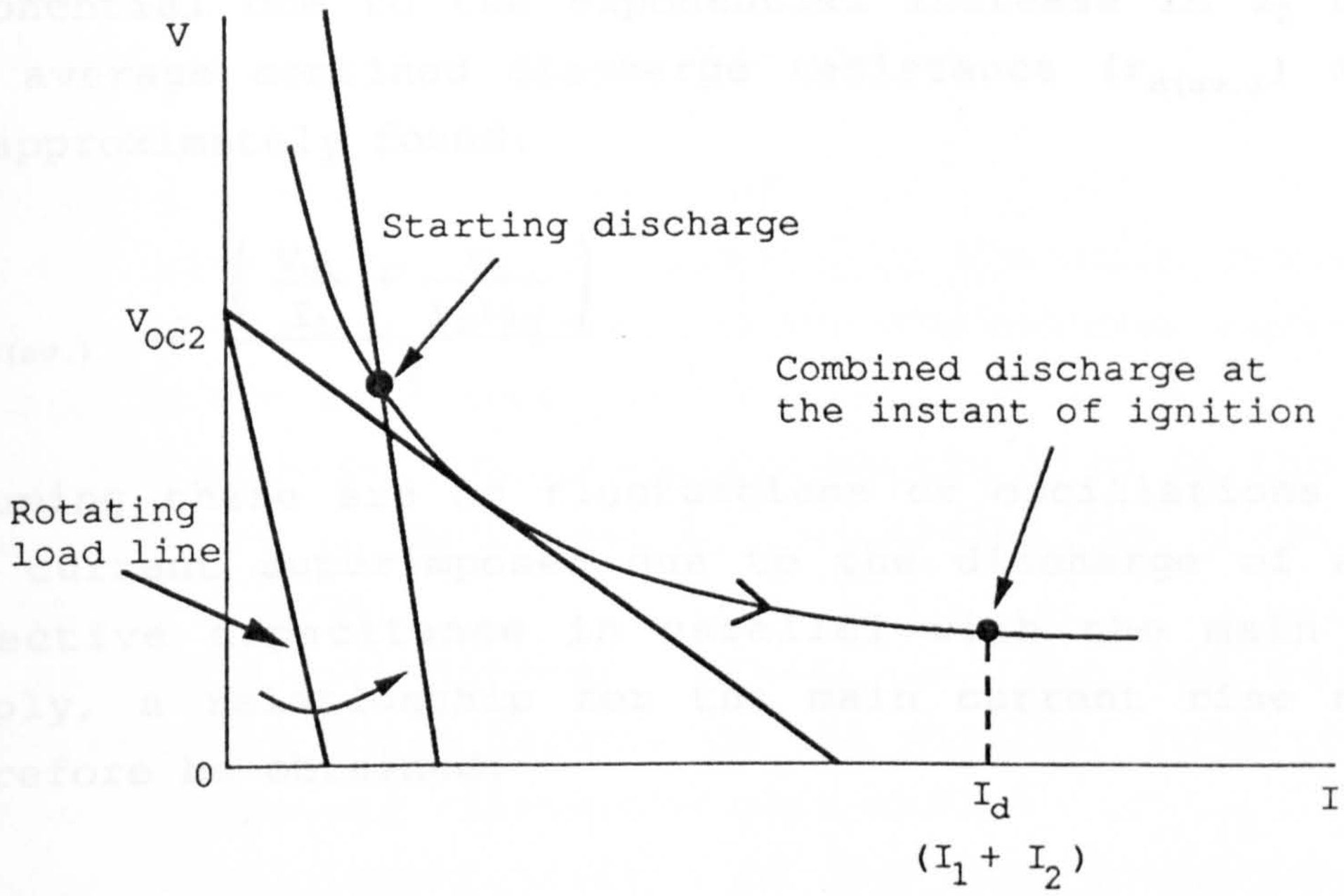

Fig.4.13 Rotating load line model.

be given by:

$$r_d = \frac{v_d}{i_1+i_2}$$

where v_d, i_1 and i_2 are variables which are interrelated during the initial current rise by equation (4.2).

The discharge resistance (r_d) decreases with time from V_{d1}/I_1 at t=0 to $v_d/(i_1+i_2)$ at t. The decrease in r_d is exponential due to the exponential increase in i_2 but the average combined discharge resistance ($r_{d(av.)}$) may be approximately found:

$$r_{d(av.)} = \frac{\left(\frac{V_{d1}}{I_1} + \frac{v_d}{i_1+i_2} \right)}{2}$$

Assuming there are no fluctuations or oscillations in the current superimposed due to the discharge of any effective capacitance in parallel with the main dc supply, a relationship for the main current rise may therefore be obtained:

$$i_2 = \frac{V_{oc2}}{r_{d(av.)} + R_2} \left[1 - e^{-\left(\frac{r_{d(av.)} + R_2}{L} \right) t} \right] \qquad (4.3)$$

and the time to reach i_2 is given by:

$$t = \frac{L}{r_{d(av.)} + R_2} \ln \left[\frac{1}{1 - \frac{i_2 \left(r_{d(av.)} + R_2 \right)}{V_{oc2}}} \right] \qquad (4.4)$$

Hence the duration of the ignition pulse (t_{min}) to allow the arc current reach I_{min} can be calculated by substituting the value of I_{min} for i_2 in equation 4.4.

4.3.5 Discussion of Results of Investigations on Arc Ignition Using DC Discharges

It has been shown that the dc starting discharge supported by the ignition source alone must have a voltage less than the open circuit voltage of the main power supply. It must exist for a time (t_{min}) given by equation (4.4) to allow the main current to reach a minimum required value to sustain the arc. The power sources and the discharge characteristics are of significance to the determination of t_{min}.

Equation 4.4 shows the effect of
(a) any inductance or resistance in the main current path which are also affected by the output current setting of the main supply;
(b) the discharge resistance during the rise in the dc current which is decreased by increasing the starting discharge current;
(c) the required minimum current for the arc to be self-sustained which depends on the physical conditions or free parameters within the gap; and
(d) the open circuit voltage of the main power supply which may be affected by ripple in its output.

The results may be used to find the minimum requirements of a dc ignition source (i.e. V_{OC1}, R_1, I_1, and t_{min}) for non-contact arc initiation by knowing the breakdown voltage of the gap, the value for I_{min} and the parameters of the main power supply (i.e. V_{OC2}, R_2, and L). The ignition of a 3 mm TIG welding arc with a breakdown voltage of about 3 kV, supplied by a dc power source of open circuit voltage of 80 V, would require a starting discharge current of at least 0.5 A to have its voltage less than 80 V. The maximum series resistance (R_1) for the ignition source can then be found:

$$R_1 = \frac{3000 - 80}{0.5} = 5840\ \Omega$$

Assuming that the main dc power supply has a maximum output current of 80 A, it will have a series resistance $R_2 = 1\ \Omega$. The series inductance L may have values up to 100 mH.

For non-contact arc ignition the cold arc V-I characteristics must be considered and a value of I_{min} for the cold arc must be used. A value of 0.4 A is suggested by Brown (1976), having a voltage of 25 V - 40 V (or higher) across it.

Therefore by applying equation (4.4), it is possible to find t_{min}

$$t_{min} = \frac{L}{r_{d(av.)} + 1} \ln \left[\frac{1}{1 - \frac{0.4 \left(r_{d(av.)} + 1 \right)}{80}} \right]$$

where $r_{d(av.)}$ is

$$r_{d(av.)} = \frac{\frac{80}{0.5} + \frac{v_d}{0.5+0.4}}{2}$$

Assuming a value for v_d of about 40 V, a series of values for t_{min} for different inductances have been calculated (Table 4.1).

L (mH)	t_{min} (μs)
2	14
4	28
8	56
16	112
32	224
50	350
100	700

Table 4.1 Variation of the minimum time required for an arc to become self-sustaining with inductance.

For a series inductance of 8 mH, the ignition source should have an output voltage of at least 3 kV with a series resistance of maximum value of 5.8 kΩ, and the output pulse should last for at least 56 μs to initiate a 3 mm TIG welding arc from cold using a dc power supply with an open circuit voltage of 80 V.

4.4 ARC IGNITION USING SINUSOIDAL HF DISCHARGES

The use of a high voltage dc pulse for arc ignition is one hundred percent reliable only if the duration of the ignition pulse is several seconds long to allow the arc to reach its steady state condition after initiation from cold. The requirement for a long duration pulse makes the high voltage dc method unsafe.

The use of spark gap oscillators to obtain hf sparks to break down and ionise the gap is relatively safe because the hf current does not penetrate the human body but tracks across the skin. Due to the short duration (5 μs - 10 μs) of each hf spark and the occurrence of many thousands of sparks before the arc strikes, severe radio frequency interference is caused (Chap. 3).

An alternative method to eliminate radio frequency interference and maintain safety, has been investigated by applying a continuous sinusoidal hf voltage to provide a single (reliable) breakdown followed by a suitable continuous hf starting discharge to allow the main arc to establish.

The purpose of the work in this section is to investigate the characteristics of steady-state ac discharges combined with dc discharges and obtain V-I curves by measuring the dc voltage and current of the ac-dc combined discharge. These represent the various stages during the continuous sinusoidal hf ignition process.

4.4.1 Test Gap Conditions and Power Sources

During the initial stages of hf ignition there is a combined ac-dc discharge which may be of short duration and difficult to investigate. Steady-state combined ac-dc discharges were used to carry out a series of tests to show the effect of ac combined with dc on the discharge characteristic.

The use of low current hf discharges of less than 100 mA, made it possible to make visual observations, they were in general easier to measure and were more stable than discharges of currents higher than about 0.4 A.

The arc during ignition from cold is a cold cathode (non-thermionic) arc even with tungsten cathodes, as a result copper electrodes were used. These were 17 mm diameter rods with rounded ends to keep the discharge central, fitted in a calibrated rack and pinion to vary the gap separation horizontally. A 3 mm gap separation in air at atmospheric pressure was chosen to represent typical gaps used for non-contact arc ignition at atmospheric pressure such as welding arcs.

Measurements were made using ac peak currents of 100 mA for the combined ac-dc glows and 1 A for arcs at a frequency of 20 kHz.

The electrical circuit is shown in Fig. 4.14. The ac current was supplied by the valve audio amplifier already described in section 4.1.1. The dc current was supplied by either a high voltage low current power supply or a low voltage high current source with LC smoothing. Capacitor C limits the ac current and blocks the dc current. L is a ferrite core inductor to block the ac current to protect the dc source and prevent loss of hf power due to diversion of the ac current. The dc current was limited by a switched bank of resistors.

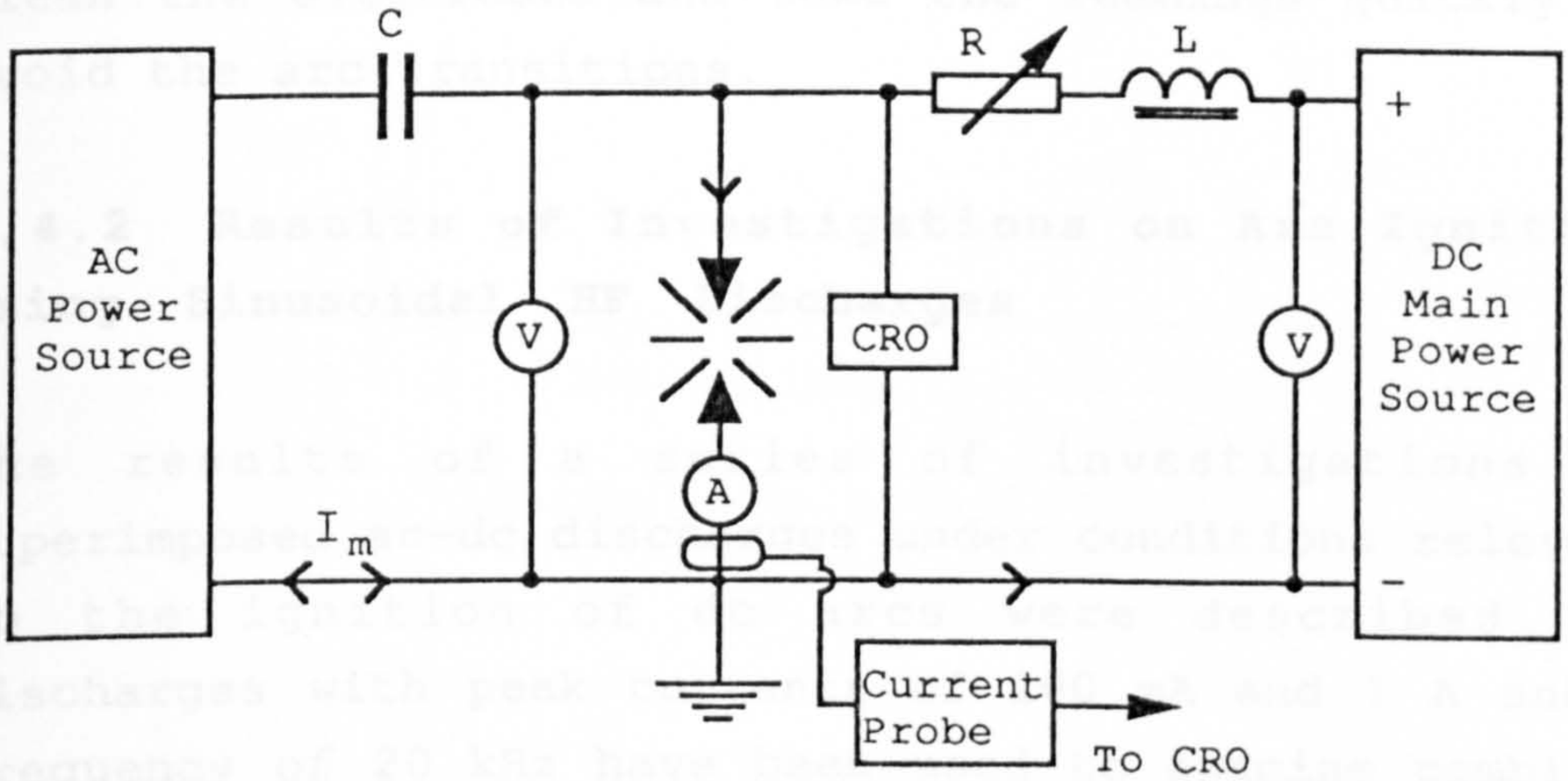

Fig.4.14 Circuit used for investigating the characteristics of combined ac-dc discharges.

The variation of the dc voltage across the combined discharge with dc current through it was measured, by first establishing an hf discharge either by breakdown, or touch started. The dc output voltage was then gradually increased for various values of series resistances. The dc voltage and dc current of the combined discharge were then measured.

When the hf discharge current was about 0.4 A - 0.6 A glow to arc transitions caused uncertainties in the measurements, and at these currents care was taken to clean the electrodes and take the readings quickly to avoid the arc transitions.

4.4.2 Results of Investigations on Arc Ignition using Sinusoidal HF Discharges

The results of a series of investigations on superimposed ac-dc discharges under conditions relevant to the ignition of dc arcs were described. HF discharges with peak currents of 100 mA and 1 A and a frequency of 20 kHz have been used to examine combined ac-dc discharges between horizontal copper electrodes at 3 mm separation in air at atmospheric pressure.

Figs. 4.15a and 4.15b show the variation in the dc voltage across the combined discharge with the dc current, for hf discharge currents of 100 mA and 1 A respectively.

The current in the discharge is made up of the sum of the ac and dc currents. When the ac and dc currents flow in the same direction (positive half cycle) through the discharge, they add up, and when they are opposite (negative half cycle), they subtract. An ac-dominated discharge indicated by the positive slope of the V-I curves is formed when the peak ac current is greater than the dc current through the discharge. A dc-dominated discharge indicated by the negative slope

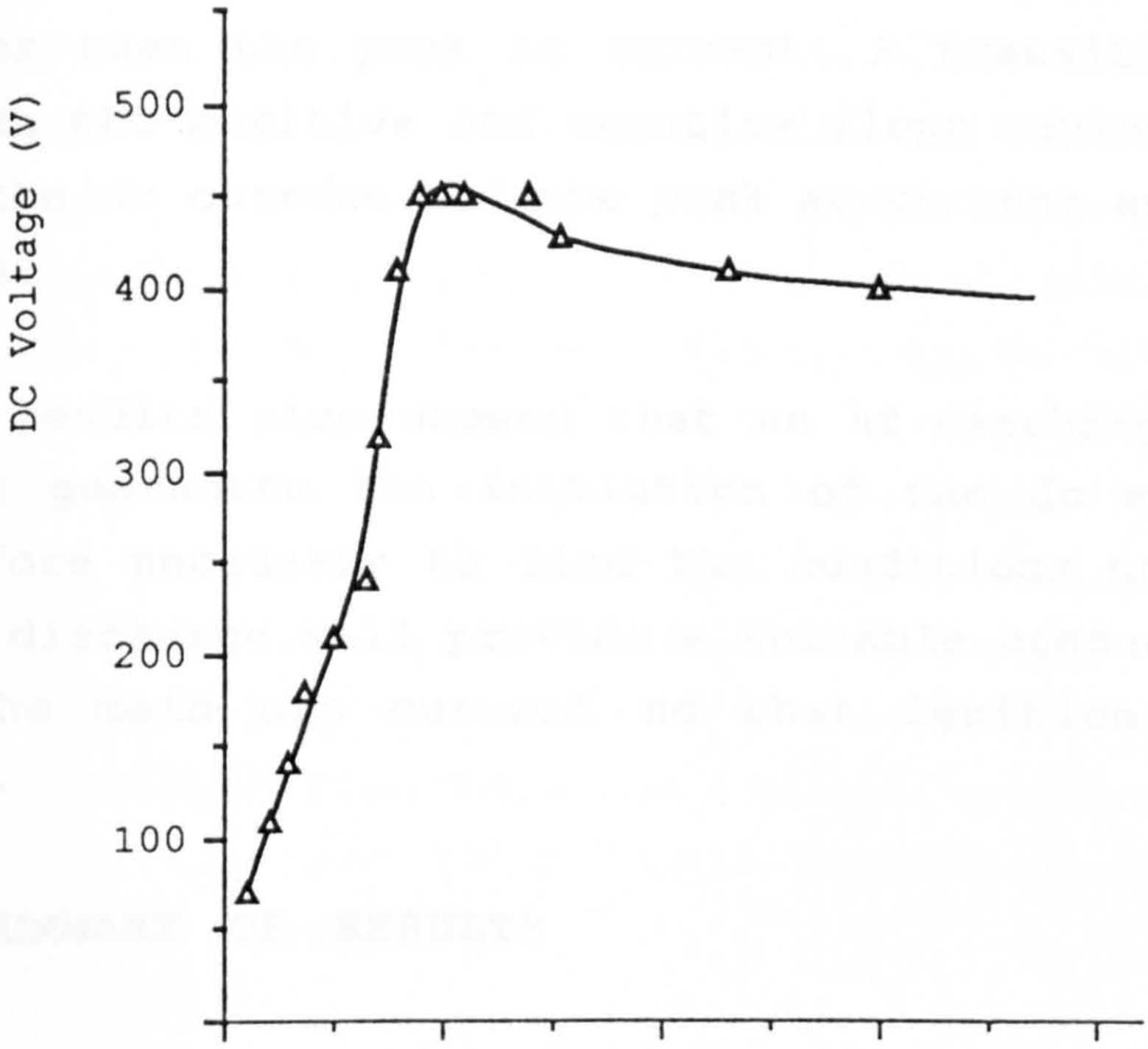

a) Combined ac-dc glow discharge

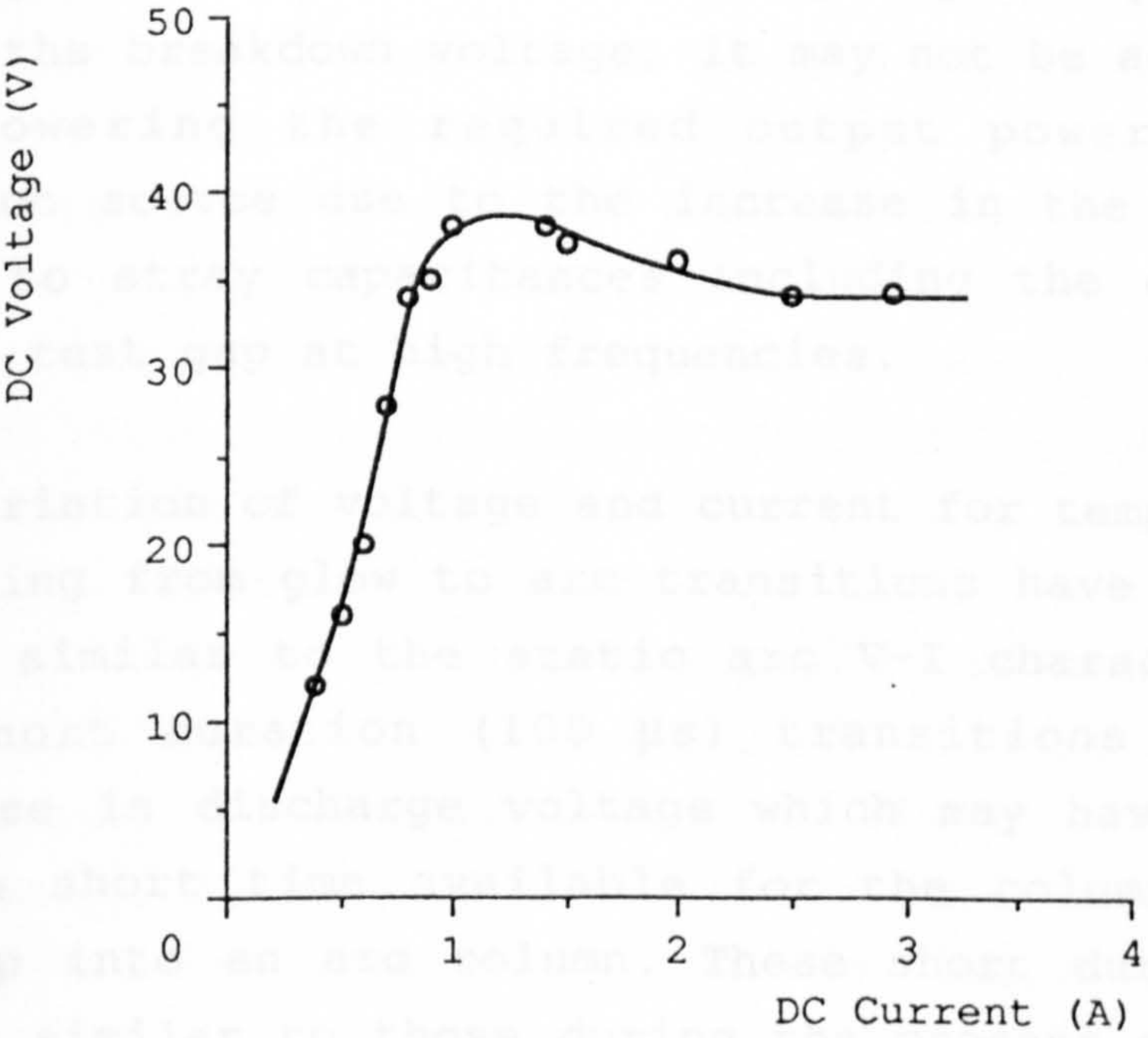

b) Combined ac-dc arc discharge

Fig.4.15 Variation of dc voltage with dc current for a combined 20 kHz discharge of ac peak current of a) 100 mA and b) 1 A.

of the V-I curve which is similar to normal dc discharge curves and is obtained when the dc current is greater than the peak ac current. A transition region between the positive and negative slope regions results when the dc current and the peak ac current approach in values.

These results also showed that an hf discharge did not always guarantee the initiation of the dc arc. It is therefore necessary to find the conditions under which an hf discharge will provide a suitable conduction path for the main arc current so that ignition may take place.

4.5 SUMMARY OF RESULTS

Measurements using frequencies up to 800 kHz did not indicate a reduction in the breakdown voltage of the arc gap. Although the use of very high frequencies may lower the breakdown voltage, it may not be advantageous for lowering the required output power from the ignition source due to the increase in the power loss owing to stray capacitances including the capacitance of the test gap at high frequencies.

The variation of voltage and current for temporary arcs resulting from glow to arc transitions have been shown to be similar to the static arc V-I characteristics. The short duration (100 μs) transitions caused an increase in discharge voltage which may have been due to the short time available for the column to fully develop into an arc column. These short duration arcs may be similar to those during the process of ignition from cold and therefore will be investigated in Chap. 5. The voltage and current of the resulting temporary arcs are affected by the electrical circuit parameters such as the open circuit voltage and series resistance.

For a non-contact dc ignition source the starting

discharge voltage should be less than the output voltage of the main source to allow the main dc current to flow and it should exist for a time determined by the transient behaviour of the circuit and the discharge supplied by the two power sources during ignition. To obtain one hundred percent reliability of ignition, the ignition pulse must exist continuously until the final steady-state arc on the static characteristic is reached. This is unsafe if a dc starting pulse is used therefore an hf voltage is necessary. To obtain the minimum requirements of a non-contact ignition system, the characteristics of arcs during ignition from cold and minimum values of current (I_{min}) for the arc to be self-sustained need to be investigated (Chap. 5).

The use of sinusoidal hf voltages has been examined as a safe, RFI-free and reliable ignition method. The investigations showed that three types of discharge exist. An ac-dominated discharge represented by the positive slope of the V-I curve, a dc-dominated discharge represented by the negative slope region similar to the normal dc glow and arc discharge V-I curves, and a transition region between the negative and positive slope regions. The existence of an hf discharge did not always guarantee arc initiation and therefore minimum requirements for a sinusoidal hf ignition source by carrying out measurements of the characteristics of combined ac-dc discharges over a wide range of frequencies (10 kHz - 800 kHz) and currents of 50 mA - 2 A for both copper electrodes in air and TIG arc gaps will be carried out in Chap. 6.

The work described in this chapter has been published as detailed below:

(1) SAIEPOUR, M., HARRY, J.E., 'Temporary arc discharges resulting from glow to arc transitions and effect of power supply parameters', International Journal of Electronics, 70, (2), pp. 459-465, 1991.

(2) SAIEPOUR, M., HARRY, J.E., 'Arc ignition using DC discharges', International Journal of Electronics, 70, (2), pp. 467-474, 1991.

CHAPTER 5

STUDY OF ARC INITIATION BY NON-CONTACT FROM COLD TO THE STEADY-STATE CONDITION

5.0 STUDY OF ARC INITIATION BY NON-CONTACT FROM COLD TO THE STEADY-STATE CONDITION

The ignition source causes spark breakdown and allows the initial developments in the arc to take place. A glow structure is first formed, a diffuse glow develops and a filamentary glow is then established, after which a transition to an arc phase takes place, all of which occur in less than 1 μs (Cavenor and Meyer 1969). The development of the arc to the steady-state condition takes place over a much longer period supported by the main power supply.

The objective of this work was to
i) determine the minimum current required for an arc to be self-sustaining after breakdown from cold,
ii) examine the different transitions leading to steady-state conditions,
iii) measure the variation of voltage with current of the thermally undeveloped (or cold) arcs and
iv) investigate the time taken to reach the final steady-state.

5.1 ELECTRODE CONFIGURATIONS, POWER SOURCES AND EXPERIMENTAL PROCEDURE

The measurements were carried out at atmospheric pressure. The maximum gap separation in air was limited to 3 mm by the breakdown voltage. The cathode was a 2.4 mm diameter copper rod or 2% thoriated tungsten rod and the anode was a 17 mm diameter copper rod; both cathode and anode had hemispherical ends to keep the discharge central. The investigations on TIG arcs used a typical TIG torch as described in Chap. 4.

Continuous power sources normally have a low rate of current rise (10^3 As^{-1} - 10^4 As^{-1}). Long duration starting pulses of the order of 1 ms to achieve ignition would be required (Chap. 4.3). These will

affect the measurements due to the addition of the starting pulse current with the main current during the current rise. A capacitor discharge supply was designed and constructed to carry out the investigations. This has the following advantages:

i) The capacitor provides an energy source with a rapid rise of arc current so that the starting pulse can be very short (less than 10 μs).
ii) The point at which the static characteristic is reached as the current decreases, is clearly indicated by a rise in arc voltage due to the negative slope of the static V-I characteristic (Fig. 5.1).
iii) The rate of supply of energy can be changed by changing the values of the capacitance, series resistance and the initial capacitor voltage.

The circuit and measuring instruments used are shown in Fig. 5.2. A single short duration (10 μs) high voltage pulse from the high voltage dc source was applied to the arc gap to cause breakdown.

The main current was supplied from a charged capacitor bank (C_1) of 10000 μF - 37500 μF which was used as a high di/dt source of arc current limited by the series resistance R_1 (1.5 Ω - 60 Ω). The arc current was measured with a current probe and the voltage was measured with a high voltage probe connected to a storage oscilloscope. The arc current decreases from an initial peak as the capacitor discharges, and an increase in arc voltage indicates that the static characteristic is followed due to the negative slope of the static V-I characteristic (Fig. 5.1). A decrease in arc voltage as the current decreases, should indicate that the static characteristic is not yet reached and is still being approached by the cold (or thermally undeveloped) arc. It was therefore possible to find the time taken for the steady-state to develop for different experimental conditions. It was also possible

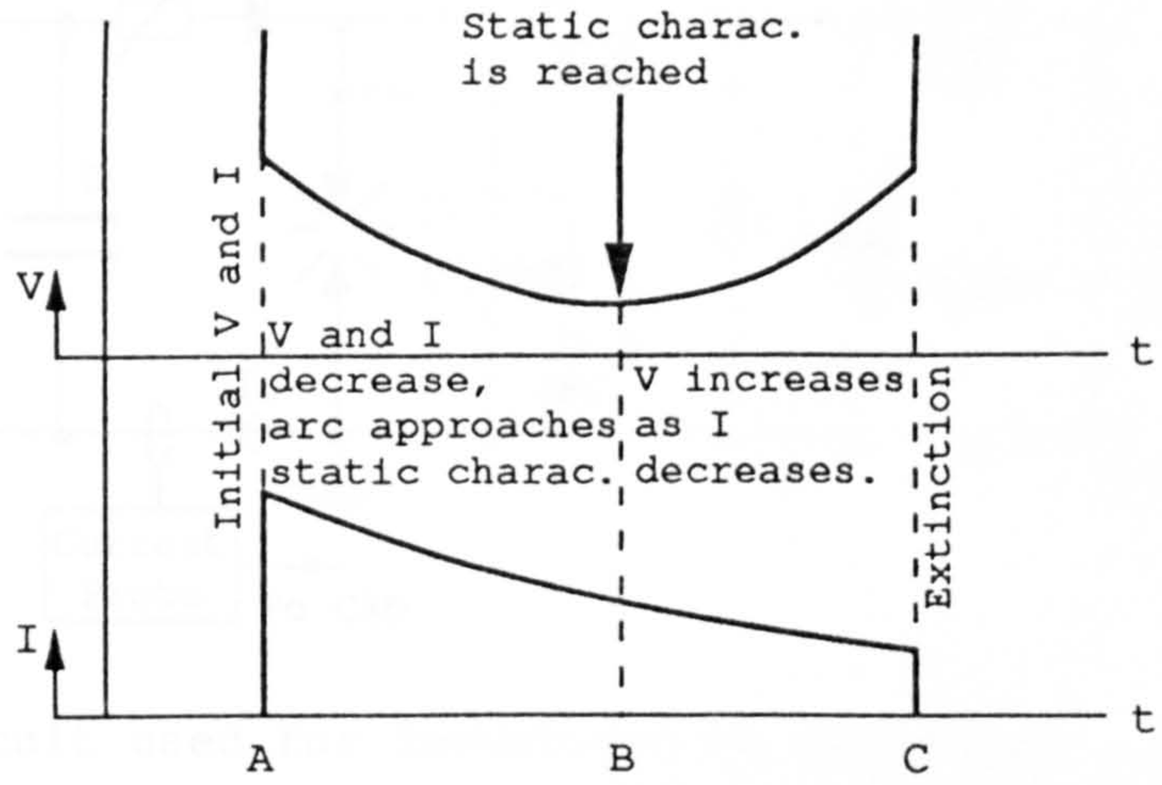

(a) A sketch of a typical oscilloscope trace showing the variation of voltage and current with time.

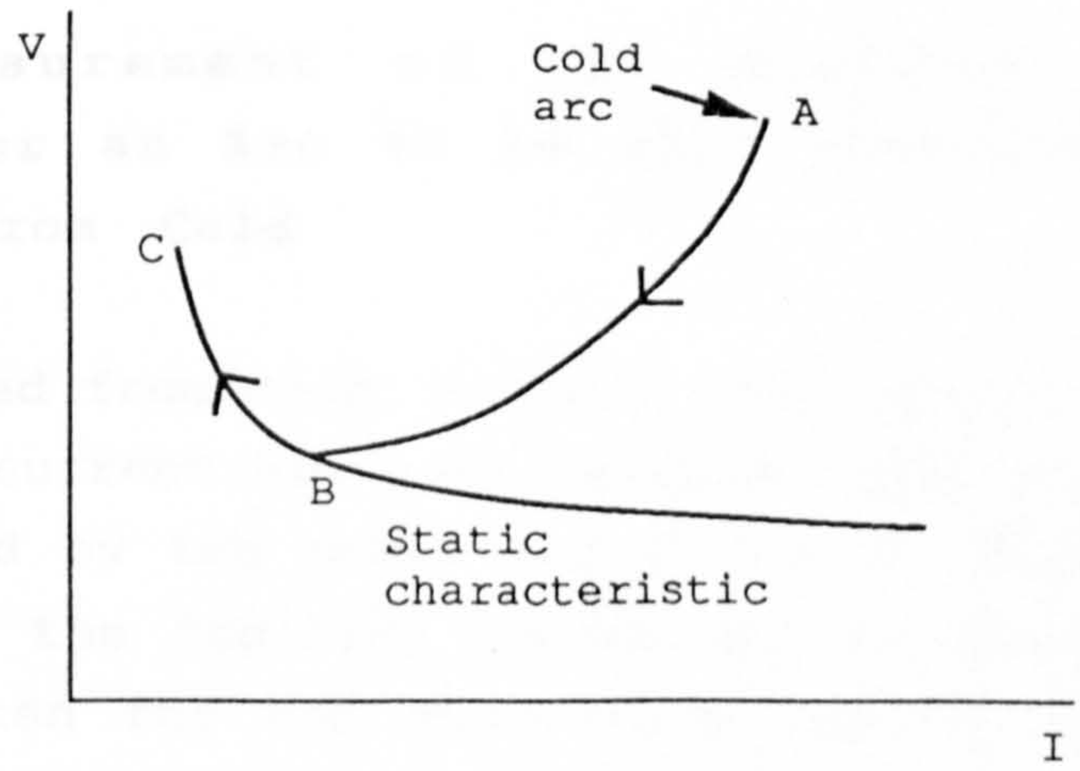

(b) Variation of voltage with current obtained from Fig.5.1a.

Fig.5.1 Variation of arc voltage and current during the development of the steady-state using the capacitor discharge technique.

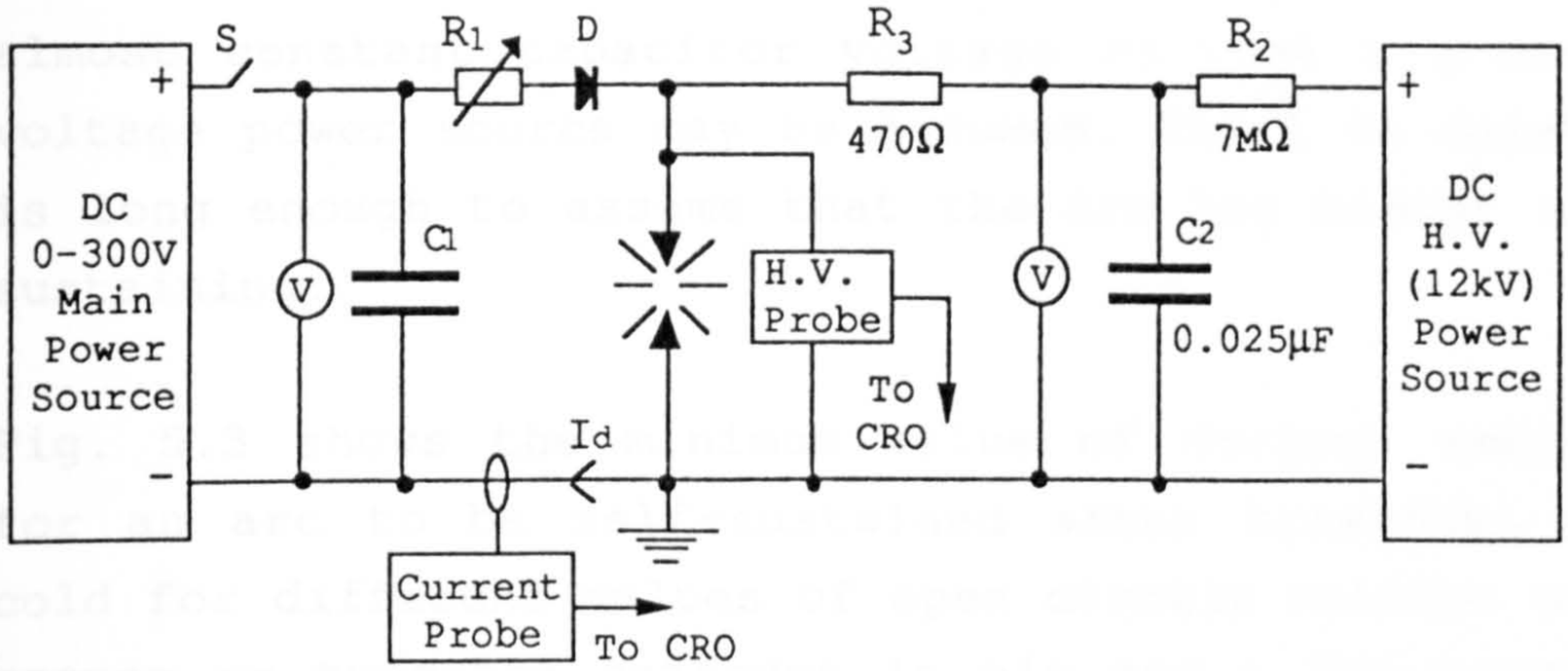

Fig.5.2 Circuit used for investigating non-contact arc initiation using a capacitor discharge technique.

by using suitable values of C_1, R_1 and V_c to make the current increase with different values of di/dt after the establishment of the initial arc current and voltage.

5.2 RESULTS

5.2.1 Measurement of the Minimum Current Required for an Arc to be Self-Sustained after Breakdown from Cold

An arc ignited from cold, becomes self-sustained when a minimum arc current has been reached. When the arc can be maintained by the power supply alone, ignition has occurred and the ignition source may be disconnected. The time taken for the main power source current to reach this minimum current determines how long the ignition source should stay on.

A series of measurements was carried out to determine the minimum current for the cold arc to be self-sustaining (I_{min}), for open circuit voltages of 50 V to 250 V. The initial value of current measured from oscilloscope traces was taken to be the value for I_{min}. The series resistance was gradually decreased until an arc of about 1 ms duration could be maintained after

breakdown. This duration was short enough to keep an almost constant capacitor voltage so that a constant voltage power source may be assumed. The 1 ms duration is long enough to assume that the arc has become self-sustaining.

Fig. 5.3 shows the minimum value of current required for an arc to be self-sustained after breakdown from cold for different values of open circuit voltage using copper or tungsten cathodes in air and a TIG torch in argon. The readings of current vary within the bands shown. The curves are derived from mean values.

Fig. 5.3 also shows that for the same open circuit voltage the values of I_{min} are higher in air than in argon especially for low open circuit voltages. This is because for the same voltage, a discharge in argon has a lower current than in air because argon needs less energy for ionisation than air (Chap. 2).

The results of this section showed that the minimum current to sustain an arc after breakdown from cold depends on the open circuit voltage of the main power supply. The physical phenomenon governing the value of I_{min} under conditions of ignition from cold is complex involving the electrical circuit parameters and the parameters of the gas and the electrodes which require a minimum amount of energy to maintain a cathode spot. The cathode fall voltage affects the electrical and thermal processes taking place at the cathode spot and it maintains at the same time at least three different processes, including electron emission from the cathode, evaporation of the cathode and ionisation of metal vapour from the cathode. It may be that the minimum current for the arc to be self-sustaining is limited by the maximum cathode fall voltage that can be reached. This in turn affects the discharge voltage which is limited by the open circuit voltage. Kesaev (1963 II) studying the stability of arcs in vacuum,

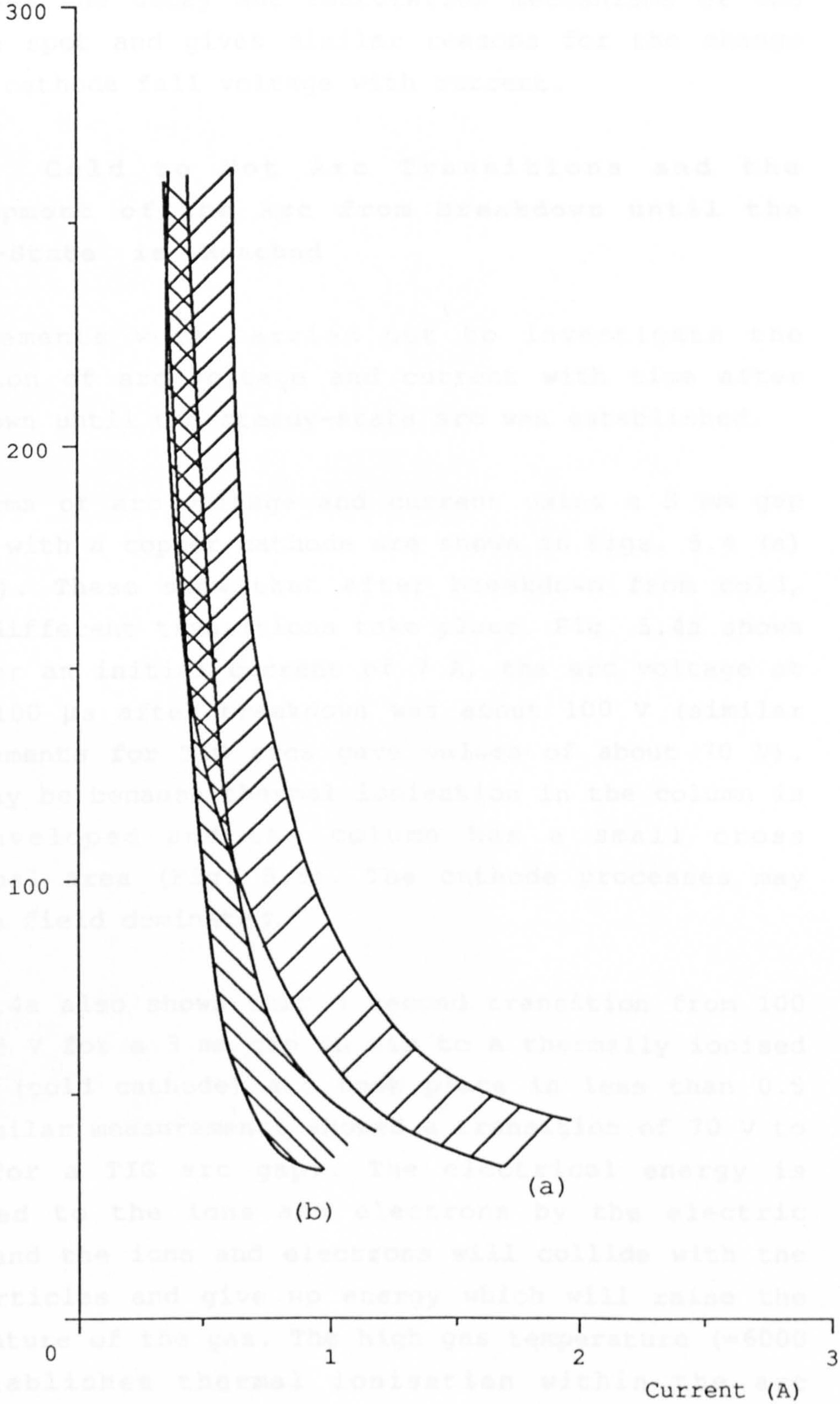

Fig.5.3 Variation of the minimum required current (I_{min}) to sustain a cold arc with open circuit voltage (V_{oc}) for (a) copper or tungsten cathodes in air, (b) TIG arc gap.

discusses the decay and restoration mechanisms of the cathode spot and gives similar reasons for the change in the cathode fall voltage with current.

5.2.2 Cold to Hot Arc Transitions and the Development of the Arc from Breakdown until the Steady-State is Reached

Measurements were carried out to investigate the variation of arc voltage and current with time after breakdown until the steady-state arc was established.

Waveforms of arc voltage and current using a 3 mm gap in air with a copper cathode are shown in Figs. 5.4 (a) and (b). These show that after breakdown from cold, three different transitions take place. Fig. 5.4a shows that for an initial current of 7 A, the arc voltage at about 100 μs after breakdown was about 100 V (similar measurements for TIG arcs gave values of about 70 V). This may be because thermal ionisation in the column is not developed and the column has a small cross sectional area (Fig. 5.5). The cathode processes may also be field dominated.

Fig. 5.4a also shows that a second transition from 100 V to 65 V for a 3 mm gap in air to a thermally ionised column (cold cathode) arc took place in less than 0.5 ms (similar measurements showed a transition of 70 V to 55 V for a TIG arc gap). The electrical energy is supplied to the ions and electrons by the electric field and the ions and electrons will collide with the gas particles and give up energy which will raise the temperature of the gas. The high gas temperature (≈6000 K) establishes thermal ionisation within the arc column. The reduction in arc voltage may have occurred as a result of increase in its cross sectional area (Fig. 5.5) and increase in free charge.

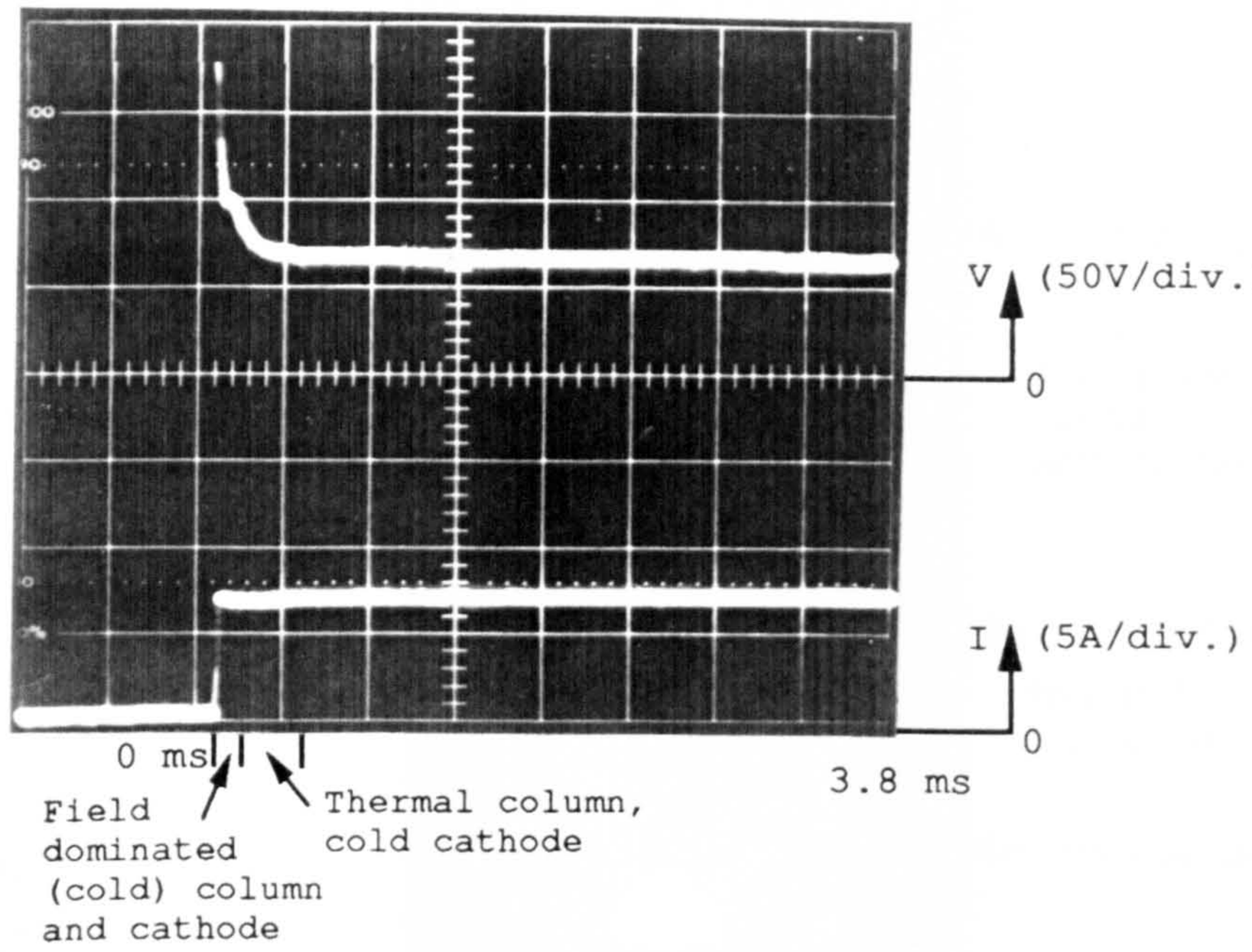

(a) Initial transitions
Time base: 0.5 ms/div.

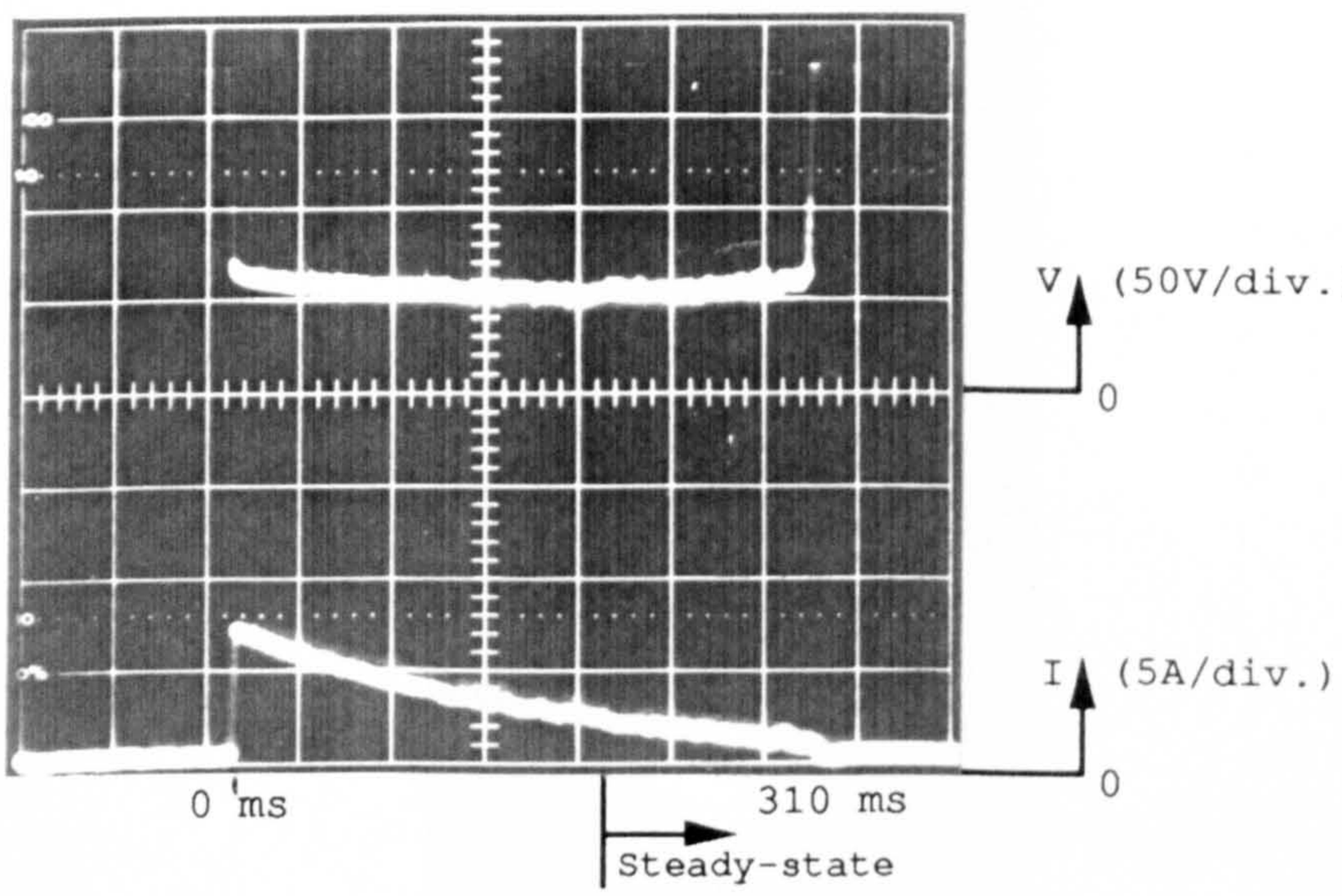

(b) Development of the steady-state
Time base: 50 ms/div.

Fig.5.4 Arc voltage and current waveforms after breakdown from cold. 3 mm gap, air, copper cathode, V_C=250 V, R_1=30 **Ω**.

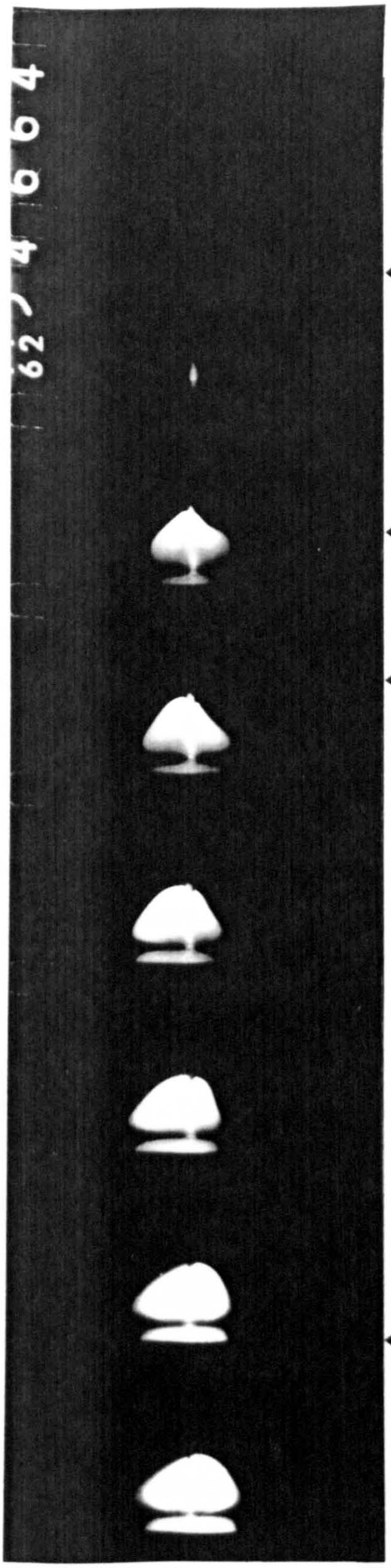

Fig.5.5 High speed ciné photographs of a 3 mm arc gap with a tungsten cathode in air before and after ignition. Initial current=7 A, Kodak TRI-X reversal film, HYCAM 16 mm camera, 3500 frames per second, aperture: f.12.5, Timing marks: 1000 per second, Exposure: 100 μs, Time between frames: 375 μs, 50 mm lens with 25 mm extension.

For short arc gaps of less than 5 mm, the effect of the column on the time taken to establish the final steady-state is insignificant because:

i) The voltage across the column may be only a small proportion of the total arc voltage.

ii) Thermal equilibrium in the arc column is normally reached in less than 1 ms.

Further evidence for the finite time (0.1 ms - 0.5 ms) required for the arc column to develop thermally, is the result obtained in section 4.2 where short duration (100 μs) arcs had higher voltages than steady-state arcs.

In order to substantiate the time taken for the development of the arc column, calculations have been carried out (Appendix 3). A cylindrically symmetrical infinitely long column with a steady-state column temperature of 6000 K and a column diameter of 3 mm has been assumed. These calculations show that under these experimental conditions, the duration required for the column in air is about 0.22 ms and that in argon is about 0.375 ms. These low theoretical values compared to the measured 0.5 ms values to establish a thermally ionised column may be due to the assumption of an arc plasma free of electrode effects which cause cooling and hence delay its development.

Fig. 5.4b shows that a third transition with a much slower reduction in voltage takes place for about 200 ms to a voltage of about 50 V at a current of about 2.5 A, lying on the static characteristic (Appendix 2), after which the voltage increases with a decrease in current following the static characteristic. The arc finally extinguishes at a current determined by the series resistance and the final capacitor voltage.

This transition may be due to heating of the cathode which enhances electron emission and evaporation of the cathode. A reduction in the cathode fall voltage

results due to the lower ionisation potential of metal vapour atoms than gas atoms, hence the arc voltage is reduced.

The time taken to reach the thermal equilibrium is governed by the establishment of a thermally stable cathode spot. This depends on processes such as convection and thermal conduction at the cathode and heat gained from the supplied electrical energy for short arc gaps of less than 5 mm. Fig. 5.6 is a plot of voltage against current determined from Fig. 5.4b which shows a typical transition to the static characteristic over a period of about 310 ms.

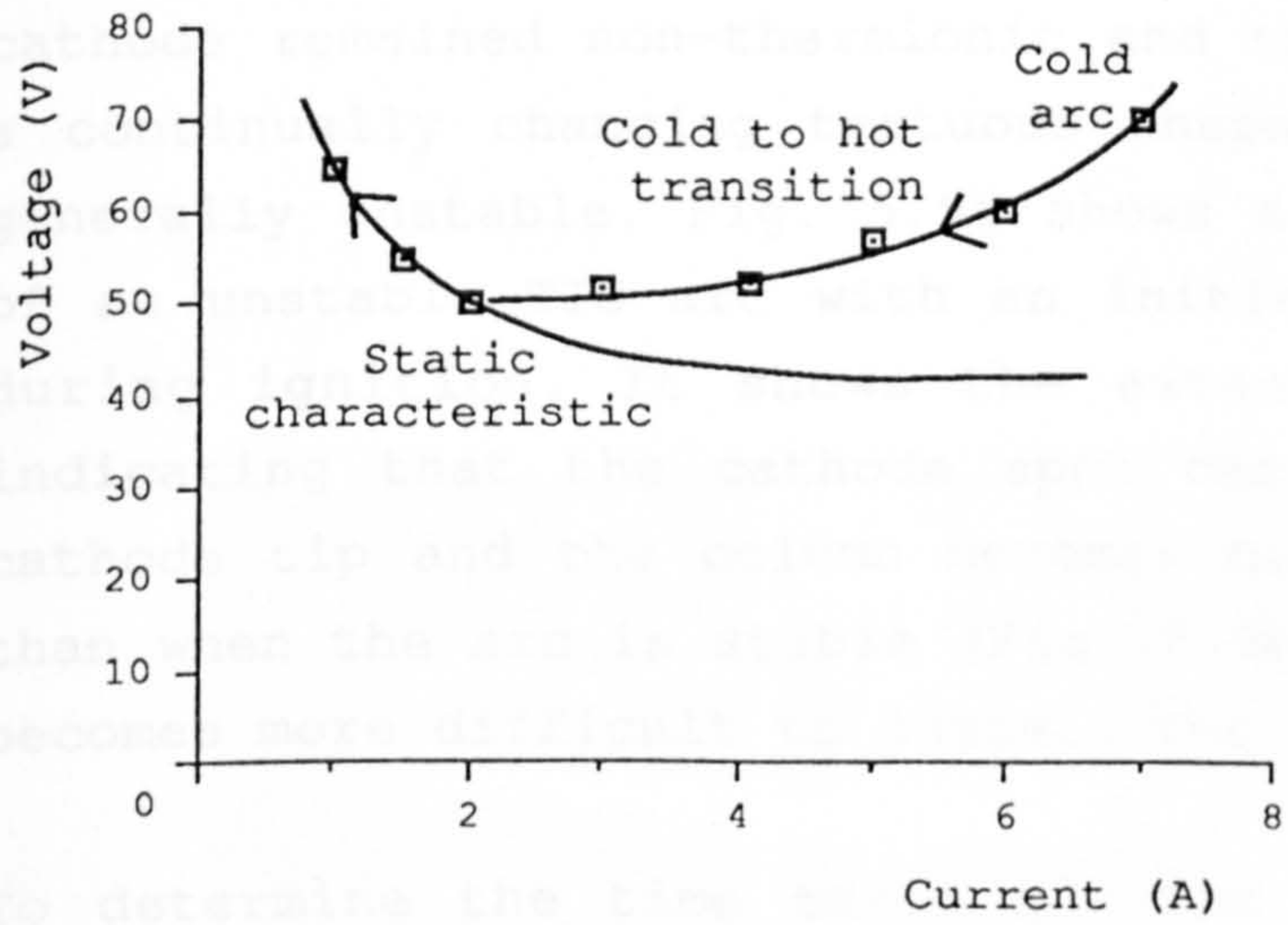

Fig.5.6 Variation of voltage with current of an arc during the cold to hot arc transition, determined from Fig.5.4b.

The initial values of arc voltage and current for both copper and thoriated tungsten cathodes in air were similar which shows that even with a tungsten cathode, the initial arc is non-thermionic. This may be due to the cathode temperature still being too low for thermionic emission to occur. The transition to the static characteristic took longer for tungsten

cathodes. The difference in the time taken to reach the steady-state becomes more apparent with long RC time-constants combined with high initial currents (Fig. 5.7). This shows the effect of the cathode material and the rate of energy supplied on affecting the time to reach the steady-state.

Investigations using TIG arcs, showed that the flow of the shielding argon gas delayed reaching the static characteristic by cooling the cathode. The static characteristic was not reached even after 280 ms for the same conditions as the previous example for a copper cathode in free air (Fig. 5.8). At initial currents of less than 5 A, although the cathode spot formed at the tip of the cathode, after about 1 ms it moved over the whole of the cathode surface. The cathode remained non-thermionic and the column took up a continually changing tortuous shape and the arc was generally unstable. Fig. 5.9a shows a still photograph of an unstable TIG arc with an initial current of 4 A during ignition. It shows the extent of instability indicating that the cathode spot can be far from the cathode tip and the column becomes considerably longer than when the arc is stable (Fig. 5.9b), as a result it becomes more difficult to sustain the arc.

To determine the time taken for the column to expand and examine the behaviour of the cathode spot in a typical TIG arc gap, high speed ciné photographs (Fig. 5.10) were taken. These show that the column in less than 0.5 ms expanded perhaps due to increasing of thermal ionisation, and the cathode spot initially formed on the cathode tip and after about 1 ms moved away.

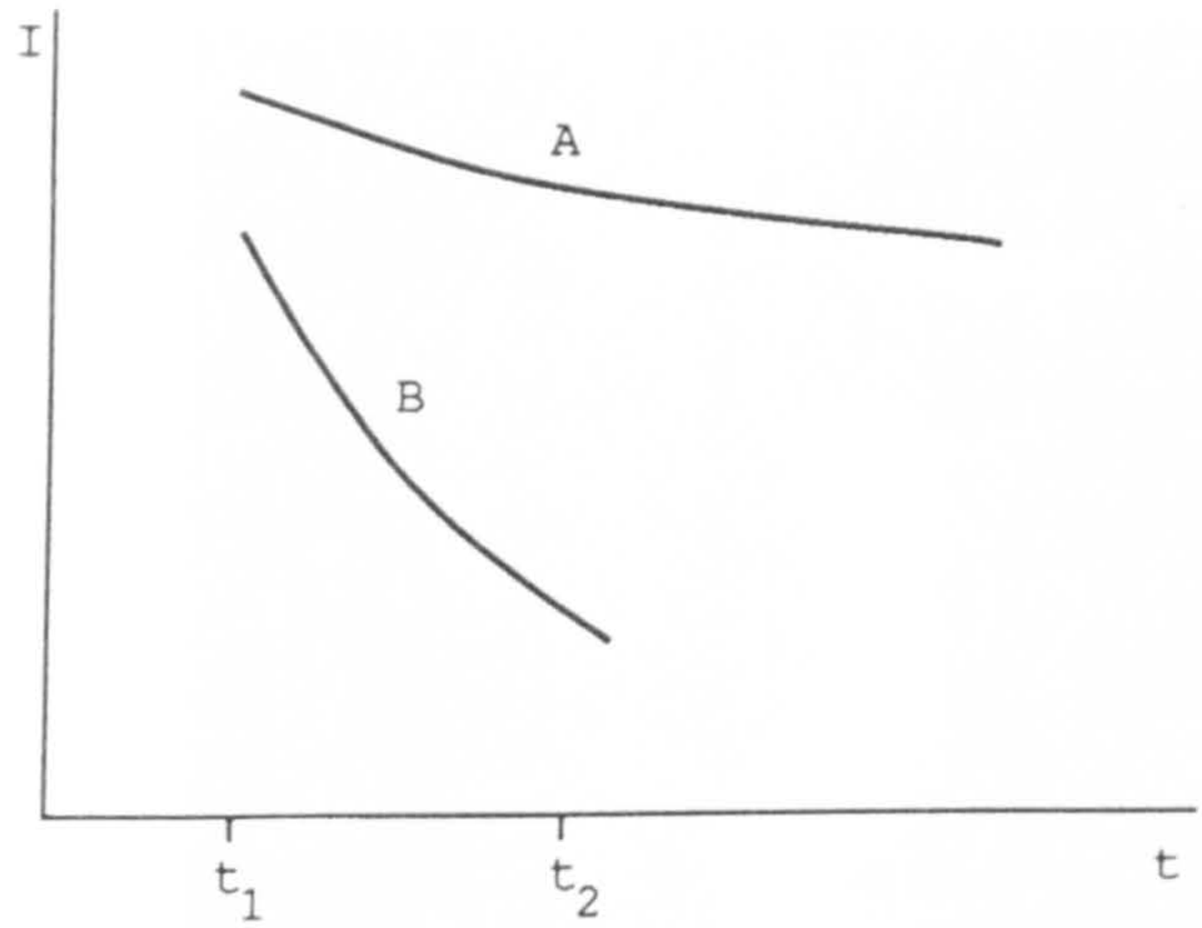

A - High initial current and long RC time-constant.
B - Low initial current and short RC time-constant.

Fig.5.7 More energy is supplied to the discharge when the initial current and/or the RC time-constant are large.

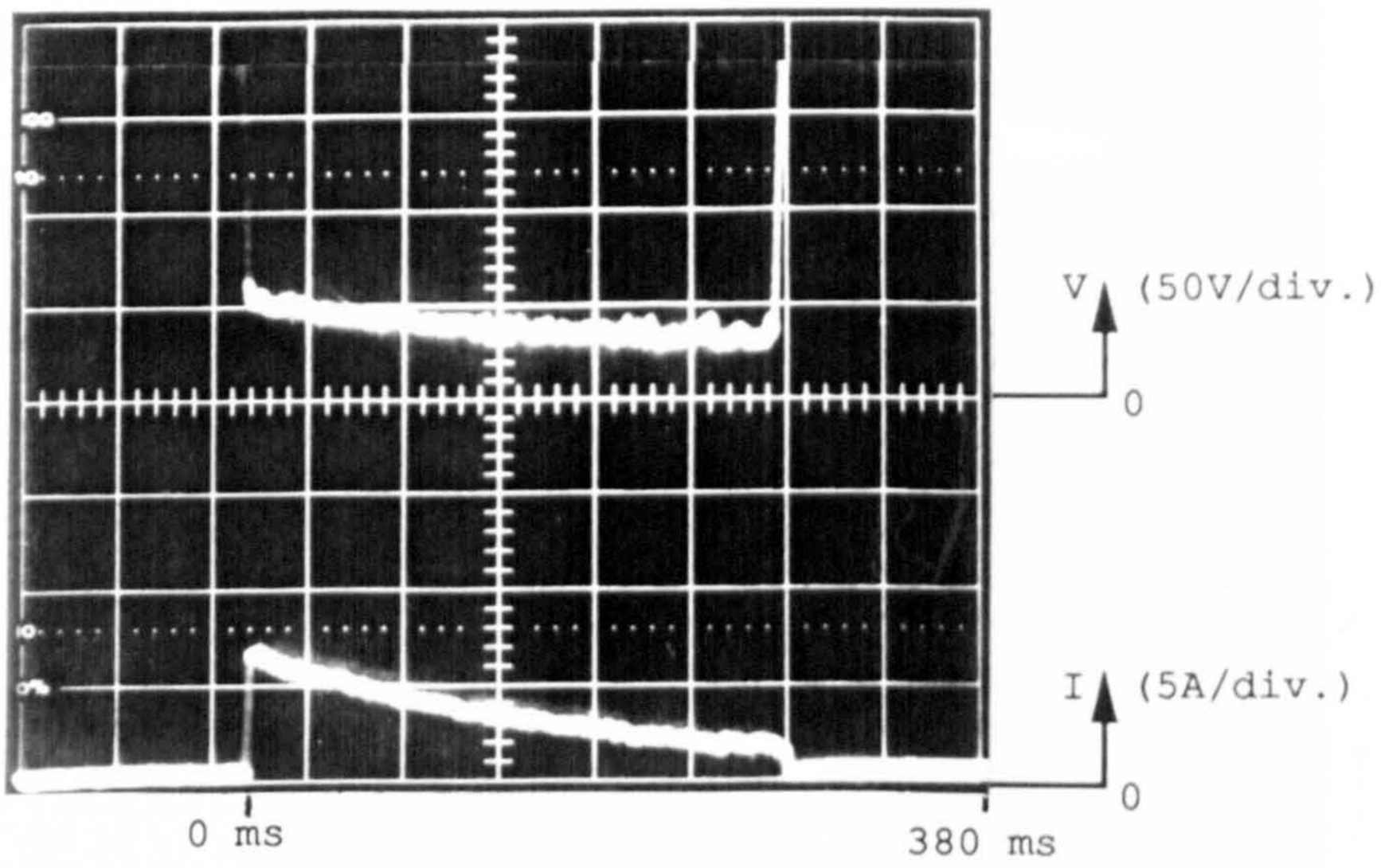

Time-base: 50 ms/div.

Fig.5.8 Arc voltage and current waveforms after breakdown from cold. 3 mm TIG arc gap, V_c=250 V, R_1=30 Ω.

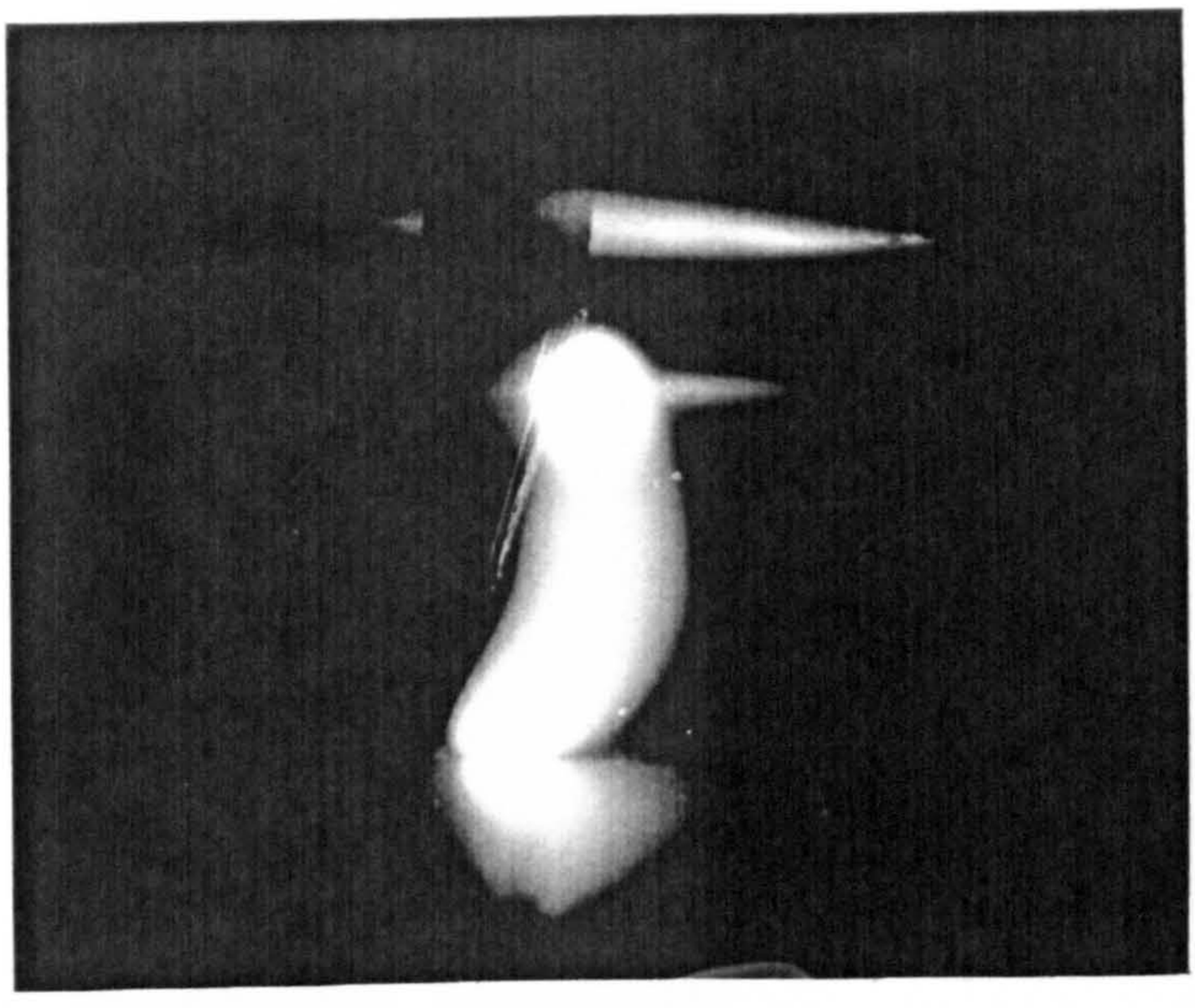

(a)

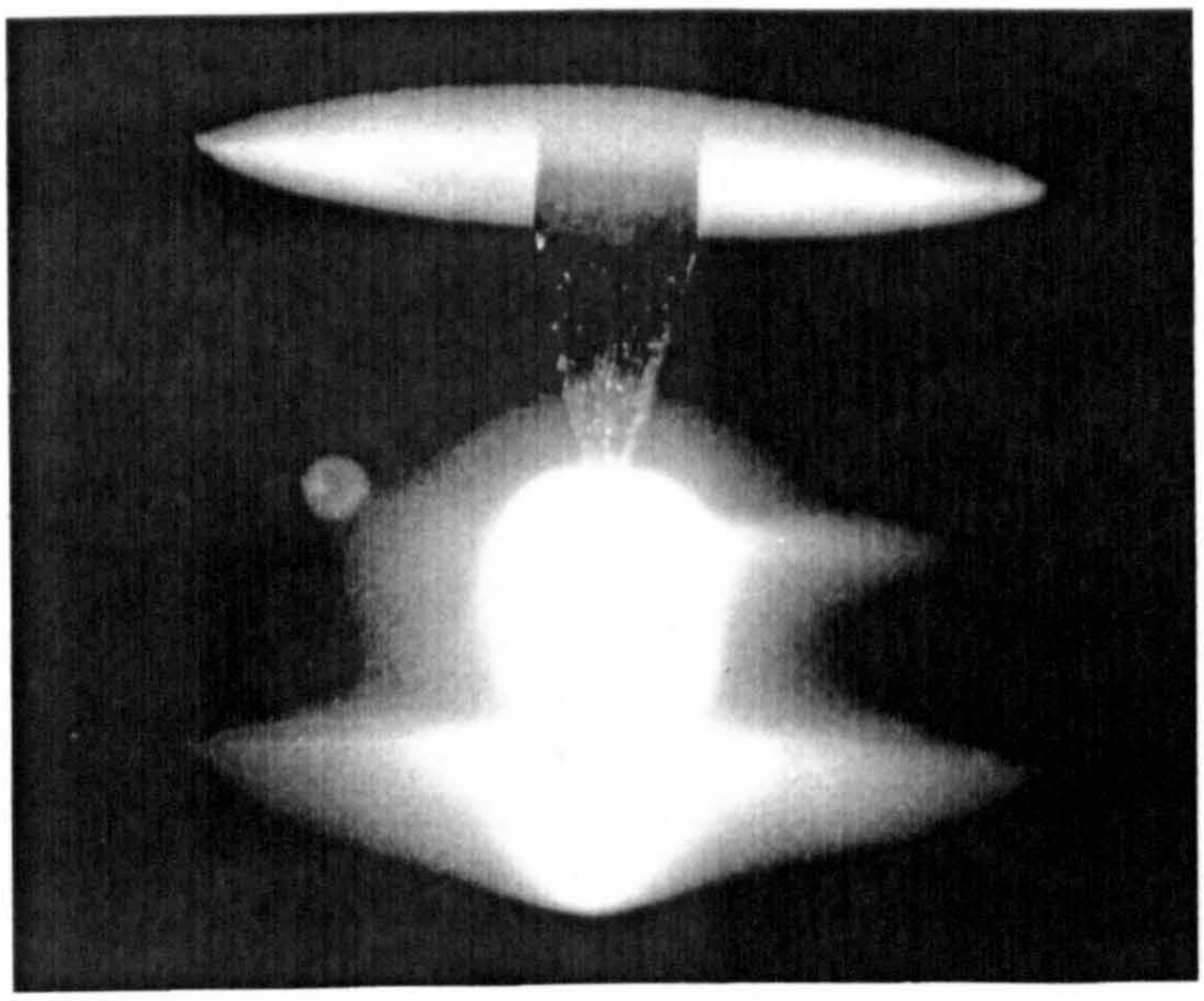

(b)

Fig.5.9 Still photographs of TIG arcs after initiation from cold. (a) unstable arc, initial current of 4 A (b) stable arc, initial current of 7 A.

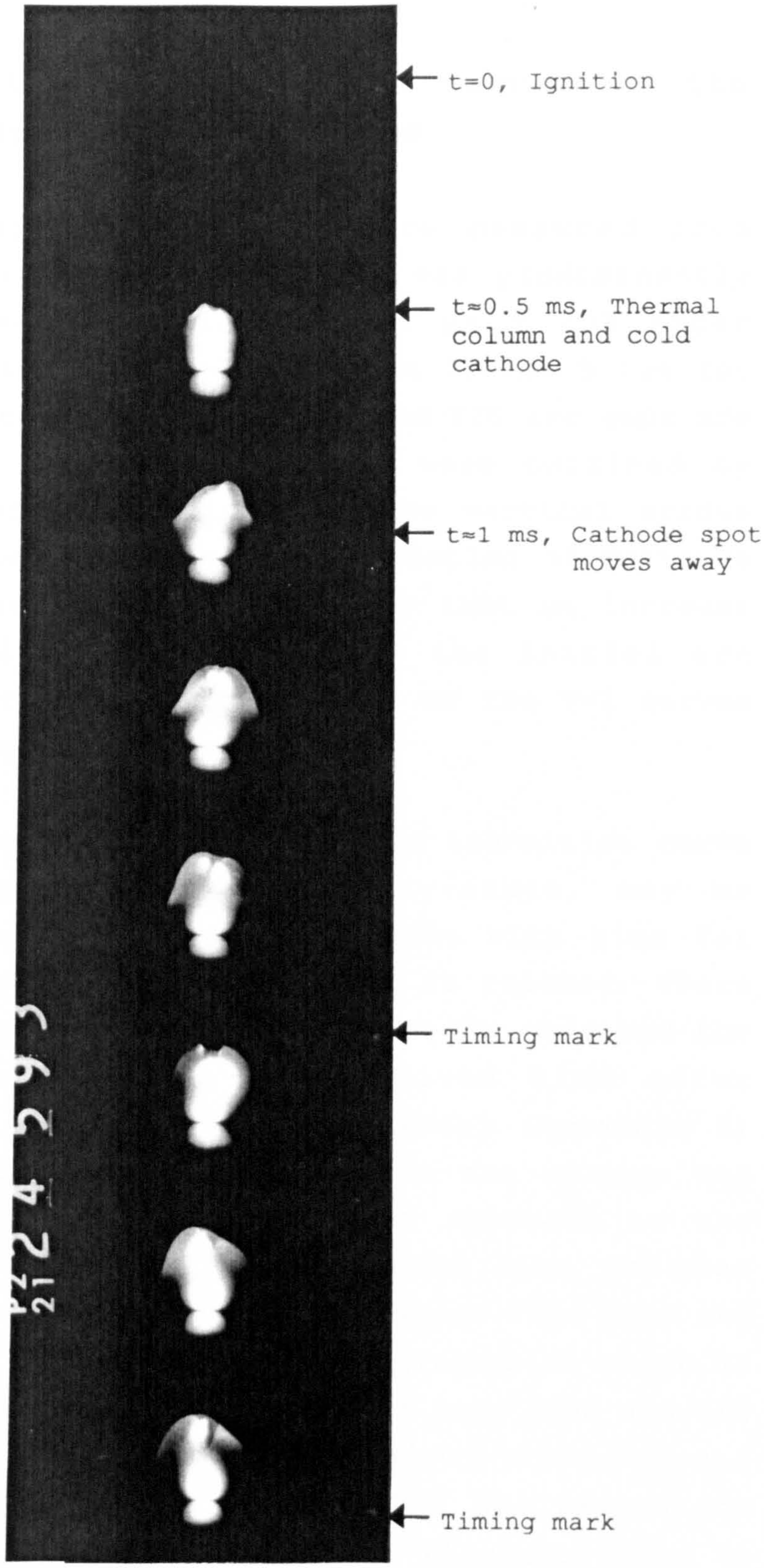

Fig.5.10 High speed ciné photographs of a 3 mm TIG arc gap before and after ignition. Initial current=4 A, Kodak TRI-X reversal film, HYCAM 16 mm camera, 2500 frames per second, aperture: f.11, Timing marks: 1000 per second, Exposure: 140 μs, Time between frames: 325 μs, 50 mm lens with 25 mm extension.

5.2.3 Variation of Voltage with Current of the Cold (Thermally Undeveloped) Arcs

The arc voltage and current were measured from oscilloscope traces while the arc was predominantly field dominated (or cold) at 100 μs ± 20% after breakdown. The cold arc V-I curves at 100 μs ± 20% for copper or tungsten cathodes in air and TIG arc gaps are shown in Fig. 5.11. These curves were obtained by averaging individual readings and the vertical arrows indicate the maximum and minimum variation of voltages recorded for each current. They show that an increase in the initial current increases the initial arc voltage, indicating a positive slope of the V-I curves for the cold arc.

The shape of the V-I cold to hot arc transition curve as the arc approaches the steady-state, may be determined. The arc voltage decreases with time for each current until the steady-state is reached. There will be a series of V-I curves between the cold and the static V-I curves each for a given time after breakdown. The rotating load line model (Appendix 5) was used to illustrate the changes in arc voltage and current that take place during the approach to the steady-state (Fig. 5.12). The load line rotates anticlockwise as the dc current increases from zero and di/dt decreases with time. The operating point which is the intersection between the rotating load line and the arc V-I characteristic at the given time, moves continuously along a V-I cold to hot arc transition curve from a value on the cold arc characteristic to the maximum value of arc current on the static characteristic. The shape of this transition curve and the durations involved depend on the discharge power as a function of time.

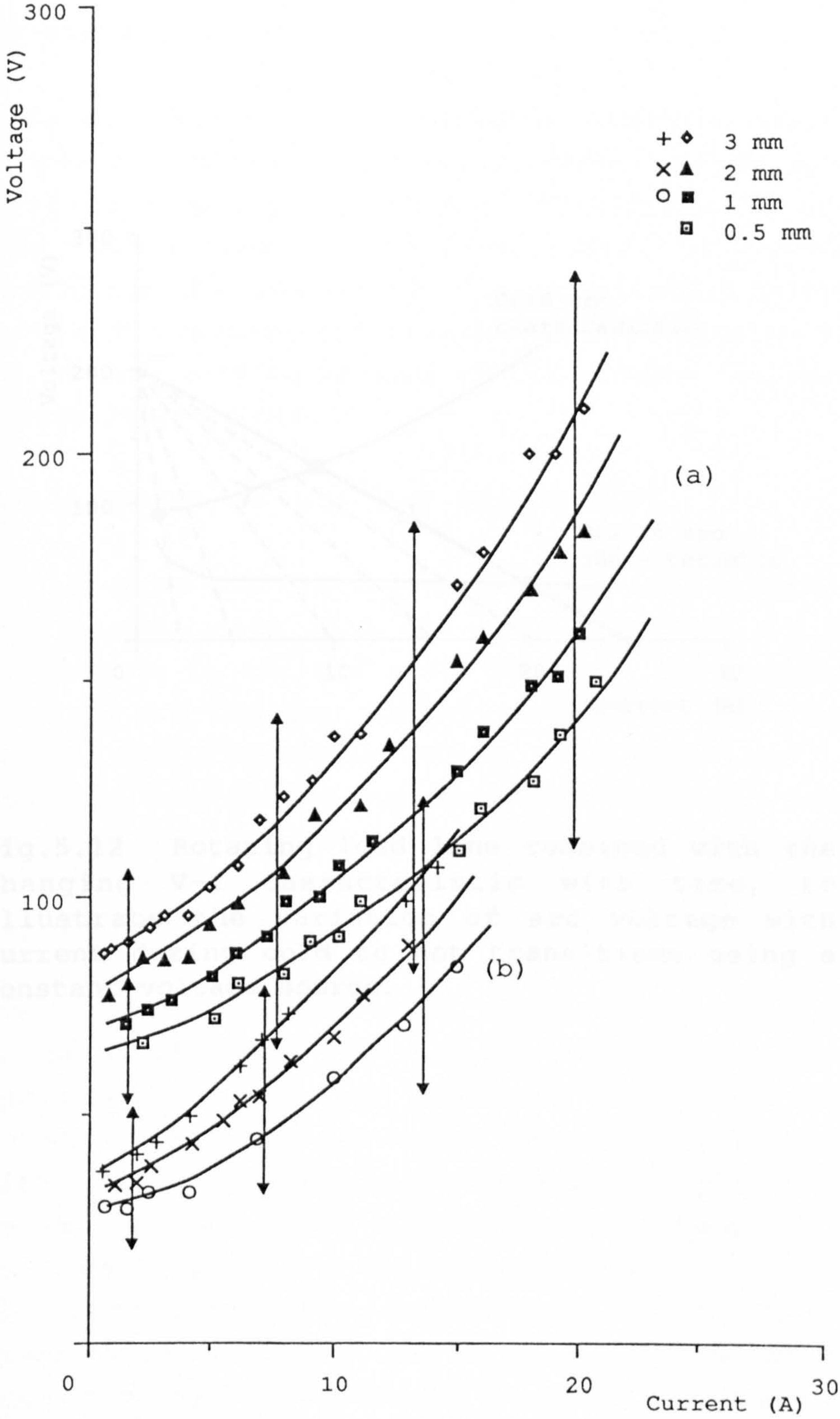

Fig.5.11 Variation of cold arc voltage with current measured at 100 μs after breakdown, using (a) copper or tungsten cathodes in air (b) TIG arc gap.

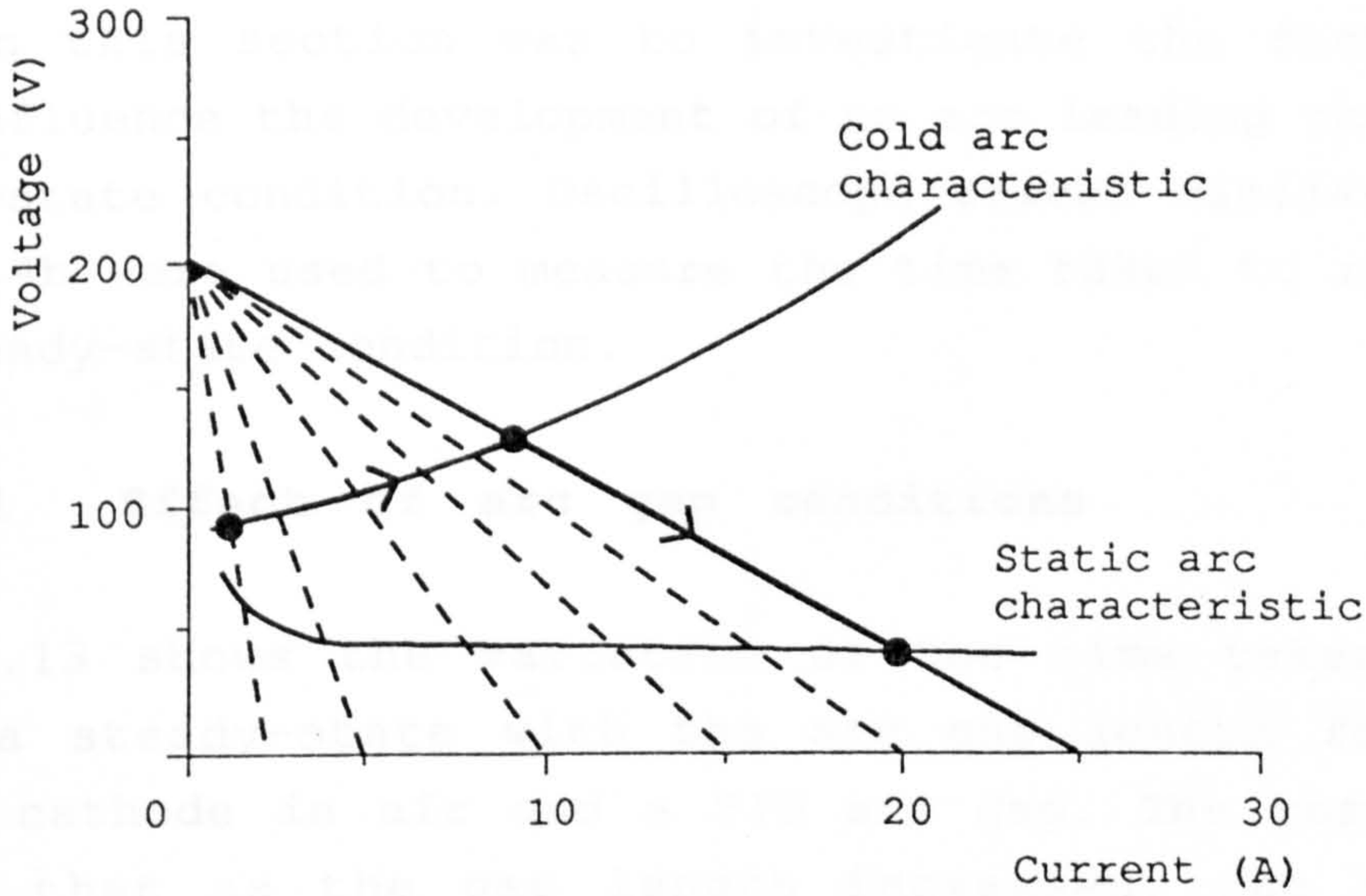

Fig.5.12 Rotating load line combined with the changing V-I characteristic with time, to illustrate the variation of arc voltage with current during cold to hot transitions using a constant voltage source.

5.2.4 Time Taken for the Development of a Steady-State Condition

The rate at which the arc resistance decreases should be maximised to obtain a thermally stable cathode spot and hence a steady-state quickly. The object of the work in this section was to investigate the factors that influence the development of an arc leading to the steady-state condition. Oscilloscope traces similar to Fig. 5.4b were used to measure the time taken to reach the steady-state condition.

5.2.4.1 Effect of arc gap conditions

Fig. 5.13 shows the variation of the time taken to reach a steady-state with the arc gap length for a copper cathode in air and a TIG arc gap. The results showed that as the gap length increased, the time decreased. The electrodes become less effective in causing heat loss as the gap length increases and most of the power will be lost by convection and radiation. The power input to the arc will mainly be conducted away by the electrodes when the gap length is reduced.

Fig. 5.14 shows the variation of the time taken to reach the steady-state with the CR time-constant with the initial current (I_i) as parameter, for a 3 mm gap in air with a copper or tungsten cathode. The initial capacitor voltage and series resistance were varied to obtain various values for I_i and CR time-constants. A longer time elapsed for the tungsten cathode than a copper cathode before a steady-state was reached, especially when I_i and the CR time-constant were large. The longer delay caused when a tungsten cathode was used may be due to the arc operating at higher cathode temperatures (≈3500 K) than that for a copper cathode of less than 3000 K. The higher decrease in the time with increasing I_i and CR time-constants shows the

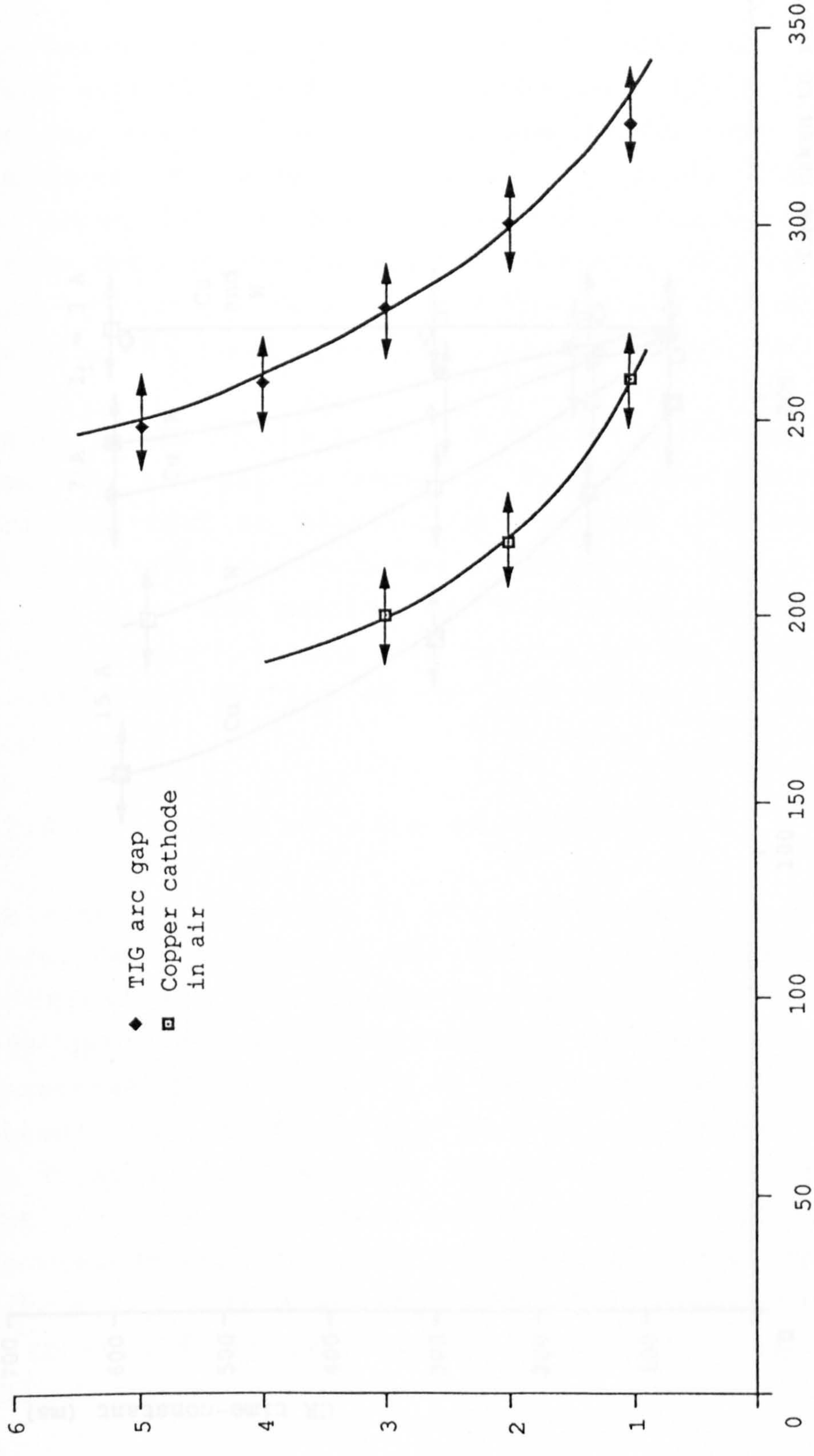

Fig.5.13 Variation of time taken to reach the steady-state with electrode separation. V_c=250 V, C_1=10,000 μF, R_1=3Ω, I_1=7 A. The arrows indicate maximum and minimum variation about the average.

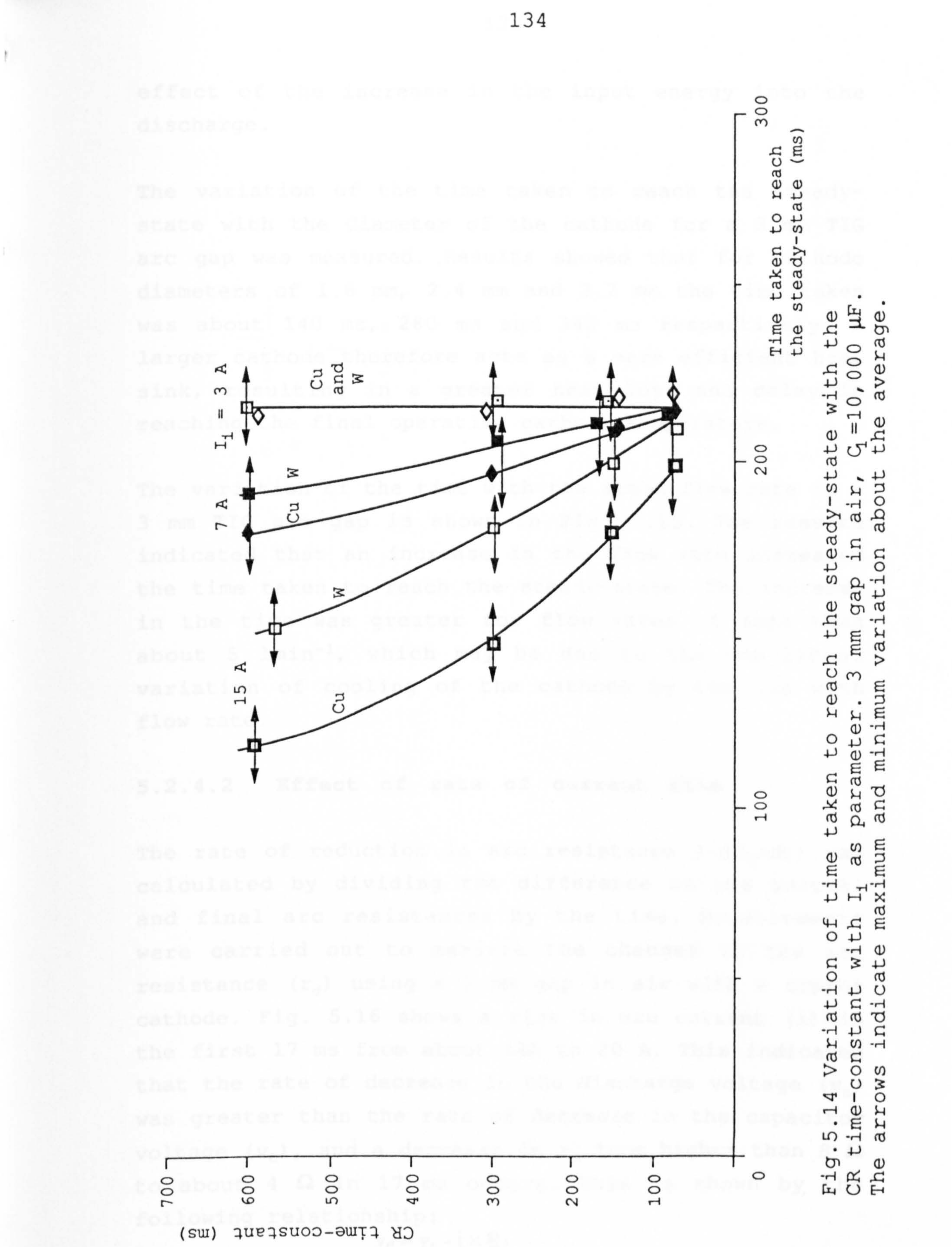

Fig.5.14 Variation of time taken to reach the steady-state with the CR time-constant with I_1 as parameter. 3 mm gap in air, C_1=10,000 μF. The arrows indicate maximum and minimum variation about the average.

effect of the increase in the input energy into the discharge.

The variation of the time taken to reach the steady-state with the diameter of the cathode for a 3 mm TIG arc gap was measured. Results showed that for cathode diameters of 1.6 mm, 2.4 mm and 3.2 mm the time taken was about 140 ms, 280 ms and 340 ms respectively. A larger cathode therefore acts as a more efficient heat sink, resulting in a greater heat loss and delay in reaching the final operating cathode temperature.

The variation of the time with the argon flow rate in a 3 mm TIG arc gap is shown in Fig. 5.15. The results indicated that an increase in the flow rate increased the time taken to reach the steady-state. The increase in the time was greater for flow rates of less than about 5 $lmin^{-1}$, which may be due to the non-linear variation of cooling of the cathode by the gas with flow rate.

5.2.4.2 Effect of rate of current rise

The rate of reduction in arc resistance ($-dr_d/dt$) was calculated by dividing the difference in the initial and final arc resistances by the time. Measurements were carried out to measure the changes in the arc resistance (r_d) using a 3 mm gap in air with a copper cathode. Fig. 5.16 shows a rise in arc current (i) in the first 17 ms from about 18A to 20 A. This indicated that the rate of decrease in the discharge voltage (v_d) was greater than the rate of decrease in the capacitor voltage (v_c), and a decrease in r_d from higher than 8 Ω to about 4 Ω in 17 ms occurs. This is shown by the following relationship:

$$v_d = v_c - i \times R_1$$

$$\frac{di}{dt} = \frac{1}{R_1}\left[\frac{dv_c}{dt} - \frac{dv_d}{dt}\right]$$

If v_d decreases faster than v_c, then i increases.

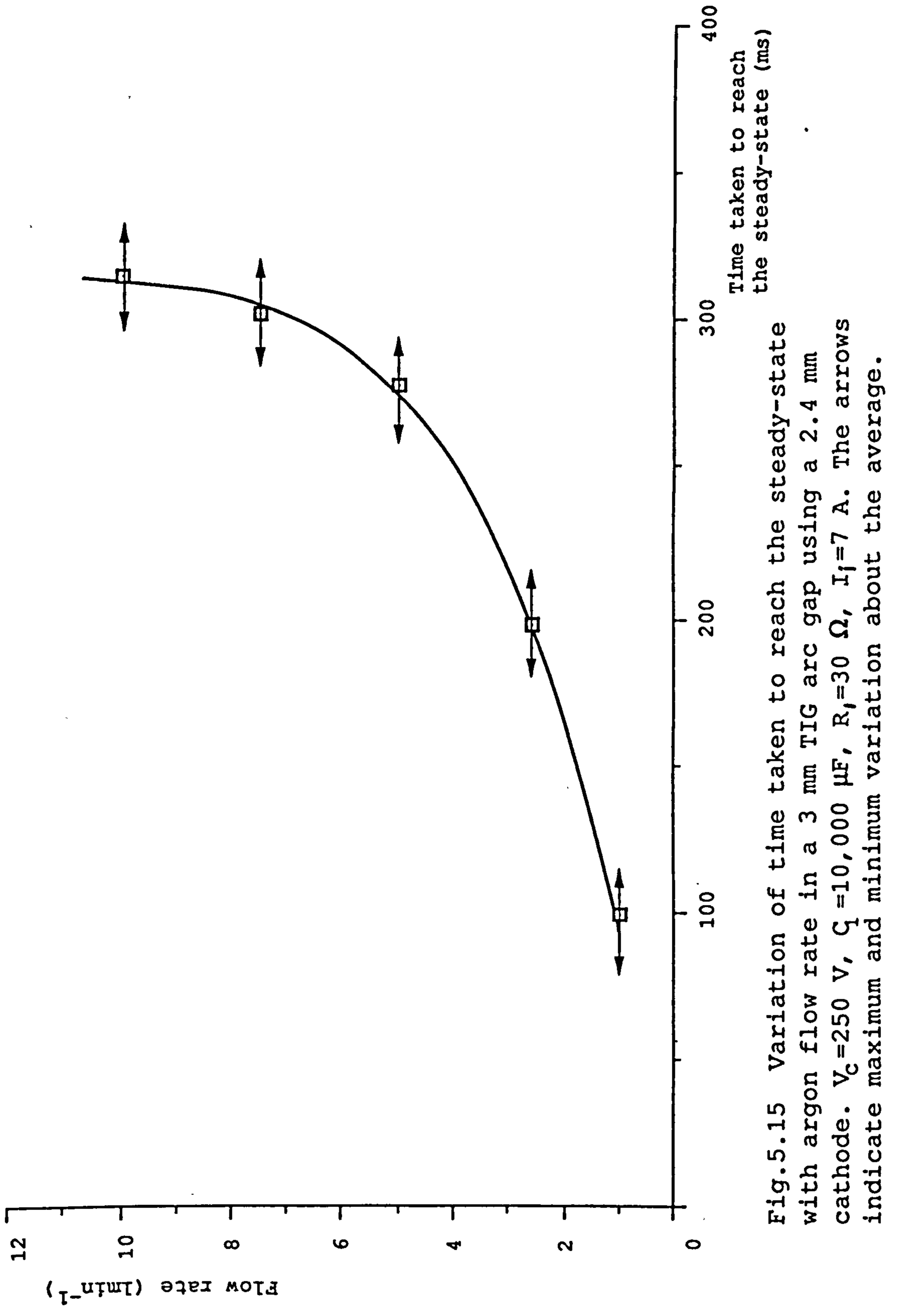

Fig.5.15 Variation of time taken to reach the steady-state with argon flow rate in a 3 mm TIG arc gap using a 2.4 mm cathode. V_c=250 V, C_1=10,000 μF, R_1=30 Ω, I_f=7 A. The arrows indicate maximum and minimum variation about the average.

The rate of rise of current (di/dt) was varied by varying V_c, C_1 and R_1 and keeping the initial current constant at about 18 A. The variation in $-dr_d/dt$ with di/dt, calculated from oscilloscope traces similar to Fig. 5.16, after establishing the same initial current of 18 A, for the arc gap mentioned above, is shown in Fig. 5.17. The results indicated that an increase in $-dr_d/dt$ occurred with increasing di/dt and the time taken for the development of the steady-state was reduced. For example a $-dr_d/dt$ of 255 Ωs^{-1} at a di/dt of 120 As^{-1} compared to 80 Ωs^{-1} at a di/dt of about 30 As^{-1} for the same initial current of 18A were measured.

A constant voltage welding power supply with a di/dt of about 10^4 As^{-1}, compared to about 120 As^{-1} in the first 17 ms in Fig. 5.16, will provide a much higher rate of gain of thermal energy. The steady-state will therefore develop more rapidly.

Fig. 5.16 also shows that when the rate of decrease in v_c becomes greater than the rate of decrease in v_d at about 17 ms after breakdown, the current decays but the arc voltage continues to decrease, indicating that the static characteristic is not yet reached. It also shows that although the static characteristic is being approached, r_d increases from 4 Ω at 17 ms to about 5 Ω at 39 ms after breakdown, showing that a decrease in ionisation occurs because of the reduction in the supplied electrical energy.

Fig. 5.18 is a plot of voltage against current determined from Fig. 5.16, and shows the cold to hot arc transitions as the load line shifts downward with a constant slope due to the drop in the capacitor voltage. Initially in the first 17 ms, due to the increased ionisation, the static characteristic at a high current is approached but then due to the decreased ionisation and increase in r_d, the static characteristic at a lower current is approached.

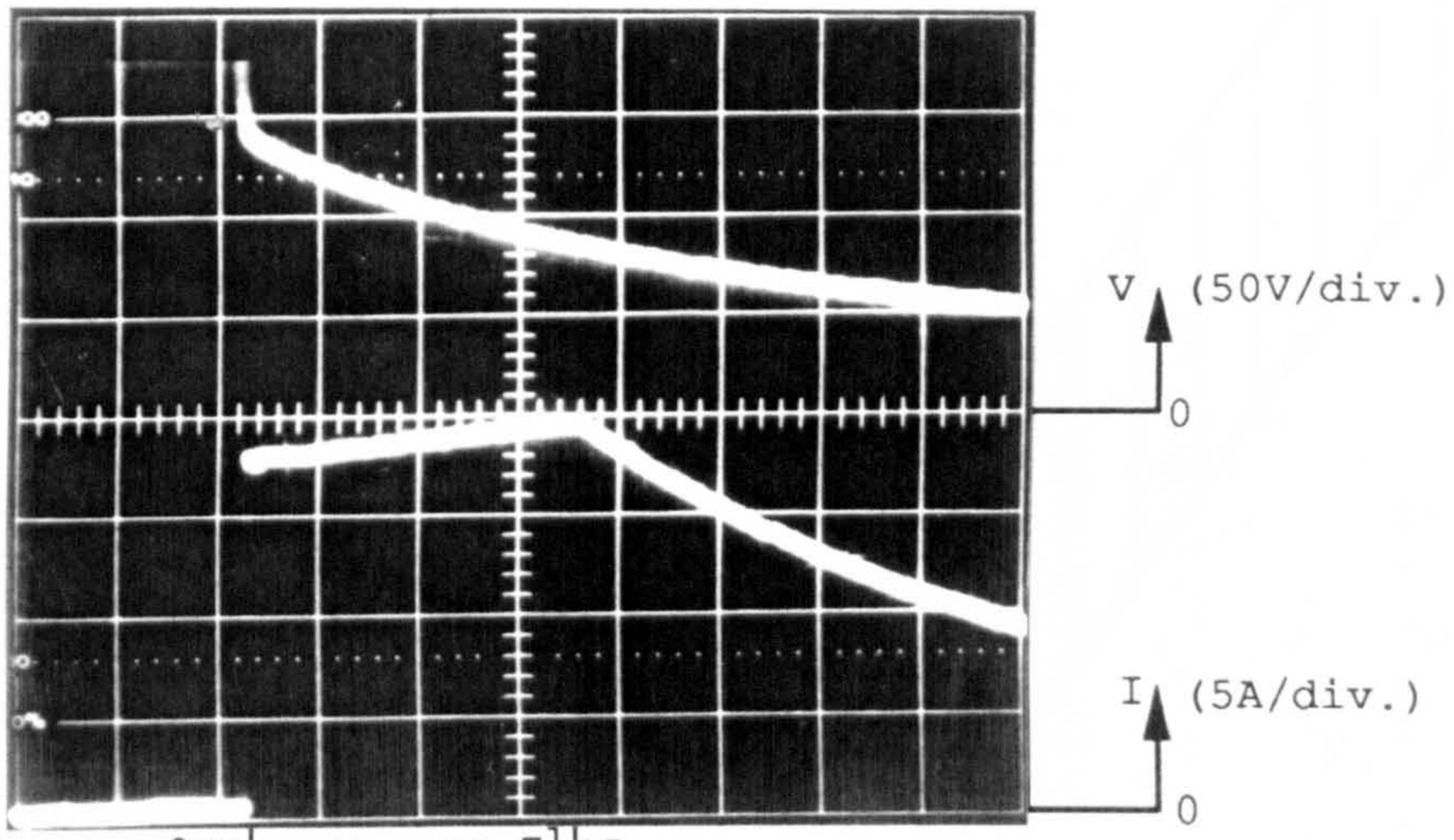

Fig.5.16 Voltage and current waveforms during cold to hot arc transitions. 3 mm gap, air, copper cathode, V_c = 200V, R_1 = 2.5 Ω. Time-base: 5 ms/div.

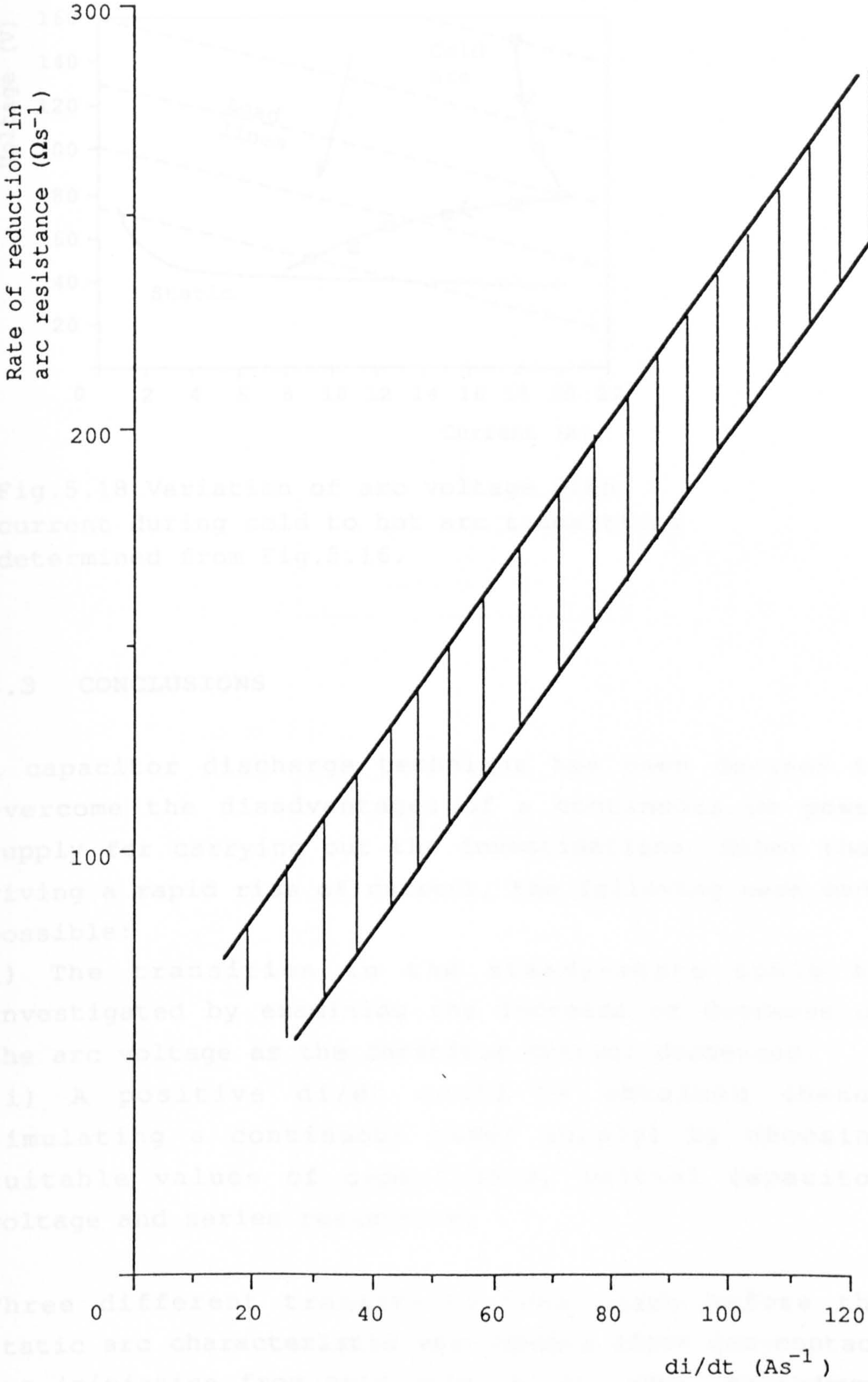

Fig.5.17 Variation of rate of reduction in arc resistance with di/dt during the transition to the steady-state. 3 mm gap, copper cathode in air. V_c=70 V - 300 V, C_1 =10,000 μF - 37,500 μF, R_1 =1.5 Ω - 7.5 Ω.

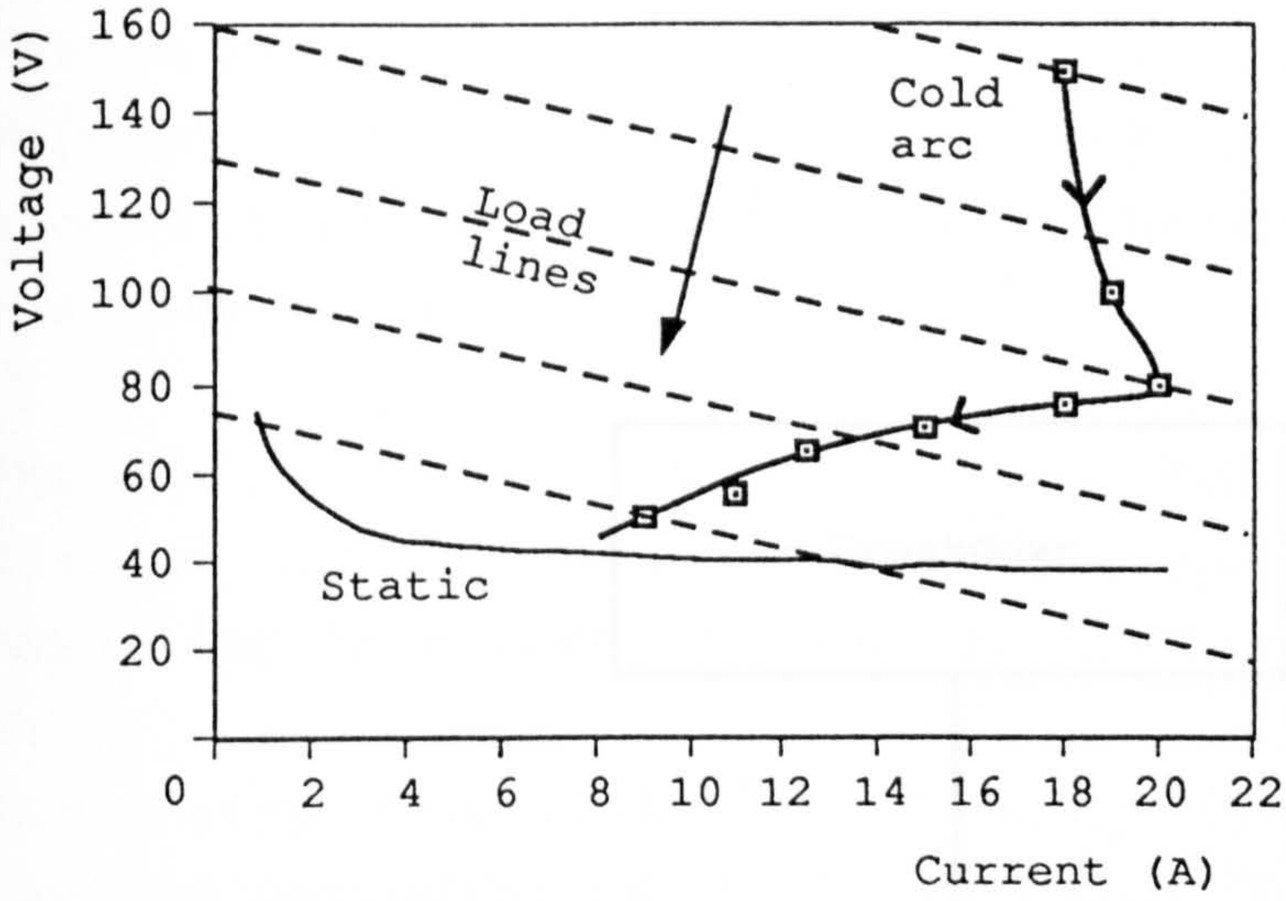

Fig.5.18 Variation of arc voltage with current during cold to hot arc transitions determined from Fig.5.16.

5.3 CONCLUSIONS

A capacitor discharge technique has been devised to overcome the disadvantages of a continuous dc power supply for carrying out the investigations. Other than giving a rapid rise of current, the following were made possible:

i) The transition to the steady-state could be investigated by examining the increase or decrease of the arc voltage as the capacitor current decreased.

ii) A positive di/dt could be obtained (hence simulating a continuous power supply) by choosing suitable values of capacitance, initial capacitor voltage and series resistance.

Three different transitions took place before the static arc characteristic was reached after non-contact arc initiation from cold (Fig. 5.19). After breakdown, an initial transition in less than 100 μs to a field dominated (cold column cold cathode) arc occurred. The initial arc voltage was similar for both thoriated tungsten and copper cathodes which suggests that the

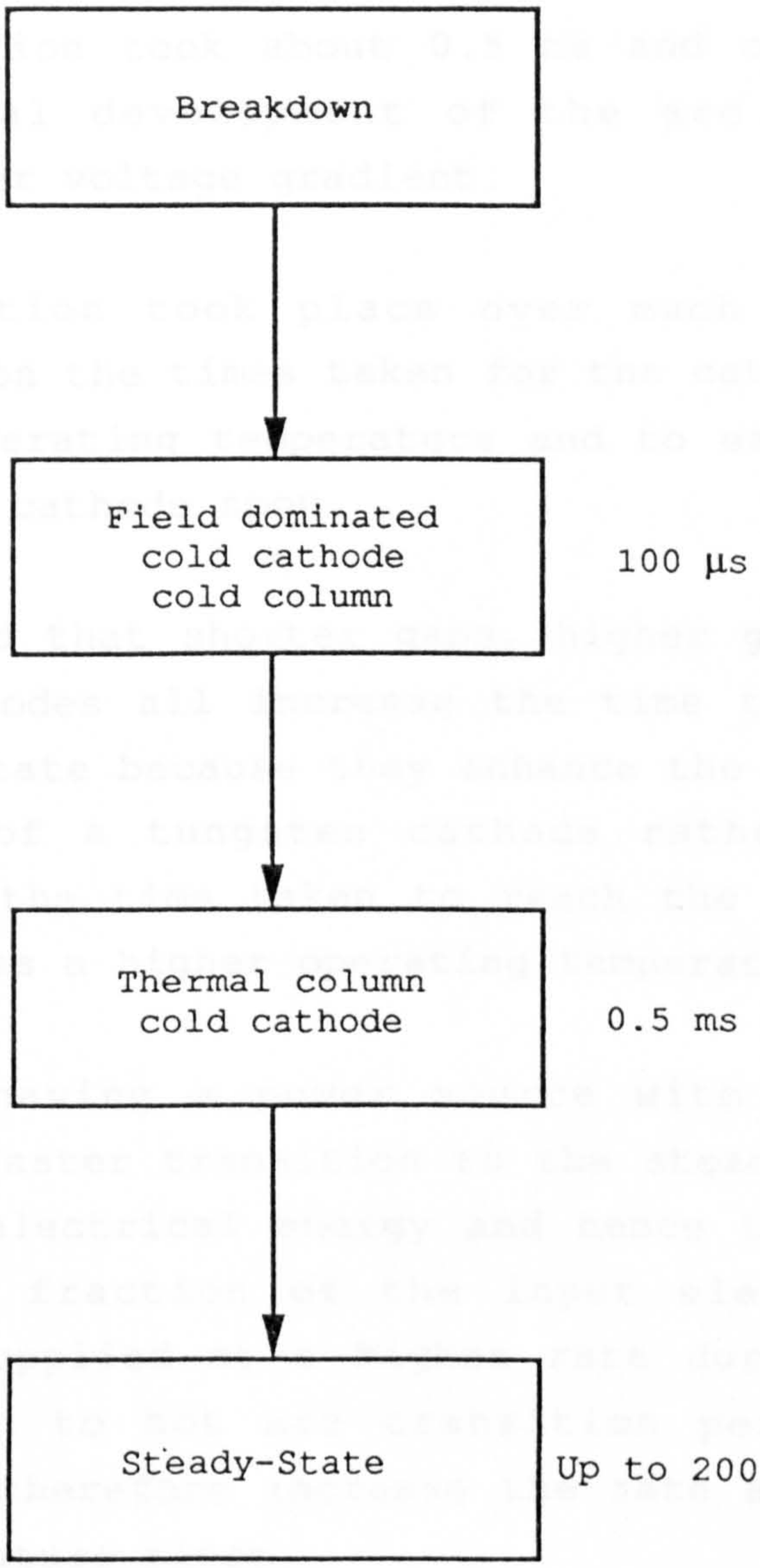

Fig.5.19 Transitions from a field dominated (cold) arc after breakdown from cold to a fully developed steady-state arc.

mechanisms of electron emission from the cathode are the same and are field dominated. The variation of voltage with current at about 100 μs after breakdown showed that the cold arc V-I characteristic has a positive slope.

The second transition took about 0.5 ms and occurred due to the thermal development of the arc column resulting in a lower voltage gradient.

The third transition took place over much longer periods depending on the times taken for the cathode to reach the final operating temperature and to establish a thermally stable cathode spot.

Measurements showed that shorter gaps, higher gas flow rates, larger cathodes all increase the time taken to reach the steady-state because they enhance the cooling effect. The use of a tungsten cathode rather than copper, increases the time taken to reach the steady-state because it has a higher operating temperature.

An advantage of having a power source with a high di/dt, is that a faster transition to the steady-state takes place. The electrical energy and hence the heat input which is a fraction of the input electrical energy, will be supplied at a higher rate during the whole of the cold to hot arc transition period. A higher di/dt will therefore increase the rate at which the cathode temperature rises.

The minimum current required to sustain an arc after breakdown from cold decreases as the open circuit voltage of the main power supply increases. This may be due to an increase in the cathode fall voltage with decrease in current resulting in a higher discharge voltage which would require a greater open circuit voltage to sustain the discharge.

The work described in this chapter has been published as follows:

SAIEPOUR, M., HARRY, J.E., 'Charateristics of arcs during non-contact ignition from cold', J. Phys. D: App. Phys., 24, (3), pp. 318-324, 1991.

CHAPTER 6

CONTINUOUS SINUSOIDAL HF ARC INITIATION

6.0 CONTINUOUS SINUSOIDAL HF ARC INITIATION

Investigations in Chapter 4 showed that hf discharges can provide a suitable conduction path for the main dc current and establish an arc.

During the initial stages of arc ignition using a continuous sinusoidal hf source, the combined ac-dc discharge is supplied by both the ignition source and the main dc supply. The resistance of the discharge decreases as the degree of ionisation increases due to the increase in the ac current. This results in a decrease in the dc voltage across the discharge for the same dc current.

The purpose of the work in this Chapter is to
i) extend the work carried out in section 4.4 on the characteristics of the combined ac-dc discharges relevant to arc ignition,
ii) obtain the minimum requirements for the ignition of dc arcs using sinusoidal hf discharges and
iii) examine the stages in the development of the arc after breakdown from cold using a continuous sinusoidal hf ignition source.

6.1 CHARACTERISTICS OF COMBINED AC-DC DISCHARGES

A series of measurements was carried out to find the variation in the dc voltage with dc current of combined ac-dc discharges, to investigate the initial stages of arc ignition. High frequency discharges with peak currents of 50 mA to 2 A and frequencies of 10 kHz to 800 kHz were investigated for 3 mm gaps using copper electrodes in air or a typical TIG torch as described in Chap. 4. The circuit used for these investigations is the same as that shown in Fig. 4.15. A circuit similar to that shown in Fig. 4.2 was used to supply the frequencies of 10 kHz to 50 kHz. The high-frequency

high-voltage generator described in section 4.1 was used to supply frequencies of 50 kHz to 800 kHz.

Fig. 6.1 shows the typical shape of the curves obtained for the variation of the dc voltage with dc current of a combined ac-dc discharge. The curve may be divided into three regions. In region OA the discharge is ac-dominated and is characterised by a positive slope of the V-I curve. Within AB the discharge is in the transition region. In region BC the discharge is dc-dominated and is characterised by a negative slope of the V-I curve.

6.1.1 Characteristics of the AC-Dominated Discharge

Figs. 6.2 and 6.4 show the variation of the dc voltage across the combined ac-dc glow discharges using copper electrodes in air and a typical TIG torch respectively. Figs. 6.3 and 6.5 show similar characteristics for the combined ac-dc arc discharges. Fig. 6.2 indicates that using copper electrodes in air, in the ac-dominated region for a dc current of 50 mA a reduction in the dc voltage across the combined ac-dc glow discharge from 310 V to 25 V occurs as the ac current increases from 100 mA to 400 mA. The reduction in voltage is due to the increase in the degree of ionisation caused by the increase in the ac discharge current. Fig. 6.4 shows that in a TIG arc gap for the same values of dc current a reduction in the dc voltage from 140 V to 40 V occurs as the ac current is increased from 100 mA to 400 mA. Fig. 6.3 shows that using copper electrodes in air, in the ac-dominated region for a dc current of 0.5 A a reduction in the dc voltage across the ac-dc arc discharge from 45 V to 8 V occurs as the ac current increases from 0.6 A to 2 A. Fig. 6.5 shows that in a TIG arc gap for the same values of currents a reduction from 20 V to 3 V occurs.

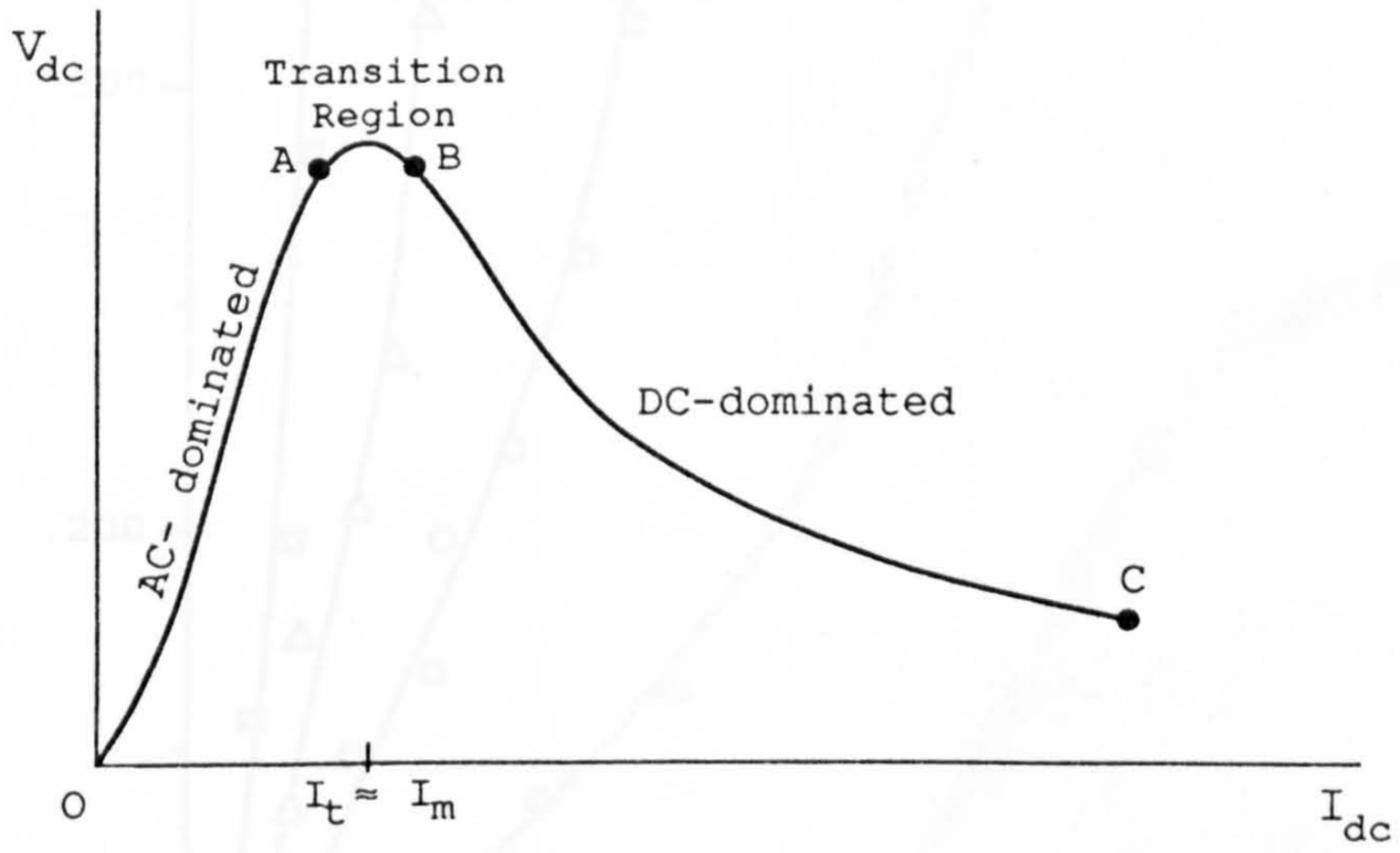

Fig.6.1 Typical shape of the curve for the variation of the dc voltage with dc current of combined ac-dc discharges.

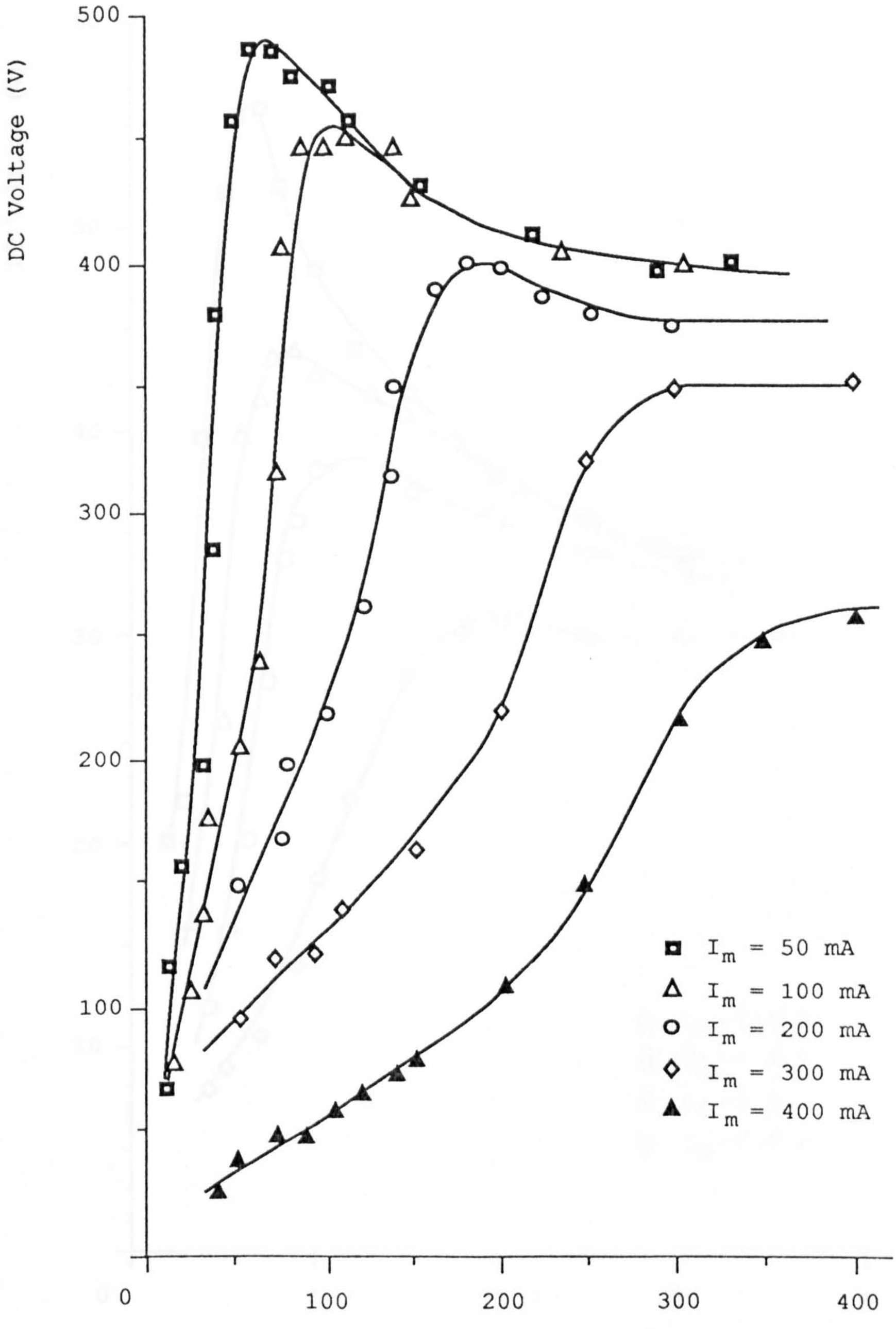

Fig.6.2 Variation of dc voltage with dc current for a combined ac-dc glow discharge in a 3 mm gap with a copper cathode in air.

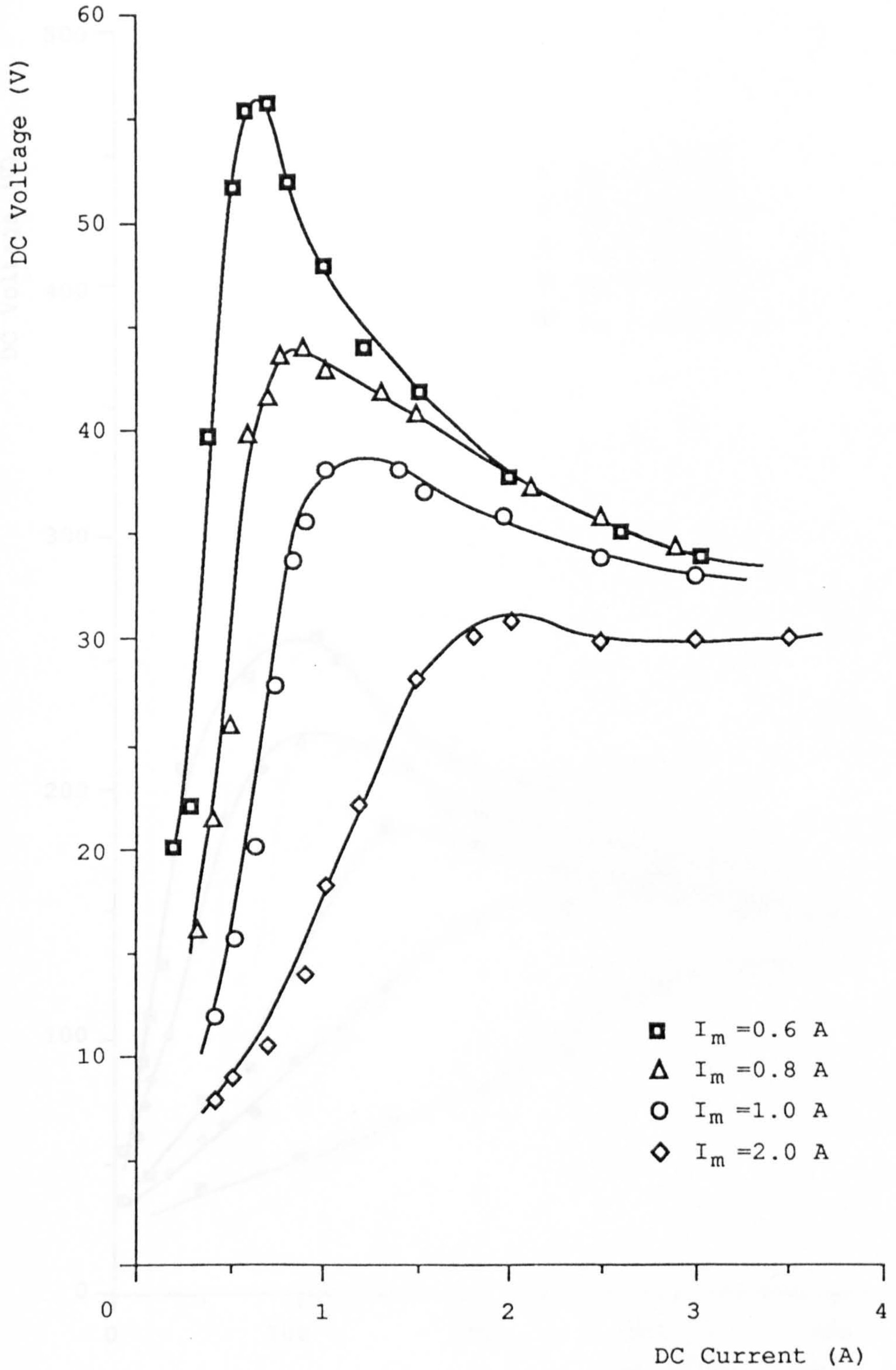

Fig.6.3 Variation of dc voltage with dc current for a combined ac-dc arc discharge in a 3 mm gap with a copper cathode in air.

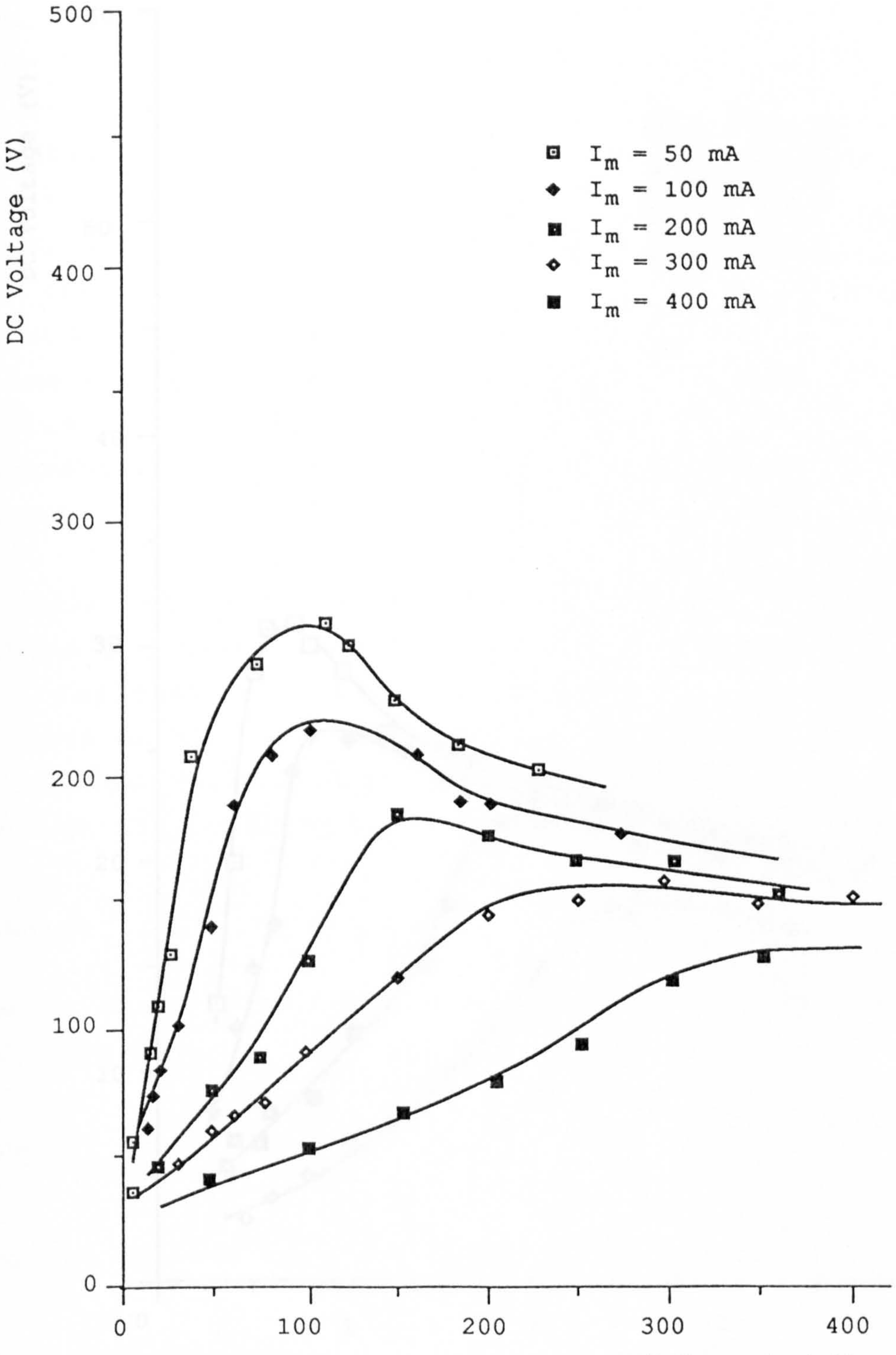

Fig.6.4 Variation of dc voltage with dc current for a combined ac-dc glow discharge in a 3 mm TIG arc gap.

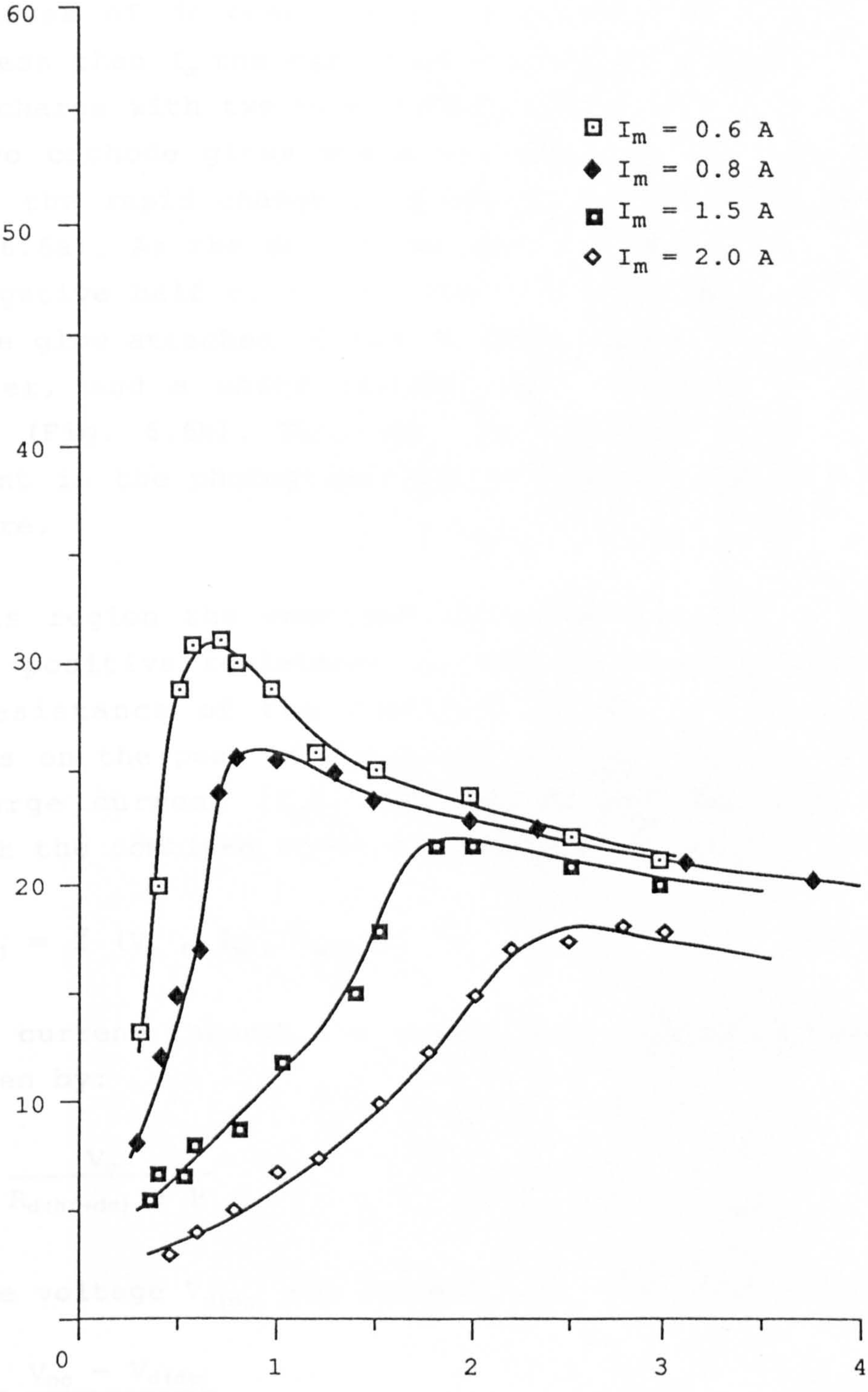

Fig.6.5 Variation of dc voltage with dc current for a combined ac-dc arc discharge in a 3 mm TIG arc gap.

The discharge was stable when operating over the positive slope region and could be maintained even with low values of dc open circuit voltages. When I_{dc} was much less than I_m the discharge was almost a sinusoidal hf discharge with two blue cathode glows at $I_m < 0.4$ A. The two cathode glows appear to exist simultaneously due to the rapid change in polarity of the electrodes (Fig. 6.6a). As the dc current was increased from zero the negative half cycle of current became smaller. The cathode glow attached to the dc anode became smaller in diameter, and a white (anode) spot appeared in its centre (Fig. 6.6b). This was clearly visible but not apparent in the photographs due to the relatively long exposure.

In this region the combined discharge acts as a non-linear positive resistance in the main current path. The resistance of the combined discharge ($R_{d(hf+dc)}$) depends on the peak hf discharge voltage (V_m), peak hf discharge current (I_m), and the dc current flowing through the combined ac-dc discharge $I_{d(dc)}$:

$$R_{d(hf+dc)} = f\ (V_m\ ,\ I_m\ ,\ I_{d(dc)}) \qquad (6.1)$$

The dc current through the steady-state ac-dc discharge is given by:

$$I_{d(dc)} = \frac{V_{oc}}{R_{d(hf+dc)} + R} \qquad (6.2)$$

and the voltage $V_{d(dc)}$ and current $I_{d(dc)}$ are related by:

$$I_{d(dc)} = \frac{V_{oc} - V_{d(dc)}}{R} \qquad (6.3)$$

where V_{oc} is the open circuit voltage of the dc source and R is the series resistance of the dc current path.

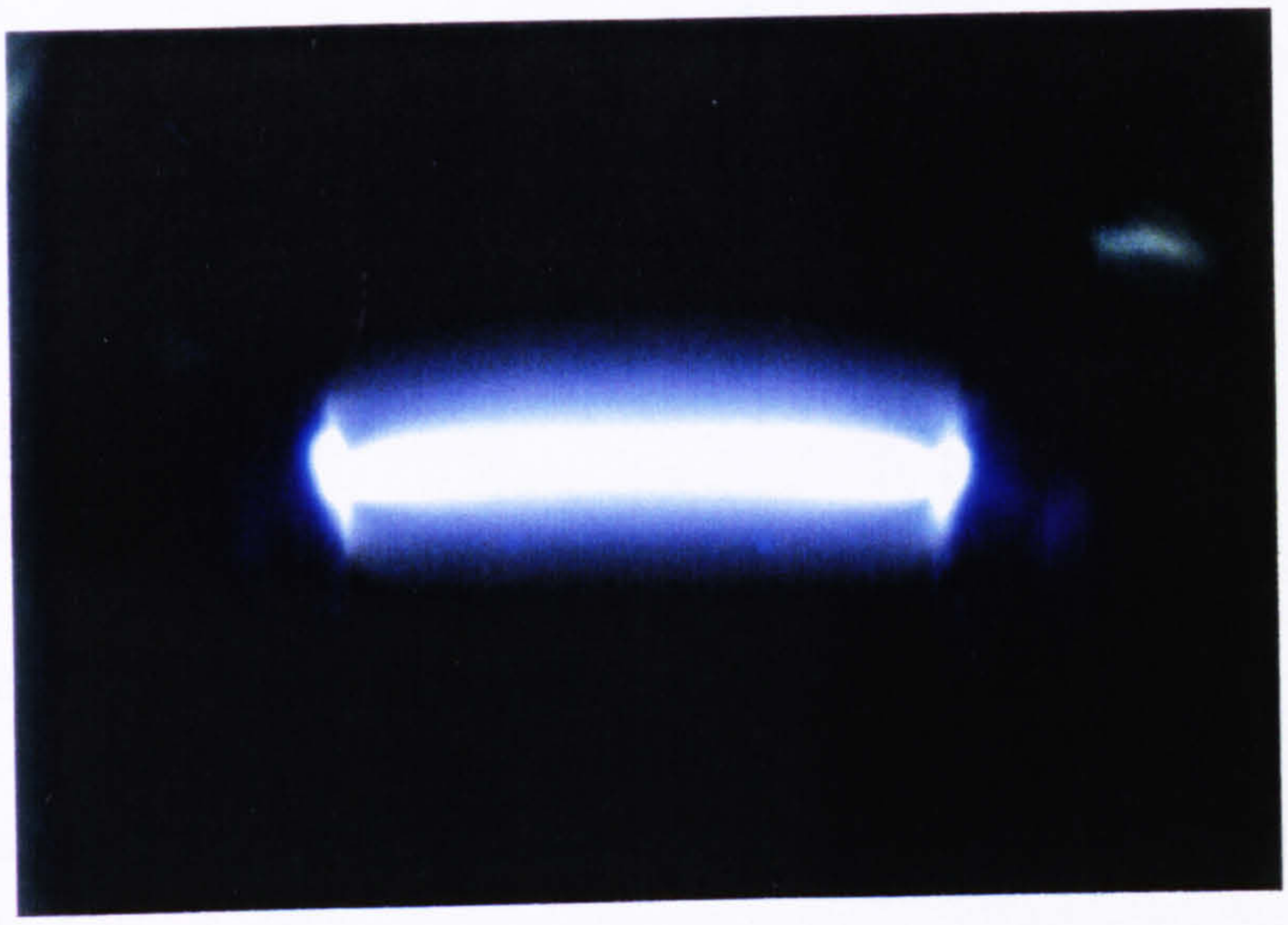

(a)

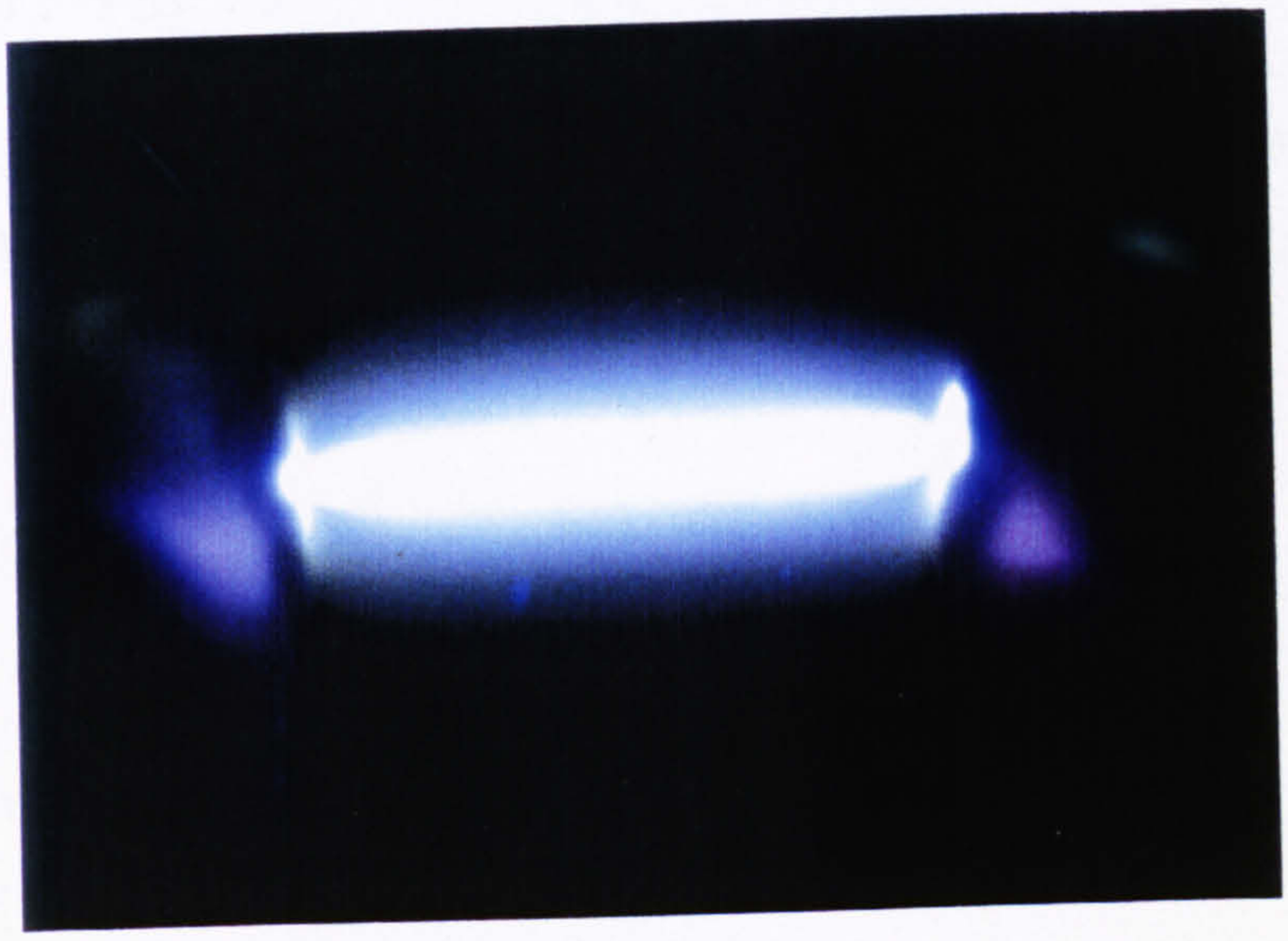

(b)

Fig.6.6 Appearance of a combined ac-dc discharge using copper electrodes in air. I_m = 100 mA, f = 40 kHz.
a) I_{dc} = 0, b) I_{dc} = 50 mA.

Fig. 6.7a shows the voltage and current waveforms for $I_{d(dc)}$=30 mA and $V_{d(dc)}$= 140 V when I_m=100 mA. The superimposed dc electric field is added or subtracted from the ac electric field and this affects the voltage across the discharge in each half cycle, giving an asymmetrical voltage waveform. The instantaneous current is dependent on the net instantaneous voltage.

6.1.2 Characteristics of the Discharge in the Transition Region

Figs. 6.2 - 6.5 show that the dc voltage at which the transition to a dc dominated discharge occurs is lowered as the ac current increases. A reduction from 450 V to 250 V occurred as the ac current increased from 100 mA to 400 mA using copper electrodes in air (Fig. 6.2). A reduction from 220 V to 130 V occurred for the same increase in ac current in a TIG arc gap (Fig. 6.4). Fig. 6.3 shows that using copper electrodes in air a reduction from 55 V to 30 V occurred for an increase of ac current from 0.6 A to 2 A and Fig. 6.5 shows that using a TIG arc gap a reduction from 31 V to 18 V for the same increase in the ac current took place.

When I_{dc} approached I_m the discharge made a hissing noise due to the rapid extinctions and reignitions. The blue cathode glow was completely replaced by the white anode spot and the discharge became generally unstable and more difficult to maintain. The amount of instability appeared to increase with a decrease in the discharge current, output voltage and series resistance of the two power sources and especially the frequency of the ac field.

There was no current flow during the negative half cycle and re-ignition peaks appeared as indicated in Fig. 6.7b which shows the waveforms for voltages and currents for I_m=100 mA and $I_{d(dc)}$=90 mA and $V_{d(dc)}$=400 V.

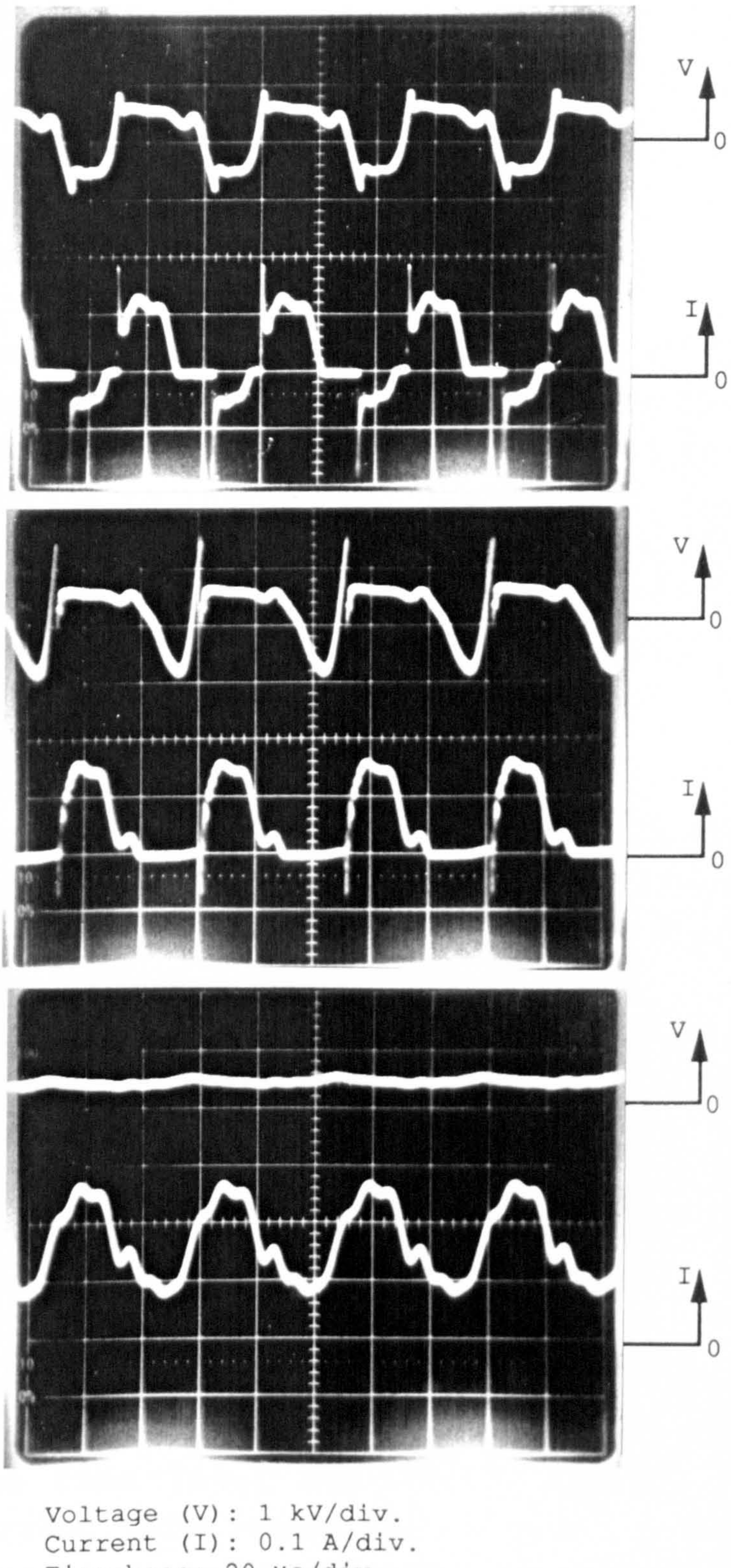

a) AC-dominated

$I_{d(dc)}$ = 30 mA,

$V_{d(dc)}$ = 140 V.

b) Transition region.

$I_{d(dc)}$ = 90 mA,

$V_{d(dc)}$ = 400 V.

c) DC-dominated

$I_{d(dc)}$ = 150 mA,

$V_{d(dc)}$ = 430 V.

Voltage (V): 1 kV/div.
Current (I): 0.1 A/div.
Time-base: 20 μs/div.

Fig.6.7 Waveforms of the combined ac-dc discharge voltages and currents for I_m = 100 mA.

The discharge processes that take place when in the transition region, may be explained as follows. When a dc electric field is superimposed on the ac field of an hf discharge, during the positive half cycle the discharge acquires a higher voltage gradient across it than in the negative half cycle. The drift velocities of the electrons and positive ions become higher and hence more current flows in the positive half cycle.

During the negative half cycle, the voltage gradient across the discharge is reduced and if the net current through the discharge becomes too small for the net voltage to sustain the discharge, the discharge current suddenly reduces to zero and ionisation ceases. The discharge will then de-ionise and disappearance of charged particles occurs by for example thermal diffusion, recombination or escape to the electrodes and the discharge may extinguish.

If the rate of de-ionisation is such that at the beginning of the next positive half cycle, the conductivity has decreased and the dielectric strength has increased due to the low amount (or absence) of ionisation, so that re-ignition is required. The value of the re-ignition voltage after the period of current zero depends on the amount of ionisation remaining from the previous positive half cycle and how much of this ionisation has been lost during the period of current zero.

Stability in the transition region may be increased by either decreasing the de-ionisation rate, or reducing the time (Δt_0) for de-ionisation (i.e. period of current zero) which may be achieved by increasing the frequency. At frequencies of less than about 15 kHz, the discharge became unstable and difficult to sustain. For I_m=100 mA, $V_{d(dc)}$=400 V, $I_{d(dc)}$=90 mA at a frequency of 14 kHz the peak re-ignition voltage(V_1) was about 1.7 kV and the period of current zero (Δt_0) about 40 μs

and at a frequency of 30 kHz, V_i was about 1.2 kV and Δt_0 about 10 μs.

6.1.3 Characteristics of the DC-Dominated Discharge

Fig. 6.3 shows that the dc voltage across an ac-dc arc discharge when operating in the dc-dominated region with a dc current of 3 A and ac current of 1 A is about 32 V using copper electrodes in air, whereas a dc static arc of the same dc current would have a voltage of higher than about 45 V. Fig. 6.5 shows that in a typical TIG arc gap for the same values of current, the dc voltage across the ac-dc arc discharge was about 20 V whereas the dc static arc voltage would be about 35 V.

Increasing the dc current beyond the transition region caused a sudden change in appearance to a brighter discharge and a sudden increase in the dc current. This indicated the sudden formation of a dc glow or dc arc, with a voltage and current mainly determined by the open circuit voltage and resistance of the dc source and the discharge V-I characteristic.

Over the negative slope region with $I_m < 0.4$ A, the discharge was similar to a dc glow with clear cathode and anode spots.
The discharge characteristics were similar to the normal dc glow and arc discharge V-I curves but with lower voltages due to the extra ionisation from the superimposed ac current.

Fig. 6.7c shows an oscillogram for the voltage and current waveforms in this region for I_m=100 mA and $I_{d(dc)}$=150 mA and $V_{d(dc)}$=430 V.

6.2 CONDITIONS FOR IGNITION OF DC ARCS USING HF DISCHARGES

The formation of a continuous hf discharge which created a conduction path for the main dc current did not always guarantee the ignition of a dc arc. It was therefore necessary to carry out a series of tests to obtain the conditions under which an hf discharge will reliably initiate a dc arc.

A series of investigations was carried out to find the limiting values of voltage, current, power and resistance of the hf starting discharge to allow arc ignition. Steady-state discharges were used and the V-I curves shown in Figs. 6.2 - 6.5 were used for the analysis.

In the first series of tests an hf discharge in a 3 mm TIG arc gap was established either by breakdown or touch started. The dc output voltage was then gradually increased keeping the series resistance constant, until a sudden change in appearance to a brighter discharge and a sudden increase in dc current occurred indicating arc ignition. The dc output voltage was greater than 180 V for an ac current of 0.3 A and series resistance of 50 Ω and it was more than 400 V for a series resistance of 500 Ω for the same ac current. In the second series of tests an hf discharge with a current of 50 mA to 2 A was established and for each test the output dc voltage was kept constant at either 200 V or 80 V. For each value of ac current and dc open circuit voltage the value of the series resistance was gradually reduced until a dc arc suddenly established. For a dc open circuit voltage of 80 V and an ac current of 0.6 A, the series resistance was less than 40 Ω and for a dc open circuit voltage of 200 V for the same hf discharge current the series resistance was less than 120 Ω for a transition to a dc arc to occur.

The results indicated that the dc output voltage, the hf discharge current and the series resistance in the dc current path had an effect on the ignition of the dc arc which may be explained by the schematic diagram of Fig. 6.8 corresponding to the results shown in Figs. 6.2 - 6.5.

Fig. 6.8 shows two curves, one for a combined ac-dc glow discharge and the other for a combined ac-dc arc discharge. Point A is the operating point on the positive slope region using an hf glow and it is stable even if the main power supply load line also cuts the dc arc region. The operating point on the ac-dominated region is stable because an increase in the dc current by for example some transient condition at point A, increases the voltage across the discharge. This reduces the difference between the dc applied voltage and the discharge voltage and therefore the current decreases; as a result when the load line cuts both the positive and negative slope curves the operating point will not transfer to the dc-dominated region and the arc will not be ignited.

Point A is also stable when the dc current decreases since the voltage across the discharge becomes smaller. This increases the difference between the dc applied voltage and the discharge voltage and therefore the current will increase and point A is again restored.

From the results of over 50 tests, it was concluded that an hf discharge will start a dc arc if the main power source load line cuts only the negative slope curve on the combined ac-dc discharge V-I curve. For a given hf discharge current the dc open circuit voltage should be greater than the highest voltage (V_t) of the transition region (Fig. 6.8) and the series resistance should be small enough to make the load line cut the dc-dominated curve without intersecting the

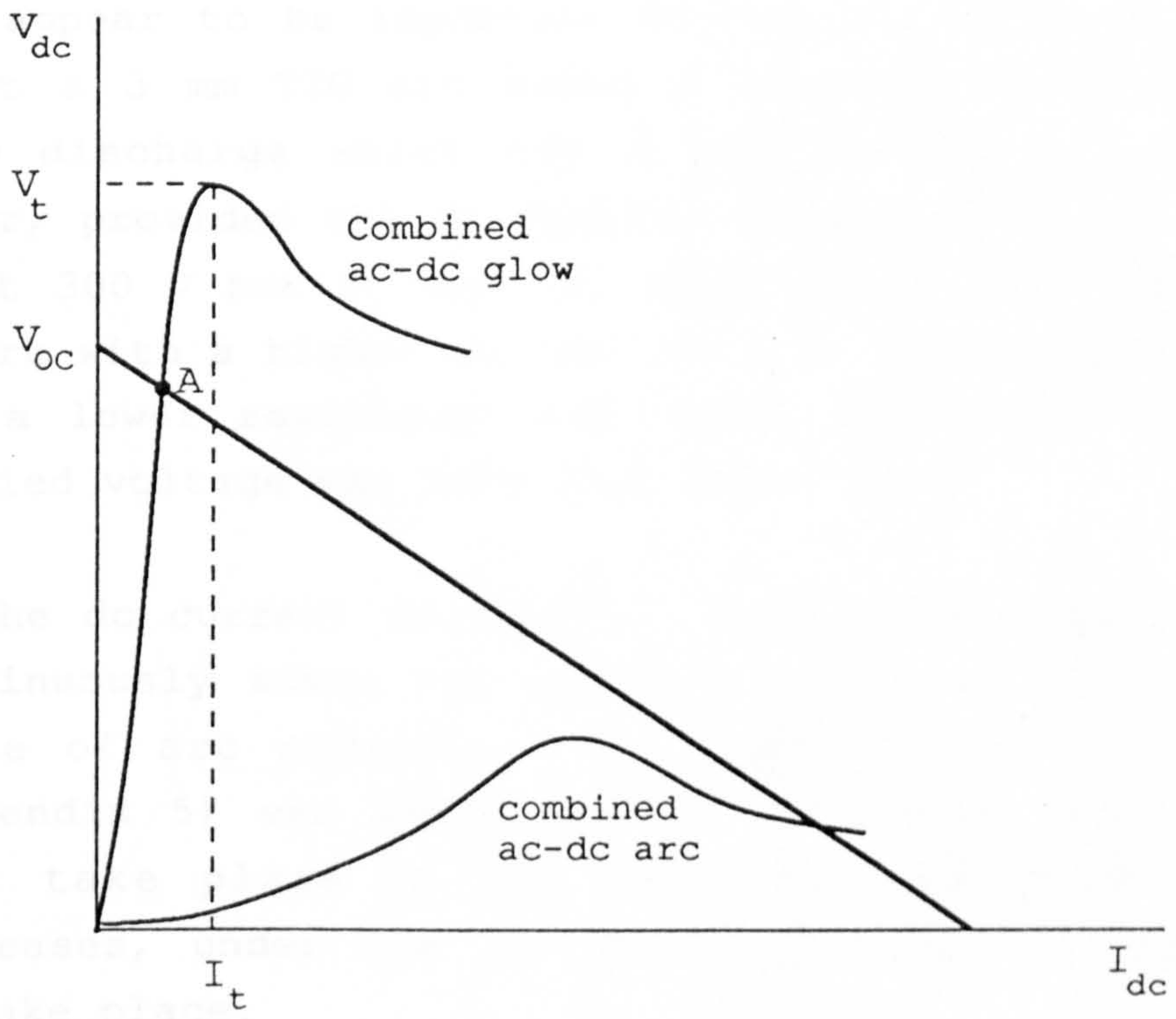

Fig.6.8 Schematic diagram showing the restriction that the hf discharge causes when the load line intersects the ac-dominated curve.

ac-dominated curve. The conditions can be represented by a relationship:

$$R < \frac{V_{oc} - V_t}{I_t}$$

where I_t is the dc current at which V_t is reached on the combined ac-dc discharge characteristic for a given hf discharge current.

The resistance or power of the starting discharge did not appear to be important because it was possible to start a 3 mm TIG arc using a low current (50 mA) hf glow discharge which has a high resistance and low power, provided the dc applied voltage was higher than about 300 V but it was not possible to start the same dc arc with a higher current (0.3 A) hf discharge which has a lower resistance and higher power, when the dc applied voltage was less than about 150 V.

As the dc current increases, the operating point moves continuously along the ac-dc curve up to the maximum value of arc current. The rotating load line model (Appendix 5) was developed to illustrate the changes that take place in the combined discharge as I_{dc} increases, under the conditions required for ignition to take place.

Fig. 6.9 shows that as the dc current increases from zero the main supply load line rotates anticlockwise because the slope of the load line decreases with time. The operating point which is the intersection between the load line and the combined discharge curve, moves continuously along the ac-dominated curve and if the load line stops rotating as the slope becomes equal to the series resistance, before it reaches the transition region, the discharge will remain ac-dominated. If, however, it carries on rotating due to having a smaller series resistance, just after the intersection with the transition region the operating point will suddenly transfer to the dc-dominated region.

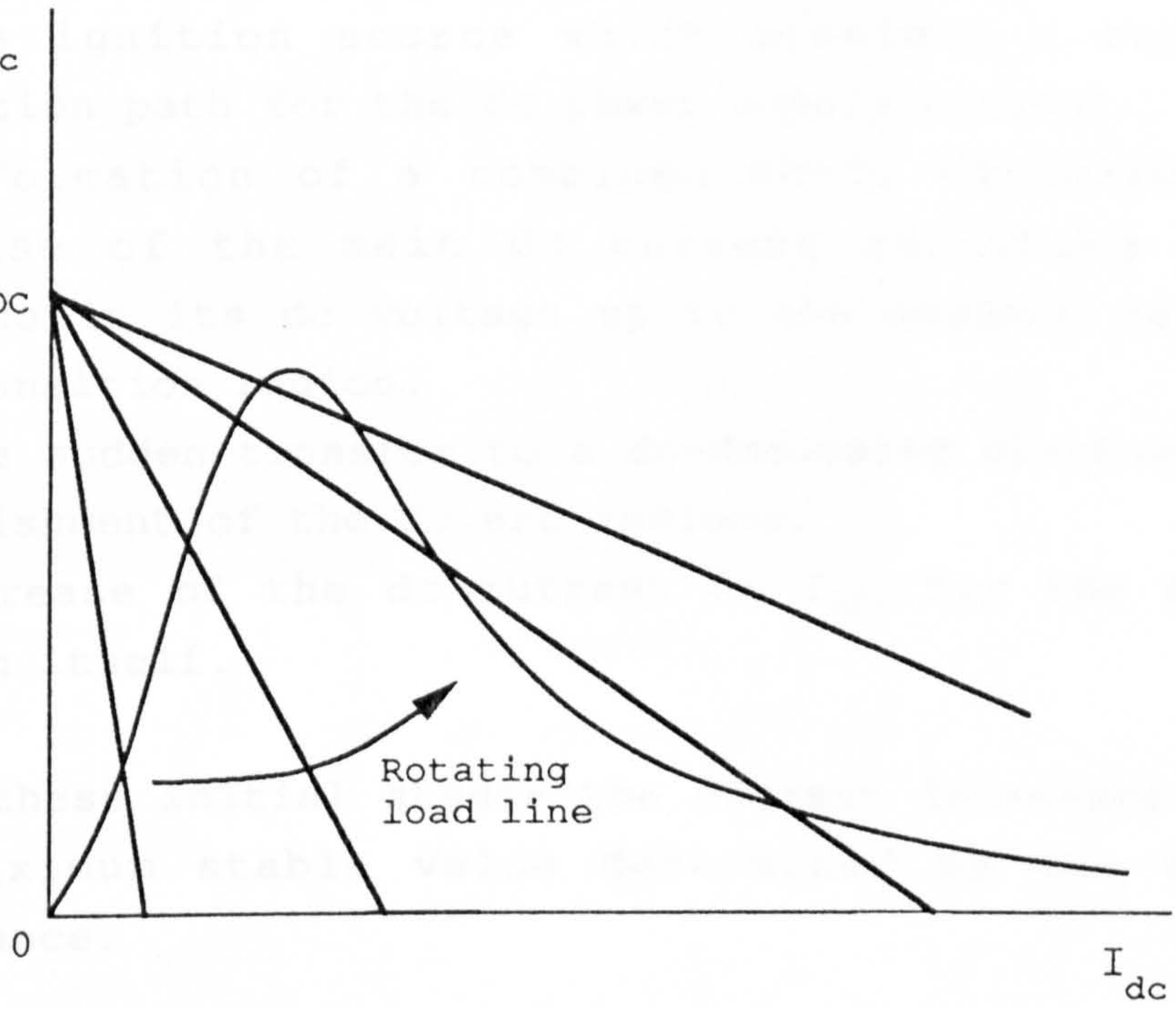

Fig.6.9 Rotating load line model

6.3 HIGH FREQUENCY ARC IGNITION FROM COLD

The non-contact hf arc ignition process may be divided into five stages:

i) Breakdown of the arc gap using an external hf high voltage source. (Breakdown of the gap does not however guarantee arc ignition).
ii) Establishment of an hf starting discharge sustained by the ignition source which provides a suitable conduction path for the dc power supply current.
iii) Formation of a combined ac-dc discharge and increase of the main dc current resulting in an increase in its dc voltage up to the maximum value at the transition region.
iv) The sudden transfer to a dc-dominated discharge and establishment of the dc arc regions.
v) Increase of the dc current to I_{min} for the arc to sustain itself.

After these initial stages the current increases up to the maximum stable value determined by the series resistance.

Fig. 6.10 shows typical voltage and current waveforms for a 3mm TIG arc gap indicating the different transitions that occur during the initial current rise after breakdown from cold using a continuous sinusoidal hf source.

Initially after breakdown from cold, field processes are responsible for ionisation in the column and the electrode fall regions (Chap. 5) and as a result the arc voltage will be higher than for the steady-state combined ac-dc discharge. The hf starting discharge current may therefore need to be higher than those found in section 6.2 which were steady-state values, to satisfy the conditions for arc ignition.

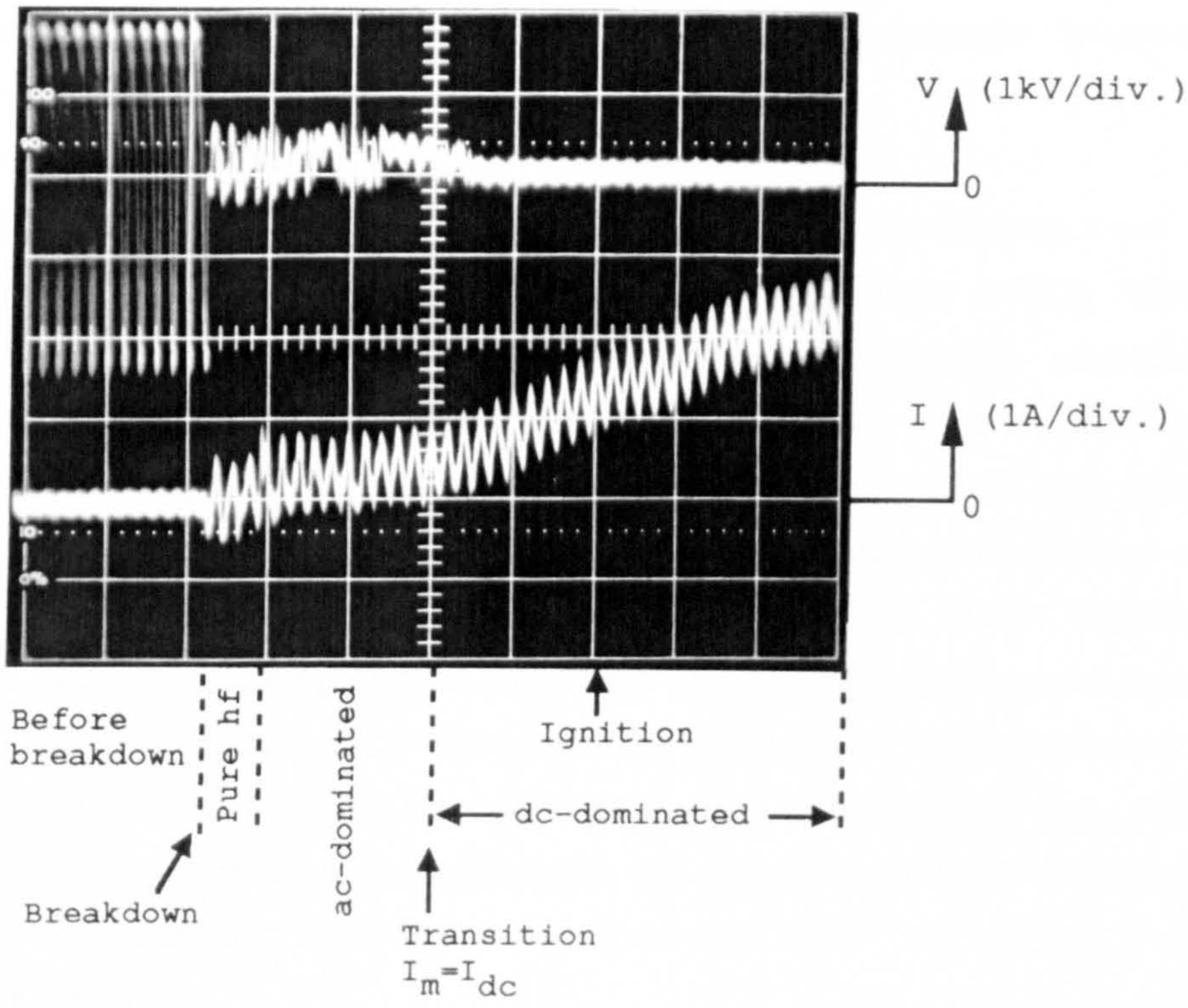

Fig.6.10 Voltage and current waveforms during ignition from cold. Time-base: 5 ms/div. Sinusoidal waveforms are affected by the sampling rate of the oscilloscope.

The results of a series of tests on ignition from cold showed that the required hf starting discharge current and hence V_t and I_t (section 6.2) are lowered if the time taken to reach the transition region is increased by for example increasing the inductance in the dc current path. The longer time (14 ms in Fig. 6.10) taken to reach the transition region allows the discharge to develop thermally and reach the V-I characteristic of a steady-state discharge shown in Figs. 6.2 - 6.5.

For a one hundred per cent reliable ignition and establishment of a self-sustained arc from cold, the dc current at which the transition region occurs should be at least equal to the minimum required arc current to sustain a cold arc. This is to allow the arc to become self-sustained at the transition region and there will be an immediate change from support by the ignition source to the support by the main power source. By reference to Fig. 5.2 estimates for the ac current for a given dc open circuit voltage can therefore be found. For a dc open circuit voltage of 80 V and 200 V, the ac current needs to be at least 0.9 A and 0.7 A respectively.

6.4 SUMMARY OF RESULTS

The variation of the dc voltage with dc current of combined ac-dc discharges for frequencies in the range of 10 kHz - 800 kHz and current of 50 mA - 2 A using copper cathodes in air or TIG arc gaps have shown that three different regions exist. An ac-dominated discharge, a dc-dominated discharge and a transition region.

A reliable, safe and RFI-free non-contact ignition may be achieved by causing one reliable breakdown followed by a suitable starting discharge using a continuous sinusoidal hf method.

For an hf discharge to ignite a dc arc, the dc applied voltage should be higher than the voltage at the transition region and the dc supply resistance should be small enough to make the dc supply load line intersect only the dc-dominated curve.

The discharge is initially a sinusoidal hf discharge because the dc current is still very small. As the dc current increases, the operating point moves up the ac-dominated curve with increasing dc voltage, reaches the transition region and then transfers to the dc-dominated region and a dc arc may be established.

For the ignition of a 3 mm TIG arc with a breakdown voltage of about 3 kV supplied by a dc source of open circuit voltage of 80 V, an hf discharge current of about 0.9 A is required. The ignition source should therefore have an output voltage of at least 3 kV and output current of 0.9 A and be designed for continuous operation to avoid the uncertainties owing to the time required for the arc to establish. The ignition system will then require high output powers of more than 1.35 kW which may not be feasible.

The work described in this chapter has been published as detailed below:

(1) SAIEPOUR, M., HARRY, J.E., 'Continuous sinusoidal HF arc initiation', J. Phys. D: App. Phys., 23, (8), pp. 1129-1131, 1990.

(2) SAIEPOUR, M., HARRY, J.E., 'Characteristics of combined high frequency and DC discharges', 25th Universities Power Eng. Conf., Robert Gordon's Inst. of Tech., Aberdeen, Scotland, 12-14 Sept., pp. 341-344, 1990.

CHAPTER 7

CONTINUOUS SINUSOIDAL SPLIT HF IGNITION SYSTEM

7.0 CONTINUOUS SINUSOIDAL SPLIT HF IGNITION SYSTEM

In any arc ignition method the requirements for electrical stability must be satisfied or the arc will not be finally established. The arc will not initiate because of the disappearance of the ionised path before the arc becomes self-sustained or even if it is formed momentarily, it will not continue to exist due to for example:

i) the decrease in current below a desired value (≈1 A) due to underdamped oscillations in the initial current rise or

ii) positional instability in the cold arc due to the movement of the cathode spot and the column.

These uncertainties make the time required to achieve ignition difficult to predict and hence a continuous starting discharge is necessary to allow the arc to initiate and thermally stabilise.

A reliable method for ignition to eliminate RFI and maintain safety is to apply a continuous sinusoidal hf voltage (Chap. 6). This provides a single reliable breakdown of the arc gap followed by a suitable continuous hf starting discharge which exists until the main arc is fully established, to eliminate the time restrictions. This method is also effective when used with a main dc supply having a low rate of current rise.

To initiate a 3 mm TIG arc from cold reliably, supplied by a dc source of open circuit voltage of 80 V, the hf ignition source should have an output voltage of about 3 kV (peak) to break down the gap and supply an output current of at least 0.9 A (peak) to sustain a suitable starting discharge. The use of a single ignition source to provide both high voltage and relatively high current simultaneously, designed for continuous

operation, requires large output powers of about 1.35 kW for a 3 mm TIG arc gap. It will therefore be bulky and expensive, even if solid-state devices are used. Table 7.1 gives approximate values for the required breakdown voltage, hf peak discharge current and the required output power from a single continuous sinusoidal hf ignition system.

This chapter describes the design of a new ignition system which maintains all the advantages such as safety, reliability of ignition and reduced RFI of a single continuous sinusoidal hf system but requires much lower powers. This ignition system is based on a continuous sinusoidal split hf technique.

7.1 BASIS OF THE DESIGN AND MINIMUM REQUIREMENTS OF THE SPLIT HF SYSTEM

A non-contact ignition source is initially required to break down the arc gap. To break down a 3 mm TIG arc gap under the conditions stated previously using frequencies up to 800 kHz a voltage of about 3 kV is needed (Chap. 4). The second requirement of the ignition system is to support the starting discharge to provide a suitable conduction path for the main dc supply. For reliable ignition an hf discharge should have a peak current of at least 0.9 A to start a 3 mm TIG arc from cold supplied by a dc power supply of output voltage of 80 V to satisfy the condition for ignition (Chap. 6).

These requirements can be met by using two separate continuous sinusoidal hf power sources. This is referred to in the text as the split hf technique. The first (HF1) causes breakdown of the arc gap and provides only a small current to sustain a low current discharge to create a conduction path for the second ignition source (HF2). The second source will support a

Type of arc gap	V_b (kV) peak	I_m (A) peak	P_{out} (kW)
Cu electrodes 3 mm gap	11	1	5.5
Cu electrodes 1 mm gap	5	1	2.5
3 mm TIG	3	0.9	1.35

Table 7.1 Required output voltage, current and power from a single hf ignition system.

higher current starting discharge and creates a suitable conduction path for the main dc supply.

Fig. 7.1 shows a schematic diagram for the complete split hf ignition process. The arc ignition process using a spilt hf technique may be divided into the following stages:

i) Breakdown of the arc gap by a high voltage produced by HF1.

ii) Formation of a low current (about 50 mA) hf discharge supported by HF1 which provides a suitable conduction path for HF2.

iii) Establishment of a double frequency (f_1 and f_2) discharge and increase of the current from HF2 resulting in an hf discharge which provides a suitable conduction path for the main power supply current.

iv) Increase of the main dc current, formation of a combined ac-dc discharge and an increase in its dc voltage up to the maximum value at the transition region.

v) The transfer to a dc-dominated discharge.

vi) Increase of the dc current to I_{min} for the arc to sustain itself.

A series of tests was carried out to determine the minimum current required from HF1 to start a higher current (≈1 A) hf discharge from HF2 of a different frequency. The results showed that the low current discharge just after breakdown by HF1 may have currents as low as 10 mA to start the second hf discharge, but a current of higher than 50 mA makes the initial discharge relatively more stable against gas flow in a typical TIG welding arc gap.

A further series of tests was carried out to determine the minimum output voltage required from HF2 to sustain an hf discharge of current of about 1 A. These results showed that an output voltage of about 300 V supplied by HF2 was sufficient to support a 1 A hf discharge.

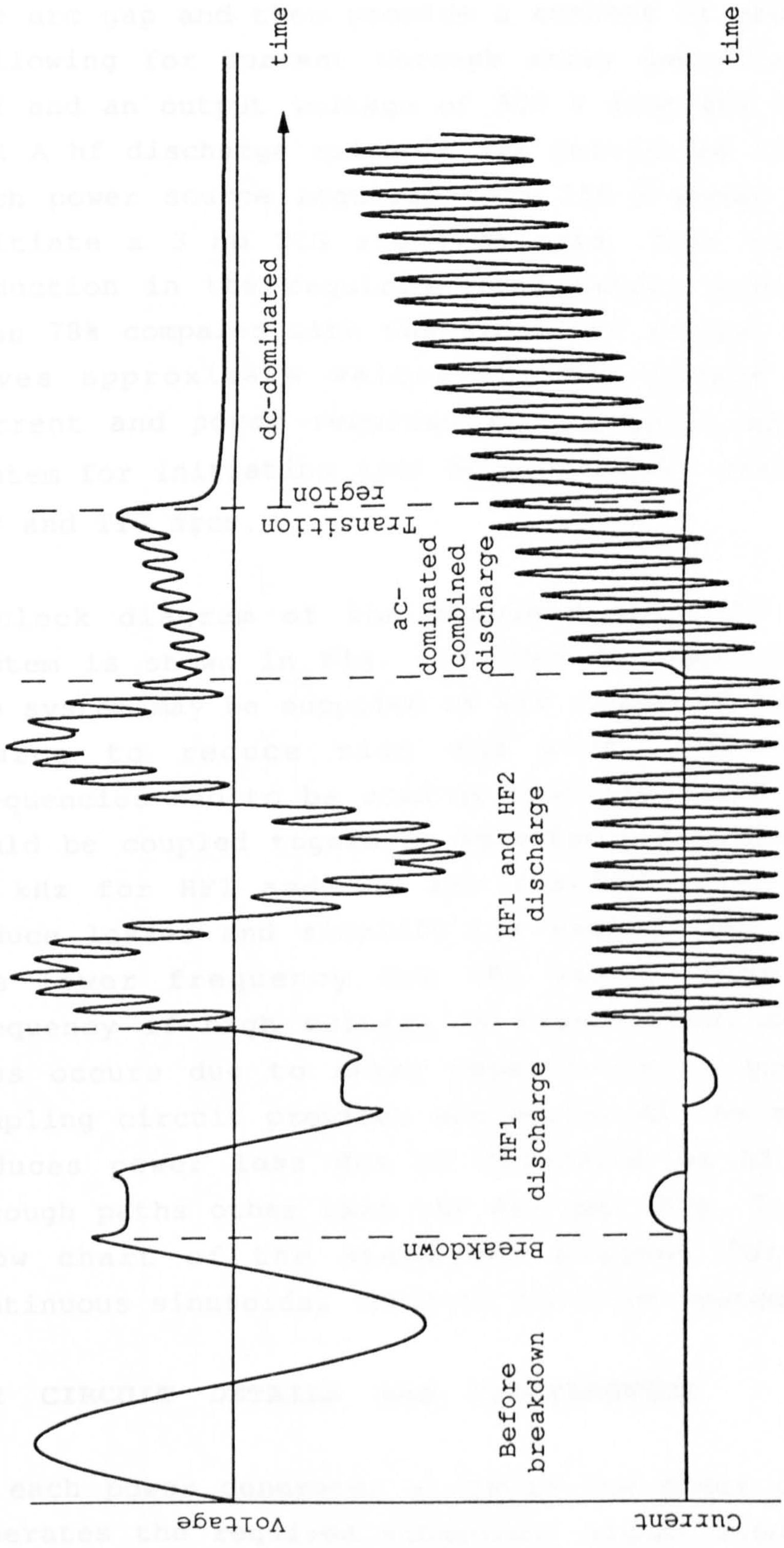

Fig.7.1 Schematic diagram showing the stages in a complete split hf ignition process.

The split hf system should therefore initially produce an output voltage of about 3 kV from HF1 to break down the arc gap and then provide a current of about 100 mA (allowing for current through stray capacitance) from HF1 and an output voltage of 300 V from HF2 to sustain a 1 A hf discharge suitable for initiating the dc arc. Each power source required only 150 W power output to initiate a 3 mm TIG arc from cold. This indicated a reduction in the required total output power of more than 78% compared with the single hf system. Table 7.2 gives approximate values for the output voltage, current and power required from a split hf ignition system for initiating arcs between copper electrodes in air and TIG arcs.

A block diagram of the complete split hf ignition system is shown in Fig. 7.2. The dc input current to the system may be supplied by the output of the main dc source to reduce size and cost. Two different frequencies had to be used so that the two hf circuits could be coupled together. Relatively low frequencies, 30 kHz for HF1 and 300 kHz for HF2 were chosen to reduce losses and simplify the design. The choice of the lower frequency for HF1 was because at high frequency if high voltage is transmitted, more power loss occurs due to stray capacitance to ground. The coupling circuit provides protection of the system and reduces power loss due to diversion of hf currents through paths other than the arc gap. Fig. 7.3 shows a flow chart of the steps and reasons for using a continuous sinusoidal split hf ignition system.

7.2 CIRCUIT DETAILS AND CONSTRUCTION

In each power generator a stable low power oscillator generates the required sinusoidal signal which after a power boost by a buffer amplifier, is used to drive a class-A amplifier the output of which is coupled to a class-B push-pull linear power amplifier to convert the

Type of arc gap	HF1			HF2			Total required output power (W)	Reduction %
	V_b (kV) peak	I_m (mA) peak	P_{out} (W)	V_{out} (V) peak	I_m (A) peak	P_{out} (W)		
Cu electrodes 3 mm gap	11	100	550	300	1	150	700	87
Cu electrodes 1 mm gap	5	100	250	300	1	150	400	84
3 mm TIG	3	100	150	300	1	150	300	78

Table 7.2 Required output voltage, current and power from a split hf ignition system.

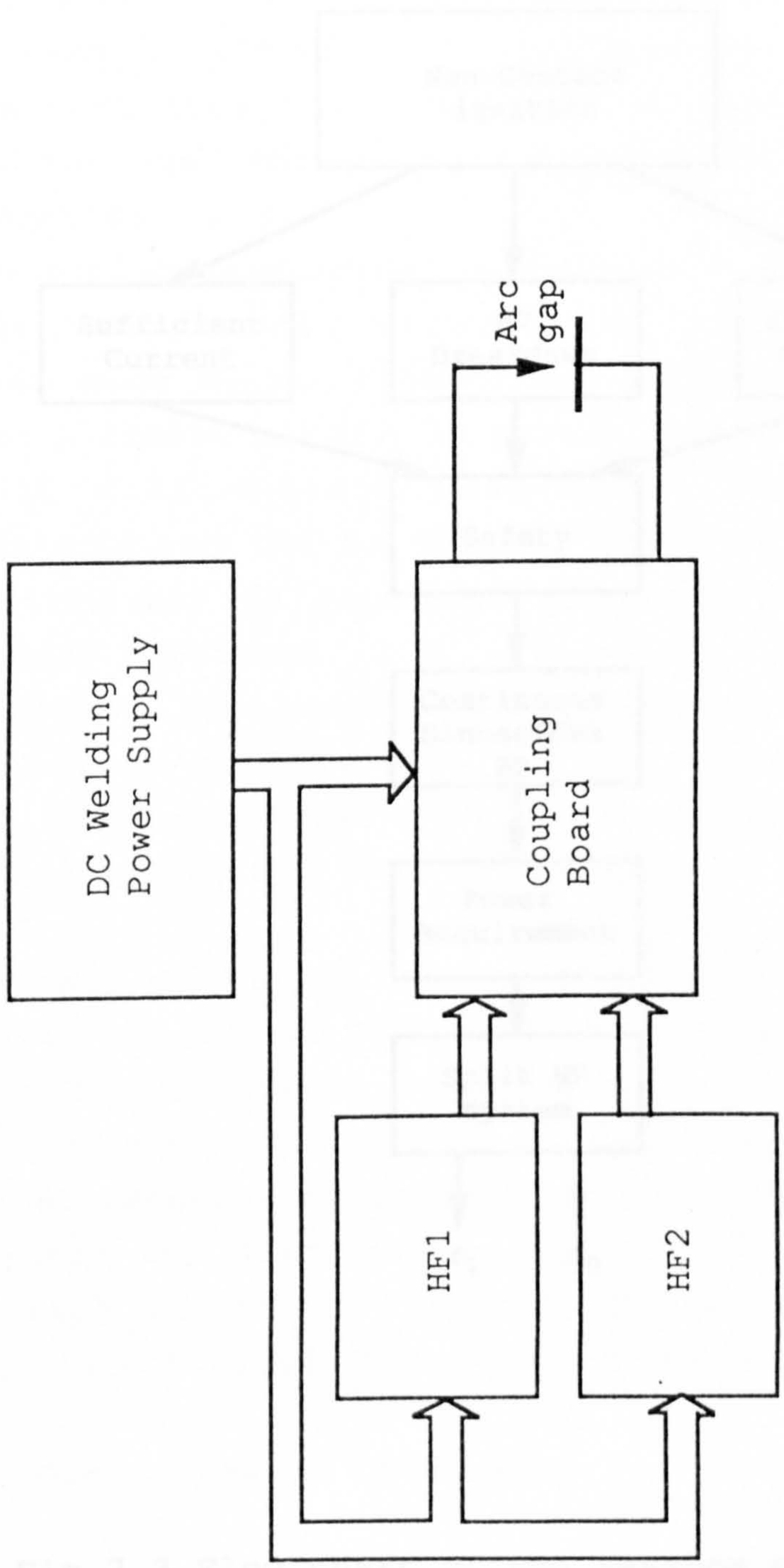

Fig.7.2 Block diagram showing the complete split HF ignition system .

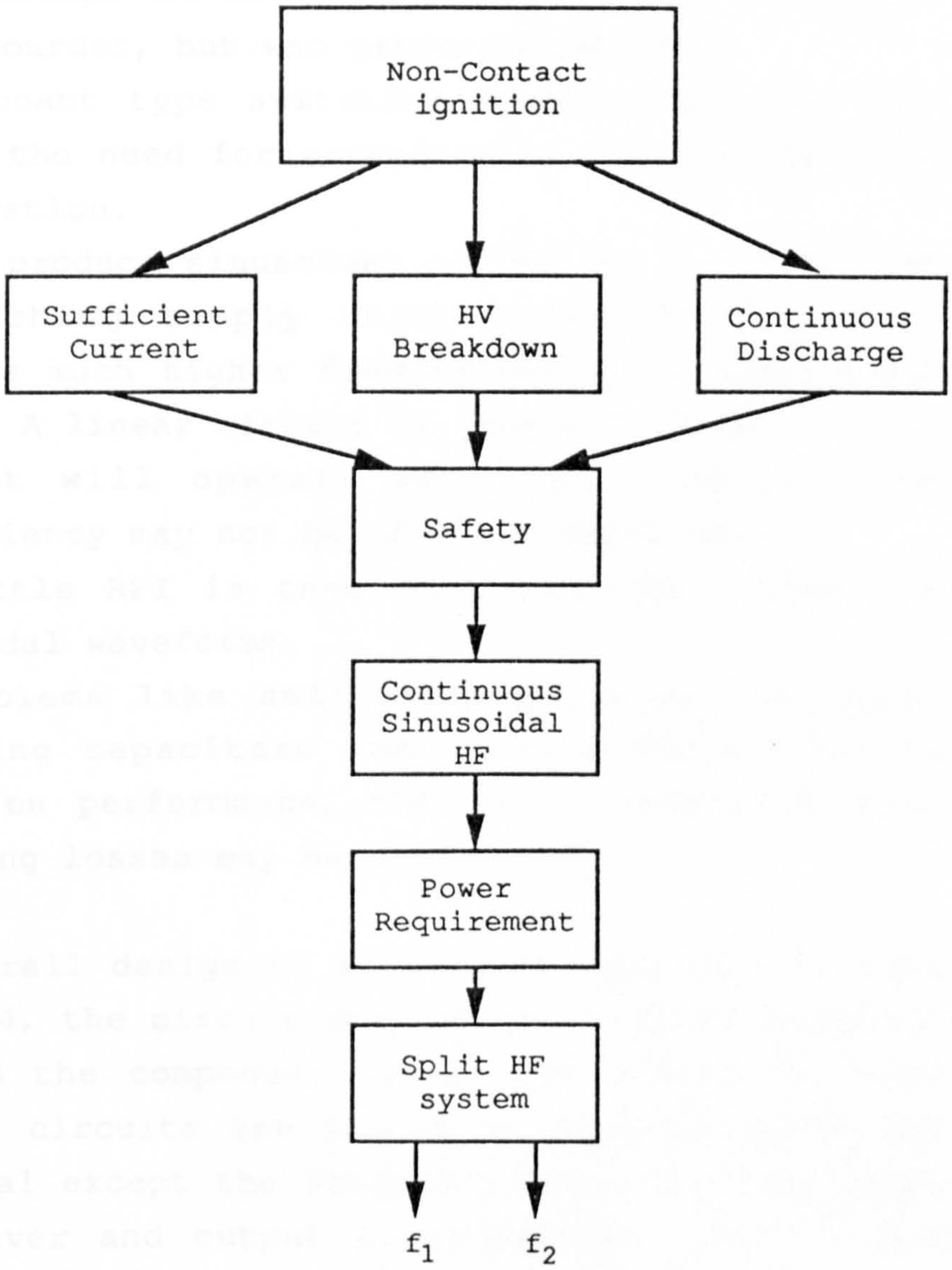

Fig.7.3 Flow chart of the reasons behind using a continuous sinusoidal split HF system.

70V dc power supply into an hf power of the required voltage and current. A linear amplifier has the disadvantage of lower efficiency than switched mode power sources, but was preferred because:

i) resonant type switching supplies are not suitable due to the need for occasionally varying the frequency of operation.

ii) to produce sinusoidal outputs at a given frequency a switching supply using pulse width modulation requires much higher frequencies which complicates the design. A linear circuit is generally simpler.

iii) it will operate only for a short time and inefficiency may not be of great importance.

iv) little RFI is generated from the circuit due to sinusoidal waveforms.

v) problems like self-oscillation can be solved by including capacitors and ferrite beads with little effect on performance, whereas in switching supplies, switching losses may be introduced.

The overall design of each power generator is shown in Fig. 7.4, the circuit diagram for each is shown in Fig. 7.5 and the component values are listed in (Appendix 4). The circuits are placed on separate pcb's and are identical except the frequency adjusting components and the driver and output transformers; Fig. 7.6 shows a photograph of one of the hf modules. The coupling circuit is contained on a separate board.

7.2.1 Output Power Amplifier

The power MOSFET's (M_1 and M_2) are the basis of the power amplifier and are connected in a common source push-pull arrangement which allows a higher efficiency and twice the output voltage for the same output transformer turns ratio and input dc voltage. The even harmonics are also suppressed and therefore less RFI and better sinusoidal outputs are achieved. MOSFET's are preferred to bipolar transistors because they are

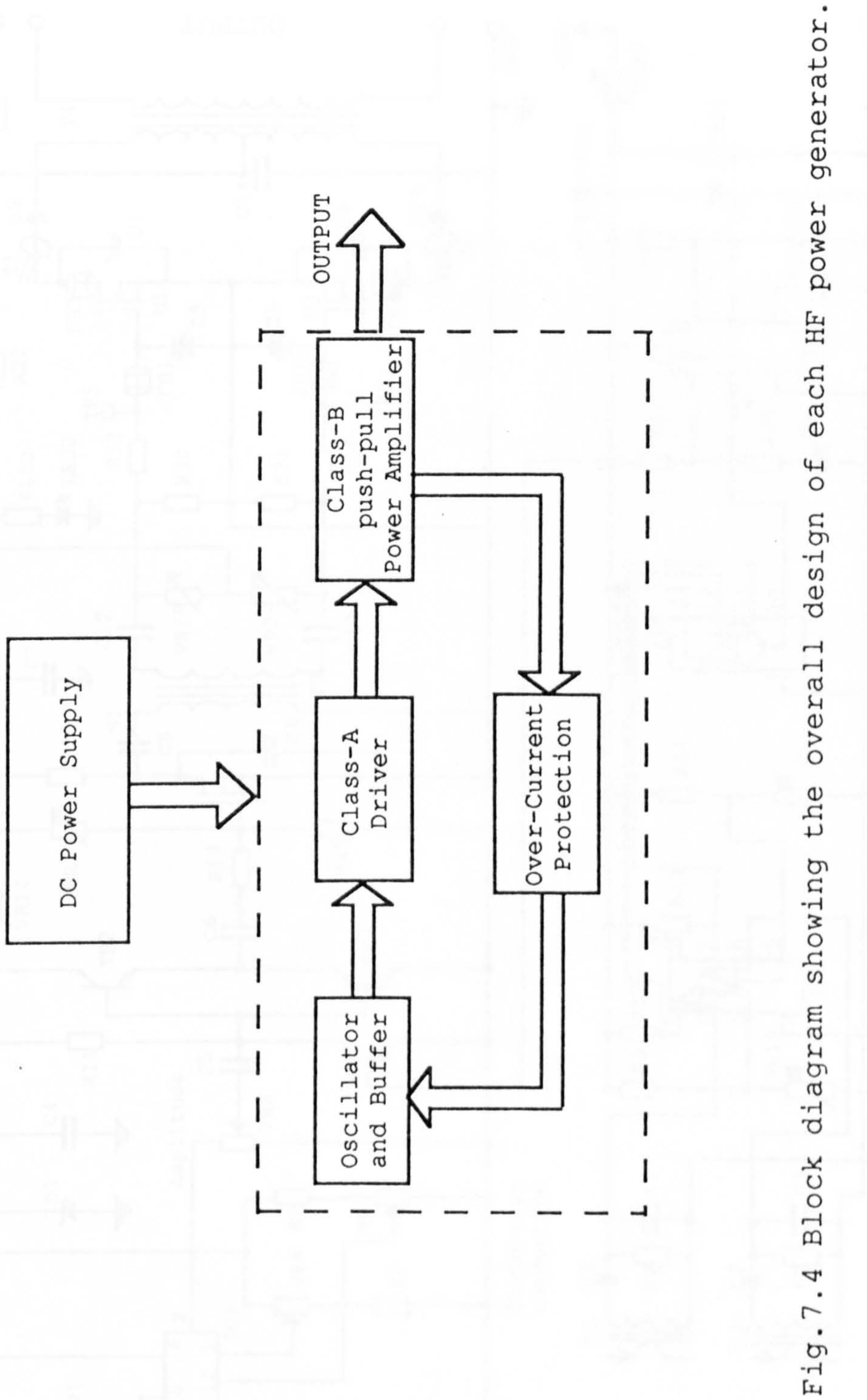

Fig.7.4 Block diagram showing the overall design of each HF power generator.

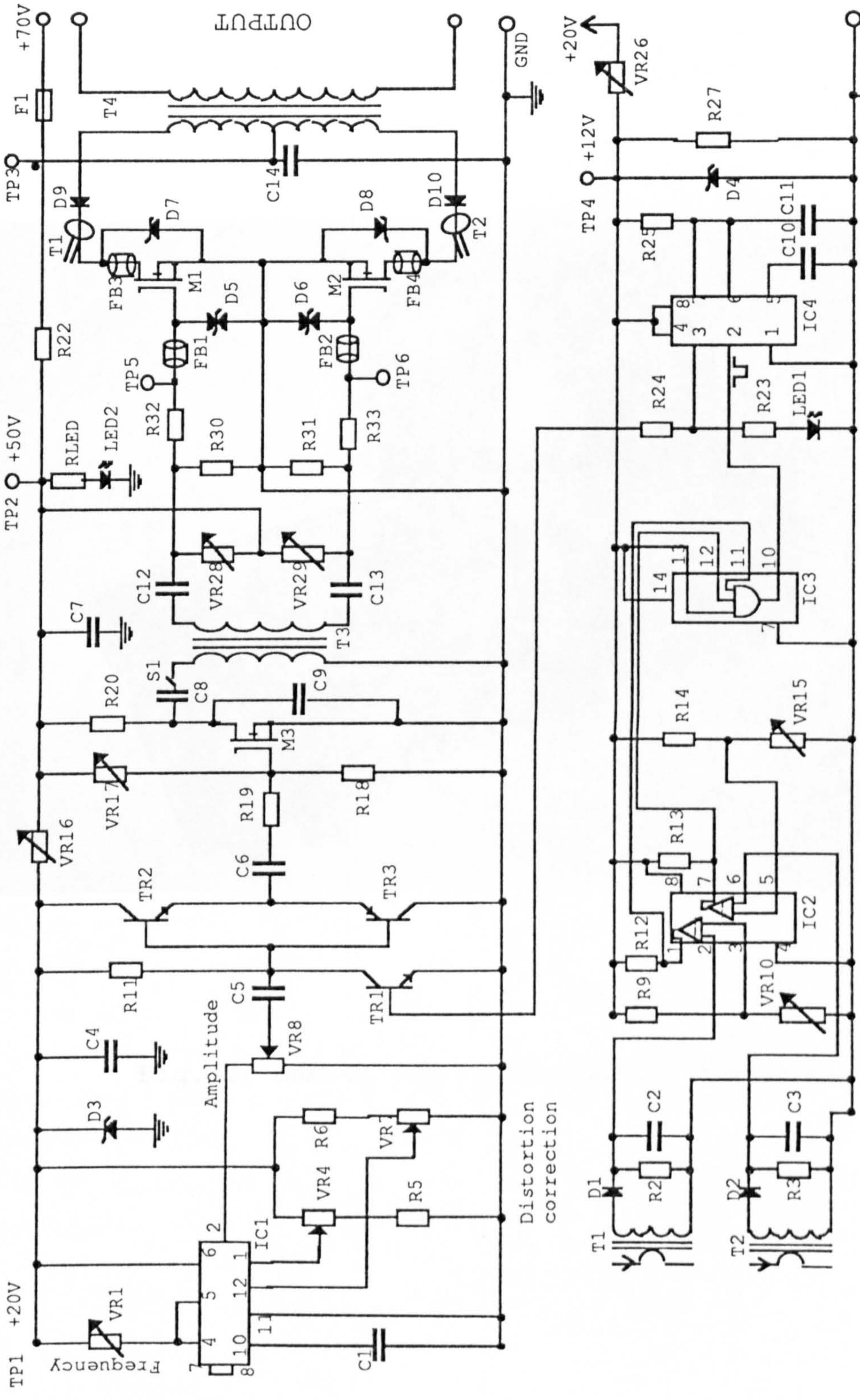

Fig.7.5 Circuit diagram for each HF power generator

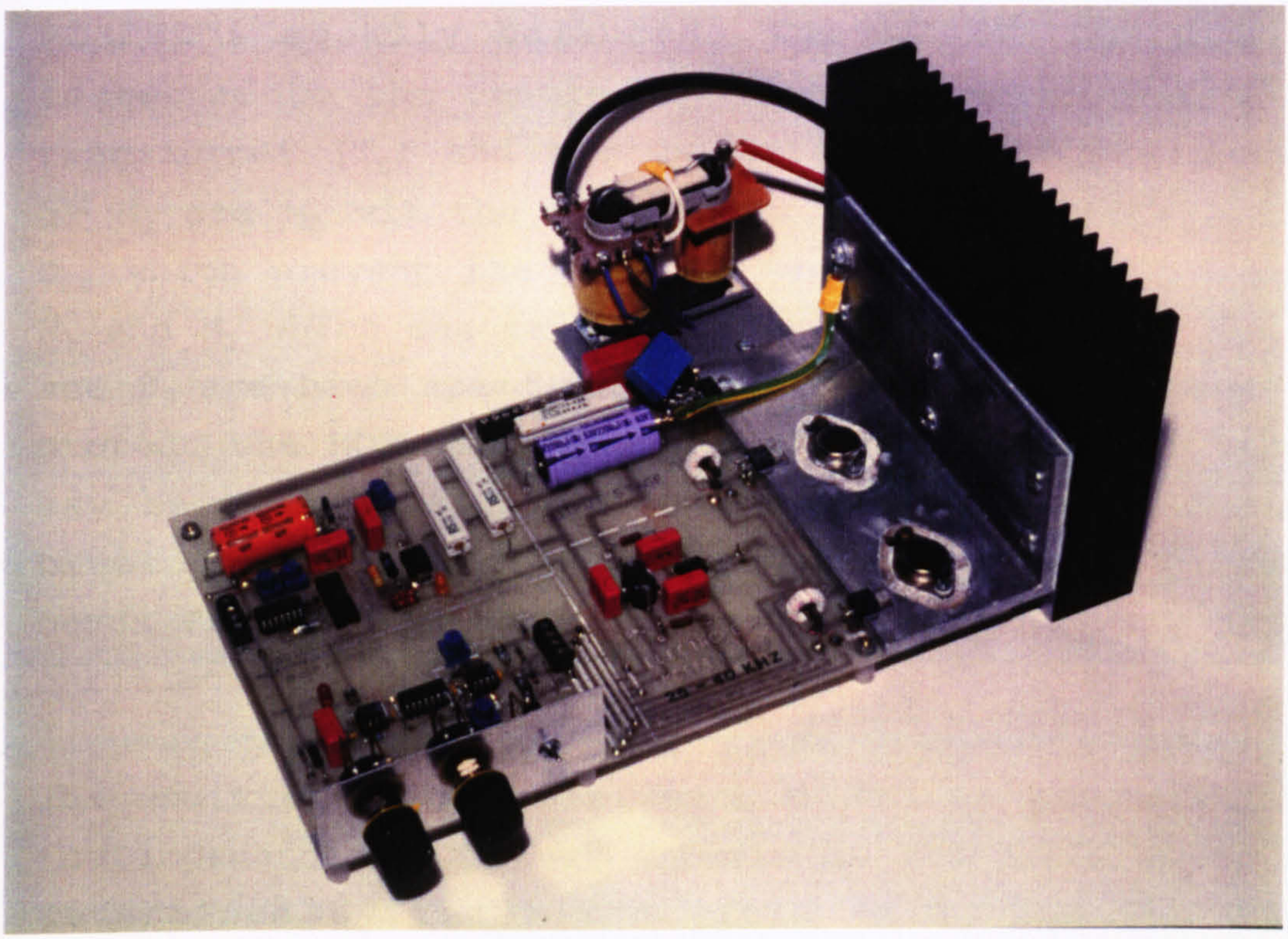

Fig.7.6 One of the prototype HF modules.

more tolerant to load mismatch which is important for ignition systems, require less drive power and simpler drive and biasing circuitry. The individual gate bias voltages are set by the biasing resistors VR_{28}, R_{30}, VR_{29} and R_{31}. The values for these resistors were made small to reduce the effect of reflected voltage from drain to gate through the MOSFET drain to gate parasitic capacitor, but this reduced the input impedance of the output stage. The gate bias voltages were set for class-B operation and care was taken to make the two MOSFET's equally balanced. The 70V dc voltage is connected to the centre-tap of the output push-pull transformer (T_4) and the current is fed to the drains of M_1 and M_2 via the high speed recovery diodes D_9 and D_{10} which prevent the flow of reverse currents through M_1 and M_2 which can cause heating and damage. D_5, D_6, D_7 and D_8 are high speed transient voltage suppressors to protect the MOSFET's against high voltage spikes which may be reflected from the arc gap especially during breakdown, through the output transformer. Ferrite beads FB_{1-4} and gate resistors R_{32} and R_{33} prevent self-oscillations.

The drain current (I_D) of each MOSFET is controlled by the impedance (R'_L) that appears at its drain which is determined by the turns ratio of T_4 and the load impedance (R_L). The proper design (or selection) of T_4 is important to match the load which may have large variations, to the output stage. The discharge controls the value of R_L which changes from almost an open circuit before breakdown of the arc gap to a low value when the 1 A hf discharge is established. The required output from HF2 is 300 V and 1 A peak from the secondary of T_4 and therefore the load impedance is:

$$R_L = \frac{300}{1} = 300\ \Omega$$

If the allowed maximum drain current for each IRF360 MOSFET is 5 A when operating in a linear mode, then:

$$R_L' = \frac{V_D}{I_D} = \frac{70}{5} = 14\ \Omega$$

but

$$R_L' = \left(\frac{N_1}{N_2}\right)^2 . R_L$$

where N_1 is half the primary turns and N_2 is the secondary
turns number. Therefore:

$$\frac{N_2}{N_1} = \sqrt{\frac{R_L}{R_L'}} = \sqrt{\frac{300}{14}} = 4.63$$

For the output transformer of HF2, Litz wire was used to reduce copper losses due to skin effect at 300 kHz and the primary inductance was made high (1.1 mH, 12 turns on each half) to reduce the magnetising current. A stack of three toroidal ferrite cores was used which reduced the leakage inductance.

Design of the output transformer for HF1 followed the same procedure. To produce the high voltage at 30 kHz a suitable television line output transformer was used in push-pull.

7.2.2 Oscillator and Driver Stage

A waveform generator (IC_1) was used to produce the sinusoidal signal of the required frequency, adjusted by VR_1 and C_1. Resistors VR_4, R_5, R_6 and VR_7 are for distortion correction and VR_8 sets the amplitude of the output. A buffer amplifier (TR_2 and TR_3) is used to give a current boost before the signal is fed to the driver MOSFET (M_3). The gate bias voltage of M_3 is set

by VR_{17} and R_{18} for class-A operation with R_{20} as the drain load resistance which is made small to lower the output impedance of the driver stage. The drain of M_3 is coupled to the input of the power stage using transformer T_3. Capacitor C_9 is placed across M_3 (drain to source) to prevent self-oscillations which are reflected through the driver transformer T_3; and Capacitors C_8, C_{12} and C_{13} are blocking capacitors. The complete system was pre-adjusted for best performance and then operated using the switch S_1.

7.2.3 Over-Current Protection

The over-current protection circuit was designed to guard against both over-current and over-heating of the power MOSFET's (M_1 and M_2). It was designed to turn off the MOSFET's if their peak drain currents exceed a certain value (i.e. 5 A for IRF360 in linear mode), thus the circuit and devices would be protected. This is achieved by sinking the input to the buffer amplifier to ground, using TR_1, hence no ac signal is fed into the MOSFET's. The drain currents (I_{D1} and I_{D2}) are sensed by the current transformers (T_1 and T_2) respectively. A dual comparator IC_2 is used to give low outputs if the input voltage representing the drain current exceeds about 5 A. The two outputs of IC_2 are fed into a 3-input AND gate (IC_3) and if any of these inputs is low, the output of IC_3 which is fed into a 555-timer (IC_4) will be low; IC_4 is then triggered which will give a positive output pulse of a given duration (i.e. 1 s) determined by R_{25} and C_{11}, and TR_1 is turned on which causes M_1 and M_2 to turn off immediately.

7.2.4 Coupling Circuit

The output of HF1 (30 kHz, 3 kV), the output of HF2 (300 kHz, 300 V), and the ouput of the main dc power supply feed the same arc gap simultaneously and the

three power sources must be protected against each other. The coupling circuit achieves this and also reduces power losses to a minimum. The circuit diagram is shown in Fig. 7.7 and a photograph of the coupling board is shown in Fig. 7.8.

Tuned circuit 1, resonates at the frequency of HF2 (300 kHz), so that it appears as a large resistance to the output of HF2. This tuned circuit is needed to eliminate the effect of C_1 at the output of HF2 at 300 kHz, by placing L_1 in parallel. C_1 is needed to suppress any high voltage spikes that may damage the output stage of HF2. Tuned circuit 2 resonates at the frequency of HF1 (30 kHz) and hence a high voltage drops across it from HF1 and therefore the 30 kHz voltage appearing at the output of HF2 will be small. This tuned circuit is capacitive to the current from HF2 (at 300 kHz) and hence to increase the required output current from HF2, an inductor L_4 is placed in series with the tuned circuit. Tuned circuit 3 resonates at the frequency of HF2 (300 kHz) and it blocks the current from HF2. Capacitors C_4 and C_6 block the dc current. L_5 and C_5 provide protection for the dc power supply and prevent loss of hf power due to the diversion of current away from the arc gap.

7.3 PERFORMANCE OF THE SYSTEM FOR ARC INITIATION

The hf power generators should be capable of operating before and after breakdown of the arc gap during which large load variations occur depending on the state of the discharge within the arc gap. Before breakdown, the arc gap is almost an open circuit and when the hf starting discharge is established its resistance may be lower than 100 Ω.

Each circuit was tested before and after breakdown of the gap by displaying the voltage waveforms at the input and output of the power stage before breakdown,

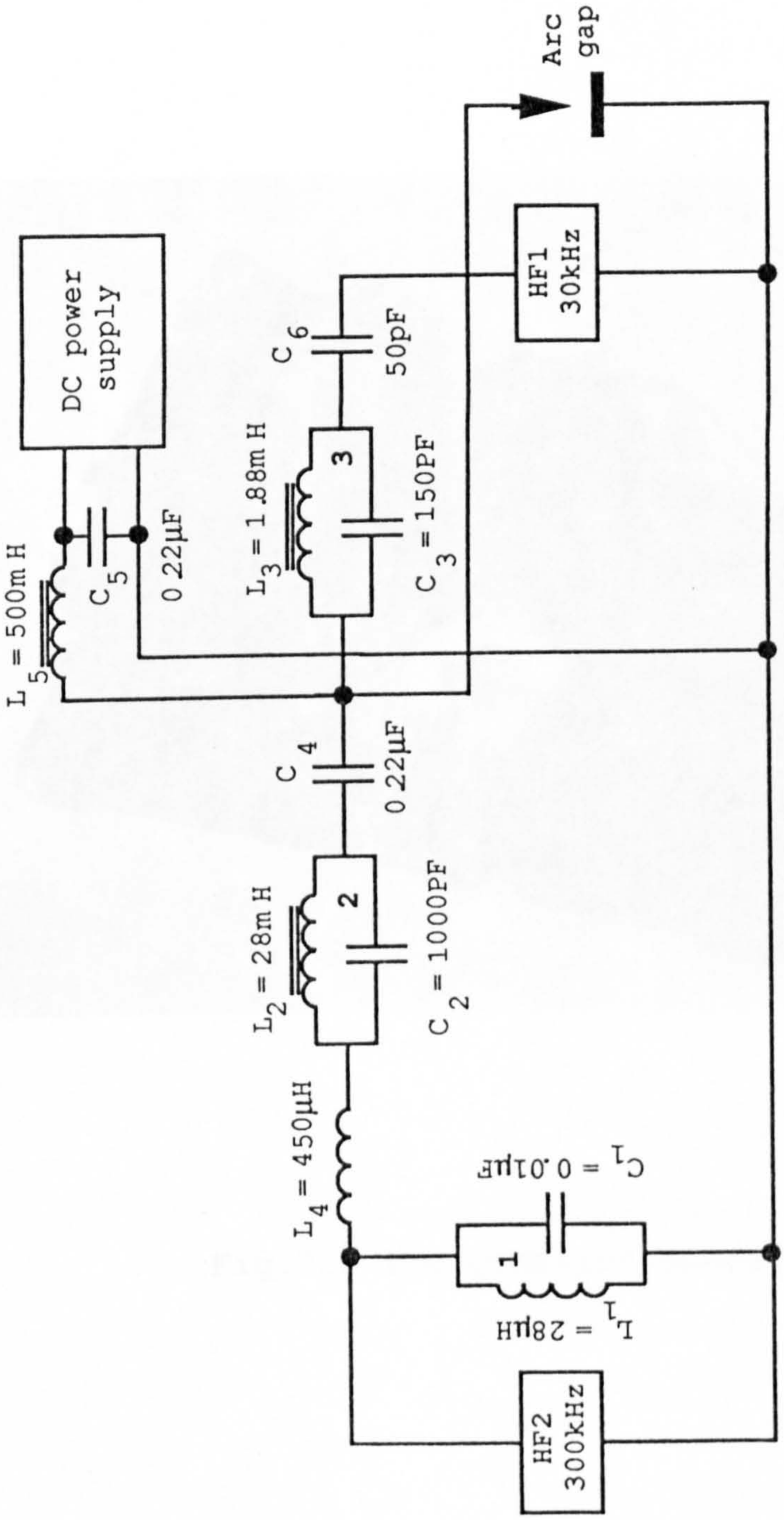

Fig.7.7 The coupling circuit.

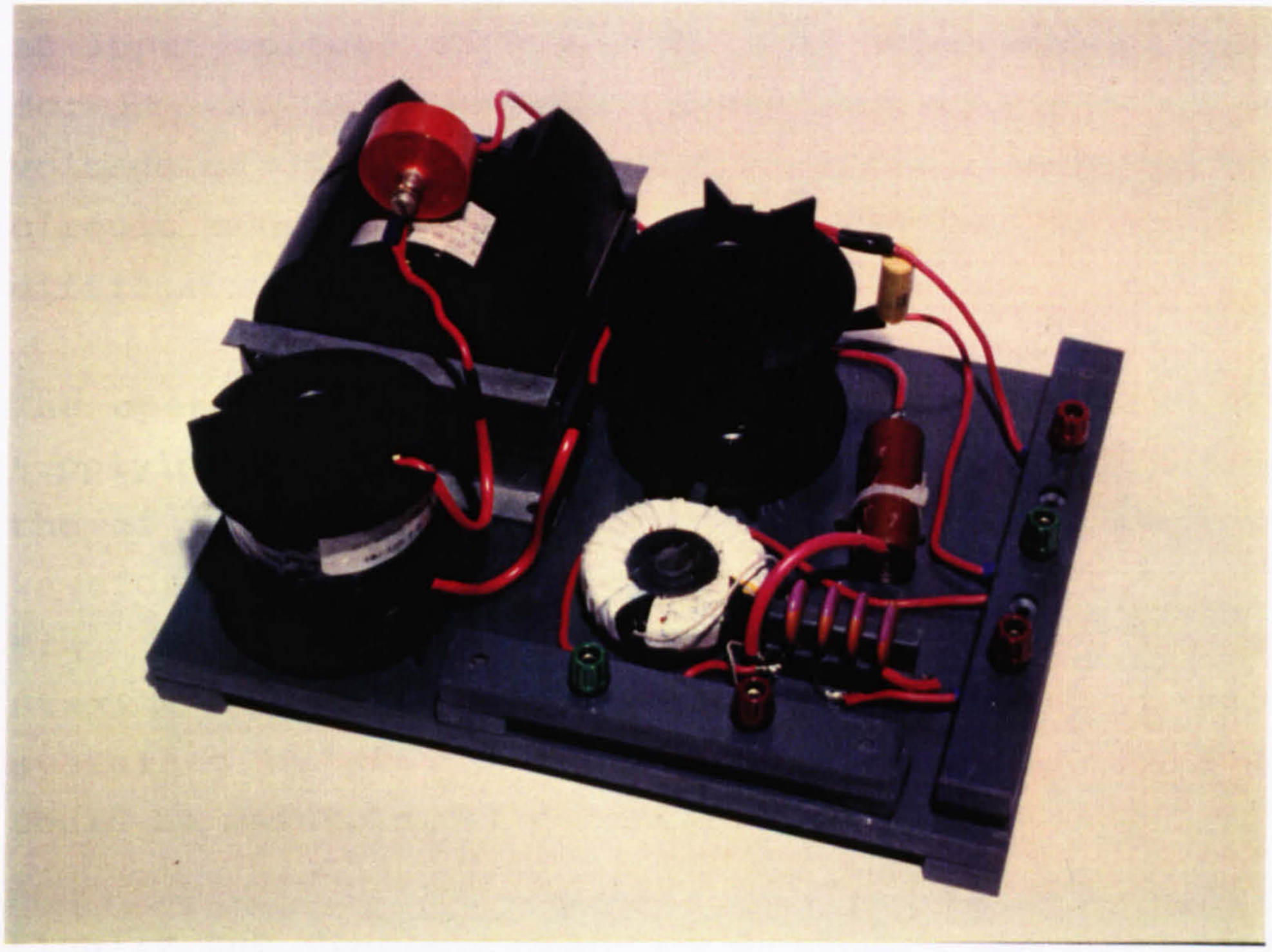

Fig.7.8 The coupling board.

and displaying the discharge voltages and currents after the required discharge was established. The input to the power stage was measured at the input to the driver transformer (T_3). The tests were carried out on a typical 3 mm TIG arc gap.

Fig.7.9a shows typical waveforms for HF1 at 30 kHz. The open circuit voltage across the arc gap was below the breakdown voltage at about 2 kV which is sinusoidal for an input voltage of 4 V. Fig. 7.9b shows the waveforms for HF2 at 300 kHz which indicates an open circuit voltage of 300 V for an input of about 6 V. Under open circuit conditions both circuits operated without any difficulties.

The operation of each circuit was then examined when supplying the required hf discharges. Fig. 7.10a shows the hf 30 kHz discharge voltage and current (≈100 mA) waveforms after breakdown when supplied by HF1, and Fig. 7.10b shows the waveforms for the hf 300 kHz starting discharge of current of about 1 A peak, sustained by HF2. Both hf disharges were stable and could be maintained for several seconds.

Finally the complete system was tested for the igntion of a 3mm TIG arc from cold with a large (500 mH) inductor in series with the main dc power supply to protect it and consequently reduced the di/dt of the main dc current. The procedure was to switch on the dc source, set the output voltage of HF1 to just below the breakdown voltage value and then switch on HF2 which will cause an increase in the voltage across the gap, therefore breakdown takes place and an hf starting discharge is established. With this new split hf system arc ignition was reliable and RFI-free. Under this condition when a spark-gap oscillator was used to ignite the arc it was impossible to initiate it and severe RFI was generated. Fig. 7.11 shows a typical voltage and current waveforms over a period of about

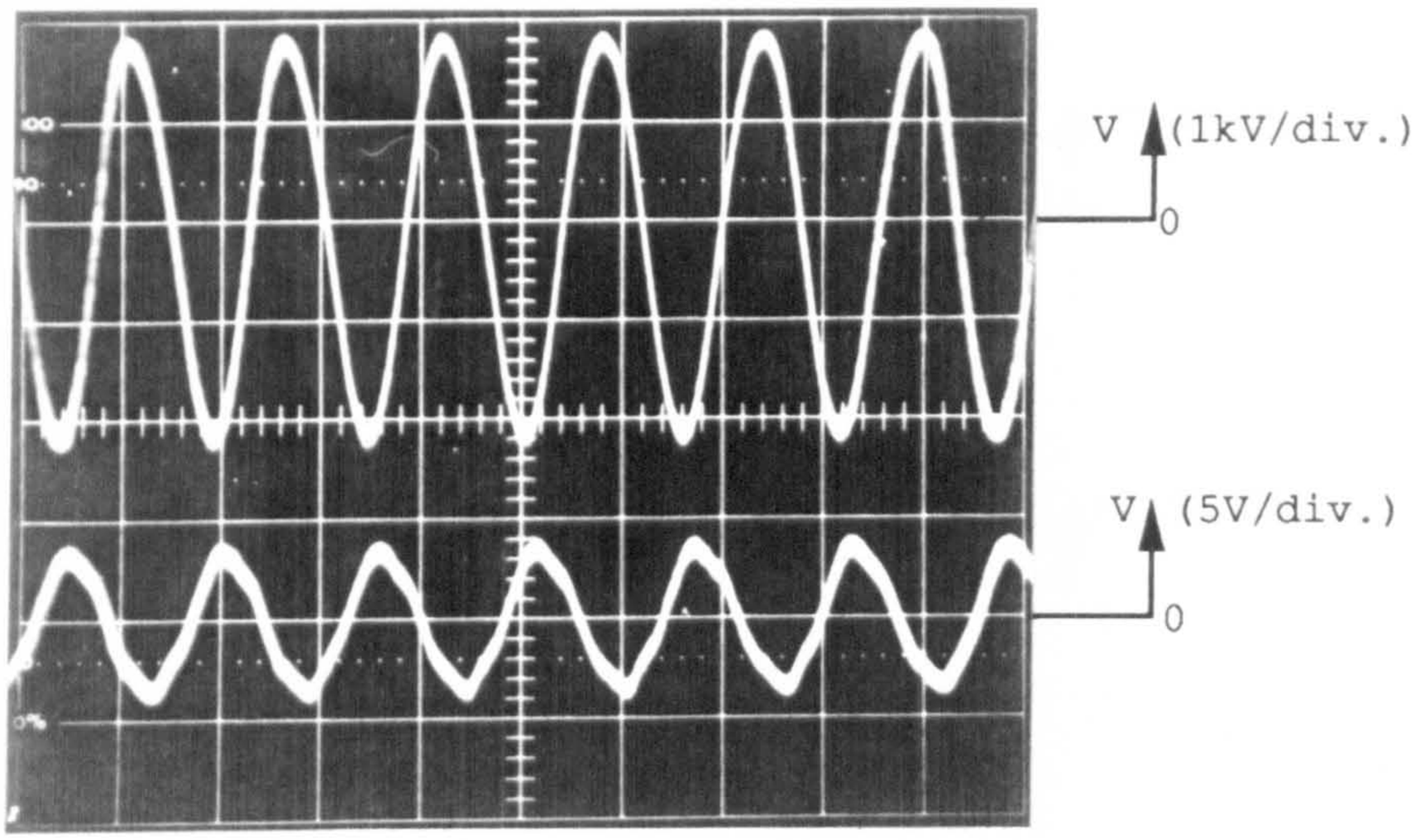

(a) Time base: 20 μs/div.

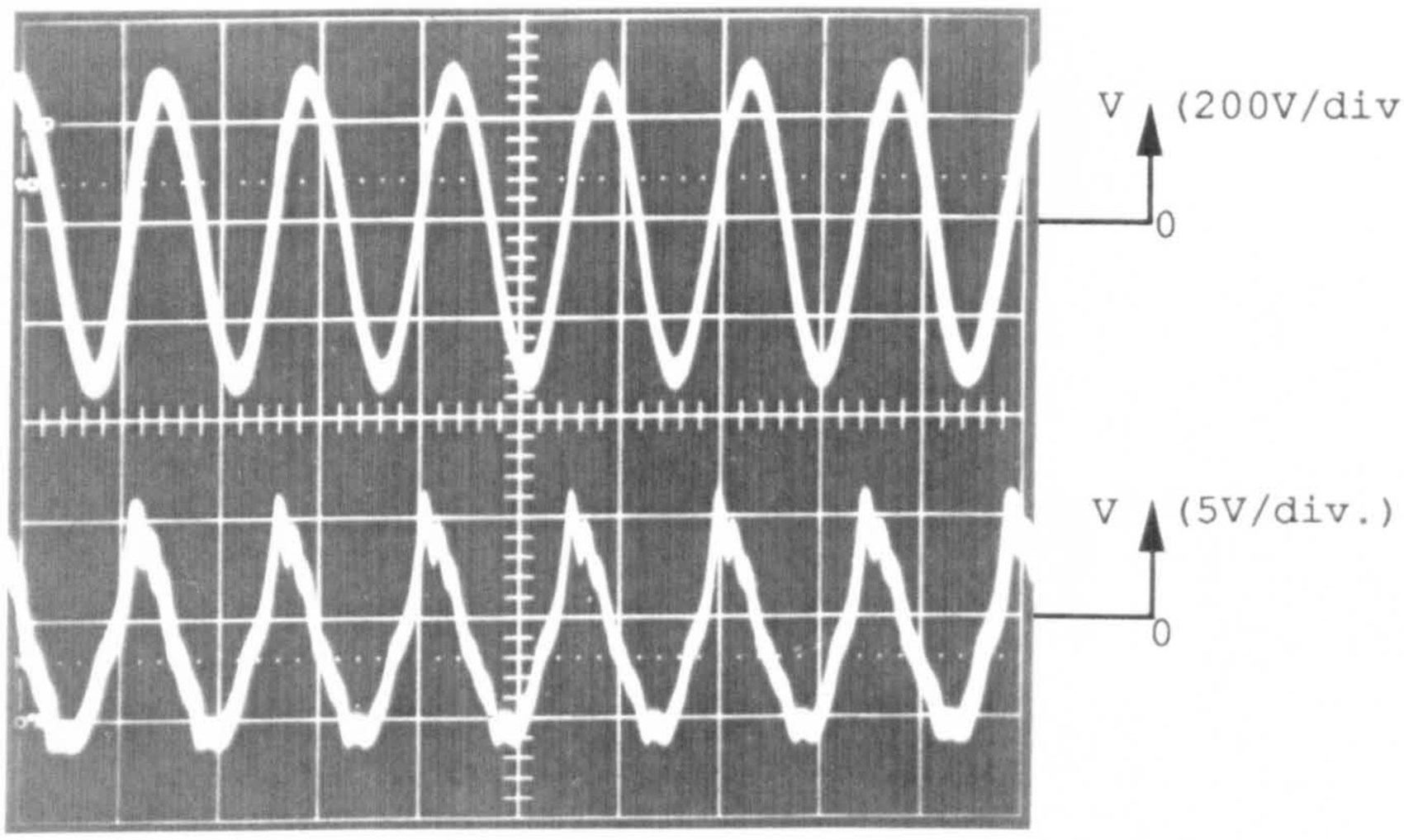

(b) Time base: 2 μs/div.

Fig.7.9 Input and output voltage waveforms of the power stage before breakdown for a) HF1 and b) HF2.

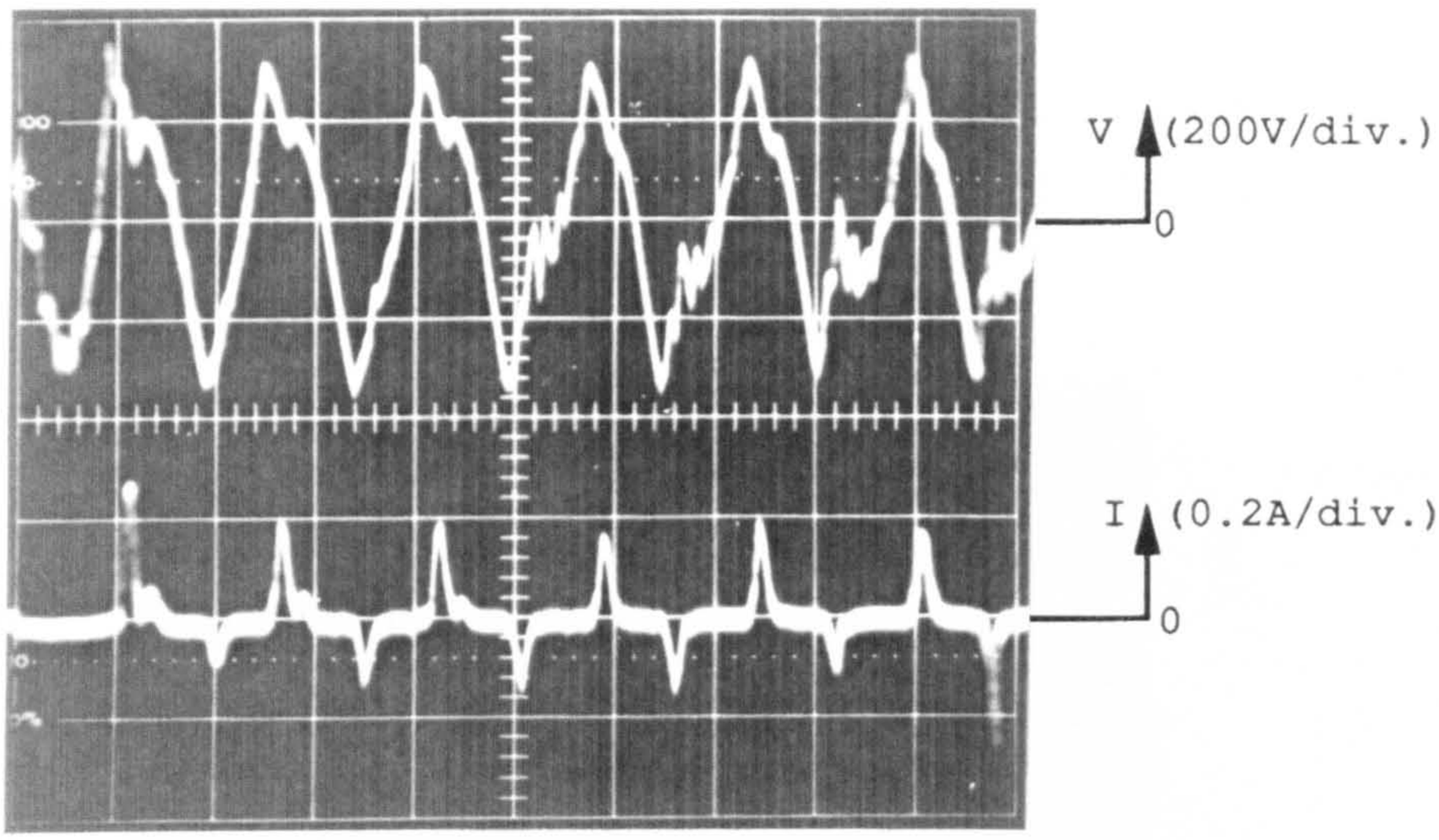

(a) Time base: 20 μs/div.

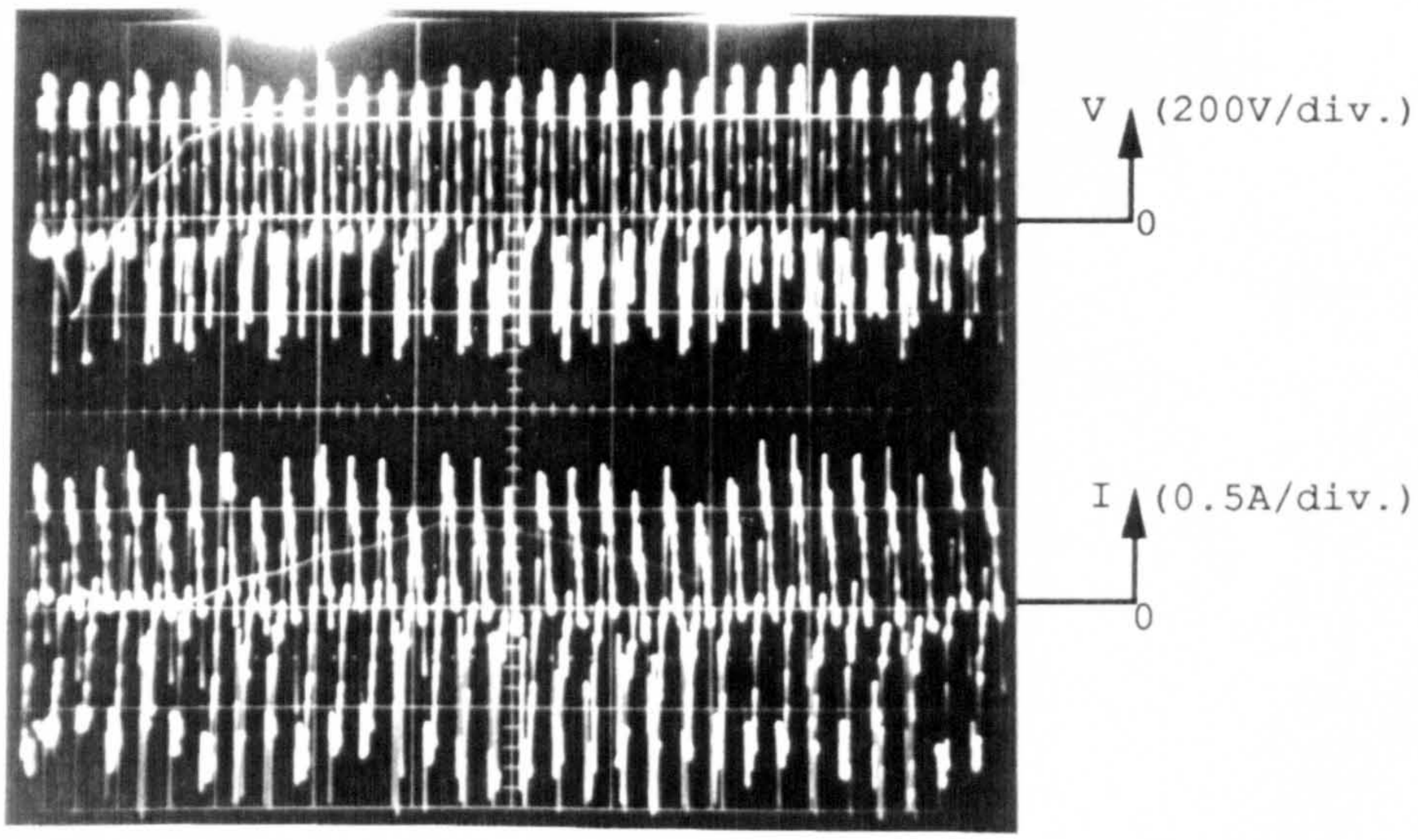

(b) Time base: 10 μs/div.

Fig.7.10 Voltage and current waveforms for the discharge supplied by a) HF1 and b)HF2.

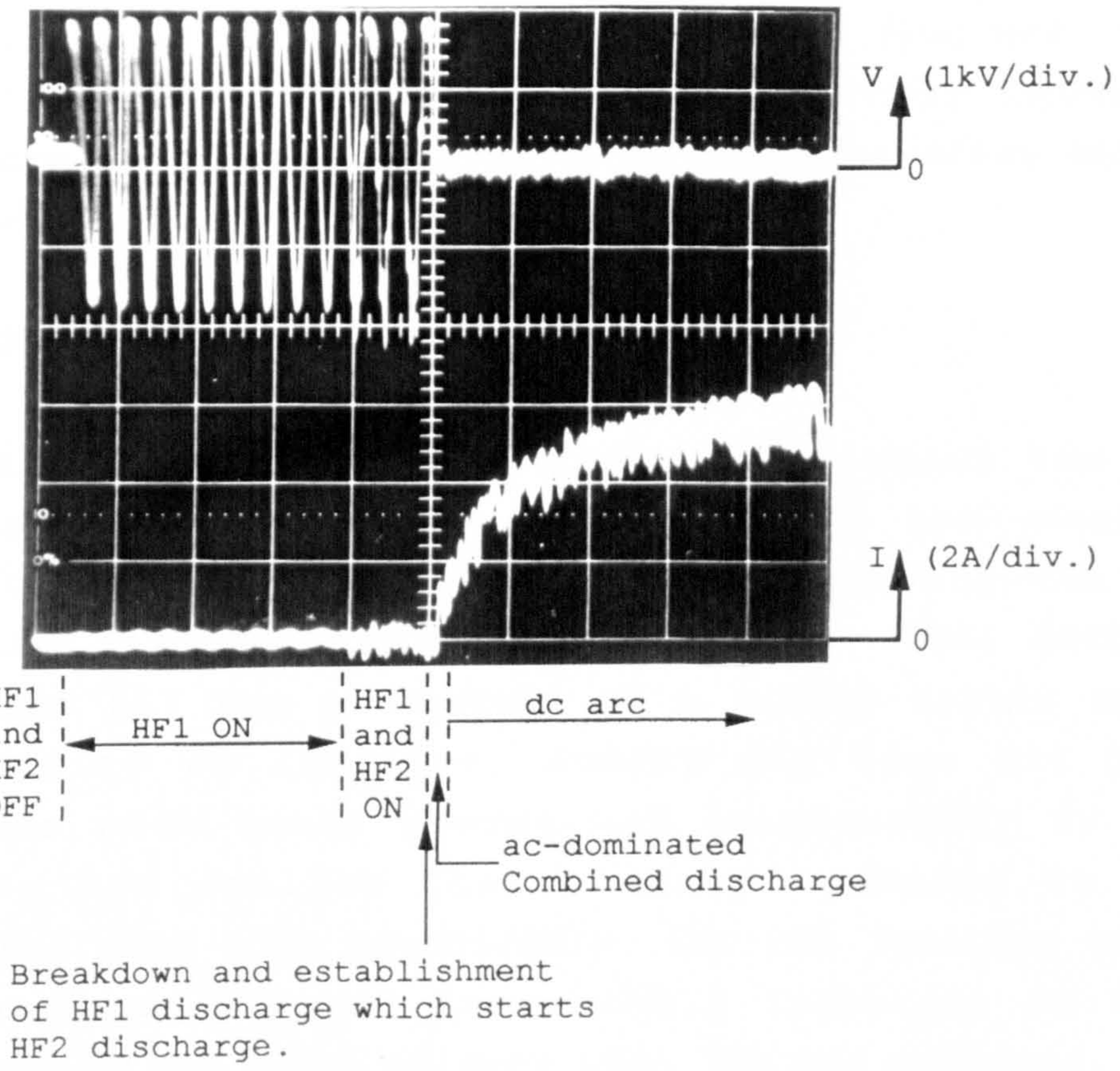

Fig.7.11 Voltage and current waveforms at the arc gap during the initial current rise after breakdown from cold. Time base: 50 ms/div. Sinusoidal waveforms are affected by the sampling rate of the oscilloscope.

500 ms after breakdown from cold. It shows that initially when HF1 is switched on a sinusoidal voltage of about 2 kV is applied to the arc gap which is not sufficient to break it down. When HF2 is swithed on its output voltage is superimposed on the output of HF1 and an increase in the voltage across the gap occurs resulting in breakdown of the arc gap. Immediately after breakdown a low current discharge from HF1 is established which starts the hf discharge from HF2. The hf discharge from HF2 allows the dc current to increase and hence an ac-dc discharge is established after which a dc arc is initiated.

7.4 CONCLUSIONS

A novel technique for arc ignition in which two hf sources are used to supply the arc gap, one causing breakdown of the gap and the other supplying the hf starting discharge has been developed. This method maintains all the advantages of a single system such reliability of ignition, safety and less RFI but requires much lower powers and consequently it is cheaper and smaller than a single system; it is therefore much more practicable. For the ignition of a typical 3 mm TIG arc from cold a reduction in the required output power of more than 78% was achieved.

A solid-state split hf ignition system based on this new idea has been designed and constructed. This system has a total output power of about 300 W. One hf circuit operated at 30 kHz for breakdown having an output voltage of about 3 kV and an output current of about 100 mA, and the other at 300 kHz for the hf starting discharge supplying a current of about 1 A. Reliable, safe and RFI-free ignition could be achieved under the conditions where a spark-gap oscillator produced severe RFI and would not initiate the arc at all.

A patent has been applied for the split hf ignition system as detailed below:

Harry, J.E., and Saiepour, M., 'Arc ignition system for a welding gun and a method of operation', U.K. Patent 9,025,597.7, Nov. 1990.

CHAPTER 8

CONCLUSIONS AND RECOMMENDATIONS FOR FURTHER WORK

8.1 Conclusions

It has been shown that a continuous sinusoidal hf discharge did not always guarantee the ignition of a dc arc. The conditions under which the hf discharge provides a suitabe conduction path for the main arc current so that ignition may take place were found; the dc applied voltage should be higher than the voltage at the transition region and the series resistance small enough to allow the arc to become dc dominated.

The minimum output voltage, current and the operating duration of a dc ignition source for non-contact ignition of dc arcs were determined. The time taken for the main current to reach the minimum required value in a combined discharge supplied by two dc power sources were obtained.

Three types of ac-dc discharges were shown to exist, indicated by the curves for the variation of dc voltage with dc current. These were an ac-dominated discharge shown by the positive slope of the V-I curves, a dc-dominated discharge shown by the negative slope of the V-I curves and a transition region between the ac-dominated and dc-dominated regions.

It has been shown that the use of a single continuous sinusoidal hf ignition source is not feasible due to the need for a high-voltage (about 3 kV) and a relatively high-current (about 1 A), and a correspondingly high power in excess of 1 kW.

A rotating load line model for a dc arc power source during the initial current rise after breakdown from cold was developed to illustrate the changes that take place in the discharge voltage and current.

A capacitor discharge method was devised to provide a versatile power source to investigate the minimum current to sustain a cold arc, the different cold to hot arc transitions and the time taken to reach the steady-state.

It has been shown that after breakdown from cold three different transitions governed by the development of thermal processes in the discharge leading to the steady-state arc take place. These were an initial field dominated cathode region and column followed by a field dominated cathode region and thermally dominated column and finally a thermal cathode region and column.

The rate of current rise was shown to affect the time taken to reach the steady-state arc after breakdown from cold. An arc power source with a high rate of current rise caused a faster transition to the steady-state than one with a lower rate of current rise.

A new continuous sinusoidal split hf ignition supply was devised to provide a safe, reliable and RFI-free ignition and which requires less than 75% of the output power of a single continuous sinusoidal hf ignition supply.

The time taken to reach the steady-state arc after breakdown from cold was found to increase as the electrode separation was reduced and as the gas flow rate and the cathode size were increased. The time to reach the steady-state was also shown to increase if tungsten cathodes were used rather than copper because of the higher operating temperature possible.

The minimum current required for an arc to be self-sustained after breakdown from cold for different

dc supply open circuit voltages was obtained to enable the determination of the minimum operating time required of the ignition source.

The review of non-contact methods of arc initiation enables the relative merits of the individual methods of arc initiation to be considered.

8.2 Recommendations for Further Work

The following recommendations are made for further work to optimise the design and minimise the power requirement of a continuous sinusoidal split hf ignition supply, in order to reduce its size so that it can be readily used in welding power sources.

The use of new semiconductor devices which require a small amount of driving power, can withstand the mismatch caused by the arc gap impedance and are tolerant towards high voltage spikes reflected back from the arc gap should be considered.

New circuit techniques for both the hf generators and the coupling circuit should be investigated and used. A possibility is to use switching techniques to increase the efficiency and reduce the size of the circuits.

The optimum combination of the frequencies used for the two ignition supplies should be determined so that the low current hf discharge reliably starts the higher current hf discharge which initiates the dc arc from cold. The possibility of decreasing the inductance in the main current path which reduces the total size of the ignition supply and increases the rate of rise of the main current resulting in a reduction in the time taken to reach the steady-state (section 5.2.4.2), should be considered.

REFERENCES

AIR REDUCTION COMPANY, 'Improvements in electric arc welding', U.K. Patent 722,494, 1955.

BAUER, A., SCHULZ, P., 'Elektrodenfälle und bogengradienten in hochdruckentladungen insbesondere bei xenon', Z. Physik, 139, pp. 197-211, 1954.

BETZ, P.L., KARRER, S., 'A characteristic of the copper arc during the formative period', J. App. Phys., 8, pp. 845-848, 1937.

BIEGELMEIER, G., ROTTER, K., 'Electrical resistances and currents in the human body', Elektrotech. u. Maschinenbau, 88, pp. 104-114, ERA Trans.-2911, July 1971.

BROWN, M.J., 'Initiation of a tungsten inert gas arc by high voltage D.C.', The Weld. Inst. Res. Report, No. 31-76-P, Dec. 1976.

BUSZ-PEUCKERT, G., FINKELNBURG, W., 'Zum anodenmechanismus des thermischen argonbogens', Z. Physik, 144, pp. 244-251, 1956.

CARY, H.B., 'Modern welding technology', Prentice-Hall, London, 1979.

CASSIE, A.M., 'The arc cathode', Nature, 181, p. 476, 1958.

CAVENOR, M.C., MEYER, J., 'The development of spark discharges in hydrogen', Aust. J. Phys., 22, pp. 155-167, 1969.

CHIHOSKI, R.A., 'The rationing of power between the gas tungsten arc and electrode', Weld, J., 49 S, (2), pp. 69-82, 1970.

CHURCHILL, R.J., PARKER, A.B., CRAGGS, J.D., 'Measurement of reignition voltage characteristics for high current spark gaps in air', J. Electronics and Control, 11, (17), pp. 17-33, 1961.

CLARK, J.C., RYAN, H.J., 'Sphere gap discharge voltages at high frequencies', Proc. AIEE, 33 I, pp. 973-987, 1914.

COBINE, J.D., 'Gaseous conductors', McGraw-Hill, London, 1958.

COBINE, J.D., FARRALL, G.A., 'Experimental study of arc stability. I', J. App. Phys., 31, pp. 2296-2304, 1960.

CORREY, T.B., ATTERIDGE, D.G., PAGE, R.E., WISMER, M.C., 'Radio frequency-free arc starting in gas tungsten arc welding', Weld. J., 65, (2), pp. 33-41, 1986.

CRAWFORD, F.W., EDELS, H., 'The reignition voltage characteristics of freely recovering arcs', Proc. IEE, 107 A, pp. 202-212, 1960.

DUSHMAN, S., 'Electron emission from metals as a function of temperature', Phys. Rev., 21, pp. 623-636, 1923.

EDELS, H., 'Properties and theory of the electric arc', Proc. IEE, IEE Reviews, 108 A, pp. 55-69, 1961.

EDELS, H., WHITTAKER, D., 'Experiments and theory on arc reignition', Symposium on the physics of the welding arc, London, pp. 41-46, 1962.

EROKHIN, A.A., BUKAROV, V.A., ISCHENKO, Y.S., 'Influence of tungsten cathode geometry on some welding arc characteristics and metal penetration', Weld. Prod., 18, (12), pp. 25-28, 1971.

FAN, H.Y., 'The transition from glow discharge to arc', Phys. Rev., 55, pp. 769-775, 1939.

FROOME, K.D., 'Rate of growth of current in arc discharges', Nature, 160, p. 129, 1947.

FROOME, K.D., 'The rate of growth of current and the behaviour of the cathode spot in transient arc discharges', Proc. Phys. Soc., 60, pp. 424-435, 1948.

GAMBLING, W.A., EDELS, H., 'The high-pressure glow discharge in air', Brit. J. App. Phys., 5, pp. 36-39, 1954.

GAMBLING, W.A., EDELS, H., 'The properties of high-pressure steady-state discharges in hydrogen', Brit. J. App. Phys., 7, pp. 376-379, 1956.

GOEBELER, E., 'Über die dielektrischen Eigenschaften der luft und einiger fester isoliermaterialien bei hochgespannter hochfrequenz', Arch. Elektrotech., 14, pp. 491-510, 1925.

GOLDMAN, K., 'Electric arcs in argon', Physics of the welding arc (A Symposium), Inst. of Welding, pp. 17-22, 1966.

GUFAN, R.M., ZOLOTYKH, V.T., 'Unit for connecting an HF ignition unit in series in a welding circuit', Weld. Prod., 12, (1), pp. 70-71, 1965.

GUILE, A.E., 'Arc-electrode phenomena', Proc. IEE, IEE Reviews, 118, (9R), pp. 1131-1154, 1971.

HANCOX, R., 'Importance of insulating inclusions in arc initiation', Brit. J. App. Phys., 11, pp. 468-471, 1960.

HARRY, J.E., EVANS, D.R., 'A large bore axial flow CO_2 laser', IEEE J. Quant. Elec., QE24, (3), pp. 503-506, 1988.

HILDEBRANDT, P., TAJBL, F., 'Method and equipment for contactless ignition of DC and AC electric current arcs under shielding gas', Schweissen u. Schneiden, 25, (4), pp. 129-132, 1973.

HIRSH, M.N., OSKAM, H.J., 'Gaseous electronics. I. Electrical discharges', Academic Press, London, 1978.

HOLLIDAY, J.H., ISAACS, G.G., 'Arc initiation at metal surfaces in a hydrogen Penning discharge', Brit. J. App. Phys., 17, pp. 1575-1583, 1966.

HOTZ, R.F., 'Experimental investigation of the relative light distribution in a high-pressure rapidly alternating dc glow discharge', J. App. Phys., 41, (4), pp. 1500-1503, 1970.

HOWATSON, A.M., 'An introduction to gas discharges', Pergamon Press, Oxford, 1976.

HOYAUX, M.F., 'Arc physics', Springer-Verlag, New York, 1968.

JACOTTET, V.P., 'Zure frage der messung von hochfrequenz spannungen und stoßspannungen kürzester dauer mit der kugelfunkenstreche', Elektrotechnische zeitschrift, 60, pp. 92-97, 1939.

JONES, G.R., FREEMAN, G.H., 'The influence of natural radial convection upon the transient behaviour of a cylindrical arc column', Z. Physik, 229, pp. 177-191, 1969.

KAMPSCHULTE, J., 'Luftdurchschlag und überschlag mit wechselspannung von 50 und 100 000 Hertz', Arch. Elektrotech., 24, pp. 525-552, 1930.

KAUFMANN, W.,'Elektrodynamische eigentumlichkeiten leitender gase', Ann. Phys., 2, (4), pp. 158-178, 1900.

KELHAM, W.O., 'The recovery of electric strength of an arc-discharge column following rapid interruption of the current', Proc. IEE, 101 II, pp. 321-334, 1954.

KESAEV, I.G., 'Stability of metallic arcs in vacuum. I', Sov. Phys. - Tech. Phys., 8, pp. 447-456, 1963.

KESAEV, I.G., 'Stability of metallic arcs in vacuum. II', Sov. Phys. - Tech. Phys., 8, pp. 457-462, 1963.

KESAEV, I.G., 'Laws governing the cathode drop and the threshold currents in an arc discharge on pure metals', Sov. Phys. - Tech. Phys., 9, pp. 1146-1154, 1965.

KING, L.A., 'The positive column of high and low current arcs', ERA Report G/XT 152, 1954.

KING, L.A., 'The voltage gradient of the free-burning arc in air or nitrogen', ERA Report G/XT 172, 1961.

KNIGHT, R., 'Multiple electric arc discharges', PhD Thesis, Loughborough Univ. of Tech., U.K. 1984.

KOHEI, A., 'A consideration on the mechanism of penetration in arc welding', J. Japan Weld. Soc., 37, (4), pp. 51-60, 1968.

KUFFEL, E., ZAENGL, W.S., 'High-voltage engineering fundamentals', Pergamon Press, Oxford, 1984.

LANCASTER, J.F., 'The physics of welding', Pergamon Press, Oxford, 1986.

LASSEN, H., 'Frequenzabhängigkeit der funkenspannung in luft', Arch. Elektrotech., 25, pp. 322-332, 1931.

LUFT, H., 'Überschlagspannungen bei hochfrequenz mittlerer wellenlänge an einfachen anodnungen', Arch. Elektrotech., 31, pp. 93-107, 1937.

LUTZ, M.A., 'The glow to arc transition - a critical review', IEEE Trans. Plasma Sci., PS2, (1), pp. 1-10, 1974.

MAKHLIN, N.M., et al, 'Suppression of radio interference caused by an arc exciter of type UPD-1', Automatic Weld., 32, (12), pp. 36-38, 1979.

MASKREY, J.T., DUGDALE, R.A., ' The role of inclusions and surface contamination in arc initiation at low pressures', Brit. J. App. Phys., 17, pp. 1025-1034, 1966.

MASON, R.C., 'Probe measurements in high pressure arcs', Phys. Rev., 51, (1), pp. 28-42, 1937.

MECHEV, V.S., EROSHENKO, L.E., 'Influence of angle of sharpening of a non-consumable electrode on the parameters of the electric arc in argon-arc welding', Weld. Prod., 23, (7), pp. 5-8, 1976.

MEEK, J.M., CRAGGS, J.D., 'Electrical breakdown of gases', John Wiley, New York, 1978.

MELTON, G.B., 'Initial current characteristics of welding sets for gas tungsten arcs', The Weld. Inst. Res. Report, No. 140-81, 1981.

MISERÉ, F., 'Luftdurchschlag bei niederfrequenz und hochfrequenz an verschiedenen elektroden', Arch. Elektrotech., 26, pp. 123-126, 1932.

MUEHE, C.E., 'AC breakdown in gases', Lincoln Lab. Tech. Report No. 380, Massachusetts, USA, Feb. 1965.

MÜLLER, F., 'Der elektrische durchschlag von luft bei sehr hohen frequenzen', Arch. Elektrotech., 28, pp. 341-348, 1934.

NASSER, E., 'Fundamentals of gaseous ionization and plasma electronics', John Wiley, London, 1971.

NEEDHAM, J.C., 'Arc stability in gas-shielded arc welding - part 2 starting the arc', The Weld. Inst. Res. Bulletin, 10, (1), pp. 14-17, 1969.

PAPOULAR, R., 'Electrical phenomena in gases', Iliffe, London, 1965.

PERSITS, L.M., GRITSENKO, M.S., SIDOROV, L.R., 'An evaluation of factors affecting the long-term

durability of tungsten electrodes and the reliability of arc ignition in argon-shielded arc welding', Weld. Prod., 26, pp. 19-23, 1979.

PFENDER, E., 'Electric arcs and arc gas heaters', in 'Gaseous electronics. I Electrical discharges', eds. HIRSH, M.N. and OSKAM, H.J., Academic Press, London, 1978.

PRICE, W.L., GAMBLING, W.A., EDELS, H., 'High-pressure glow-to-arc transitions with tungsten and copper cathodes', Nature, 176, pp. 28-29, 1955.

PROWSE, W.A., 'The initiation of breakdown in gases subject to high frequency electric fields', J. Brit. IRE, 10, pp. 333-347, 1950.

PYKAL, M., 'Welding arc ignition in TIG welding', International Inst. Weld., Doc. No. IIW-212-330, 1975.

REUKEMA, L.E., 'The relation between frequency and spark-over voltage in a sphere-gap voltmeter', Trans. AIEE, 47, pp. 38-48, 1928.

RICHARDSON, O.W., 'The emission of electricity from hot bodies', Longmans Green, London, 1921.

ROMALO, D., 'Conditions for spark-starting of a plasma torch', Metal construction and Brit. weld. J., 1, pp. 457-459, 1969.

SAIEPOUR, M., HARRY, J.E., 'Arc ignition using DC discharges', Int. J. Electronics, 70, (2), pp. 467-474, 1991.

SAVAGE, W.F., STRUNCK, S.S., ISHIKAWA, Y., 'The effect of electrode geometry in gas tungsten-arc welding', Weld. J., 44 S, (11), pp. 489-496, 1965.

SCHWAB, H.A., 'Electrical properties of radio frequency glow discharges in air at atmospheric pressure', U.S. Naval Weapons Lab., Dahlgren, Virginia, Rep. No. 2124, 1967.

SCHWAB, H.A., 'Some properties of radio frequency gas discharges in air at atmospheric pressure', Proc. IEEE, 59, (4), pp. 613-616, 1971.

SCHWAB, H.A., HOTZ, R.F., 'Reignition voltage in a high-pressure rf discharge', J. App. Phys., 41, (4), pp. 1503-1507, 1970.

SLEPIAN, J., 'Extinction of an A-C arc', Trans. AIEE, 47, pp. 1398-1407, 1928.

SLEPIAN, J., 'Extinction of a long A-C arc', Trans. AIEE, 49, pp. 421-430, 1930.

SOMERVILLE, J.M., 'The electric arc', John Wiley, New York, 1959.

SUITS, C.G., 'High pressure arcs', General Electric Rev., 39, pp. 194-200, 1936.

SUITS, C.G., 'High pressure arcs in common gases in free convection', Phys. Rev., 55, pp. 561-567, 1939.

THOMSON, J.J., THOMSON, G.P., 'Conduction of electricity through gases', Cambridge Univ. Press, Cambridge, 2, 1933.

USHIO, M., MATSUDA, F., 'Study on gas-tungsten-arc electrode', Weld. Res. Inst., Japan, IIW Doc. 212-648-86, pp. 1-10, 1986.

VON ENGEL, A., 'Ionized gases', Clarendon Press, Oxford, 1965.

VON ENGEL, A., 'Electric plasmas: their nature and uses', Taylor and Francis, London, 1983.

VON ENGEL, A., STEENBECK, M., 'Elektrische gasentladungen lhre physik und technik', 2, Springer-Verlag, Berlin, 1934.

VOLFF, C.L., HAMMERSLAG, J., 'High-frequency unit for inert gas arc welding', U.S. Patent 2,574,514, 1951.

APPENDICES

APPENDIX 1

Table A.1.1 Components List for the HF HV Generator

Resistors:

R_1 and R_7	570 kΩ
R_2 and R_6	6 kΩ (15 W)
R_3	140 Ω
R_4	25 kΩ (8 W)
R_5	100 kΩ
R_8 and R_9	560 kΩ
R_{10}	22 kΩ (100 W)
R_{11}	100 kΩ (5 W)
R_{12}	9.99 MΩ (high voltage)

Inductors:

L_1 and L_2	Common mode inductors L=9 mH each, stack of 8 toroidal ferrite cores Fair-Rite material 77 Part No.5,977,003,801.
L_3	0.1 H, 150 mA, DC choke

Capacitors:

C_1	0.22 μF
C_2	0.2 μF (500 V)
C_3	0.1 μF (250 V)
C_4	0.1 μF
C_5 and C_6	1200 pF
C_7	0.1 μF (1500 V)
C_8	500 pF (1500 V)
C_9	3000 pF (15 kV)

Transformer:

T_1	Push-Pull transformer, solenoidal air core primary and secondary made of 200 turns of 2.23 mm diameter copper wire.

Valves:

V_1 and V_2	Type 807 Pentodes.
V_3 and V_4	EEV-C1136 Power Tetrodes.

APPENDIX 2

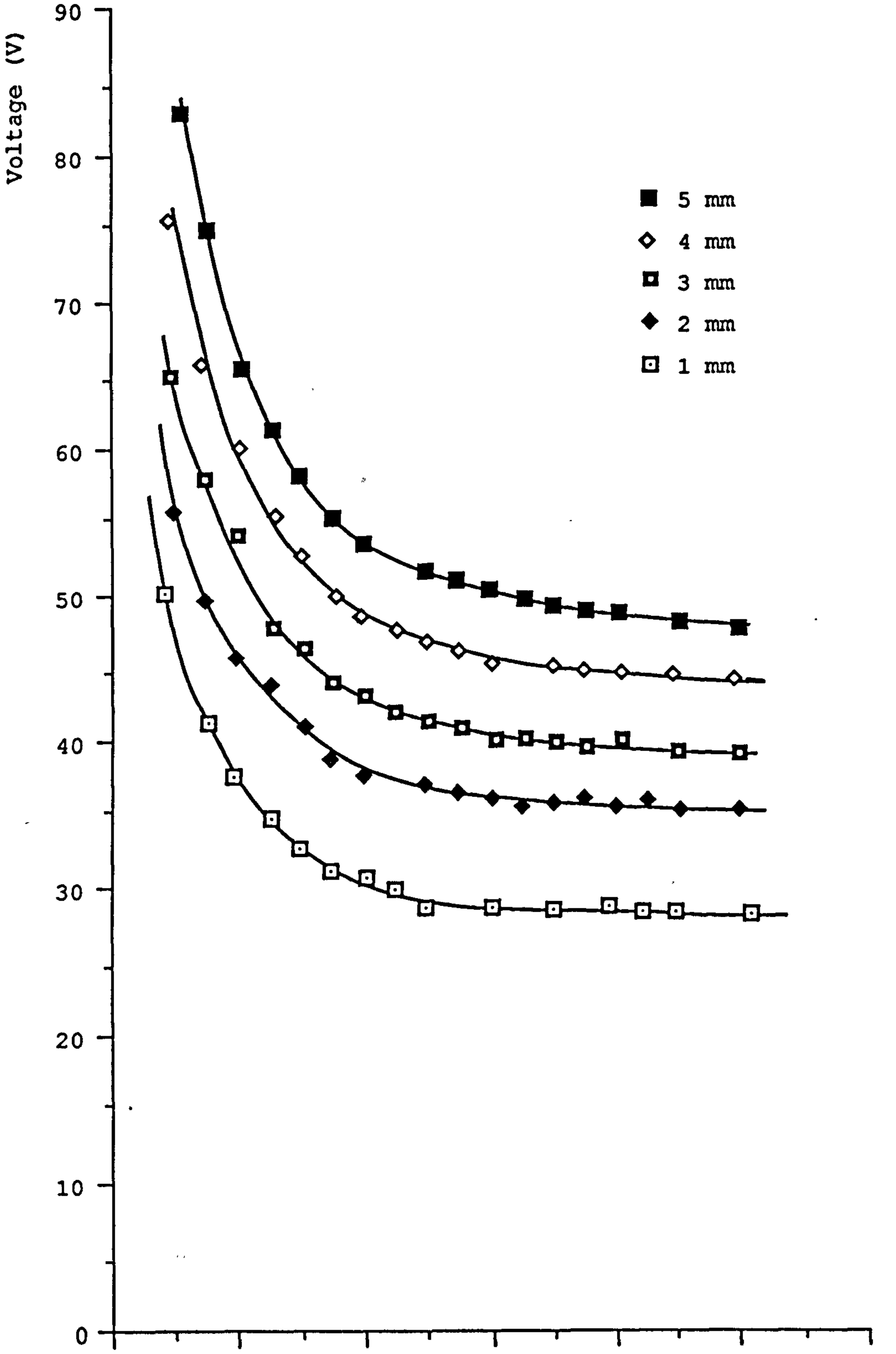

Fig.A.2.1 Static arc V-I characteristics using a copper cathode in air

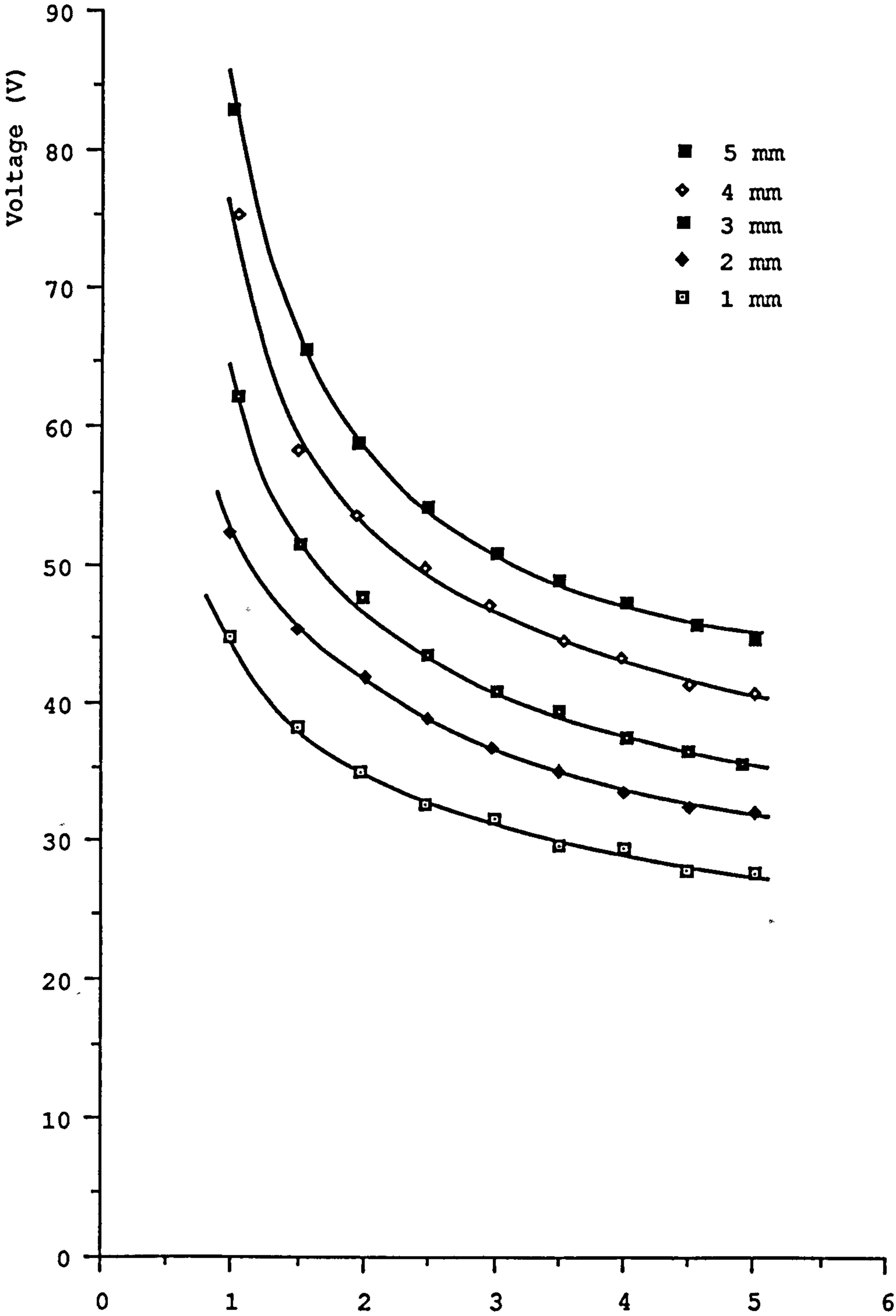

Fig.A.2.2 Static arc V-I characteristics using a tungsten cathode in air.

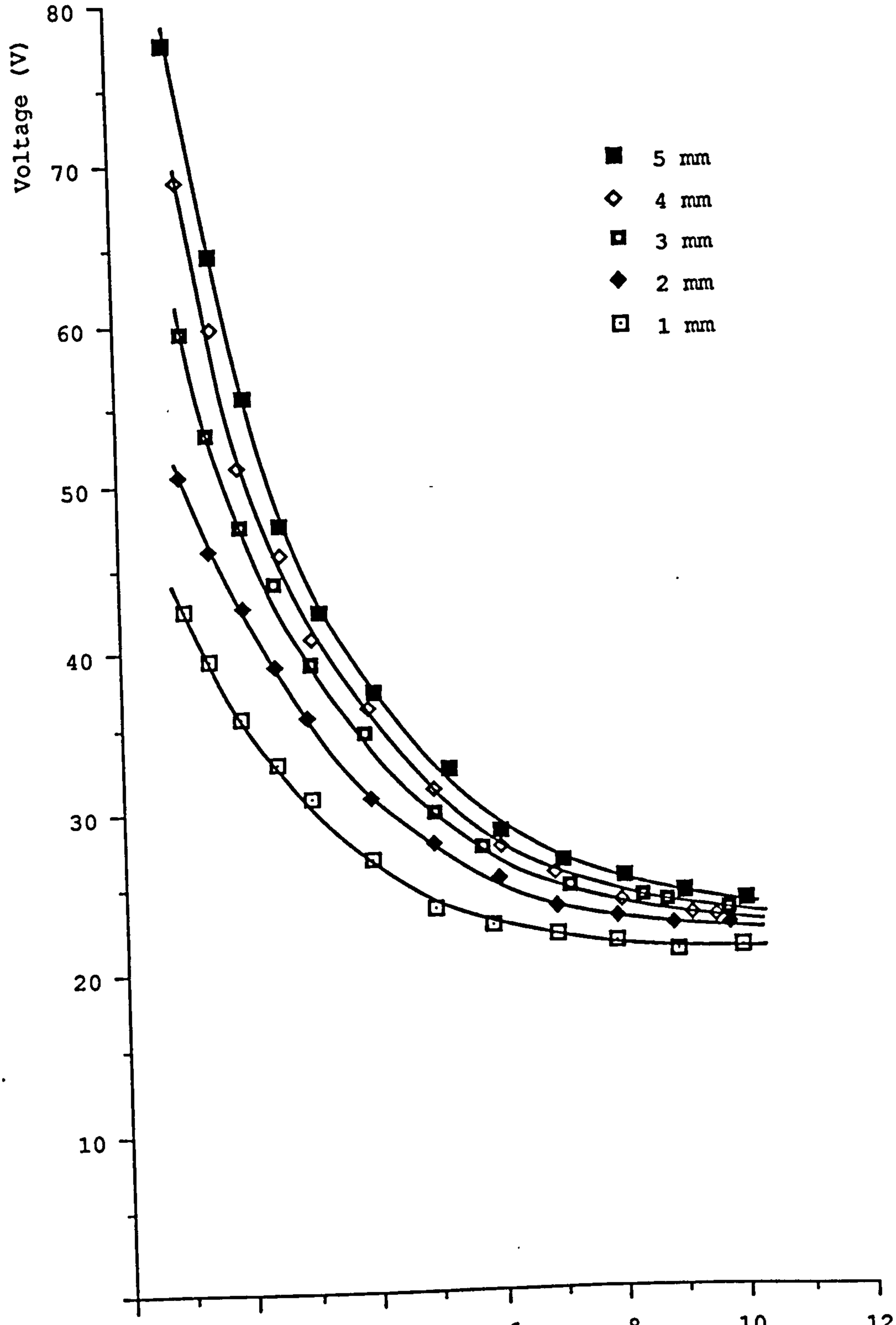

Fig.A.2.3 Static V-I characteristics for TIG arcs.

APPENDIX 3

DETERMINATION OF THE TIME TAKEN FOR AN ARC COLUMN TO THERMALLY DEVELOP AFTER INITIATION FROM COLD.

Assuming a cylindrically symmetrical infinitely long arc column, the energy required to raise its temperature by ΔT is given by:

$$\rho_{av.}.C_p.\Delta T.l.\pi D^2/4$$

where $\rho_{av.}$ is the average gas density, C_p is the specific heat capacity at constant pressure, ΔT is the rise in temperature, l is length of the column and D is the column diameter.

The input electrical energy to the discharge during the development of the column is:

$$I\left(\frac{V_1-V_2}{2}\right)t$$

where I is the current, t is the time taken for the arc to thermally develop and V_1 and V_2 are the arc voltages before and after the development of the column respectively. From section 5.2.2 the measured values of V_1 and V_2 for a 3 mm gap in air are 100 V and 65 V and in argon are 70 V and 55 V respectively.

The gas density (ρ_2) at 6000 K may be calculated using the volume coefficient of expansivity of gases which may be expressed in terms of the gas density:

$$\rho_2 = \frac{\rho_0}{\left(\frac{T_2-T_1}{273}+1\right)}$$

where ρ_0 = density at 0 °C which may be assumed approximately equal to the density at room temperature for the purpose of these calculations. Therefore for air $\rho_0 \approx 1.293$ kgm^{-3} and for argon $\rho_0 \approx 1.784$ kgm^{-3}. Hence for $T_2-T_1 \approx 6000$ K, in air $\rho_2 \approx 0.056$ kgm^{-3} and $\rho_{av.} \approx 0.675$ kgm^{-3}; in argon $\rho_2 \approx 0.078$ kgm^{-3} and $\rho_{av.} \approx 0.931$ kgm^{-3}.

These values for ρ_2 are very close to those indicated by Jones and Freeman (1969).

If I=7 A, D=3 mm and C_p for air and argon are 993 Jkg^{-1}K^{-1} and 524 Jkg^{-1}K^{-1} respectively then:

in air **t ≈ 222 μs** and

in argon **t ≈ 376 μs.**

These theoretical values are lower than the experimental values (≈0.5 ms) obtained in chap. 5 and this may be owing to the assumption of an arc plasma free of electrode effects which cause cooling and hence delay the development of a thermally ionised column.

APPENDIX 4

Table A.4.1 Components list for each HF generator module used in the new split hf system

Resistors:

VR_1*, VR_{10}	1 kΩ, variable
R_2	120 Ω
VR_4, VR_7, VR_8, VR_{17}.	100 kΩ, variable
R_5, R_6, R_{12}, R_{13}, R_{23}, R_{24}.	10 kΩ
R_9, R_{14}	1 kΩ
R_{11}	8.2 kΩ
VR_{15}	1 kΩ, variable
VR_{16}	5 kΩ, variable
R_{18}	68 kΩ
R_{19}, R_{32}, R_{33}	47 Ω
R_{20}	47 Ω (2 in series),(11 W)
R_{22}	68 Ω (11 W)
R_{25}	560 kΩ
VR_{26}	100 Ω, variable
R_{27}	240 Ω
VR_{28}, VR_{29}	10 kΩ, variable
R_{30}, R_{31}	330 Ω (2.5 W)
R_{LED}	4.7 kΩ (1 W)

Capacitors:

C_1*	470 PF (Polypropylene)
C_2, C_3,	1 nF (Polypropylene)
C_4	2200 µF(40 V), Electrolytic
C_5, C_6, C_8, C_{12}, C_{13}	1 µF
C_7	2200 µF(63 V), Electrolytic

C_9	0.22 µF (Polypropylene)
C_{10}	0.01 µF
C_{11}	2.2 µF
C_{14}	6.8 µF (100 V)

Semiconductors:

IC_1	ICL 8038 waveform generator.
IC_2	LM393N
IC_3	4073B
IC_4	555 timer
TR_1, TR_2	ZTX 451
TR_3	ZTX 551
M_1, M_2	IRF 360 (or SMM 24N40)
M_3	IRF 520
D_1, D_2	OA 202
D_3	Zener diode, 27 V, 5 W
D_4	Zener diode, 15 V, 5W
D_5, D_6	1.5KE10CP, Bidirectional transient suppressor (TRANSIL).
D_7, D_8	BZW 50-150, Unidirectional transient suppressor (TRANSIL).
D_9, D_{10}	BYV29-400, Fast recovery diode.
LED_1	Over-current (red)
LED_2	Power (yellow)

Transformers:

T_1, T_2 100:1, FX4063 toroidal core, sensing current transformers.

T_3* Driver transformer, 1:1, Siemens RM6 core (T38 material), 2 mH for 300 kHz, 20 mH for 30 kHz.

T_4* Push-pull Transformer, for 300 kHz, 3 Toroids of Fair-Rite 77, total N_P=24 turns and N_S=64 turns, using Litz wire, for 30 kHz, Philips (G8) television horizontal output transformer, pins 1,2,3, are the primary with pin 2 as the centre tap and pins 11, 15 are the HV output.

Fuses:

F_1 5 A (Antisurge)

Ferrite beads:

FB_1, FB_2, FB_3, FB_4 RS 238-283

Heatsink:

0.4 °C/W, Farnell type 148-123

* Different for each HF unit.

APPENDIX 5

ROTATING LOAD LINE MODEL

A model was devised and used in chapters 4, 5 and 6 to illustrate the changes that take place in the discharge voltage and current during the current rise after breakdown from cold. This model is discussed below.

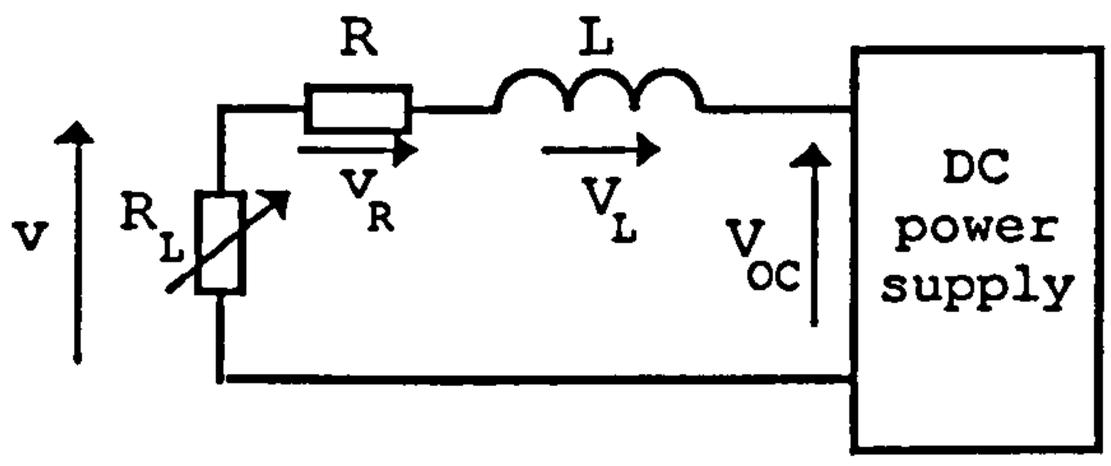

Fig. A.5.1 RL transient circuit

During the current rise in an RL transient circuit (Fig. A.5.1), the magnitude of V_{OC} stays constant but the phase of v_R and v_L change with respect to V_{OC} (Fig. A.5.2). At t=0, V_{OC} and v_L are equal and in phase. At the steady-state V_{OC} and v_R become equal and in phase.

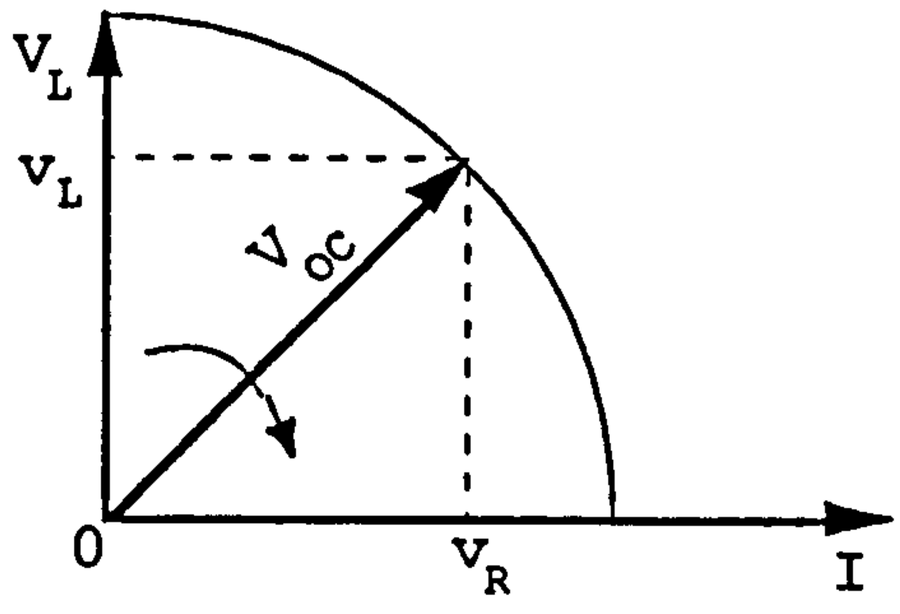

Fig. A.5.2 Vector diagram during the current rise

V-I diagrams are two dimensional graphical representations which show only magnitudes and not phases (Figs. A.5.3 - A.5.5). Although the I-axis is shown perpendicular to V_{OC} in these diagrams, during

APPENDIX 5

ROTATING LOAD LINE MODEL

A model was devised and used in chapters 4, 5 and 6 to illustrate the changes that take place in the discharge voltage and current during the current rise after breakdown from cold. This model is discussed below.

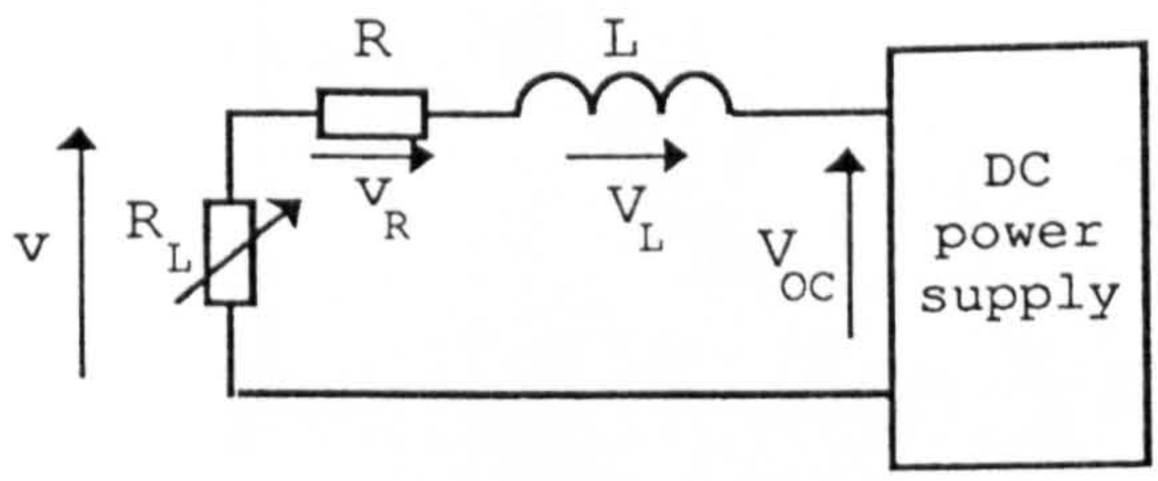

Fig. A.5.1 RL transient circuit

During the current rise in an RL transient circuit (Fig. A.5.1), the magnitude of V_{OC} stays constant but the phase of v_R and v_L change with respect to V_{OC} (Fig. A.5.2). At t=0, V_{OC} and v_L are equal and in phase. At the steady-state V_{OC} and v_R become equal and in phase.

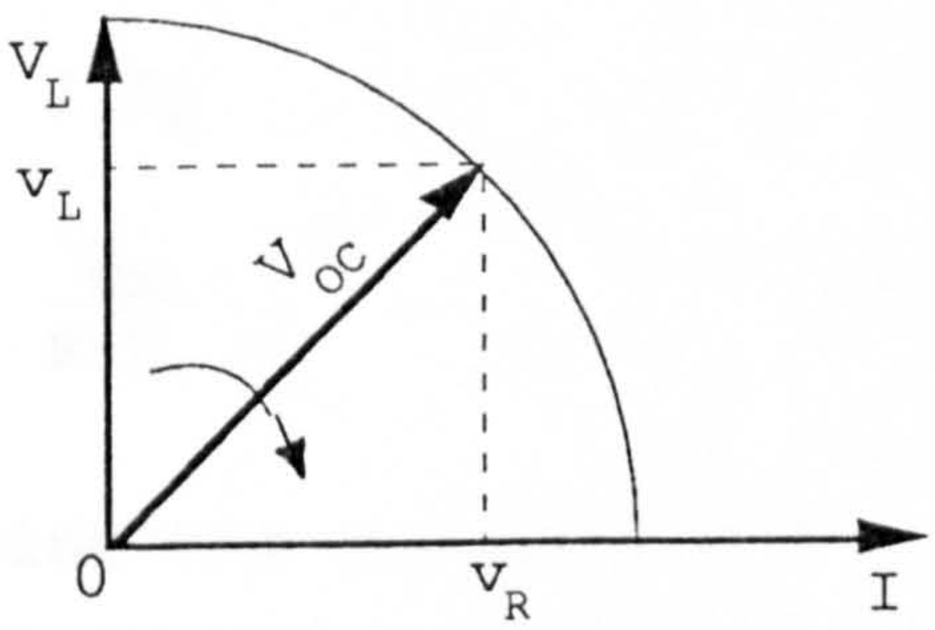

Fig. A.5.2 Vector diagram during the current rise

V-I diagrams are two dimensional graphical representations which show only magnitudes and not phases (Figs. A.5.3 - A.5.5). Although the I-axis is shown perpendicular to V_{OC} in these diagrams, during

the current rise I may be at different phases to V_{OC}. Although V_{OC} is shown fixed in a V-I diagram, its phase changes with respect to the current as shown in the vector diagram of Fig. A.5.2.

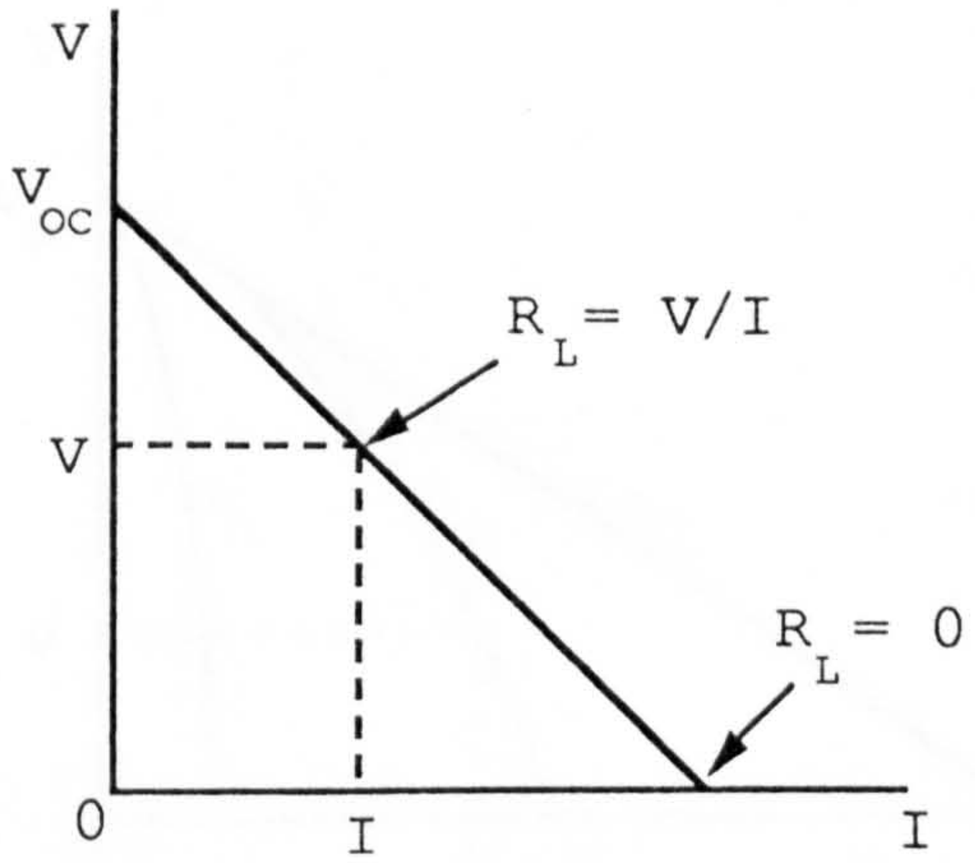

Fig. A.5.3 Steady-state load-line model

Fig. A.5.3 shows the load line for a circuit in the steady-state. The line shows the variation of the voltage across the load R_L with current for values of $R_L = 0 - \infty$. The voltage and current for each value of R_L are given by:

$$V = I.R_L \qquad (A.5.1)$$

$$I = \frac{V_{OC}}{R+R_L} \qquad (A.5.2)$$

During the current rise in a transient RL circuit, the voltage and current are related by:

$$v = i.R_L \qquad (A.5.3)$$

$$i = \frac{V_{OC}}{R+R_L}\left[1 - e^{-\left(\frac{R+R_L}{L}\right)t}\right] \qquad (A.5.4)$$

For each value of time t a curve can be plotted for the variation of v with i for values of R_L = 0 - ∞. The general shape of this load curve is shown in Fig. A.5.4.

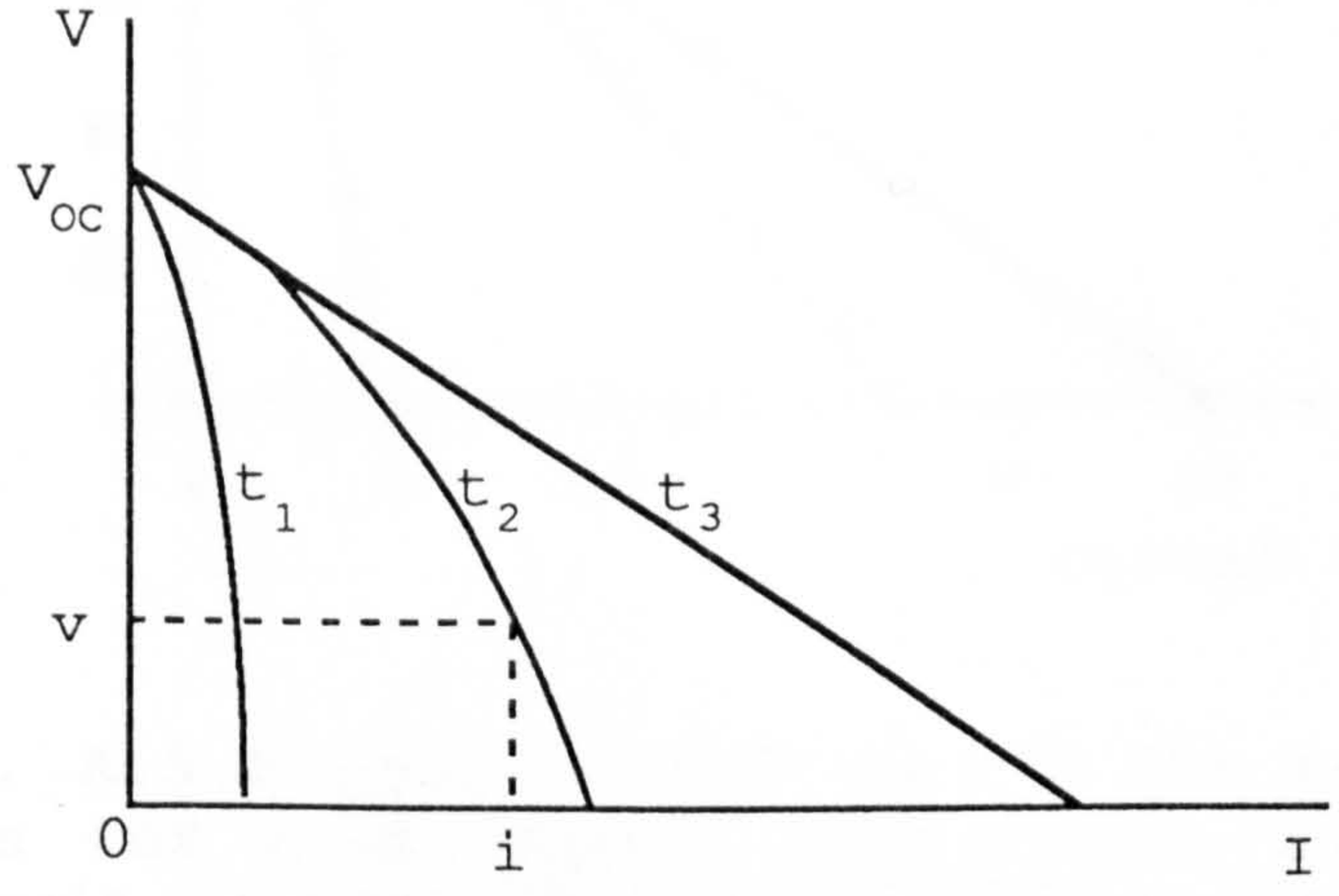

Fig. A.5.4 Shape of the load curves during the current rise in an RL transient circuit.

Because Fig. A.5.4 is a two dimensional V-I diagram of magnitudes of V and I the voltage across R and L is not equal to $(V_{OC}-v)$.

Each load curve can be approximated to a load line except at times just after breakdown when the inductive voltage component is much greater than the resistive voltage component.

Example

Considering a dc power supply with an open circuit voltage of 100 V, series resistance of 2 Ω and series inductance of 1 mH. For values of t equal to 100 μs, 500 μs and 3000 μs equations A.5.3 and A.5.4 were used to find the load currents and voltages for R_L = 0 - ∞. Fig. A.5.5 shows the load curves for each value of time.

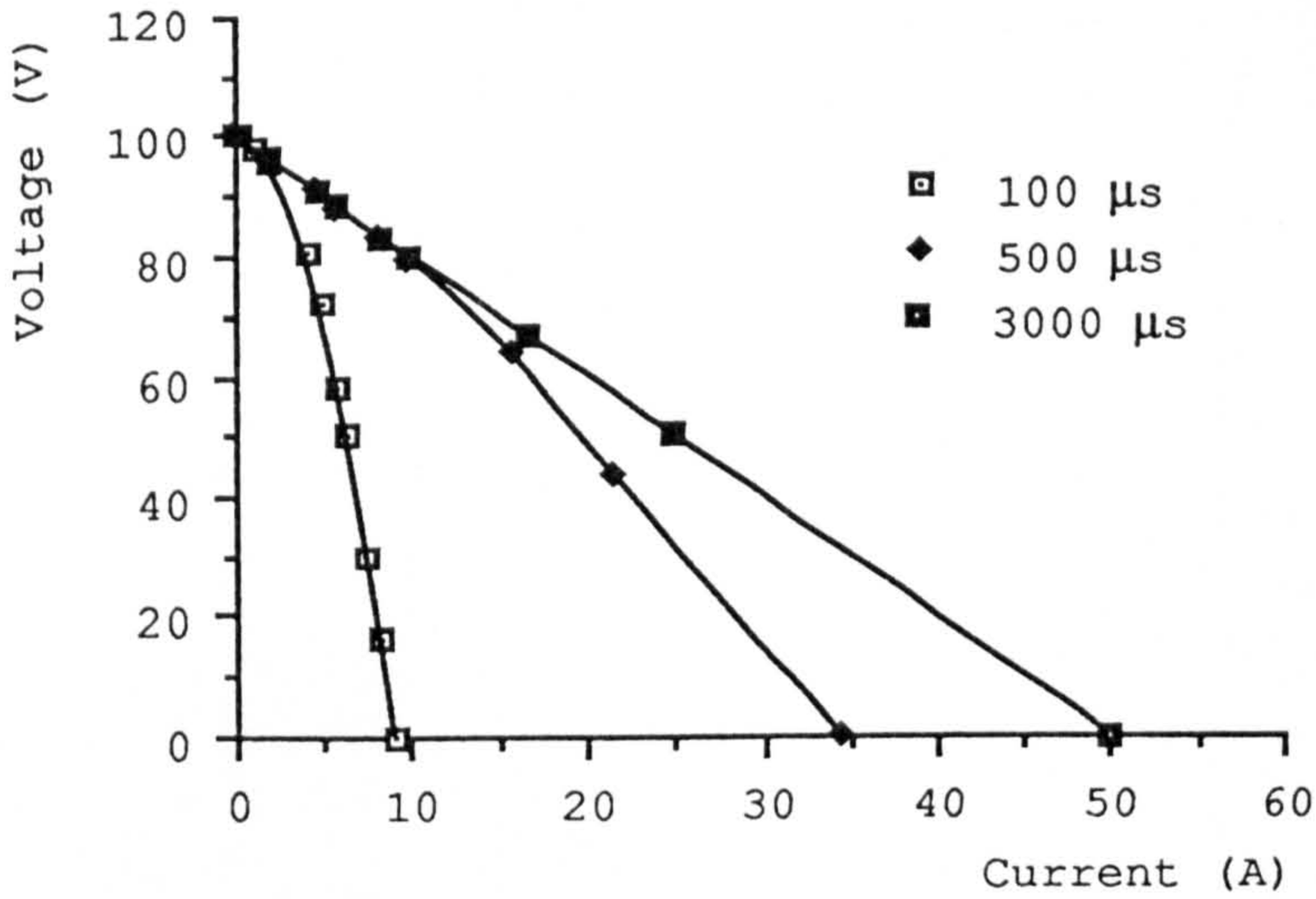

Fig. A.5.5 Load curves during the current rise for a dc power supply with an open circuit voltage of 100 V, series resistance of 2 Ω and series inductance of 1 mH.

The slope of these load curves or approximately load lines, decreases as time increases. The load line therefore rotates anticlockwise about the point V_{OC}.